

**Optimizing Anaerobic Treatment to Enhance Energy Recovery from
High-Strength Waste and Wastewater**

by

Anqi Mou

A thesis submitted in partial fulfillment of the requirements for the degree of

Doctor of Philosophy

in

Environmental Engineering

Department of Civil and Environmental Engineering

University of Alberta

© Anqi Mou, 2024

ABSTRACT

Anaerobic digestion (AD) is a promising technology for the sustainable treatment of high-strength waste and wastewater, offering the potential for energy recovery. However, various factors can inhibit the AD process, requiring well-balanced operational strategies to optimize different stages of the AD process, enhancing overall energy recovery, and investigating the dynamics of microbial communities to understand the mechanisms behind these optimizations.

The research chain began by examining pre-treatment methods to accelerate the initial hydrolysis step of AD. Specifically, the efficiency of calcium hypochlorite pre-treatment on thickened waste activated sludge (TWAS) was investigated. The optimal dosage of calcium hypochlorite was determined to minimize sludge volume after aerobic digestion, with a focus on enhancing solubilization and biodegradability of TWAS. After the pre-treatment with $0.1 \text{ gCa(ClO)}_2/\text{gtotal solids (TS)}$, volatile solids (VS) of TWAS were reduced by 65% after 20 days of aerobic digestion - nearly double the reduction observed in un-pretreated TWAS.

Subsequently, the thesis shifted focus to improving syntrophic interactions between four steps of AD. The feasibility of anaerobic calcium phosphate granulation for blackwater treatment was assessed in continuous reactors operated under mesophilic conditions. CaP granules were developed in the up-flow anaerobic sludge blanket (UASB) reactor. An organic loading rate (OLR) of 16.0 g/L/d and hydraulic retention time (HRT) of 0.25 days were achieved, with a total chemical oxygen demand (COD) removal rate of 75.6%, and a methane production rate of $8.4 \text{ gCH}_4\text{-COD/L/d}$.

This thesis also explored co-digestion methods to reduce the volatile fatty acids (VFAs) accumulations, thereby balancing the four steps of AD. The feasibility of long-term operation for co-digestion of spent caustic wastewater and pot ale wastewater was assessed. The methane yield of co-digestion reactor was higher than that of the pot ale wastewater reactor. The organic loading capacity of co-digestion reactor reached 13.6 g/L/d, which was higher than 7.6 g/L/d achieved in pot ale wastewater reactor. Meanwhile, the co-digestion also improved the hydrolysis efficiency of co-digestion substrates.

In the final stages, this thesis accelerated methanogenesis, the last step of AD process. The effects of granular activated carbon (GAC) spatial distribution in UASB reactors on methane production were examined. Three different GAC placement strategies (top, bottom, and top+bottom) were evaluated to enhance methane production throughout the reactor depth, particularly focusing on treating different solid-content wastewater and enhancing organic loading capacities. Under low OLR (2 g/L/d) treating high solid-content wastewater, the highest methane yield was observed for UASB supplemented with self-floating GAC (74%), which was followed by settled +self-floating GAC reactor (65%), then settled GAC reactor (58%). When treating low solid-content wastewater, all UASBs achieved improved methane yield, and settled +self-floating GAC reactor achieved the highest methane yield (83%). Under high OLR (6 g/L/d) treating high solid-content wastewater, the UASB supplemented with GAC at both bottom and top achieved the highest methane yield (66%), whereas the UASB supplemented with GAC at the top failed.

Throughout the AD process, the role of microorganisms was important. The dynamics of microbial communities in augmented systems were analyzed to highlight their critical role in optimizing performance. This thesis demonstrated the significance of balancing whole AD processes through strategic treatment modifications and highlights the need to consider organic loading capacities

and feedstock characteristics, thereby contributing to the development of more sustainable wastewater treatment solutions.

PREFACE

This thesis is an original work by Anqi Mou. I designed and conducted the research involved in this thesis at the University of Alberta under the supervision of Dr. Yang Liu. I was responsible for performing all the experiments, data collection and analysis, and manuscript composition. Dr. Yang Liu was the supervisory author and was involved with conceptualization, review, and editing of the manuscript. Other contributions made by my colleagues are listed below.

A version of **Chapter 3** has been published as Mou, A., Yu, N., Zhang, L., Sun, H., and Liu, Y. 2022. Calcium hypochlorite pretreatment enhances waste-activated sludge degradation during aerobic digestion. *Journal of Environmental Engineering*, 148(4), 04022002. Dr. Najiaowa Yu, Dr. Lei Zhang, and Dr. Huijuan Sun contributed to methodology.

A version of **Chapter 4** has been published as Zhang, L.¹, Mou, A.¹, Sun, H., Zhang, Y., Zhou, Y., and Liu, Y. 2021. Calcium phosphate granules formation: Key to high rate of mesophilic UASB treatment of toilet wastewater. *Science of the Total Environment*, 773, 144972. (¹Equal contributions). Dr. Lei Zhang contributed to methodology and conceptualization. Dr. Huijuan Sun, Dr. Yingdi Zhang, and Dr. Yun Zhou contributed to methodology.

A version of **Chapter 5** has been submitted as Mou, A., Yang, X., Yu, N., Mohamed A., and Liu, Y. Anaerobic co-digestion of pot ale and spent caustic wastewater: Impacts on performance stability and microbial community dynamics. Xinya Yang, Dr. Najiaowa Yu, and Abdul Nayeem Mohamed contributed to methodology.

Part of **Chapter 6** has been published as Mou, A., Yu, N., Sun, H., and Liu, Y. 2022. Spatial distributions of granular activated carbon in up-flow anaerobic sludge blanket reactors influence

methane production treating low and high solid-content wastewater. *Bioresource Technology*, 363, 127995. Dr. Najiaowa Yu, Dr. Lei Zhang, and Dr. Huijuan Sun contributed to methodology. Additionally, part of **Chapter 6** has been submitted as Mou, A., Yu, N., Yang, X., Khalil, M., and Liu, Y. Enhancing methane production in up-flow anaerobic sludge blanket (UASB) reactor: the role of granular activated carbon (GAC) placement and substrate solid content on biofilm community dynamics. Dr. Najiaowa Yu, Xinya Yang, and Mostafa Khalil contributed to methodology.

A version of **Chapter 7** has been published as Mou, A., Yu, N., Yang, X., and Liu, Y. 2024. Enhancing methane production and organic loading capacity from high solid-content wastewater in modified granular activated carbon (GAC)-amended up-flow anaerobic sludge blanket (UASB). *Science of The Total Environment*, 906, 167609. Dr. Najiaowa Yu and Xinya Yang contributed to methodology.

DEDICATION

To my dear parents

To my dear grandparents

ACKNOWLEDGMENTS

A decade ago, my visit to UCLA planted the seed of aspiration within me – to one day become Dr. Mou, inspired by the university's vibrant academic environment. Today, as that dream materializes, I reflect on the arduous yet enriching journey of my Ph.D. studies.

I extend my deepest gratitude to my esteemed supervisor, Professor Yang Liu, whose exemplary dedication, and passion for research have profoundly influenced my academic path. Since my master's studies at Nankai University, Dr. Liu has been a beacon of guidance, inspiring me with her innovative ideas and patient mentorship. Her unwavering support and encouragement have been instrumental in my decision to pursue my Ph.D. at the University of Alberta, a choice I have never regretted. Dr. Liu embodies the epitome of a mentor and researcher, treating her students with unparalleled kindness and patience. I am profoundly thankful for the opportunity to learn and grow under her guidance, aspiring to emulate her excellence in my future endeavors. I also express my heartfelt appreciation to my undergraduate supervisor, Dr. Xianqiu Zhang from Nanjing Normal University, and my master's supervisor, Dr. Qixing Zhou from Nankai University. Their ongoing support and care have been invaluable. My gratitude extends to the members of my supervisory committee for their insightful feedback and contributions to my research.

Special thanks go to my colleague and friend, Dr. Najiaowa Yu, for her invaluable collaboration and mentorship in anaerobic digestion research. Her assistance with experimental challenges, paper revisions, and career advice has greatly enriched my professional journal. I am grateful for the knowledge shared by Abdul on industrial applications and engineering perspectives, and for the camaraderie and shared experimental ventures with Xinya Yang. My appreciation also extends to Dr. Lei Zhang for his foundational teachings in anaerobic digestion and experimental techniques.

To my colleagues, Dr. Bing Guo, Dr. Hongyu Dang, Dr. Huijuan Sun, Dr. Huixin Zhang, Dr. Mengjiao Gao, Tong Liu, Xin Zou, and Dr. Yun Zhou, thank you for the collective wisdom and support that have greatly contributed to my learning experience. I am grateful for my lifelong friends, from childhood to university, for their enduring support and warmth. Dr. Chengjia Qu, Hua'an Zhang, Huan Qiu, Jingjing Liu, Lei Li, Dr. Najiaowa Yu, Dr. Rugeng Liu, Siwen Wang, Tong Liu, Wenfei Pan, Wentao Wang, Xu Zhu, Yanqi Ye, Yiyu Lu, Dr. Yuening Li, Yuming Wu, and Dr. Yuzhuo Li - your presence has been a comfort through every season of life. To my partner, Tae Hyun Chung, and his family. Your unwavering support and care, especially during challenging times, have been a source of immense strength.

The deepest gratitude is reserved for my family, whose unwavering support has been the cornerstone of my journey. My mother, Yonghong Lu, a paragon of leadership and dedication, has always held herself to the highest standards, guiding me with her wisdom and strength. Without her, the pursuit of my Ph.D. in Canada would have remained a mere dream. Her ability to provide solutions and support for any problem has been my guiding light. My father, Jianguang Mou, is the embodiment of kindness, always there to offer comfort and the most delicious meals, making sure I felt loved and supported at every step. To my beloved grandmothers, your love and caring have always been a source of comfort. My grandfathers left me with memories filled with love and wisdom that continue to guide me. I miss them dearly and am grateful for the moments we shared. Farewell to my grandfathers. And to my cherished pets - Diandian, Baobao, Mimi, Cookie, and Cocoa - your companionship has been a source of joy and comfort, adding brightness to my days.

Finally, my gratitude extends to the financial sponsors of my research: China Scholarship Council, Natural Sciences and Engineering Research Council of Canada, Canada Research Chair Program, Alberta Innovates, WaterWerx, and City of Edmonton, for their generous support.

TABLE OF CONTENTS

ABSTRACT	II
PREFACE	V
DEDICATION	VII
ACKNOWLEDGMENTS	VIII
TABLE OF CONTENTS	X
LIST OF FIGURES	XVII
LIST OF TABLES	XXIV
ABBREVIATIONS	XXV
CHAPTER 1 INTRODUCTION AND RESEARCH OBJECTIVES	1
1.1 Background and motivations	1
1.2 Research objective and approach	2
1.3 Thesis layout	7
CHAPTER 2 LITERATURE REVIEW	11
2.1 Anaerobic digestion process	11
2.2 The effects of operational parameters on anaerobic digestion	13
2.2.1 Organic loading rates	13
2.2.2 Feedstocks	14

2.3 High-strength waste and wastewater from different wastewater systems	16
2.3.1 Waste activated sludge (WAS) in centralized wastewater systems	17
2.3.2 Blackwater in decentralized wastewater systems	18
2.3.3 Distillery wastewater	20
2.4 Pre-treatment methods to enhance hydrolysis of WAS.....	22
2.5 Blackwater anaerobic digestion.....	25
2.6 Anaerobic co-digestion	27
2.7 Direct interspecies electron transfer (DIET).....	29
2.8 Research gaps	33

CHAPTER 3 CALCIUM HYPOCHLORITE PRE-TREATMENT

ENHANCES THICKENED WASTE-ACTIVATED SLUDGE

DEGRADATION DURING AEROBIC DIGESTION 36

3.1 Introduction.....	37
3.2 Materials and methods	38
3.2.1 Sludge source	38
3.2.2 TWAS pre-treatment with $\text{Ca}(\text{ClO})_2$.....	39
3.2.3 Aerobic digestion.....	39
3.2.4 Analytical methods.....	40
3.2.5 Kinetic modeling of VS degradation	42
3.2.6 Microbial community analysis	42
3.2.7 Statistical analysis.....	43

3.3 Results and discussion	43
3.3.1 <i>Ca(ClO)₂ pre-treatment</i>	43
3.3.2 <i>Aerobic digestion</i>	50
3.3.3 <i>Microbial community</i>	54
3.3.4 <i>Potential implication in WWTPs</i>	56
3.4 Conclusions.....	57
CHAPTER 4 CALCIUM PHOSPHATE GRANULES FORMATION: KEY TO HIGH RATE OF MESOPHILIC UASB TREATMENT OF TOILET WASTEWATER	58
4.1 Introduction.....	59
4.2 Materials and methods	61
4.2.1 <i>Mesophilic UASB reactor set-up</i>	61
4.2.2 <i>Water quality characterization and biogas analysis</i>	64
4.2.3 <i>Characterization of granular sludge</i>	65
4.2.4 <i>Microbial community analysis</i>	66
4.2.5 <i>Statistical analysis</i>	67
4.3 Results	67
4.3.1 <i>Reactor performance</i>	67
4.3.2 <i>COD mass balance</i>	69
4.3.3 <i>Sludge bed development</i>	70
4.3.4 <i>Granules size and granule EPS content</i>	73
4.3.5 <i>Characteristics of granular sludge in the reactor</i>	75

4.3.6 <i>Microbial community</i>	78
4.4 Discussion.....	81
4.4.1 <i>Anaerobic granules significantly increased the performance of the UASB</i>	81
4.4.2 <i>Formation of anaerobic granules in anaerobic toilet wastewater treatment</i>	82
4.5 Conclusions	85
CHAPTER 5 ANAEROBIC CO-DIGESTION OF POT ALE AND SPENT CAUSTIC WASTEWATER: IMPACTS ON PERFORMANCE STABILITY AND MICROBIAL COMMUNITY DYNAMICS	86
5.1 Introduction.....	87
5.2 Materials and Methods.....	90
5.2.1 <i>Distillery wastewater and inoculum</i>	90
5.2.2 <i>Batch co-digestion experiments</i>	90
5.2.3 <i>Reactor operation</i>	91
5.2.4 <i>Analytical methods</i>	91
5.2.5 <i>Sludge characteristics</i>	92
5.2.6 <i>Microbial community analysis</i>	93
5.3 Results and discussion	93
5.3.1 <i>Wastewater characteristics</i>	93
5.3.2 <i>Batch experiments of co-digestion</i>	94
5.3.3 <i>Reactor performance</i>	96
5.3.4 <i>COD mass balance and hydrolysis efficiency</i>	99
5.3.5 <i>Sludge characteristics</i>	102

5.3.6 <i>Microbial community</i>	105
5.3.7 <i>Implications</i>	109
5.4 Conclusion	109
 CHAPTER 6 SPATIAL DISTRIBUTIONS OF GAC IN UASB REACTORS	
INFLUENCE METHANE PRODUCTION TREATING LOW AND HIGH	
SOLID-CONTENT WASTEWATER	
	111
 6.1 Introduction	 112
6.2 Materials and methods	115
6.2.1 <i>Reactor design and operation</i>	115
6.2.2 <i>Seed sludge and substrates</i>	116
6.2.3 <i>Analytical methods</i>	116
6.2.4 <i>Sludge characterization</i>	117
6.2.5 <i>Microbial community analysis</i>	118
6.2.6 <i>Microbial community analysis and gene predictions</i>	118
6.3 Results and Discussion	119
6.3.1 <i>Wastewater characteristics</i>	119
6.3.2 <i>Reactor performance</i>	120
6.3.3 <i>Sludge characteristics</i>	124
6.3.4 <i>Microbial community</i>	126
6.3.5 <i>Microbial community of GAC-biofilms</i>	130
6.3.6 <i>Predictions of functional genes</i>	138
6.3.7 <i>Principal component analysis (PCA)</i>	141

6.3.8 <i>Correlation matrix analysis</i>	142
6.3.9 <i>Implications</i>	145
6.4 <i>Conclusions</i>	146
CHAPTER 7 ENHANCING METHANE PRODUCTION AND ORGANIC LOADING CAPACITY FROM HIGH SOLID-CONTENT WASTEWATER IN MODIFIED GRANULAR ACTIVATED CARBON (GAC)-AMENDED UP-FLOW ANAEROBIC SLUDGE BLANKET (UASB).....	148
7.1 <i>Introduction</i>	149
7.2 <i>Materials and methods</i>	151
7.2.1 <i>Design and operation of the reactors</i>	151
7.2.2 <i>Seed sludge and wastewater</i>	153
7.2.3 <i>Analytical techniques and calculations</i>	153
7.2.4 <i>Sludge characterization</i>	155
7.2.5 <i>Analysis of microbial community</i>	155
7.2.6. <i>Analysis of statistical significance</i>	156
7.3 <i>Results and Discussion</i>	156
7.3.1 <i>Reactor performance</i>	156
7.3.2 <i>Hydrolysis efficiency</i>	161
7.3.3 <i>Volatile fatty acids (VFAs) concentrations</i>	163
7.3.4 <i>Sludge stability</i>	165
7.3.5 <i>Specific methanogenic activities of sludge</i>	168
7.3.6 <i>Microbial community</i>	172

7.3.7 <i>Implications</i>	177
7.4 Conclusions	178
CHAPTER 8 CONCLUSIONS AND RECOMMENDATIONS	179
8.1 Thesis overview	179
8.2 Conclusions	181
8.3 Recommendations	185
BIBLIOGRAPHY	188

LIST OF FIGURES

Fig. 1.1. Overview of thesis.....	8
Fig. 2.1. Different stages of anaerobic digestion process for biogas generation.....	13
Fig. 2.2. Schematic showing a malt whisky distillation process, traditional by-products (draff, pot ale, and spent caustic wastewater).....	21
Fig. 2.3. Schematic diagram of IET (A) and DIET (B: DIET via conductive pili; C: DIET via membrane-bound electron transport proteins; D: DIET via abiotic conductive materials.) between organics-oxidizing bacteria and methanogenic archaea. This figure is a modification of a schematic presented in a previous paper (Park et al., 2018).	31
Fig. 3.1. SCOD concentrations during 24 h Ca(ClO)₂ pre-treatment of TWAS.....	44
Fig. 3.2. a: Confocal laser scanning microscopy (CLSM) images of TWAS at different Ca(ClO)₂ pretreatment concentrations (green/red color represents live/dead cells); b: The percentage of live cells (green) and dead cells (red) in TWAS at different Ca(ClO)₂ pretreatment concentrations.....	45
Fig. 3.3. EEM contour plot of soluble organics (a) and EEM area volume of soluble organics (b) after 24 h Ca(ClO)₂ pre-treatment of TWAS: I: tyrosine-like proteins; II: soluble microbial by-product-like substances; III: tryptophan-like substances; IV: fulvic acid-like substances; V: humic acid-like substances (RU represents relative unit).	47
Fig. 3.4. Concentrations of soluble protein and polysaccharide after 24 h Ca(ClO)₂ pre-treatment of TWAS.....	48
Fig. 3.5. Specific resistance to filtration (SRF) after pretreatment of TWAS with different Ca(ClO)₂ concentrations.	49

Fig. 3.6. Soluble chemical oxygen demand (SCOD) concentrations during aerobic digestion of TWAS.	50
Fig. 3.7. The rates of SCOD concentration changes during aerobic digestion of TWAS in three phases.	51
Fig. 3.8. VS reduction during 20 days of aerobic digestion of WAS and kinetic modeling analysis of the hydrolysis rate (<i>k</i>) of TWAS pretreated with different doses of Ca(ClO)₂. ..	53
Fig. 3.9. The relative abundance of predominant bacteria at family level in sludge (The taxonomic names were shown for family level or higher level; family: f_; order: o_; class: c_).	55
Fig. 3.10. Predicated metagenome functions of sludge after aerobic digestion treatment. ..	56
Fig. 4.1. Performance of UASB reactor during seven operation phases (A: Influent and effluent total COD concentrations and COD removal rate; B: Methane yield; C: Methane production rate).	68
Fig. 4.2. COD mass balance of UASB reactor treating toilet wastewater at different hydraulic retention time (HRT), the partition of influent COD considered includes COD for methane production, effluent COD, COD accumulation in sludge, COD in discharged sludge and unknown COD.	70
Fig. 4.3. The concentrations of TSS and VSS and the ratio of VSS/TSS (A), the influent COD_{solids} hydrolysis efficiency (B), and methanogenic activity (C) of UASB reactor treating toilet wastewater at different organic loading rates (OLR). Error bars represent one standard deviation.	72
Fig. 4.4. Protein and polysaccharide contents in EPS of the granules (A), granules diameter and PN/PS ratio (B) during the operation phases.	74

Fig. 4.5. EEM fluorescence spectra of sludge EPS during anaerobic sludge granulation (A) Phase I and (B) Phase IV..... 75

Fig. 4.6. Granular sludge and particle size distribution in UASB reactor (A: Granule formation in the UASB reactor; B: Particle size distribution of granular sludge; C: SEM pictures of granular sludge; D: SEM-EDS images of granules; E: XRD pattern of a granule). 77

Fig. 4.7. Relative abundances of top 10 bacterial genera (A) and top 6 archaeal genera (B) in the anaerobic granules. Unidentified genera were named using higher taxonomic levels, family and order (f__ and o__). 79

Fig. 4.8. Pearson's correlation between sludge granules microbial community and granules size and PN/PS ratio in the EPS of the granules. The color key indicates the strength of correlation coefficient. (A) Correlation between Bacterial and granular sludge formation; (B) Correlation between Achaea and granular sludge formation. 80

Fig. 5.1. SCOD/TCOD ratios and pH of different spent caustic wastewater: pot ale wastewater (S:P) volume ratio co-digestion wastewater (A) and biochemical methane potential (BMP) of different S:P volume ratio co-digestion wastewater (B). The mixing time for co-digestion wastewater was one hour. 96

Fig. 5.2. Methane production rate of control reactor (pot ale wastewater) (A) and co-digestion reactor (B) and influent TCOD, effluent TCOD, and COD removal rates of control reactor (C) and co-digestion reactor (D) after long-term operation at different stages..... 98

Fig. 5.3. COD balance of control reactor (pot ale wastewater) (A) and co-digestion reactor (B) and hydrolysis efficiency (C) of two reactors after long-term operation at different stages. 102

Fig. 5.4. Sludge-specific methanogenic activity (SMA) of control reactor (pot ale wastewater) (A) and co-digestion reactor (B) and sludge stability (C) of two reactors after long-term operation at different stages. The organic loading rates (OLR) of R1 at Stage 1, 2, and 3 were 3.7 g/L/d, 7.6 g/L/d, and 11.2 g/L/d, respectively. The OLR of R2 at Stage 1, 2, 3, and 4 were 3.9 g/L/d, 8.8 g/L/d, 11.8 g/L/d, and 13.6 g/L/d, respectively. 105

Fig. 5.5. Heatmap for the relative abundance of main bacterial communities (A) and archaeal communities (B) of inoculum anaerobic granular sludge (GS), control reactor (R1, pot ale wastewater), and co-digestion reactor (R2) after long-term operation at different stages. R1-1 represents Stage 1 of R1. (family: f_; order: o_; class: c_; p: phylum) if not identified at the genus level. 108

Fig. 6.1. The schematic layout of three UASB reactors. 115

Fig. 6.2. Methane yield in R1, R2, and R3 during the three stages of reactor operations. 121

Fig. 6.3. COD balance in R1, R2, and R3 reactors (A: stage 1; B: stage 2; C: stage 3)..... 123

Fig. 6.4. Hydrolysis efficiency of high solid-content wastewater in stage 1 of reactor operations..... 123

Fig. 6.5. Spatial sludge specific methanogenic activity (SMA) for acetate and H₂/CO₂ in three stages of reactor operations..... 124

Fig. 6.6. Relative abundance of bacterial communities at the genus level. Taxonomic names are shown for genus level or higher level (family: f_; order: o_; class: c_; p: phylum) if not identified at the genus level. The Shannon diversity is reported at the bottom of the heatmap. 127

Fig. 6.7. Relative abundance of archaeal communities at the genus level. Taxonomic names are shown for genus level or higher level (family: f_; order: o_; class: c_) if not identified at the genus level. The Shannon diversity is reported at the bottom of the heatmap..... 129

Fig. 6.8. Relative abundance of the main bacteria genera (A) and syntrophic bacteria ratio (B) of suspended sludge surrounding GAC and biofilm attached on GAC of three reactors (R1: bottom GAC-amended UASB; R2: top GAC-amended UASB; R3: bottom+top GAC-amended UASB) under three stages (Stage 1: high solid-content wastewater; Stage 2: medium solid-content wastewater; Stage 3: low solid-content wastewater). Taxonomic names are shown for genus level or higher level (family: f_; order: o_; class: c_; p: phylum) if not identified at the genus level..... 133

Fig. 6.9. Relative abundance of archaea genera (A) and Shannon index (B) of flocs surrounding GAC and biofilm attached on GAC of three reactors (R1: bottom GAC-amended UASB; R2: top GAC-amended UASB; R3: bottom+top GAC-amended UASB) under three stages (Stage 1: high solid-content wastewater; Stage 2: medium solid-content wastewater; Stage 3: low solid-content wastewater). Taxonomic names are shown for genus level or higher level (family: f_; order: o_; class: c_; p: phylum) if not identified at the genus level..... 136

Fig. 6.10. Predicated metagenome functions of flocs surrounding GAC and biofilm attached on GAC of three reactors (R1: bottom GAC-amended UASB; R2: top GAC-amended UASB; R3: bottom+top GAC-amended UASB) under three stages. Stage 1: high solid-content wastewater (A); Stage 2: medium solid-content wastewater (B); Stage 3: low solid-content wastewater (C)..... 138

Fig. 6.11. Principal component analysis (PCA) of bacteria (A) and archaea (B) community of flocs and biofilm of three reactors (R1: bottom GAC-amended UASB; R2: top GAC-amended UASB; R3: bottom+top GAC-amended UASB) under three stages (Stage 1: high solid-content wastewater; Stage 2: medium solid-content wastewater; Stage 3: low solid-content wastewater).	141
Fig. 6.12. Correlation of operational parameters with reactor performance, sludge activities, and microbial community. The color bar indicates Pearson correlation coefficient. Significance labeled (*) for $p < 0.05$, (**) for $p < 0.01$, (***) for $p < 0.001$.	144
Fig. 7.1. The top-GAC bio-balls.	152
Fig. 7.2. Reactor performances: (A) Methane yield, (B) effluent chemical oxygen demand (COD) concentrations and (C) effluent pH.	157
Fig. 7.3. Chemical oxygen demand (COD) mass balance of three reactors (R1: bottom GAC; R2: top GAC; R3: bottom+top GAC) at different organic loading rates (OLRs).	160
Fig. 7.4. Hydrolysis efficiency of three reactors at different organic loading rates (OLRs).	162
Fig. 7.5. Volatile fatty acids (VFAs) concentrations in terms of acetate, propionate, and butyrate of top layer (A) and bottom layer (B) of three reactors at different organic loading rates (OLRs).	164
Fig. 7.6. Sludge stability of top layer (A) and bottom layer (B) of three reactors at different organic loading rates (OLRs). Stage 1: OLR was 2.0 ± 0.2 g/L/d; Stage 2: OLR was 4.0 ± 0.3 g/L/d; Stage 3: OLR was 6.0 ± 0.2 g/L/d.	166
Fig. 7.7. Sludge specific methanogenic activities (SMAs) of top layer (A) and bottom layer (B) of three reactors at different organic loading rates (OLRs).	169

Fig. 7.8. Relative abundance of main bacterial (A) and archaeal (B) communities at the genus level of three reactors (R1: bottom GAC; R2: top GAC; R3: bottom+top GAC) at top and bottom sludge. 172

LIST OF TABLES

Table 3.1. Characteristics of the thickened WAS tested.	39
Table 4.1. Profiles of COD, VFA, TS and NH₄⁺-N concentrations in influent (untreated toilet wastewater) and effluent and COD_{total} removal efficiency in phases I-VII (unit: g/L, standard deviation is in brackets).....	63
Table 4.2. Profiles of Ca²⁺, PO₄³⁻-P, and pH in phases I-VII (unit: mg/L, standard deviation is in brackets).....	64
Table 5.1. Characteristics of spent caustic wastewater, pot ale wastewater, and co-digestion wastewater (S:P=1:5). The values are average ± standard deviation.	94
Table 6.1. Synthetic wastewater characteristics in the three stages of reactor operations. The values are average ± standard deviation.....	120

ABBREVIATIONS

ACP	amorphous calcium phosphate
AD	anaerobic digestion
APHA	American Public Health Association
APSD	anaerobic phased solids digester
BMP	biomethane potential
BOD	biochemical oxygen demand
C/N	carbon-to-nitrogen
CLSM	confocal laser scanning microscopy
COD	chemical oxygen demand
CSTR	continuous stirred tank reactors
DIET	direct interspecies electron transfer
EDX	energy dispersive X-ray spectroscopy
EEM	three-dimensional excitation-emission matrix
EPS	extracellular polymeric substances
FRI	fluorescence region integration
GAC	granular activated carbon
GC	gas chromatography
HRT	hydraulic retention time
IET	interspecies electron transfer
IFT	interspecies formate transfer
IHT	interspecies hydrogen transfer

KEGG	Kyoto Encyclopedia of Genes and Genomes
NCBI	National Center for Biotechnology Information
OLR	organic loading rate
PBS	phosphate-buffered saline
PCR	polymerase chain reaction
PE	polyethylene
PICRUS	Phylogenetic Investigation of Communities by Reconstruction of Unobserved States
S:P	spent caustic wastewater: pot ale wastewater volume ratio
SCOD	soluble chemical oxygen demand
SD	standard deviation
SEBAC	sequential batch anaerobic composting
SEM	scanning electron microscope
SF	self-floating
SMA	specific methanogenic activity
SRF	specific resistance to filtration
TAN	total ammonia nitrogen
TCOD	total chemical oxygen demand
TCP	tricalcium phosphate
THP	thermal hydrolysis process
TN	total nitrogen
TP	total phosphorous
TS	total solids

TSS	total suspended solids
TWAS	thickened waste activated sludge
UASB	up-flow anaerobic sludge blanket
VFA	volatile fatty acids
VS	volatile solids
VSS	volatile suspended solids
WAS	waste activated sludge
WWTP	wastewater treatment plant
XRD	X-ray diffraction

CHAPTER 1 INTRODUCTION AND RESEARCH OBJECTIVES

1.1 Background and motivations

As the industry continues to expand, the increased consumption of fossil fuels has contributed to both climate change and energy shortages. Therefore, there is an urgent need for renewable energy sources that can help reduce greenhouse gas emissions (Deng et al., 2012). Among these, bioenergy stands out due to its low emissions and affordability, playing a crucial role in meeting the growing demand for sustainable energy solutions. Methane, a renewable bioenergy source, can be produced under anaerobic conditions from various high-strength substrates, including sewage sludge, blackwater, and industrial wastewater (Li et al., 2019).

Anaerobic digestion (AD) emerges as a promising technology for harnessing renewable energy, alongside the treatment and recycling of organic wastes. The widespread adoption of AD is driven by the potential for energy recovery and the stabilization of various organic waste and wastewater, proving to be more cost-effective than conventional wastewater treatment technologies (Pasalari et al., 2021). Optimizing AD to enhance methane production from diverse high-strength wastes can help reduce reliance on non-renewable energy sources. The AD process comprises four crucial steps: hydrolysis, acidogenesis, acetogenesis, and methanogenesis (Yu et al., 2022). When any of these steps become rate-limiting, it can destabilize the AD process, leading to unsatisfactory performance. Addressing these inhibitions requires specific strategies that consider the unique characteristics of the substrates involved.

Recent advancements in anaerobic digestion technology have significantly enhanced its efficiency and economic viability. However, challenges persist. For example, when the first step - hydrolysis

- is inhibited, it can upset the balance of the entire AD process, notably through slow hydrolysis rates, resulting in longer hydraulic retention time (HRT) and a larger footprint (Mou et al., 2022b; Sun et al., 2022; Yu et al., 2022; Zhang et al., 2021b). Furthermore, the AD process can be impeded by the inefficient conversion of crucial intermediates like volatile fatty acids (VFAs), attributed to the slow syntrophic interactions in AD process. Also, methanogenesis can be inhibited by slow growth rates of anaerobes during methanogenesis and inefficient electron transfer (Yang et al., 2020; Yu et al., 2021c). Therefore, addressing these inhibitions requires specific strategies that adjust according to the specific step being limited. Innovations such as pre-treatment methods to accelerate hydrolysis, the use of anaerobic granular sludge and/or co-digestion to enhance the syntrophic interactions between four steps of AD process, and the addition of conductive materials to improve methanogenesis, have markedly improved the AD performance and system balance (Duguma et al., 2024; Wang et al., 2023). These developments have not only reduced operational costs but also enhanced the overall feasibility of waste-to-energy conversions (Dhar et al., 2017).

1.2 Research objective and approach

The primary objective of this thesis is to optimize each step of the AD process using cost-effective and efficient strategies, focusing on overcoming specific inhibitions and uncovering the microbial mechanisms crucial for enhancing energy recovery from high-strength waste and wastewater. To achieve this aim, the following objectives have been outlined:

1) Pre-treatment to accelerate hydrolysis process: investigating the impacts of calcium hypochlorite pre-treatment on the solubility and biodegradability of thickened waste activated sludge (TWAS).

The degradation of TWAS is usually limited by the slow hydrolysis rate and low biodegradable rate. This objective focused on the efficiency of pre-treating TWAS with varying concentrations of $\text{Ca}(\text{ClO})_2$ to determine the optimal dosage that minimizes volatile solids (VS) of TWAS after aerobic digestion. Firstly, the potential of $\text{Ca}(\text{ClO})_2$ as a pre-treatment method for TWAS prior to aerobic digestion was investigated. The solubilization and biodegradability of TWAS after adding different amounts of $\text{Ca}(\text{ClO})_2$ under aerobic pre-treatment conditions for 24 hours were compared to values obtained in TWAS with no $\text{Ca}(\text{ClO})_2$ addition. Following the pre-treatment process, TWAS that was not pre-treated was used as seed sludge for processing the pre-treated TWAS through 20-day aerobic digestion. The volume reduction of TWAS after aerobic digestion was examined to determine the optimal dosage of $\text{Ca}(\text{ClO})_2$ pre-treatment. Additionally, a kinetic model was applied to underscore the mechanisms by which $\text{Ca}(\text{ClO})_2$ pre-treatment enhances TWAS volume reduction.

2) Anaerobic granular sludge to improve syntrophic interactions: assessing the feasibility of anaerobic calcium phosphate granulation for blackwater treatment in continuous reactors operated under mesophilic conditions.

Hydrolysis and methanogenesis processes are both limited in anaerobic blackwater treatment due to the presence of both particulate and soluble organics. In this objective, anaerobic granular sludge was formed and then promoted hydrolysis and methanogenesis of blackwater in UASB reactor, aiming for elevated organic loading rate (OLR) treatment efficiencies. A lab-scale up-flow anaerobic sludge blanket (UASB) reactor, inoculated with anaerobic floc sludge, was operated continuously for 250 days to investigate the viability of anaerobic granulation for blackwater treatment under mesophilic conditions. Following the successful formation of granular sludge, the HRT was markedly reduced from 8 days to 0.25 days, while the OLR significantly increased from

0.4 to 16.0 g COD/L/d. This objective evaluated the energy recovery efficiency, focusing on the rate and potential of methane production. Additionally, sludge characteristics were thoroughly analyzed to understand the qualitative and quantitative aspects of the granules formed. And then, the mechanisms of the granular sludge formation were also discussed.

3) *Anaerobic co-digestion to enhance syntrophic activities: investigating the impacts of anaerobic co-digestion of pot ale wastewater and spent caustic wastewater on energy recovery in continuous UASB reactors to enhance syntrophic activities.*

Anaerobic digestion of distillery wastewater faces limitations due to the presence of particulate organics such as lignin and crude protein, and soluble organics such as VFA, which restrict both hydrolysis and methanogenesis processes. This objective explored the anaerobic co-digestion of pot ale wastewater and spent caustic wastewater using inoculated anaerobic granular sludge. Two UASB reactors, each with a working volume of 1 L, were operated under mesophilic conditions for 200 days. The reactors differed in feedstocks: one treated pot ale wastewater, while the other treated a co-substrate of pot ale and spent caustic wastewater (volume ratio 5:1, mixed for 1 hour). The organic loading rates of co-digestion reactor were incrementally increased from 3.9 g/L/d to 13.6 g/L/d. This study evaluated the energy recovery efficiency, with a focus on the methane production rate, and conducted the in-depth analysis of sludge characteristics to assess microbial communities.

4) *Conductive material to accelerate methanogenesis process: examining the effects of granular activated carbon (GAC) spatial distributions in up-flow anaerobic sludge blanket (UASB) reactors on methane production to accelerate methanogenesis process.*

Recent studies by our group have highlighted the enhanced performance of UASB reactors with self-floating GAC (by encasing GAC in plastic carriers) amendment, as compared to settled GAC, treating glucose as the carbon source (Yu et al., 2021c). This objective was to extend these findings by assessing the effectiveness of settled and floating GAC in treating wastewater with more complex characteristics.

4.1) Assessing the impacts of granular activated carbon (GAC) spatial distributions in up-flow anaerobic sludge blanket (UASB) reactors on methane production treating different solid-content wastewater.

This objective constructed UASB reactors amended with settled and self-floating GAC to increase contact between microorganisms and GAC, aiming to boost methanogenesis through the whole reactor depth. Three laboratory-scale UASB reactors, each supplemented with 25 g/L of settled, self-floating, or a combination of settled and self-floating GAC, were operated continuously under mesophilic temperature (35 °C) for 170 days. The reactors processed feedstocks with varying solid-content ratios (SCOD/ TCOD: <10 % for high, 40 %-60 % for medium, and >90 % for low solid-content) across different stages. The impacts of the spatial distributions of GAC on the UASB reactor performance were evaluated, and the mechanisms that promoted anaerobic digestion with self-floating GAC were investigated.

4.2) Evaluating the effects of granular activated carbon (GAC) spatial distributions in up-flow anaerobic sludge blanket (UASB) reactors on methane production and organic loading capacity treating high solid-content wastewater.

Addressing the challenge of anaerobic digestion of high solid-content wastewater, which is often limited by high OLRs, this objective involved the continuous operation of three lab-scale UASB

reactors at a mesophilic temperature (35 °C) for 150 days. The reactors were distinguished by their GAC placement: bottom GAC, top GAC, and bottom+top GAC, each with 25 g/L GAC. The OLRs increased stepwise, from 2.0 ± 0.2 g/L/d to 6.0 ± 0.2 g/L/d, through decreases in HRT from 7.0 days to 2.3 days. The performances of three reactors at different OLRs treating high solid-content wastewater were evaluated. Further experiments of spatial distributions of sludge stability and specific methanogenic activities (SMAs) were studied.

5) Investigating the microbial community dynamics in enhanced AD systems treating high-strength waste and wastewater to reveal the underlying mechanisms.

The microbial community structure and diversity in advanced AD systems were analyzed, providing ecological insights for these cost-efficient treatment technologies. This research evaluated the development of the methanogenic pathway through approaches of 16S rRNA gene sequencing to examine microbial communities under different treatment and operational conditions:

- i) Comparing microbial communities in pre-treated versus untreated TWAS after aerobic digestion to underscore the mechanisms by which pre-treatment accelerates the hydrolysis process.
- ii) Evaluating shifts in microbial community within anaerobic granular sludge subjected to increased OLR treating blackwater to clarify the mechanisms of the enhancement of syntrophic interactions by anaerobic granular sludge.
- iii) Investigating changes in microbial community in anaerobic co-digestion systems with increased OLR treating distillery wastewater to reveal the underlying mechanisms of improved hydrolysis and methanogenesis processes.

- iv) Assessing the distribution of microbial community in GAC-amended UASB reactors to uncover the mechanisms of enhanced methanogenesis process.
- v) Determining the impact of GAC placement and substrate solid content on the dynamics of biofilm communities to explore the mechanisms by which GAC biofilms impact overall reactor performance.
- vi) Exploring the dynamics of microbial community in GAC-amended systems under high OLR conditions treating high solid-content wastewater to understand the mechanisms of improved organic loading capacity.

The objective analyzed and compared microbial communities developing at different stages and in various reactor zones, including GAC biofilms. The dynamic shifts in microbial communities and the establishment of methanogenic pathways were correlated with performance in treating high-strength waste and wastewater.

1.3 Thesis layout

This thesis is a paper-based format, comprising a total of eight chapters, each contributing to a coherent exploration of the study's objectives. The structure of the thesis is represented in **Fig. 1.1**, providing an overview of the organization.

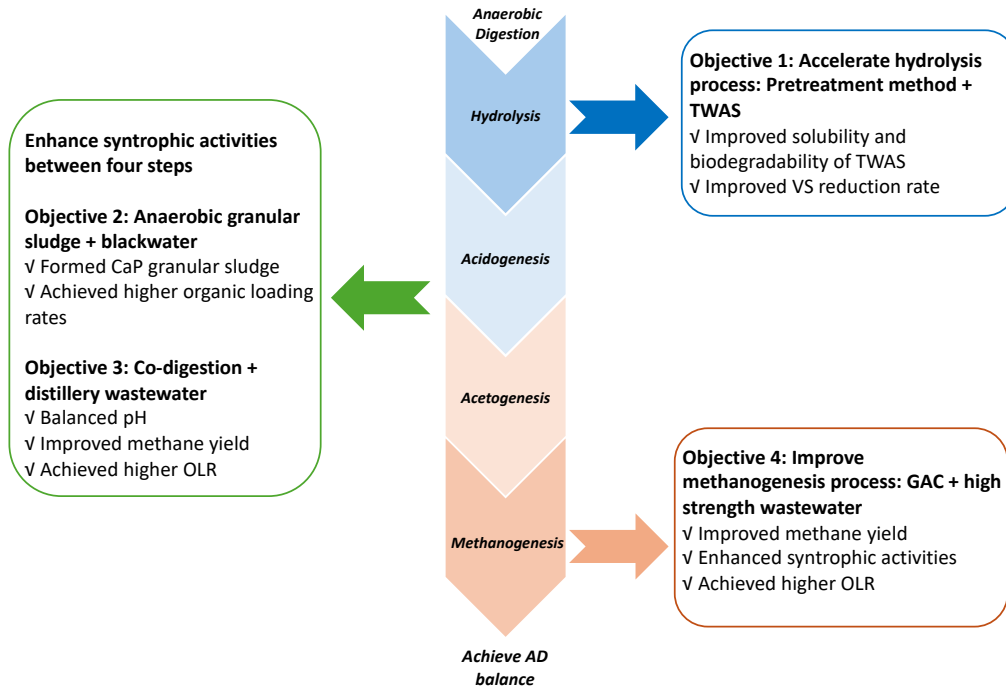


Fig. 1.1. Overview of thesis.

Chapter 1 introduces the background, problem statement, and motivation behind the research. It outlines the objectives and approaches adopted to address the research questions.

Chapter 2 reviews the AD process, the factors inhibiting the AD process, and the sources and characteristics of the targeted waste and wastewater, such as WAS, blackwater, and distillery wastewater. It summarizes existing literature on pre-treatment methods of WAS, anaerobic granular sludge, co-digestion, and DIET process, highlighting the limitations in current studies and proposing different novel and cost-efficient strategies to enhance AD process.

Chapter 3 explores the application of calcium hypochlorite as a pre-treatment strategy to accelerate the hydrolysis of TWAS. It involves laboratory experiments with TWAS, studying the effects of using calcium hypochlorite as a pre-treatment method on TWAS solubilization, volume reduction,

and microbial community dynamics after aerobic digestion. This chapter addresses objectives 1 and 5.

Chapter 4 examines the potential of anaerobic calcium phosphate granulation in continuous reactors operating under mesophilic conditions for blackwater to improve the syntrophic interactions of AD processes. Long-term operation of a lab-scale UASB reactor was conducted using anaerobic floc sludge as inoculum to study the feasibility of anaerobic granulation for blackwater treatment at mesophilic conditions. With the formation of granular sludge, the HRT decreased gradually to enhance organic loading rates. The reactor performance was evaluated. The sludge characteristics and the structure of microbial community were analyzed. This chapter is directed to objectives 2 and 5.

Chapter 5 explores the impacts of anaerobic co-digestion of pot ale wastewater and spent caustic wastewater on energy recovery in continuous UASB reactors to enhance the syntrophic activities. The effects of combining these two wastewater streams to optimize methane production and overall system stability were evaluated. The setup and maintenance of reactors operating under mesophilic conditions were described, focusing on the effects of co-digestion on organic loading rates, methane yield, and sludge activities. Analytical methods were employed to assess changes in microbial community structures and functional dynamics, crucial for optimizing the anaerobic digestion process. This chapter is directed to objectives 3 and 5.

Chapter 6 describes modified UASB reactors through the integration of bottom and/or top GAC, facilitating a semi-two-phase AD process treating different solid-content high-strength wastewater to accelerate methanogenesis process. Three UASB reactors were supplied with GAC in different locations: bottom, top, and bottom+top. The performances of three reactors treating different solid-

content wastewater were evaluated. The spatial distributions of microbial communities in the reactors with bottom GAC and top GAC were analyzed. Chapter 6 also compares microbial communities on settled and floated GAC biofilms in UASB reactors to clarify the effect of the GAC biofilms on methane production when treating different solid-content wastewater. Syntrophic microbial functions in biofilms and surrounding sludge flocs in the bottom GAC and top GAC reactors were investigated along with the structure, diversity, and correlation of the microbial communities. This chapter fulfills objectives 4.1 and 5.

Chapter 7 investigates the effects of GAC spatial distributions in UASB reactors on methane production and organic loading capacity treating high-strength wastewater. Three UASB reactors were used, as described in Chapter 6. The performances of three reactors at different OLRs treating high-strength wastewater were evaluated. Further studies on spatial distributions of sludge stability, SMAs, and microbial communities under different OLRs were analyzed. This chapter aligns with objectives 4.2 and 5.

Chapter 8 concludes a comprehensive summary of the research, highlighting key findings and principal conclusions. It also outlines recommendations for future studies in related fields.

The bibliographies from all chapters are combined and presented at the end.

CHAPTER 2 LITERATURE REVIEW

2.1 Anaerobic digestion process

The urgent shift away from fossil fuels towards green technology underscores the search for alternative methods for generating sustainable renewable energy. Anaerobic digestion has emerged as an effective wastewater treatment method that also facilitates bioenergy recovery. This process produces biogas, which can be harnessed for electricity and heat generation, highlighting its dual benefits (Chae et al., 2008). Beyond treating organic waste, AD plays a crucial role in nutrient and biogas recovery, integrating with current renewable energy technologies (Jadhav et al., 2024). For handling high-strength wastewater, high-rate anaerobic bioreactors are favored due to their dual advantages: they produce less sludge and simultaneously generate energy (Hamza et al., 2016).

AD is a complex biochemical process that operates under strictly anaerobic conditions (oxidation reduction potential (ORP) less than -200mV), where a diverse microbial consortium efficiently converts organic matter into primarily CO_2 and methane (CH_4) (Appels et al., 2008). This process is divided into four successive phases: hydrolysis, acidogenesis, acetogenesis, and methanogenesis (**Fig. 2.1**). In the hydrolysis phase, complex and insoluble organic substances including proteins, carbohydrates, and fats are decomposed into soluble molecules like amino acids, sugars, and fatty acids (Appels et al., 2008). Particularly when treating high solid-content wastes, hydrolysis often becomes the rate-limiting step due to low efficiency of fermentative bacteria (Aquino and Stuckey, 2008; Ghyyoot and Verstraete, 1997; Kumar and Samadder, 2020; Wang et al., 1999). The hydrolysis process can be accelerated by applying pre-treatment methods to the substrates, including biological, chemical, and physical pre-treatment (Yuan and Zhu, 2016). Following hydrolysis, the acidogenesis stage involves the further breakdown of these simpler compounds into

short-chain fatty acids, alongside the production of hydrogen, carbon dioxide, and other minor by-products (Appels et al., 2008). Then, during acetogenesis, these organic acids are transformed into acetic acid, hydrogen, and CO₂ (Appels et al., 2008). The final phase, methanogenesis, is characterized by the activities of two types of methanogens: one type converts acetic acid into methane and CO₂, while the other type utilizes intermediates like hydrogen, and CO₂ to form methane (Kumar and Samadder, 2020). The overall efficiency of AD, particularly in low solid-content wastewater treatment, is often constrained by the slow pace of methanogenesis, although recent findings suggest that this can be augmented through direct interspecies electron transfer between syntrophic bacteria and methanogens (Lee et al., 2016).

Recent advancements in anaerobic digestion technology have significantly enhanced its efficiency and economic viability. Innovations including pre-treatment methods, the use of anaerobic granular sludge, co-digestion of varied waste streams, and process optimization, have markedly improved the performance and cost-effectiveness of these systems (Duguma et al., 2024; Wang et al., 2023). These developments have not only reduced operational costs but also improved the overall feasibility of waste-to-energy methods (Dhar et al., 2017).

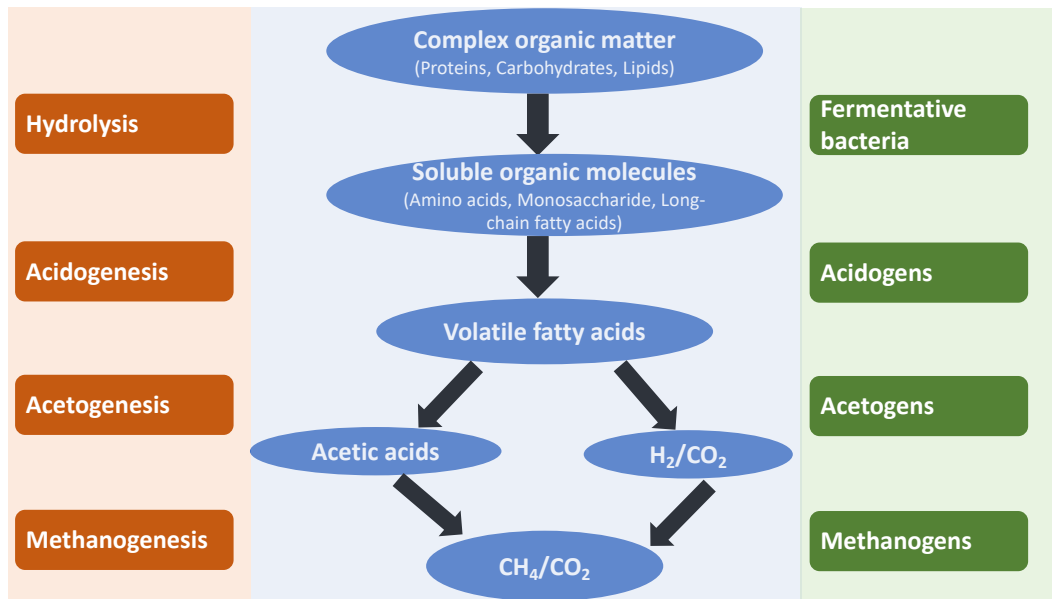


Fig. 2.1. Different stages of anaerobic digestion process for biogas generation.

2.2 The effects of operational parameters on anaerobic digestion

The significance of AD process technology in generating biogas has sparked an interest in enhancing and managing this process more effectively. The AD process is influenced by numerous factors, including the pH, organic profile of the substrate, process kinetics, and microbial diversity (Nkuna et al., 2022). The nature of the substrate, in terms of its composition or physical state, impacts the required pre-treatment and mixing within the reactor, thereby shaping the entire AD system's configuration (Nkuna et al., 2022). These aspects play crucial roles in ensuring process stability, designing the process, and achieving process efficiencies.

2.2.1 Organic loading rates

OLR is a critical factor in biogas production, potentially affecting the process either positively or negatively. While high conversion efficiencies are achievable at low OLRs, overly low rates may lead to microbial death or inactivity due to nutrient scarcity, affecting metabolic activities (Kothari

et al., 2014). Conversely, high OLRs can cause microbial inhibition and washout, degrading process performance (Nsair et al., 2020). Excessive feeding volume in AD systems can lead to rapid production of VFAs by bacteria during hydrolysis and acidogenesis processes, which can inhibit both the hydrolysis process and the activity of methanogenic archaea (Gadirli et al., 2024). Thus, maintaining an appropriate OLR is vital for ensuring the efficiency and stability of AD processes, as it directly influences microbial activity and degradation rates. Many studies have focused on challenging the OLR or finding the optimal OLR in anaerobic digestion (Gao et al., 2019b; Zhang et al., 2021a). However, the highest OLR achieved in previous studies varies based on the feedstock composition, operational temperature, and process technology. The main challenge in increasing OLR for high solid-content wastes is hydrolysis efficiency. The main challenge in increasing OLR for low solid-content wastes is the accumulation of VFA and a sharp decrease in pH, which can inhibit the methanogenesis process.

2.2.2 Feedstocks

The choice of feedstock is important in biogas production, significantly influencing AD process's efficiency and methane yield. Feedstocks vary in their characteristics, impacting biodegradability and methane production potential. Understanding these properties is essential to optimize process parameters, including temperature, pH, moisture content, and the availability of organic matters. For a substrate to be considered suitable for the AD process, it must fulfill specific criteria. Primarily, it should be rich in easily biodegradable organic matter, facilitating efficient conversion to biogas (Gadirli et al., 2024). Additionally, the substrate must contain minimal levels of inhibitory substrates such as heavy metals, pesticides, and antibiotics, which can hinder microbial activity and overall process effectiveness (Gadirli et al., 2024).

Feedstocks for anaerobic digestion can be categorized based on their moisture content into solids, slurries, and liquids (Cabrita and Santos, 2023). When considering their biodegradability, these feedstocks range from easily degradable wastewater to more complex, high-solid wastes (Cabrita and Santos, 2023). Typically, high solid-content wastes include animal manure, sludge, food wastes, energy crops, and other organic wastes are defined as high solid content wastes (Cabrita and Santos, 2023; Vavilin et al., 2003). Feedstocks such as blackwater, distillery wastewater, leachate wastewater as considered to have medium solid content (Cabrita and Santos, 2023; Gao et al., 2020). Municipal wastewater and molasses wastewater are examples of low solid-content wastewater (Mallick et al., 2010a). Liquid-based substrates are generally more manageable compared to those with a high solid content. The amount of solids in a substrate determines the mixing requirements of the system, whereas the nutritional profiles influence degradation rates and biogas production through altered interactions between the substrate and microbes (Nkuna et al., 2022).

To enhance methanogenesis and address the limitations of practical methane yield, a variety of strategies have been implemented. Understanding the specific properties of various substrates and their interactions during the AD process is essential for effectively enhancing this process. For wastes with high solid content, the high TCOD does not correlate with a high SCOD, which limits the efficiency of hydrolysis (Kumar and Samadder, 2020). Therefore, it is necessary to adapt hydrolysis enhancements to the properties and behaviors of these substrates, including the pre-treatment of substrates prior to AD (Jain et al., 2015). For low solid-content wastes with high VFA, the main challenge is that excessive VFA can cause a sudden drop in system pH and inhibit methanogenesis. Therefore, different methods need to be employed to improve methanogenesis efficiency, such as adding conductive materials to enhance DIET (Nguyen et al., 2021). For

medium solid-content wastewater, with high particulate COD and soluble COD, the hydrolysis and methanogenesis process may be both rate-limiting steps in AD. To accelerate the whole AD process, the syntrophic relationships between different microorganisms need to be improved. For example, granule structure of anaerobic granular sludge could promote syntrophic interaction by providing closer physical associations among syntrophic partners, facilitating electron transfer, and enhancing the presence of functional microorganisms (Zhang et al., 2022a).

2.3 High-strength waste and wastewater from different wastewater systems

High-strength wastewater is characterized by high biochemical oxygen demand (BOD), total suspended solids (TSS), and significant concentrations of fats, oils, grease, and additional pollutants compared to typical domestic wastewater (Paritosh and Kesharwani, 2024). Conversely, wastewater with low strength features BOD₅ values ranging from 10 to 300 mg/L, TSS between 100 and 350 mg/L, and chemical oxygen demand (COD) not exceeding 1 g/L (Turkdogan-Aydinol et al., 2011). High-strength variants, however, may demonstrate COD levels up to 1200 g/L, greatly exceeding those typical of residential wastewater (Hai et al., 2018). The discharge of untreated high-strength wastewater into freshwater ecosystems could lead to a critical reduction in dissolved oxygen levels, thereby posing a substantial risk to environmental sustainability (Lau and Trzcinski, 2022). Notable sources of high-strength wastewater include distilleries, dairy, pulp and paper, slaughterhouses, petroleum, pharmaceutical, high saline, livestock, food waste, waste activated sludge (WAS), and blackwater, among others (Lau and Trzcinski, 2022; Paritosh and Kesharwani, 2024; Zou et al., 2022).

2.3.1 Waste activated sludge (WAS) in centralized wastewater systems

Publicly operated centralized wastewater treatment systems are engineered to handle large volumes of wastewater from urban areas (Wilderer and Schreff, 2000). These systems involve complex infrastructure, including pipelines, pumps, and treatment facilities, to collect and treat wastewater away from its source (De Anda et al., 2018). Such operations, marked by their energy intensity and high costs, primarily involve mechanical, chemical, and biological processes (Fernández del Castillo et al., 2022). Aerobic treatment processes, notably activated sludge methods that necessitate mechanical aeration, are widely utilized due to their effectiveness in treating wastewater (Lee and Welander, 1996). These methods are not only critical to the treatment process but also contribute significantly to operational costs, with the generation and handling of sludge alone accounting for 45-75% of the operational costs of a conventional treatment plant (Rosso et al., 2008). Additionally, the disposal of WAS presents a substantial financial burden, representing up to 50% of wastewater treatment plants (WWTPs) operating costs (Muga and Mihelcic, 2008). In WWTPs, primary and secondary sludge are often merged and condensed into thickened waste activated sludge (TWAS) for additional treatment steps (Appels et al., 2008).

WAS, a semi-solid by-product of the wastewater treatment process, is rich in nutrients but also contains harmful pathogens, heavy metals, and odorous compounds, posing significant environmental and health risks if not managed properly (Kavitha et al., 2013). Its composition is dual phased: a particulate phase comprising organic and inorganic matter, and a watery phase containing dissolved substances like carbohydrates, fatty acids, and salts (Godvin Sharmila et al., 2022). The presence of non-readily biodegradable compounds further complicates the reuse of sludge without pre-treatment (Godvin Sharmila et al., 2022). Given its high biodegradability and the potential for environmental contamination, sludge demands thorough treatment to reduce its

volume, stabilize its organic content, and ensure it meets regulatory standards for disposal (Chon et al., 2011).

The necessary WAS treatment processes in WWTPs involve several steps: reducing the water content to decrease volume, transforming putrescible matter into more stable forms, and conditioning the final residue to comply with disposal regulations (Appels et al., 2008; Dewil et al., 2007; Van de Velden et al., 2008). Despite various treatment strategies explored, including sanitary landfills, incineration, and composting, each method comes with its challenges (Liang et al., 2021). Sanitary landfills, for example, are cost-effective but risk groundwater contamination (Park et al., 2012). Incineration, while extensively studied, requires drying the sludge beforehand, which is energy-intensive and costly, and may release pollutants like dust, dioxins, and acid gases into the atmosphere (Hong et al., 2005).

The composition of dried WAS frequently contains over 45% organic matter, with nitrogen and phosphorous making up about 3-4% and 1-10% of the WAS's dry weight, respectively (He et al., 2021; Liang et al., 2021). Therefore, WAS is valued as a biomass resource, highlighting its potential for sustainable treatment and disposal strategies rather than traditional disposal methods (Ambaye et al., 2020; Luo et al., 2020). The pursuit of sludge minimization strategies and the integration of WAS management with renewable energy generation are considered forward-thinking solutions for WAS treatment (Ambaye et al., 2020). These strategies not only aim to reduce operating costs but also support the WWTP's shift towards carbon-neutral operations.

2.3.2 Blackwater in decentralized wastewater systems

Blackwater, originating from decentralized wastewater systems, is primarily composed of feces, urine, flush water, and toilet paper (Chiang et al., 2023). These systems, by treating wastewater

on-site or near its generation point, offer significant advantages such as reduced transport and operational costs (De Anda et al., 2018). This efficiency, coupled with streamlined collection and treatment processes, highlights the effectiveness of decentralized approaches (Capodaglio et al., 2017). An additional benefit is the potential for on-site reuse of treated wastewater in applications such as cultivation, irrigation, and toilet flushing (Capodaglio et al., 2017; Singh et al., 2014). Particularly in rural communities, where large-scale collection infrastructures are economically impractical, decentralized systems present a viable solution (Fernández del Castillo et al., 2022).

Blackwater presents a significant environmental challenge due to its high pollution load, primarily from human excreta (Chiang et al., 2023). Its characteristics vary widely, influenced by factors such as age, gender, health, income, geographic location, and sociocultural background (Rose et al., 2015). This variability, coupled with a range of collection and storage systems, complicates the assessment of blackwater's typical properties (Welling et al., 2020). Blackwater classification depends on the toilet technology used: conventional flush toilets (using 9-12 L per flush), dual-flush toilets (3/6 L per flush), and low-flush systems like vacuum toilets (0.5-2 L per flush) (Noutsopoulos et al., 2018).

Blackwater consistently exhibits high concentrations of solid organics and ammonia (Wen et al., 2024). On average, the suspended COD comprises 62-72% of the TCOD, and the total ammonia nitrogen (TAN) accounts for 54-62% of the total nitrogen (TN) (Wen et al., 2024). The role of toilet paper is significant, contributing substantially to TCOD and TSS (Friedler et al., 1996). Specifically, flushing toilet paper can increase TCOD and TSS loads by 7 and 10 %, respectively (Almeida et al., 1999; Friedler et al., 1996). Despite representing only about 30% of domestic sewage by volume, blackwater contributes disproportionately to the pollution load - around 60% of organic matter, 92% of total nitrogen, 75% of phosphorous, and 76% of potassium

(Noutsopoulos et al., 2018). This imbalance underscores the potential efficiency gains in energy and nutrient recovery from blackwater.

Traditionally, blackwater has been managed through a combined discharge-collection-treatment system, which imposes significant burdens on WWTPs by increasing energy use, operational costs, and resource wastage, while depleting essential nutrients (Chiang et al., 2023). Adopting source separation for wastewater in areas undergoing renovation or development can mitigate these challenges, enhancing resource recovery (Chiang et al., 2023). Notably, blackwater separation systems can recover 4 times more phosphorus and over 30 times more nitrogen than the centralized system in rural areas (Malila et al., 2019). Therefore, the rich concentration of organic and inorganic substances in blackwater not only facilitates biogas production but also enhances the recovery of critical nutrients like nitrogen and phosphorous (de Graaff et al., 2010; Gao et al., 2019b). This advantage becomes particularly pronounced with anaerobic digestion, which maximizes the potential for energy production and nutrient recovery from blackwater's unique properties.

2.3.3 Distillery wastewater

The distillery manufacturing processes consist of four primary steps: mashing, fermentation, first distillation, and second distillation (**Fig.2.2**). These stages generate substantial amounts of high-strength co-products, such as pot ale wastewater from the first distillation process (spirit still) and spent caustic wastewater from second distillation process (wash still).

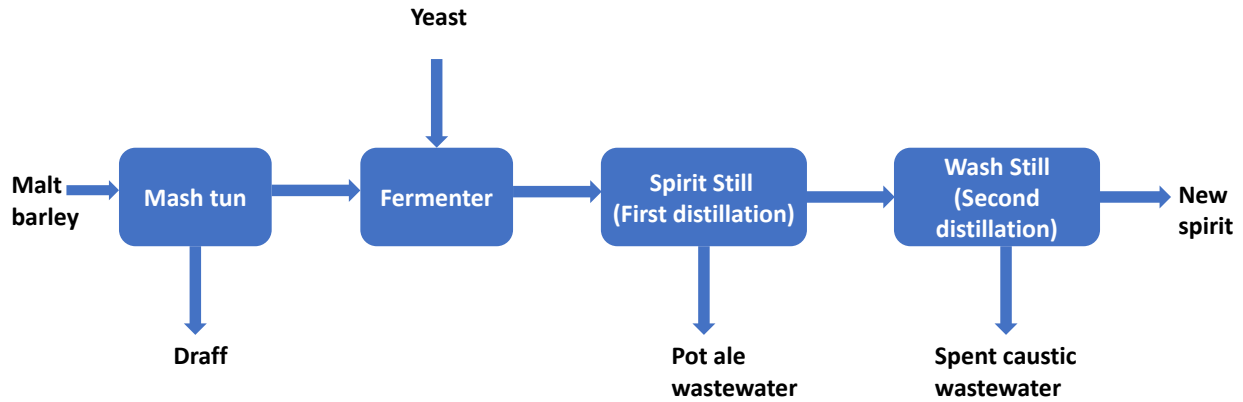


Fig. 2.2. Schematic showing a malt whisky distillation process, traditional by-products (draff, pot ale, and spent caustic wastewater).

Produced in large quantities each year, pot ale wastewater poses significant environmental challenges due to its high COD, phosphorus, and ammonia (Graham et al., 2012). Traditional disposal or treatment options for pot ale include release into the ocean, application on land as fertilizer, concentration through evaporation into pot ale syrup, and processing via anaerobic digestion (Dionisi et al., 2014). However, these methods present various challenges. Ocean disposal is limited to distilleries near coastlines. Using pot ale as fertilizer on land can be problematic due to the harmful effects of its pollutants (Dionisi et al., 2014). Moreover, other explored treatment techniques for distillery wastewater, such as coagulation-flocculation, adsorption, and oxidation methods including Fenton's oxidation, ozonation, and electrochemical oxidation, along with membrane processes, have proven less than ideal due to their substantial chemical use and high operational cost (Mohana et al., 2009; Satyawali and Balakrishnan, 2008).

Research into pot ale treatment has increasingly concentrated on biological methods, focusing on anaerobic digestion alone or in combination with aerobic treatment stages (Goodwin et al., 2001; Mallick et al., 2010a; Strong and Burgess, 2008). Anaerobic digestion has been identified as a

potentially promising treatment process for pot ale wastewater to produce biogas due to the high COD (Barrena et al., 2018; Gunes et al., 2021a; Gunes et al., 2021b; Mallick et al., 2010b). However, the distillery industry has been limited in adopting this technology. This is partly due to challenges posed by particulate organics, low pH, yeast cells, lignin, and proteins, which can make stable long-term digestion difficult to achieve (Barrena et al., 2018). To address these issues, various pre-treatment methods have been employed before AD process, including enzymatic pre-treatment, pH amendment coupled with solid-liquid phase separation, deproteination pre-treatment, and thermal pre-treatment (Barrena et al., 2018; Dionisi et al., 2014; Gunes et al., 2019; Mallick et al., 2010a).

Spent caustic wastewater is an alkaline waste with characteristics such as a high pH level (over 13), elevated salinity (above 4%), and substantial pollutant content, with COD ranging from 10 to 20 g/L. Various treatment strategies for this type of wastewater are broadly divided into five principal categories: thermal processes, chemical oxidation, biological treatments, membrane separation technologies, and electrochemical methods (Alipour and Azari, 2020). In the biological treatment category, specific microorganisms, including *Aspergillus* sp. *SMHS-3* and *Thiobacillus RAI01*, were employed to degrade organic pollutants via biochemical oxidation (de Graaff et al., 2011; Gholipour et al., 2018). However, these biological processes often require substantial dilution and neutralization steps to adjust pH and total dissolved solids (TDS) to levels suitable for the effective functioning of the microorganisms (Gholipour et al., 2018).

2.4 Pre-treatment methods to enhance hydrolysis of WAS

Various digestion methods, including CSTR, sequential batch anaerobic composting, UASB, have been employed to treat high solid-content wastewater (Jain et al., 2015; Tyagi et al., 2018). To

optimize the fermentation and methanogenesis process individually, two-step or multi-step anaerobic digestion has been utilized (Abu-Dahrieh et al., 2011; Li et al., 2019). However, the effectiveness of these reactors in treating high solid-content wastewater can be hindered by the slow biodegradation of certain components and waste's heterogeneous nature (Gagliano et al., 2020). Hydrolysis of WAS presents a significant bottleneck in digestion process, leading to prolonged sludge retention times and diminished organic degradation (Tiehm et al., 2001; Weemaes and Verstraete, 1998). This challenge is compounded by the inherent recalcitrance of sludge's cell walls and EPS, which are crucial but difficult-to-degrade components of the organic fraction (Xu et al., 2020). The semi-rigid structure of microbial cell envelopes, composed of glycan strands cross-linked by peptide chains, provides resistance to biodegradation, thus limiting the efficiency of hydrolysis (Appels et al., 2008; Xu et al., 2020). To address these challenges, a variety of pre-treatment methods have been developed, aiming to disrupt the cell walls and solubilize EPS, thereby facilitating the release of readily available organic material for further degradation by acidogenic microorganisms (Appels et al., 2008).

Pre-treatment strategies include physical, chemical, and biological techniques, each targeting different aspects of sludge to improve biogas production and AD efficiency. Physical methods such as thermal, ultrasound, and electric pulse treatments effectively disrupt sludge structures, enhancing the solubilization of organic matter (Tiehm et al., 2001). Chemical pre-treatments, including alkaline and Fenton reactions, further aid in breaking down EPS and facilitating organic matter hydrolysis (Xu et al., 2020). Meanwhile, biological pre-treatments, notably aerobic digestion and enzyme addition, specifically target and break down complex biopolymers, improving the biodegradability of the sludge (Kavitha et al., 2013; Xu et al., 2020). These pre-

treatments convert slowly degradable, particulate organic material into low molecular weight, readily biodegradable compounds, effectively bypassing the rate-limiting hydrolysis stage.

Recent studies have explored oxidative pre-treatment technologies for WAS destruction, such as ozonation and peroxidation, using hydroxyl radicals' strong oxidative potential to degrade sludge without producing hazardous by-products (Appels et al., 2008; Chen et al., 2016). Some studies explored alternative oxidants that offer increased biogas production and require less severe reaction conditions (Erkan, 2019). Chlorination, a cost-effective oxidation method widely used in WWTPs for tertiary treatment, employs chlorite or chlorite-based compounds to eliminate pathogens (Luo et al., 2020). Hypochlorite pre-treatment involving the dissolution of hypochlorite salt in water, generates hypochlorite acid, which decomposes into highly oxidative species such as OCl^- , Cl^- , and $\cdot\text{OH}$ (Yu et al., 2022). The strong oxidative abilities of the $\cdot\text{OH}$ and OCl^- generated in this process contribute significantly to pollutants' decomposition (Yu et al., 2022; Yu et al., 2021d). This process efficiently breaks down EPS, promotes cell lysis, and improves WAS dewaterability.

Although these pre-treatment methods show potential in enhancing solubilization and hydrolysis, thus improving the digestion process, economic considerations, often limit the broader application of these pre-treatments to laboratory-scale investigations. Despite this, the accumulated evidence highlights the indispensable role of pre-treatment in addressing the hydrolysis bottleneck in digestion processes, underscoring the necessity for ongoing research and development to render these technologies more economically feasible for large-scale applications.

2.5 Blackwater anaerobic digestion

AD is considered a viable option for treating blackwater due to its benefits in terms of sanitation, energy recovery, and nutrient preservation (Chen et al., 2008). Nonetheless, the effectiveness and stability of AD processes for blackwater treatment frequently encounter significant obstacles (Wen et al., 2024). The presence of inhibitory compounds such as free ammonia, sulfides, and pharmaceuticals in blackwater can interfere with the AD process, especially by disrupting the cooperative activities between bacteria and methanogens (Martins et al., 2018). The hydrolysis step, crucial for methane production from relatively recalcitrant substrates, is often hindered by solid materials like toilet paper and undigested plant matter found in blackwater (Yu et al., 2020; Zeeman and Sanders, 2001). Moreover, the methanogenic organisms involved in AD are particularly sensitive to environmental fluctuations and toxic substances, which exacerbates the instability of the process, particularly when dealing with high concentrations of solid organics and ammonia in blackwater.

Strategies aimed at improving methane recovery efficiency include appropriate pre-treatment methods, co-digestion with high carbon content wastes, and enrichment of methanogens (Wen et al., 2024). However, previous studies have demonstrated limited success, with achieved OLR remaining low, necessitating long HRT and bulky digesters (Gao et al., 2019b; Wen et al., 2024). Increasing OLR to enhance efficiency is hindered by blackwater's high solid organic content. Pre-treatments focusing on enhancing blackwater hydrolysis, such as mechanical, thermal, and micro-aeration methods, have been investigated (Wen et al., 2024; Yu et al., 2020). However, these pre-treatment methods often require high operation costs and energy input. Among the microorganisms involved in AD, methanogens are particularly vulnerable. The presence of inhibitory substances, such as free ammonia and sulfides, in blackwater commonly inhibits methanogens, thereby also

making the methanogenesis process a rate-limiting step in blackwater AD process (Wang et al., 2016; Yenigün and Demirel, 2013). Enriching methanogenesis process through co-digestion with food waste has shown promise in enhancing blackwater treatment efficiency by boosting methanogenic activities (Wen et al., 2024). The low carbon-to-nitrogen (C/N) ratio inherent in blackwater mono-digestion leads to ammonia toxicity and process instability, highlighting the importance of co-digestion with high-carbon-content wastes to optimize the substrate C/N ratio and increase biogas yields (Wen et al., 2024).

The use of anaerobic granular sludge in wastewater treatment is highly efficient and well-established. Anaerobic granular sludge is characterized by diverse microorganisms that congregate and form granules (Faria et al., 2019). These dense microbial clusters have a high sedimentation velocity, which makes them resistant to washout even under high hydraulic loads (Lim and Kim, 2014). Furthermore, anaerobic granular sludge consists of diverse microorganisms, capable of degrading complex organics in wastewater (Tassew et al., 2019). For high solid-content wastewater, hydrolysis process often becomes the limiting factor. This limitation is primarily due to the diffusion-controlled interactions between substrate particles and hydrolytic enzymes (Tassew et al., 2019). Since most extracellular enzymes are either bound to or maintained within bacterial structures, the hydrolysis rate is inherently linked to the density of active bacterial populations. Anaerobic granular sludge can enhance the hydrolysis stage by promoting the aggregation of microorganisms into compact clusters that settle effectively (Subramanyam, 2013; Tassew et al., 2019). Research indicates that bacteria on the surface of granules utilize extracellular polymeric substances to capture and digest feed particles (Tassew et al., 2019). Also, the granular structure of the sludge could create different micro-environments within the granule, which are conducive to different types of microorganisms involved in each step of the AD process. This

distinct layered community structure formed within these granules plays a critical role in fostering syntrophic relationships among bacteria, enhancing the overall efficiency of the AD process (Faria et al., 2019; Van Lier et al., 2016). The proximity provided by the granule structure enhances syntrophic interactions, facilitates electron transfer, and fosters functional microorganisms (Zhang et al., 2022a).

Although it was traditionally thought that blackwater conditions were unsuitable for forming anaerobic granular sludge due to the need for high up-flow velocities and low solids content (Faria et al., 2019). However, recent studies have shown that anaerobic granular sludge can form in UASB systems treating blackwater at low temperature (25 °C) after extensive operational periods (over 500 days), even under low up-flow velocities (< 0.1 m/h), allowing for the retention and proliferation of methanogens (Tervahauta et al., 2014a). Therefore, utilizing anaerobic granular sludge for blackwater treatment holds promise for efficient and sustainable wastewater treatment, as it enhances syntrophic interactions between bacteria for hydrolysis and archaea for methanogenesis, as well as facilitating nutrient recovery.

2.6 Anaerobic co-digestion

The production of biogas through the anaerobic digestion of various organic materials such as food waste, agricultural residues, landfill waste, and sewage sludge, has gained attention (Awasthi et al., 2018; Duguma et al., 2024; Phayungphan et al., 2020). However, the reliance on a single substrate often results in limited biogas yield due to the insufficient essential trace elements, nutrients and microbial communities' quality of one substrate (Duguma et al., 2024; Velmurugan et al., 2010). To address these limitations, recent studies have focused on the anaerobic co-digestion of multiple substrates (Evidente et al., 2021; Matheri et al., 2017; Velmurugan et al.,

2010). This approach not only enhances biogas production but also ensures economic sustainability. By utilizing substrates with complementary characteristics, co-digestion facilitates the sharing of treatment facilities, which reduces both initial investment and operational costs (Bamba et al., 2021). Additionally, it provides a buffer against variations in waste composition, dilutes toxic compounds, improves pH buffering capacity, and achieves a more nutrient balance, offering substantial improvements in both energy production and wastewater management practices (Bamba et al., 2021; Duguma et al., 2024; Ripoll et al., 2020).

Pot ale wastewater, a by-product of the distillery spirit still industry, varies in composition based on factors such as fermentation processing, sugarcane varieties, nutrient usage, and other environmental factors (Mallick et al., 2010a; Mallick et al., 2010b). It is rich in biodegradable volatile solids, typically constituting over 80% of its mass, making it a suitable candidate for AD processes. Nevertheless, the presence of hydrophobic lignin, non-degradable fibrous materials, and yeast hinders microbial activities, thus slowing the hydrolysis process. Various biological and biochemical pre-treatment methods have been employed to enhance hydrolysis of AD without the need for costly equipment (Goodwin and Stuart, 1994; Gunes et al., 2019). Additionally, the low pH of pot ale wastewater can restrict the methanogenesis process with VFA accumulations. Among the treatment for pot ale wastewater, AD is a cost-effective solution with numerous environmental benefits, including the production of renewable energy and a reduction in greenhouse gas emissions (Gunes et al., 2019). However, its high nitrogen content and low C/N ratio limit biogas production, as high protein leads to ammonia accumulation, which inhibits the microbial activities of AD process. Previous studies have demonstrated that co-digestion with other organic waste can optimize the C/N ratio and pH, thereby enhancing methane yield (Gunes et al., 2021b; Ripoll et al., 2022).

Spent caustic wastewater emerges from a variety of sources including the wash still unit, molasses, and the cleaning chemicals used on equipment and tanks (Li et al., 2021a). The environmental challenge posed by this wastewater stems from its extremely alkaline pH, high organic content, and the presence of recalcitrant pollutants such as polyphenols and caustic soda. Distilleries are compelled to manage this wastewater effectively to adhere to environmental regulations (Alipour and Azari, 2020; de Graaff et al., 2011; Gholipour et al., 2018). Given its high pH, high COD and high salinity, and at the same time, pot ale wastewater requires high pH and liquid waste for digestion. Therefore, spent caustic wastewater can be used as the co-substrate since it also has potential in chemical pre-treatment of refractory organics to enhance biogas production, as well as dilute toxic or inhibitory compounds. This integration not only facilitates the handling of wastewater and avoids disposal issues but also improves the economic viability of the treatment process. Furthermore, using spent caustic wastewater as the co-substrate enhances the C/N ratios of pot ale substrate. This integration offers a straightforward enhancement to biomethane production in distilleries, circumventing the need for more costly and complex pre-treatment strategies.

2.7 Direct interspecies electron transfer (DIET)

The stability and efficiency of AD processes are often reliant on the syntrophic relationships among microorganisms, where interspecies electron transfer (IET) is essential for the metabolic cooperation needed to oxidize organic compounds and reduce CO₂ to CH₄ (**Fig. 2.3A**) (Batstone et al., 2006). Electrons are conveyed between microorganisms via soluble electron shuttles such as H₂ and formate, known as interspecies hydrogen transfer (IHT) and interspecies formate transfer (IFT) (Zhang et al., 2023). However, the relatively slow and indirect nature of electron transfer via shuttles like H₂ and formate hinders efficiency due to diffusion limitations and large intercellular

distances (Li et al., 2021b). Moreover, the accumulation of VFAs from thermodynamically unfavorable propionate or butyrate degradation in the presence of high H₂/formate concentrations inhibits methane production and decreases AD efficiency, suggesting that IET via H₂/formate restricts methanogenesis (Barua and Dhar, 2017).

The discovery of DIET has expanded our understanding of electron flux options among microorganisms, offering a potentially more efficient mechanism for interspecies electron exchange under anaerobic conditions compared to traditional IET via H₂/formate (Liu et al., 2012). DIET, which does not rely on H₂ as an electron carrier, overcomes thermodynamic limitations under high hydrogen partial pressure (Baek et al., 2018; Chen et al., 2022). Mathematical models have shown DIET's superiority over IHT, with an electron transfer rate approximately 8.57 times higher (Storck et al., 2016). DIET relies on direct cell-to-cell electron exchange facilitated by electrically conductive pili, membrane-bound electron transport proteins, or conductive materials, such as biochar, granular activated carbon, carbon cloth, and graphite rod (Barua and Dhar, 2017; Park et al., 2018) (**Fig. 2.3**).

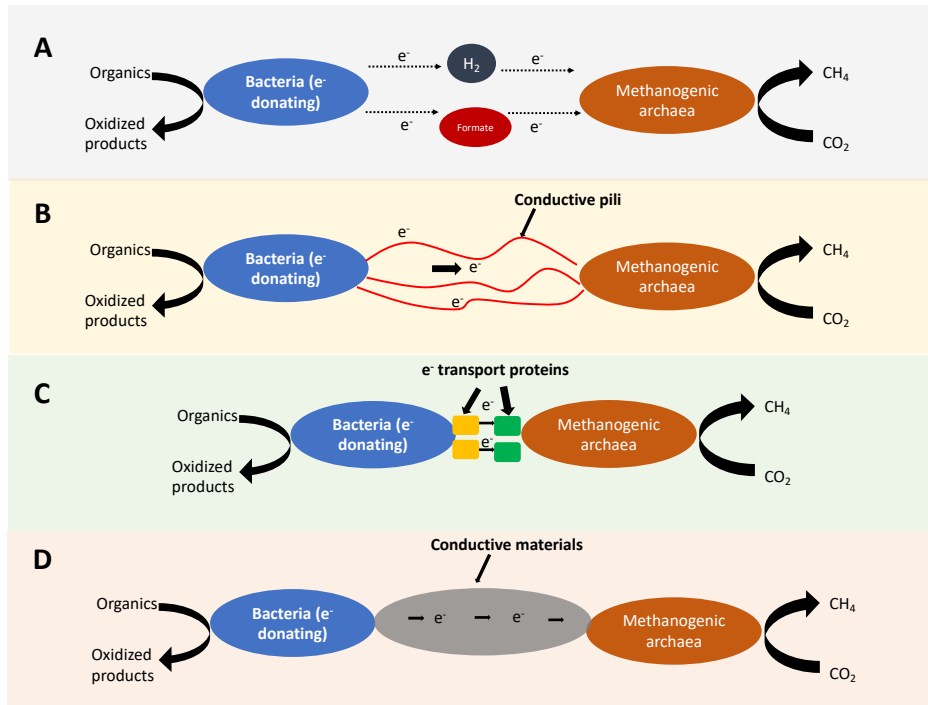


Fig. 2.3. Schematic diagram of IET (A) and DIET (B: DIET via conductive pili; C: DIET via membrane-bound electron transport proteins; D: DIET via abiotic conductive materials.) between organics-oxidizing bacteria and methanogenic archaea. This figure is a modification of a schematic presented in a previous paper (Park et al., 2018).

Amending conductive materials to stimulate DIET enhances the efficiency of AD across various substrates and operating conditions (Chen et al., 2022; Luo et al., 2015; Wang et al., 2020a; Yin and Wu, 2019). Particularly, GAC has been extensively employed for this purpose due to its accessibility, simplicity in reactor setup, and advantageous properties typical of carbon-based materials. These include a larger particle size, a compact outer surface, robust adsorption capacity, high mechanical durability, and significant chemical stability (Liu et al., 2012; Zhang et al., 2023). Previous studies have shown that methane yield significantly increases with GAC addition, ranging from 1.8 to 18 times compared to controls without GAC (Dang et al., 2016; Dang et al., 2017).

The amendment of GAC in AD processes could improve overall efficiency. GAC accelerates hydrolysis rate, providing more substrates for subsequent stages and promoting the growth of syntrophic microorganisms capable of DIET, thus enhancing electron transfer and organic matter degradation (Peng et al., 2018; Yang et al., 2017). In addition to its effects on pH regulation and VFAs, GAC supplementation has the potential to facilitate direct electron exchange, enhancing the bioconversion of VFAs into methane and consequently increasing methane production (Capson-Tojo et al., 2018; Zhang et al., 2023). Furthermore, research on the effects of GAC on methane yield and DIET processes, considering varying inoculum concentrations and compositions, has consistently shown that GAC addition enhances methane production. This enhancement is often linked to the selective enrichment of DIET-associated bacteria and archaea on the surfaces of GAC (Kang et al., 2019; Kang et al., 2021). Additionally, GAC has been observed to improve microbial resilience against high OLRs and to create a more conductive environment for microbial communities (Zhang et al., 2023).

The increase in methane production in AD systems with GAC is largely due to its role in facilitating DIET, enhancing reaction stability, and providing colonization sites for crucial microorganisms (Zhang et al., 2023). These findings underscore the significant potential of GAC supplementation in optimizing AD processes and boosting bioenergy production. However, the settling of GAC at the bottom of reactors due to its high-density limits contact between sludge and GAC (Yu et al., 2021c). Recent research into novel reactor configurations, such as self-floating GAC in UASB reactors, has shown promising results, achieving substantially higher methane production compared to conventional settled GAC-amended UASB reactors (Yu et al., 2021c). Hence, further strategies, including reactor configuration adjustments, hold promise for enhancing the efficiency of GAC-amended AD systems.

2.8 Research gaps

Anaerobic digestion has emerged as a cost-effective and environmentally sustainable technology for high-strength waste and wastewater, and simultaneously recovery energy. However, the effectiveness of AD aligns with the balance of its four main steps. Challenges in any of these steps can impede the overall process, requiring the need for specific strategies that enhance each step according to the specific properties of the waste being processed. High-strength waste and wastewater, such as waste activated sludge, blackwater, and distillery wastewater, are suitable for energy recovery by biological treatment. However, these substrates can inhibit different steps of the AD process, potentially leading to unsatisfactory performance. Therefore, there is a critical need to develop innovative approaches to overcome the limitations imposed by the inherent characteristics of the substrates and ensure each step of the AD process is effectively balanced.

For the first step of AD process - hydrolysis, substrates containing high-strength, refractory waste like WAS usually experience rate limiting conditions. To address this, a variety of pre-treatment techniques to accelerate hydrolysis steps has been investigated, including chemical, physical, and biological methods designed to pre-hydrolyze substrates. These methods can improve the biodegradability and the solubility of complex organic materials, thus enhancing overall AD efficiency (Yu et al., 2020). However, despite their effectiveness, these techniques often come with high energy requirements and operational costs. Consequently, there is a need for more cost-effective and energy-efficient solutions to optimize AD processes for such challenging wastes. Recent studies suggest that oxidative pre-treatment methods, such as chemical oxidation, can enhance the hydrolysis efficiency in AD by increasing hydrolysis rates and improving the solubility and biodegradability of recalcitrant wastes (Gautam et al., 2019; Yu et al., 2022).

For the syntrophic interactions of AD process, substrates with challenges such as high VFA, high solid content, and high solubility often require effective syntrophic activities to improve both hydrolysis and methanogenesis processes. Employing anaerobic granular sludge in wastewater treatment is a highly efficient and well-established approach (Zhang et al., 2022a). Anaerobic granular sludge comprises diverse microorganisms capable of breaking down complex organics in wastewater (Tassew et al., 2019). It has been observed that the granular structure fosters syntrophic interactions by providing proximity to syntrophic partners, enhancing electron transfer, and enriching functional microbes (Zhang et al., 2022a). Therefore, anaerobic granular sludge is a promising option for efficient and sustainable treatment of high-strength wastewater, potentially enhancing hydrolysis rates and methanogenesis process. Moreover, anaerobic co-digestion also plays a critical role as it provides opportunities to reduce the inhibition and enhance syntrophic activities of AD process (Duguma et al., 2024). For example, in the distillery industry, challenges posed by particulate organics, extreme pH, high VFAs, and other inhibitory compounds have limited AD adoption (Sillero et al., 2024). Therefore, there is a need to explore co-digestion methods to optimize the anaerobic treatment of distillery wastewater.

At the final step of AD process - methanogenesis, substrates with high soluble organics often face inhibition due to inefficient electron transfer from bacteria to archaea. Conductive materials, such as biochar, carbon nanotubes, iron-based oxide, granular activated carbon (GAC), powdered activated carbon, and magnetite, have been identified as electron conduits, promoting direct interspecies electron transfer (DIET) and, ultimately, methane production (Barua and Dhar, 2017; Park et al., 2018). Moreover, to further optimize the AD process, alternative digestion techniques, such as two-step or multi-step anaerobic digestion, have been used to optimize the fermentation and methanogenesis processes separately (Jain et al., 2015). However, the widespread industrial

adoption of two-stage AD system is hindered by economic considerations related to the construction and maintenance of a second digester (Rajendran et al., 2020). Therefore, innovative reactor configurations that facilitate phase separation within a single reactor hold economic appeal but have yet to be thoroughly explored and demonstrated.

**CHAPTER 3 CALCIUM HYPOCHLORITE PRE-TREATMENT
ENHANCES THICKENED WASTE-ACTIVATED SLUDGE
DEGRADATION DURING AEROBIC DIGESTION**

A version of this chapter has been published in Journal of Environmental Engineering.¹

¹ Mou, A., Yu, N., Zhang, L., Sun, H., Liu, Y. 2022. Calcium hypochlorite pretreatment enhances waste-activated sludge degradation during aerobic digestion. Journal of Environmental Engineering, 148(4), 04022002.

3.1 Introduction

Large amounts of sludge are produced in wastewater treatment plants (WWTPs). Treatment of sludge from sewage and industrial wastewater can account for 35-60% of a WWTP's operation costs (Appels et al., 2008). Waste activated sludge (WAS) can be treated before disposal (Zhang et al., 2020b). WAS digestion (either anaerobic or aerobic digestion) is the key technology used in WWTPs for WAS management. Anaerobic digestion of WAS recovers bioenergy in the form of biomethane, but requires large reactor footprints, due to the slow hydrolysis and methanogenesis rates during the anaerobic treatment. In comparison, aerobic digestion process is flexible and requires small reactor volumes, hence is widely used for sludge stabilization and volume reduction in small-scale WWTPs (Duan et al., 2012; Kavitha et al., 2016; Wang and Yuan, 2015).

As the presence of extracellular polymeric substances (EPS) and cell walls in sludge limits degradation and hydrolysis, pre-treatment methods (Wang et al., 2018b; Yuan et al., 2016) using chemical (oxidative; acid, alkaline hydrolysis) (Merrylin et al., 2014; Song et al., 2010a; Wang et al., 2018a; Wang and Yuan, 2015; Wu et al., 2018), physical (thermal, ultrasound) (Burger and Parker, 2013; Gonzalez et al., 2018; Kennedy et al., 2007; Layden et al., 2007) biological (bacterial, enzyme hydrolysis) (Burgess and Pletschke, 2008; Gonzalez et al., 2018; Ushani et al., 2017), and combinations (Jin, 2018; Kavitha et al., 2016; Kavitha et al., 2013; Tyagi and Lo, 2012) are employed. Although these aforesaid pre-treatment methods can be quite effective, they are expensive and are associated with large chemical consumptions, high energy requirements, and complex implementation methods (Wu et al., 2018; Zhu et al., 2018).

Recent studies reported that hypochlorite could cause cell lysis and EPS disintegration, releasing protein and polysaccharide into the soluble media (Erkan, 2019); the active chlorine species are

HClO and OCl⁻ (Equations (3-1) and (3-2)). Cell lysis and the disintegration of EPS release orthophosphate (PO₄³⁻), protein, and polysaccharide into the soluble medium (Erkan, 2019).



Several studies examined the role of hypochlorite pre-treatment for anaerobic digestion (Luo et al., 2020; Yuan et al., 2016; Zhang et al., 2020b). However, no information is available on the usage of Ca(ClO)₂ to treat WAS in aerobic digestion process. This study pretreated WAS with different dosages of Ca(ClO)₂ to identify the optimal dose for reducing WAS VS during aerobic digestion. A kinetic model was used to determine why WAS degradation was enhanced with Ca(ClO)₂ pre-treatment. The microbial community after aerobic digestion was also assessed to reveal the impacts and mechanisms of Ca(ClO)₂ pre-treatment on WAS.

3.2 Materials and methods

3.2.1 Sludge source

Thickened WAS (TWAS) was collected after the thickening process of secondary sedimentation tank sludge from a full-scale WWTP in Alberta, Canada, and was used within 48 hours. Characteristics of thickened WAS are shown in **Table 3.1**.

Table 3.1. Characteristics of the thickened WAS tested.

Parameters	Unit	Quantity
pH		6.3
TS	g L ⁻¹	48.0
VS	g L ⁻¹	33.0
VS/TS		0.69
Total chemical oxygen demand (TCOD)	g L ⁻¹	45.0
Soluble chemical oxygen demand (SCOD)	g L ⁻¹	1.3
Total phosphorous (TP)	mg P L ⁻¹	1385
Soluble phosphate	mg P L ⁻¹	255
Soluble calcium	mg Ca L ⁻¹	285
Soluble ammonia	mg N L ⁻¹	615

3.2.2 TWAS pre-treatment with Ca(ClO)₂

Five reactors (P1, P2, P3, P4, and P5) with a working volume of 0.5 L each were assembled. Each reactor was dosed with 0.2 L of sludge. P1, the control, contained untreated TWAS. Ca(ClO)₂ (0.01, 0.05, 0.1, and 0.2 gCa(ClO)₂/gTS, respectively) was added to P2, P3, P4, and P5. All reactors were mixed continuously for 24 hours at 120 rpm at room temperature. Each reactor was prepared and treated in triplicate. Samples from each reactor were collected every 1-5 hours and filtered by 0.45 µm filter to measure the soluble chemical oxygen demand (SCOD). After 24 hours of treatment, soluble protein, polysaccharide, and organics were measured; live/dead cell viability was analyzed, and specific resistance to filtration (SRF) was measured in all reactors.

3.2.3 Aerobic digestion

To evaluate whether the aerobic digestion of TWAS could be enhanced by pre-treatment of TWAS with Ca(ClO)₂, 100 mL of TWAS from P1, P2, P3, P4, and P5 reactors were transferred to other five 0.5 L reactors (hereafter, aerobic digestion reactors), which were denoted as A1, A2, A3, A4,

and A5, each containing 0.1 L untreated TWAS as seed sludge for aerobic microbes. The seed sludge to pretreated sludge ratio was 1:1. Each reactor was conducted in triplicate.

All aerobic digestion reactors were continuously mixed with a shaker set to 120 rpm at room temperature for 20 days. Samples were obtained every two days from the aerobic digestion reactors to measure TS, VS, and SCOD.

3.2.4 Analytical methods

3.2.4.1 Soluble protein and polysaccharide

Samples (10 ml) from the pre-treatment reactors were centrifuged (2000 rpm, 15 min), and the supernatant of each sample was filtered by membrane filters (0.22 μm) to measure protein and polysaccharide. Coomassie Brilliant Blue G-250 method was used to measure protein (Bradford, 1976); the sulfuric acid-phenol method was used to measure polysaccharides (Li et al., 2014).

3.2.4.2 Three-dimensional excitation-emission matrix (EEM)

The filtered supernatants of samples from pretreatment reactors were analyzed with an EEM, using a Varian fluorescence spectrophotometer with an excitation range of 220 nm to 450 nm and an emission range of 250 nm to 550 nm. Excitation and emission intervals were 10 nm and 1 nm, respectively, with a scanning rate of 600 nm/min. EEM area volume was indicated by the fluorescence region integration (FRI) method to quantitatively investigate the compositions of dissolved organic matter (Chen et al., 2003; Zhou et al., 2013).

3.2.4.3 Cell viability analysis

Live and dead cells in TWAS were counted using confocal laser scanning microscopy (CLSM). Samples were extracted from reactors after 24-hour pretreatment (Zhu et al., 2018). Viable cells and non-viable cells were stained using the LIVE/DEAD™ BacLight™ Bacterial Viability Kit (Thermo Fisher Scientific). Cells were dyed by adding 2 µL dye mixture to 2 mL of diluted TWAS samples. And then, the samples were incubated in the dark (room temperature, 1 hour). Each stained sample (5 µL) was deposited in an optical petri dish (18 mm). A Zeiss LSM 710 confocal microscope (Carl Zeiss Micro Imaging GmbH, Germany) was used to examine a series of optical slices.

3.2.4.4 SRF

SRF used the Buchner funnel method to assess the dewaterability of TWAS (Zhu et al. 2018). The SRF was calculated with Equation (3-3):

$$SRF = 2PA^2b/\mu W \quad (3-3)$$

where P is the pressure of filtration (Pa), A is the area of filter (m²), b is the slope of the filtrate discharge curve (s/m⁶), μ is filtrate viscosity (S Pa), W is solids mass per unit volume of filtrate (kg/m³), and SRF is the specific resistance of the sludge to filtration (m/kg).

3.2.4.5 TS, VS, and SCOD analyses

TS, VS, and SCOD were measured by the Standard Methods (Baird et al., 2017). The rates of SCOD changes were calculated by Equation (3-4):

$$\text{rates of SCOD changes} = |SCOD_{t2} - SCOD_{t1}|/|t2 - t1| \quad (3-4)$$

Where $SCOD_{t2}$ is the SCOD value at time $t2$ (days), the unit of *rates of SCOD changes* is g/L/d.

3.2.5 Kinetic modeling of VS degradation

The first-order exponential decay of VS degradation was modeled to estimate the hydrolysis rate constant (k), using Equation (3-5):

$$Y = Y_0 * (1 - \exp(-kt)) \quad (3-5)$$

where Y is the degraded percentage of TWAS (%) at time t (days), Y_0 is the initial TWAS degradable percentage (%), t (days) is the digested time, and k is the hydrolysis rate constant (d^{-1}).

3.2.6 Microbial community analysis

Sludge samples (1 mL) were obtained from reactors after 20 days of aerobic digestion. After centrifuging for 5 mins at 10,000 g, the supernatant of the samples was discarded, and the rest sludge was washed using PBS buffer (Zhang et al., 2021b). The genomic DNA of each sample was extracted using DNeasy PowerSoil Kit (QIAGEN, Hilden, Germany) following the manufacturer's protocol. MiSeq sequencing was performed by an Illumina MiSeq platform and processed using the QIIME 2 DADA2 algorithm. The Greengenes database (version 13_8) with 99% similarity was used as the reference database. The Phylogenetic Investigation of Communities by Reconstruction of Unobserved States (PICRUSt) program was used to investigate the prediction of microbial functions using the Kyoto Encyclopedia of Genes and Genomes (KEGG) database (Yu et al., 2020). Raw sequence files were deposited in the NCBI Sequence Read Archive database and assigned accession No. SRR14929592.

3.2.7 Statistical analysis

Sample analysis results were measured in triplicate, and the arithmetic mean value was reported. The significance of the results was determined using a *t-test*; $p < 0.05$ was considered statistically significant.

3.3 Results and discussion

3.3.1 $\text{Ca}(\text{ClO})_2$ pre-treatment

3.3.1.1 Effect of $\text{Ca}(\text{ClO})_2$ pre-treatment on sludge solubilization

Sludge solubilization was evaluated using the SCOD of TWAS. As shown in **Fig. 3.1**, the initial SCOD concentration increased right after $\text{Ca}(\text{ClO})_2$ addition, which may be attributed to the organics released from the EPS decomposition and cell lysis. The SCOD increased with the introduced dosage of calcium hypochlorite during 0 to 8 hours. The highest SCOD in the P1 control reactor (no $\text{Ca}(\text{ClO})_2$), was 1.45 ± 0.05 g/L during 24 hours of pre-treatment. In the test samples containing $\text{Ca}(\text{ClO})_2$, the highest SCOD values were 1.55 ± 0.02 g/L, 3.20 ± 0.15 g/L, 4.26 ± 0.06 g/L, and 4.15 ± 0.34 g/L in P2, P3, P4, and P5 reactors, respectively.

In the P1 and P2 reactors, the general trends of SCOD concentration changes were similar between each other during the 24 h pre-treatment, where the SCOD concentration increased in the first two hours and then decreased after two hours of pre-treatment. After 12 hours of pre-treatment, the concentrations of SCOD in P1 and P2 reactors had decreased, which may be attributed to the SCOD consumption by microbes in the TWAS. Also, the concentrations of SCOD in control P1 and P2 reactors were similar ($p=0.22$), although 0.01 g $\text{Ca}(\text{ClO})_2$ /gTS was supplied in P2 reactor.

This may be explained by the low calcium hypochlorite dosage and the uptake of organics released from EPS and cell lysis.

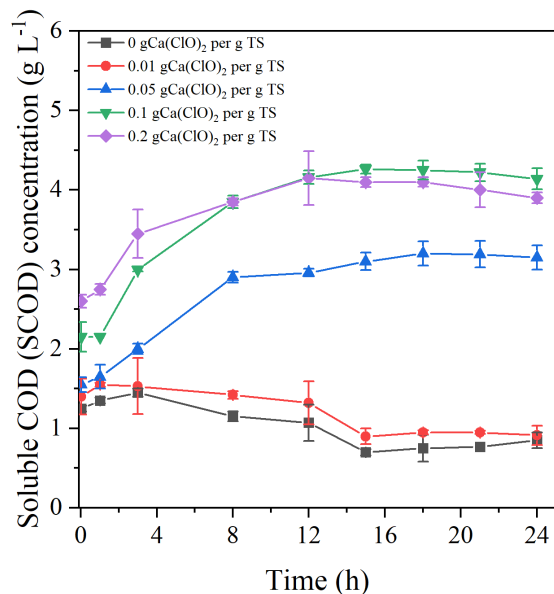


Fig. 3.1. SCOD concentrations during 24 h Ca(ClO)₂ pre-treatment of TWAS.

In P3, P4, and P5 reactors, the SCOD concentrations rapidly increased from 0 h to 12 h after the hypochlorite addition, which may be attributed to the release of organic molecules from TWAS as OCl⁻ broke the microbial cell walls and decomposed EPS in the sludge. A similar observation of an increase in SCOD after hypochlorite treatment was reported previously for anaerobic sludge digestion (Luo et al., 2020; Yuan et al., 2016). After 12 hours of pre-treatment, the concentrations of SCOD in P3, P4, and P5 reactors were stable.

Fig. 3.2a shows confocal laser scanning microscopy (CLSM) images of TWAS in different Ca(ClO)₂ concentrations. The green/red color represents live/dead cells. The percentage of live cells (**Fig. 3.2 b**) was 98.58%, 64.12%, 36.39%, 21.55% and 5.40%, in P1, P2, P3, P4, and P5 reactors, respectively. As over 50% of the cells in P1 and P2 reactors were alive, there were enough

microbes in the sludge to continuously degrade SCOD, as observed in Fig. 3.1. However, fewer than 40% of the cells were alive in P3, P4, and P5 reactors, allowing SCOD concentrations to remain stable during pretreatment.

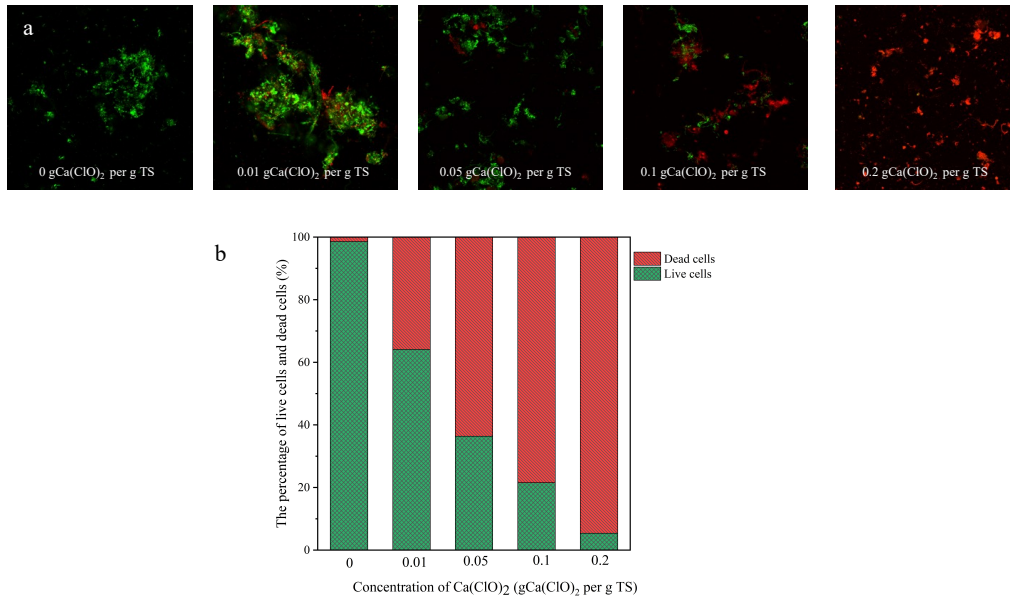


Fig. 3.2. a: Confocal laser scanning microscopy (CLSM) images of TWAS at different $\text{Ca}(\text{ClO})_2$ pretreatment concentrations (green/red color represents live/dead cells); b: The percentage of live cells (green) and dead cells (red) in TWAS at different $\text{Ca}(\text{ClO})_2$ pretreatment concentrations.

Although more $\text{Ca}(\text{ClO})_2$ was added to P5 reactor than to P4 reactor, the highest SCOD reached in P5 reactor was lower than the highest SCOD reached in P4 reactor. Therefore, the best concentration and the pre-treatment time under tested experiment conditions were determined to be 0.1 g $\text{Ca}(\text{ClO})_2$ /gTS and 12 hours, respectively.

3.3.1.2 Effect of pre-treatment on soluble organics

The organic portions of TWAS are mostly in aggregated forms, such as located in cell envelopes, EPS, and intracellular materials (Wang et al., 2018a; Zhu et al., 2018). To facilitate solids reduction, these organisms need to be discharged into the liquid media in the TWAS treatment procedure.

EEM fluorescence was used to characterize soluble organics (**Fig. 3.3a**). The dissolved organics could be classified into five types according to EEM spectra, which are region I (such as tyrosine-like proteins, Ex/Em= 220 nm-250 nm / 280 nm-330 nm), region II (such as soluble microbial by-product-like substances, Ex/Em= 250 nm-450 nm / 280 nm-380 nm), region III (such as tryptophan-like substances, Ex/Em= 220 nm-250 nm / 330 nm-380 nm), region IV (such as fulvic acid-like substances, Ex/Em= 220 nm-250 nm / 380 nm-550 nm), and Region V (such as humic acid-like substances, Ex/Em= 250 nm-450 nm / 380 nm-550 nm) (Zhang et al., 2020b). Among these regions, region I and region II are usually considered as biodegradable substrates, whereas region III, IV, and V are often considered to be substrates with low biodegradability, which mainly include tryptophane-like, fulvic acid-like, and humic acid-like substances (Wang et al., 2018b). EEM area volumes were calculated (**Fig. 3.3b**) to provide a more comprehensive characterization of organics. The results indicated that the total area of EEM graphs in regions I and II increased with an increasing dose of $\text{Ca}(\text{ClO})_2$, revealing that the addition of $\text{Ca}(\text{ClO})_2$ to TWAS enhanced the biodegradability of the substrates. The sum of the EEM area volumes of five regions increased from P1 to P5 reactors, in accordance with SCOD results.

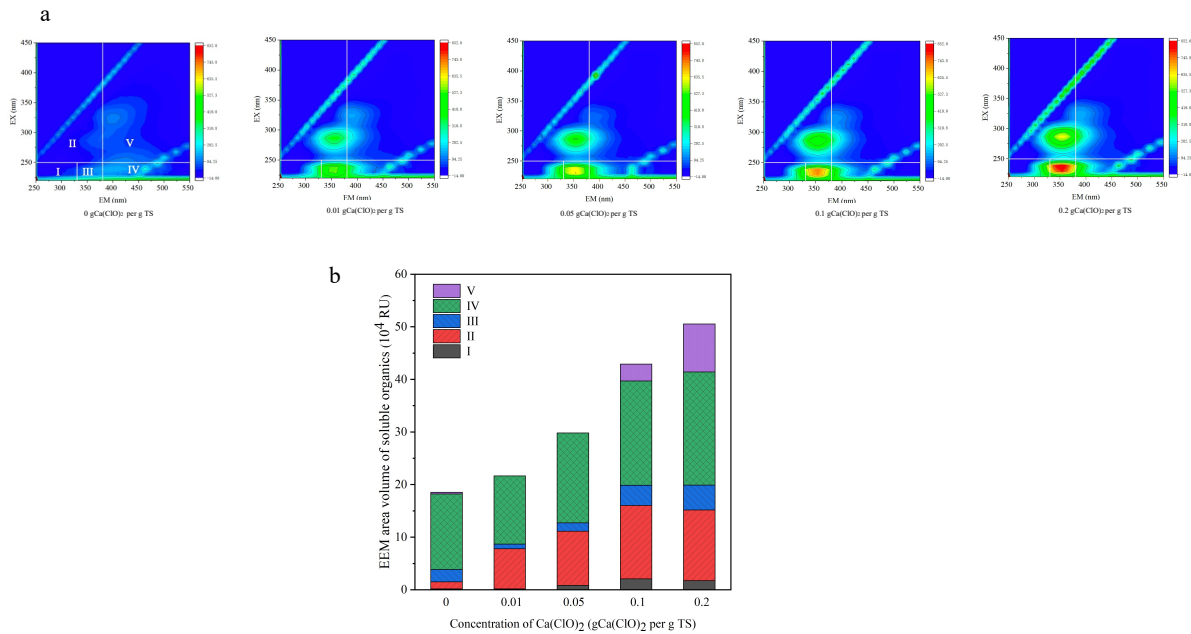


Fig. 3.3. EEM contour plot of soluble organics (a) and EEM area volume of soluble organics (b) after 24 h $\text{Ca}(\text{ClO})_2$ pre-treatment of TWAS: I: tyrosine-like proteins; II: soluble microbial by-product-like substances; III: tryptophan-like substances; IV: fulvic acid-like substances; V: humic acid-like substances (RU represents relative unit).

The soluble protein and polysaccharide concentrations in TWAS at different $\text{Ca}(\text{ClO})_2$ pre-treatment concentrations are shown in **Fig. 3.4**. The concentrations of protein and polysaccharide increased from P1 reactor to P4 reactor, then decreased from P4 reactor to P5 reactor, which may be due to the excess OCl^- induced oxidation of protein and polysaccharide. The major components of TWAS are proteins and polysaccharides (Zhang et al., 2020b). The release of the intracellular compounds and cell surface bound EPS after $\text{Ca}(\text{ClO})_2$ pre-treatment may result in a rise in soluble protein and polysaccharide, as also demonstrated previously (Liang et al., 2019; Zhang et al., 2020b; Zhu et al., 2018).

The highest release of protein, polysaccharide, and biodegradable substrates into the soluble medium was achieved when 0.1 gCa(ClO)₂/gTS pre-treatment was applied to TWAS.

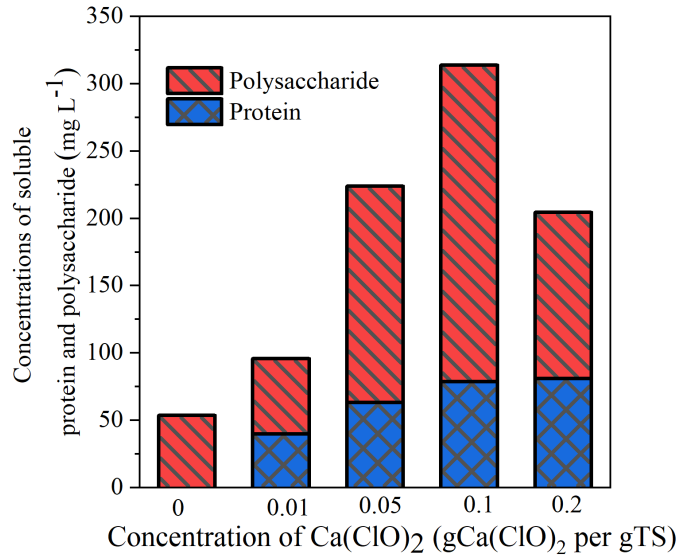


Fig. 3.4. Concentrations of soluble protein and polysaccharide after 24 h Ca(ClO)₂ pre-treatment of TWAS.

3.3.1.3 Effect of Ca(ClO)₂ pre-treatment on sludge dewaterability

SRF was used to characterize the effect of Ca(ClO)₂ on sludge dewaterability, as illustrated in **Fig. 3.5**. In general, a low SRF value shows good sludge dewaterability (Chen et al., 2016). When the Ca(ClO)₂ dose was increased, the SRF initially dropped. The SRF then rose, which was consistent with the SRF trends in a previous study that used Ca(ClO)₂ to treat TWAS (Zhu et al., 2018). In that study, the trend of the first decrease and then increase was displayed, and when Ca(ClO)₂ dosage was 0.04 gCa(ClO)₂/gTS, the SRT declined to minimum value (Zhu et al., 2018). In this study, at P3 and P4 (0.05 and 0.1 gCa(ClO)₂/gTS) reactors, the values of SRF declined to 3.02×10^{10} m/kg and 3.13×10^{10} m/kg, respectively, which was due to the disruption of floc integrity

and structure and the release of extracellular and intracellular contents (Feng et al., 2009). However, the SRF value increased when the dosages of $\text{Ca}(\text{ClO})_2$ were raised, indicating an evident deterioration in sludge dewaterability. Hence, the excessive release of biopolymers into the solution with high dose of $\text{Ca}(\text{ClO})_2$ is undesired. Previous studies also demonstrated that the release of biopolymers with high affinity for water can lead to an increase in the sludge's viscous properties (Wang et al., 2006). Also, high dose of $\text{Ca}(\text{ClO})_2$ can lead to an alkaline condition which may further inhibit sludge dewatering capacity (Liang et al., 2019; Liang et al., 2015).

Overall, pre-treatment with $\text{Ca}(\text{ClO})_2$ improved TWAS solubilization and dewaterability by adding OCl^- , which had an oxidative effect on cell lysis, EPS decomposition, and the release of organic substances. The best time and dosage of $\text{Ca}(\text{ClO})_2$ pre-treatments that were found under tested experimental conditions were 12 h and 0.1 g $\text{Ca}(\text{ClO})_2/\text{gTS}$, respectively.

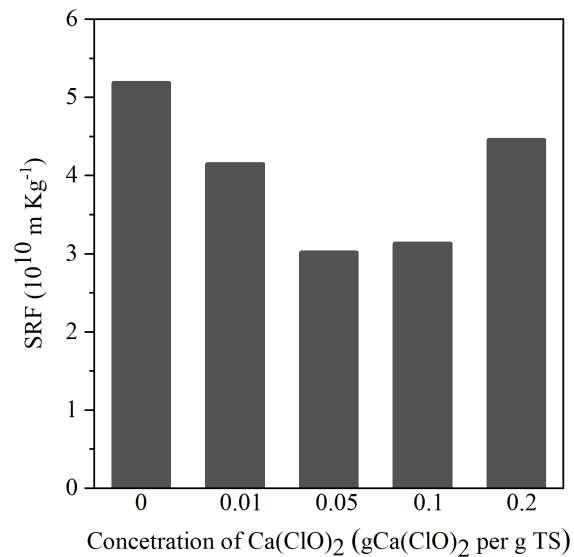


Fig. 3.5. Specific resistance to filtration (SRF) after pretreatment of TWAS with different $\text{Ca}(\text{ClO})_2$ concentrations.

3.3.2 Aerobic digestion

3.3.2.1 Effect of aerobic digestion on sludge solubilization

Changes in the SCOD during anaerobic digestion were characterized using sludge SCOD changes (Fig. 3.6). The profile of SCOD concentration changes can be separated into 3 phases (Fig. 3.7). Phase 1 (from 0 days to 4 days) was characterized by a fast release phase; Phase 2 (4 to 12 days) showed a rapid degradation phase, and Phase 3 (12 to 20 days) displayed a slow SCOD decrease phase. This trend was similar to the results reported by a previous study on ultrasonic aided bacterial pretreatment for TWAS aerobic treatment (Kavitha et al., 2016).

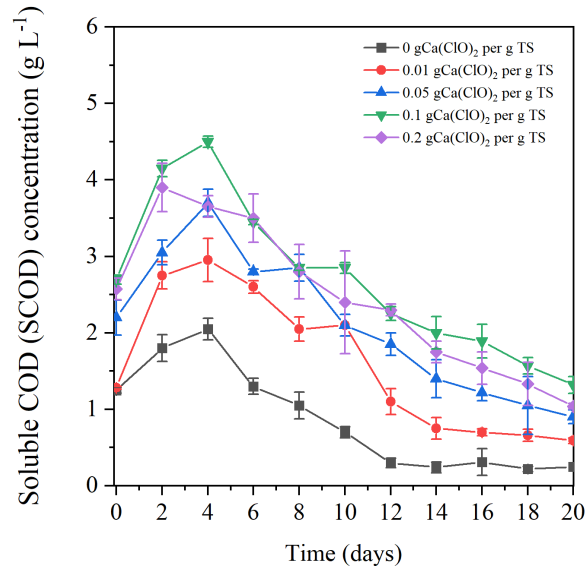


Fig. 3.6. Soluble chemical oxygen demand (SCOD) concentrations during aerobic digestion of TWAS.

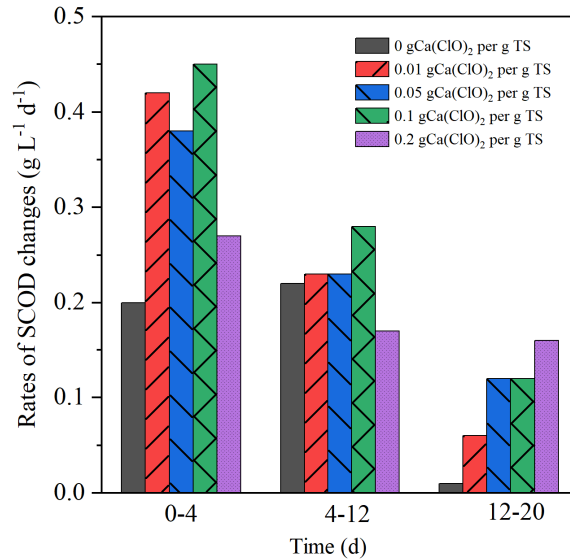


Fig. 3.7. The rates of SCOD concentration changes during aerobic digestion of TWAS in three phases.

During the rapid increase of SCOD phase (0-4 days), increased release of organics (highest COD measured-initial COD after pretreatment) was observed for $\text{Ca}(\text{ClO})_2$ pretreated sludge. The highest SCOD concentrations were 2.05 ± 0.14 g/L, 2.95 ± 0.28 g/L, 3.70 ± 0.18 g/L, 4.50 ± 0.07 g/L, and 3.90 ± 0.32 g/L, respectively, at A1, A2, A3, A4 and A5 reactors during aerobic digestion, with the highest COD concentration release observed in the A4 reactor.

In the degradation process (4-20 days), the degradations in different reactors were all characterized by fast initial degradation from 4-12 days, followed by slow degradation after day 12 (**Fig. 3.7**). For the A1, A2, and A3 reactors, the rates of SCOD changes during 4-12 days were similar, ranging from 0.22-0.23 g/L/d. In comparison, the A4 reactor achieved the highest SCOD release rate (0.28 g/L/d). The SCOD reduction slowed down during 12-20 days, which means the degradation of SCOD mainly happened in the first 4-12 days.

The SCOD data indicated that the best $\text{Ca}(\text{ClO})_2$ dosage for aerobic digestion under tested experimental conditions was $0.1 \text{ gCa}(\text{ClO})_2/\text{gTS}$.

3.3.2.2 *Effect of aerobic digestion on VS reduction*

The degradation percentages of VS in A1 to A5 reactors during 20-day aerobic digestion of TWAS are shown in **Fig. 3.8**. VS reduction percentages reached $36.29 \pm 0.49 \%$ in A1 reactor, $49.42 \pm 0.01 \%$ in A2 reactor, $55.81 \pm 0.01 \%$ in A3 reactor, $65.05 \pm 2.68 \%$ in A4 reactor, and $51.24 \pm 6.78 \%$ in A5 reactor after 20 days of aerobic digestion. The degradation percentage of VS during the aerobic digestion of TWAS was the highest in A4 reactor with $0.1 \text{ gCa}(\text{ClO})_2/\text{gTS}$ pre-treatment.

A considerable reduction in VS was observed in the first 12 days of aerobic digestion, in accordance with the values of SCOD during aerobic digestion. In 12 days, the reduction rates of VS were $29.91 \pm 1.86\%$, $42.16 \pm 2.55\%$, $48.35 \pm 0.79\%$, $61.55 \pm 2.41\%$, and $45.01 \pm 6.58\%$ in A1, A2, A3, A4, and A5 reactors, respectively. Therefore, an HRT of 12 days was ideal for effective aerobic degradation after $\text{Ca}(\text{ClO})_2$ pre-treatment.

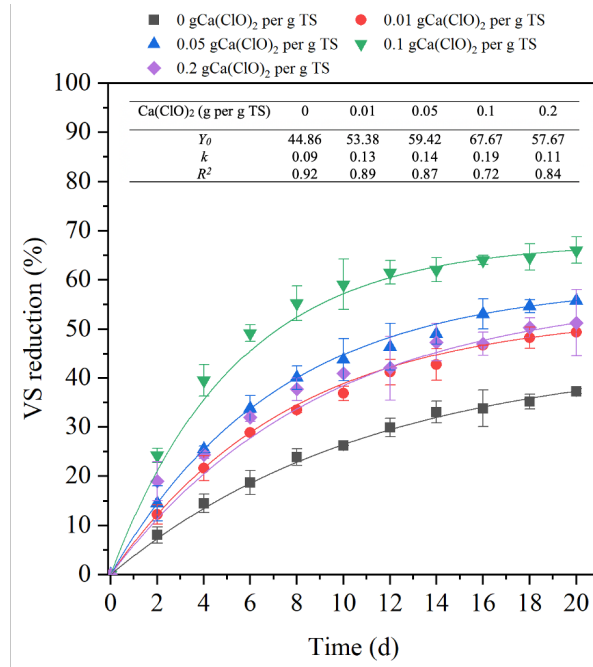


Fig. 3.8. VS reduction during 20 days of aerobic digestion of WAS and kinetic modeling analysis of the hydrolysis rate (k) of TWAS pretreated with different doses of $\text{Ca}(\text{ClO})_2$.

3.3.2.3 Kinetic modeling of VS reduction

To investigate the effect of $\text{Ca}(\text{ClO})_2$ pretreatment on the aerobic digestion of sludge (on a VS basis), the first-order kinetic modeling was performed (**Fig. 3.8**). The modeling of VS degradation was evaluated using R^2 values. The R^2 values of the first-order kinetic model ranged from 0.72 to 0.92. The hydrolysis rates (k) at different pre-treatment dosages were determined by kinetic modeling. The k value of the control reactor, A1, was 0.09 d^{-1} , which was lower than the k values found in experimental reactors (A2-A5) with $\text{Ca}(\text{ClO})_2$ pretreatments. This confirmed that pretreatment of TWAS with $\text{Ca}(\text{ClO})_2$ improved the hydrolysis efficiency of TWAS. The k value increased from 0.13 d^{-1} in A2 to 0.19 d^{-1} in A4 reactor, then decreased to 0.11 d^{-1} in A5 reactor. The hydrolysis rate in A4 reactor was the fastest, a result concomitant with the SCOD results and

the VS reduction. Y_0 was the initial TWAS degradable percentage, which means the biodegradable capacity of TWAS. The values of Y_0 in $\text{Ca}(\text{ClO})_2$ pretreated reactors were higher than the control group, with the A4 reactor achieving the highest Y_0 value (67.67%), in accordance with the results of **Fig. 3.1**.

3.3.3 Microbial community

Fig. 3.9 shows the relative abundance of predominant bacteria at the family level after aerobic digestion treatment. The dominant bacteria at family level in original TWAS consist of *f_Rhodocyclaceae* (17.2%), *f_Comamonadaceae* (10.1%), *f_Moraxellaceae* (6.6%), *o_Thiobacterales* (4.8%), *o_Sphingobacteriales* (4.8%), *f_Xanthomonadaceae* (4.7%) and *f_Cytophagaceae* (3.9%). However, the relative abundance of dominant bacteria changed after 20 days of aerobic digestion treatment. Without adding $\text{Ca}(\text{ClO})_2$, the main bacteria were *f_Rhodocyclaceae* (~15.0%), *f_Xanthomonadaceae* (~11.1%), *f_Comamonadaceae* (~7.7%), *f_Cytophagaceae* (~6.4%), *f_Intrasporangiaceae* (~6.0%), *c_Betaproteobacteria* (~5.6%) and *f_Saprospiraceae* (~5.5%) after aerobic digestion treatment.

The relative abundance of bacteria after aerobic digestion varied significantly pretreated with different dosages of $\text{Ca}(\text{ClO})_2$. The relative abundance of *f_Cryomorphaceae*, which could metabolize a wide variety of organics and had a solid capacity to ingest proteins, cellulose, and lipids with high molecular weight, increased from 1.4% in A1 reactor to 23.1 % in A3 reactor (Song et al., 2021). On the other hand, the abundance of *f_Rhodocyclaceae*, which had been observed to be abundant in WAS, was reduced from 17.2% in the control reactor to 3.5 % in the 0.05 $\text{gCa}(\text{ClO})_2/\text{gTS}$ reactor after aerobic digestion treatment (Wei et al., 2020). After adding 0.1 $\text{gCa}(\text{ClO})_2/\text{gTS}$, *f_Xanthomonadaceae*, known as hydrocarbon utilizing bacteria (Wei et al., 2020),

became the main bacteria at the family level (~44.0%). The relative abundances of *o_Saprospirales*, *f_Cytophagaceae* and *f_Cryomorphaceae* increased to 9.8%, 8.3% and 4.5%, respectively. *f_Cytophagaceae* and *f_Cryomorphaceae* have been linked to the degradation of bio-recalcitrant hydrocarbons (Xia et al., 2017). *o_Saprospirales* has been reported to decompose organics with high molecular weight and polymers (Xia et al., 2017). Overall, the efficient VS reduction was the consequence of a combination of variables, such as the concentration of bioavailable organics and the activities of the microbial community. *Xanthomonadaceae* and *Cryomorphaceae* were significantly related to the presence of $\text{Ca}(\text{ClO})_2$ after aerobic digestion treatment.

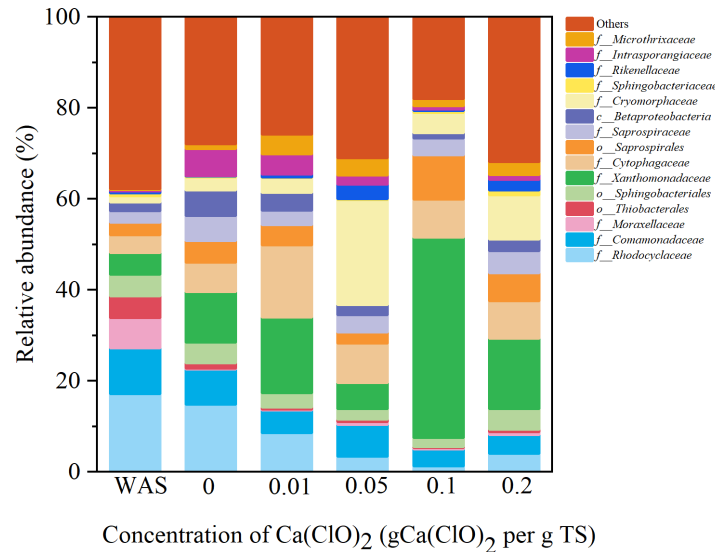


Fig. 3.9. The relative abundance of predominant bacteria at family level in sludge (The taxonomic names were shown for family level or higher level; family: f_; order: o_; class: c_).

A reference database was used to examine the functional genes based on data from 16S rRNA gene amplicon (Langille et al., 2013). As shown in **Fig. 3.10**, different concentrations of $\text{Ca}(\text{ClO})_2$ aided different functional groups. The dose of 0.1 gCa(ClO)₂/gTS displayed the highest frequency

of replication and repair and folding, sorting, and degradation in genetic information processing, which can be linked to the decomposition of cells and high concentrations of soluble organic compounds in TWAS. The A4 reactor also showed the highest prevalence of cellular processes and signaling, as well as cellular processes functions of cell motility, revealing the active growth of cells, which may have been caused by increased microorganisms activity (Yu et al., 2020).

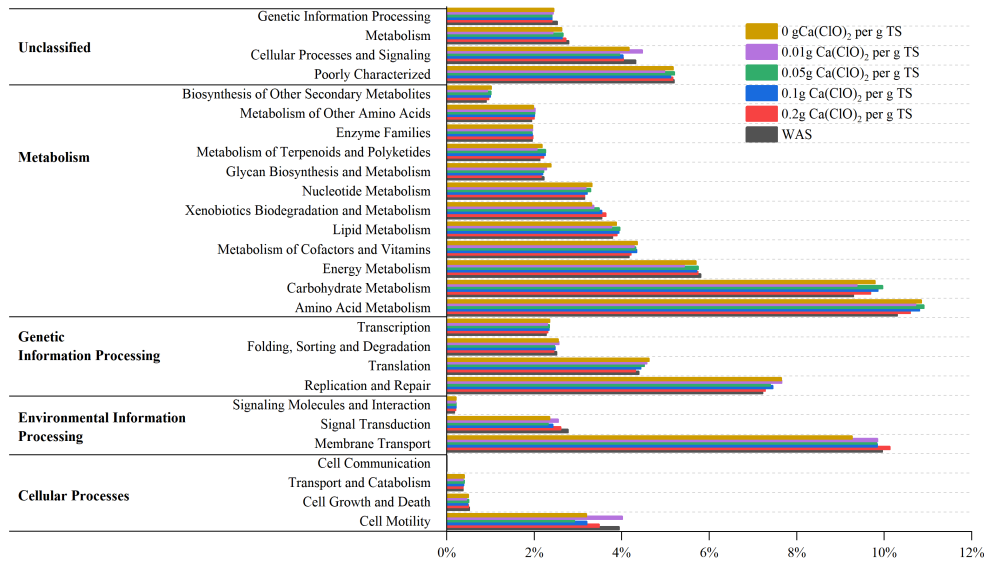


Fig. 3.10. Predicated metagenome functions of sludge after aerobic digestion treatment.

3.3.4 Potential implication in WWTPs

In this study, it was demonstrated that calcium hypochlorite pre-treatment before TWAS aerobic digestion can effectively improve the TWAS treatment performance. Experimental results in this study revealed that with Ca(ClO)₂ pre-treatment at a dose of 0.1 g Ca(ClO)₂/gTS, sludge retention time can be reduced to 12 days. However, pre-treatment conditions should be further optimized in future studies before full-scale application of the process can be adopted.

3.4 Conclusions

Laboratory tests were carried out to investigate the feasibility of improving VS reduction of thickened WAS by aerobic digestion after $\text{Ca}(\text{ClO})_2$ pre-treatment. The $\text{Ca}(\text{ClO})_2$ pre-treatment improved the solubilization and dewaterability of TWAS and reduced the presence of VS during aerobic digestion. Kinetics analysis showed that the hydrolysis rates of WAS were improved after $\text{Ca}(\text{ClO})_2$ pre-treatment. In addition, the relative abundance of dominant bacteria varied significantly with $\text{Ca}(\text{ClO})_2$ addition. The laboratory tests provided basic information (appropriate dosage, retention time, and mechanisms) for the calcium hypochlorite pre-treatment method. However, future large-scale studies are needed to further evaluate this process for full-scale applications. The microbial community changes before and after the pre-treatment should also be assessed in future studies.

**CHAPTER 4 CALCIUM PHOSPHATE GRANULES FORMATION: KEY
TO HIGH RATE OF MESOPHILIC UASB TREATMENT OF TOILET
WASTEWATER**

A version of this chapter has been published in Science of the Total Environment.²

² Zhang, L.¹, Mou, A.¹, Sun, H., Zhang, Y., Zhou, Y., Liu, Y. 2021. Calcium phosphate granules formation: Key to high rate of mesophilic UASB treatment of toilet wastewater. Science of the Total Environment, 773, 144972. (¹Equal contributions)

4.1 Introduction

Novel decentralized infrastructure reduces the amounts of waste at source, improves recycling or reuse at the site, and eliminates wastewater collection components; thus, can reduce more than 60% operation and maintenance costs compared to those of centralized systems (Capodaglio, 2020; Kujawa-Roeleveld et al., 2006; Massoud et al., 2009; Singh et al., 2014). The development of suitable decentralized wastewater treatment systems that focus on resource recovery and fit communities of various scales has been intensively studied in recent years (Chaggu et al., 2007; Cunha et al., 2020; Zhang et al., 2020a; Zhou et al., 2020). In particular, greywater (laundry and kitchen wastewater) and toilet wastewater (feces, urine, and flush water) can be managed separately for nutrients, and to reduce greenhouse gas emissions (Gros et al., 2020). Toilet wastewater contains more than 50% organics and more than 90% of nutrients of municipal wastewater, and only accounts for 10–30% of the household wastewater volume (Zhang et al., 2019). Energy contents from source-diverted toilet wastewater can be recovered in the form of methane through anaerobic digestion processes (Kujawa-Roeleveld et al., 2005). Anaerobic toilet wastewater treatment recovers energy locally and is particularly suitable for areas with source-diverted toilet wastewater collection, and/or limited public sewer networks (Mainardis et al., 2020). However, process optimization focusing on toilet wastewater anaerobic digestion is still limited.

Different anaerobic reactor types have been evaluated for source-diverted toilet wastewater treatment, including continuous stirred tank reactors (CSTR) (Wendland et al., 2007), up-flow anaerobic sludge bed reactors (UASB) (de Graaff et al., 2010; Slompo et al., 2019) and accumulation systems (Chaggu et al., 2007). For instance, De Graaff et al. studied the application of a UASB reactor for toilet wastewater treatment under 25 °C and achieved a maximum organic loading rate (OLR) of 1.1 g COD/(L·d) and an HRT of 8.7 d (de Graaff et al., 2010). Recently,

Gao et al. optimized a mesophilic UASB treating vacuum toilet collected wastewater through controlling free ammonia inhibition and achieved a high OLR of 4.1 g COD/(L·d) with an HRT of 2.6 d (Gao et al., 2019b). Co-digestion of toilet wastewater and kitchen food residuals was a simple and sound way to increase the OLR (Gao et al., 2020; Kujawa-Roeleveld et al., 2006; Zhang et al., 2020c). However, no other strategies have been reported to further improve the OLR of anaerobic toilet wastewater digestion.

Anaerobic granulation is a proven approach to increase the OLR of anaerobic treatment of organic wastewater due to its high biomass density and resistance towards environmental stress (Faria et al., 2019; Liu and Tay, 2004). Interestingly, only two studies reported the development of anaerobic granular sludge for toilet wastewater treatment (Tervahauta et al., 2014b; Zhang et al., 2021a), and both studies reported calcium phosphate-rich anaerobic granular sludge formation during toilet wastewater treatment. Significantly improved OLR and methane recovery were observed by Zhang et al., which has been attributed largely to the sludge granulation under thermophilic conditions (Zhang et al., 2021a). Our traditional understanding of the anaerobic granular sludge formation suggests that sludge granulation process requires stringent conditions, e.g. low solids contents in feedstock (< 0.3 g COD/L), high liquid up-flow velocity (> 1 m/h) and certain reactor types with high height/diameter ratios (Alphenaar, 1994; McHugh et al., 2003; Tay et al., 2006; Zhang et al., 2021a). Interestingly, both toilet wastewater granulation studies applied low liquid up-flow velocity, and toilet wastewater has high solids contents (> 5.0 g COD/L). For instance, the shear force caused by biogas production was low in Tervahauta et al.'s study, due to its low OLR and low methane production because of low temperature operation (25 °C) (Tervahauta et al., 2014b). Therefore, understanding the anaerobic granulation mechanisms involved in anaerobic toilet wastewater treatment is essential for the reactor design and operation.

Factors including localized environment (pH and mixing condition), CaP formation, and proper hydrolysis rate were pointed out to be crucial for the granulation in anaerobic toilet wastewater treatment (Cunha et al., 2018a; Cunha et al., 2018b; Zhang et al., 2021a). However, no study has demonstrated anaerobic granulation under mesophilic conditions for toilet wastewater treatment.

In the present study, the feasibility of anaerobic granulation for toilet wastewater treatment using a mesophilic UASB was investigated. Long-term operation of a lab-scale UASB reactor was carried out using anaerobic floc sludge from a waste activated sludge (WAS) digester as the inoculum. With the formation of granular sludge, the HRT was significantly shortened from 8 d to 0.25 d with a clear OLR increased from 0.4 to 16.0 g COD/(L·d). The energy recovery efficiency (methane production rate and potential) was evaluated, and the sludge characteristics and the structure of microbial community were analyzed. The mechanisms of the granular sludge formation were discussed in detail. The results of the present study provide new understanding of anaerobic granulation processes.

4.2 Materials and methods

4.2.1 Mesophilic UASB reactor set-up

A 1 L (working volume) laboratory-scale polymethyl methacrylate UASB reactor was used to treat vacuum toilet wastewater under mesophilic conditions (Height×Diameter: 350 mm × 60 mm). The start-up time was 30 days, and the operation was 250 days. The reactor temperature (35 °C) was controlled by a water jacket using circulating water provided with a heated bath circulator (HW-2 L, Walter Products Inc., Canada). Mesophilic anaerobic sludge inoculum was collected from a full-scale anaerobic digester treating municipal biosolids in Edmonton (Alberta, Canada). Toilet wastewater was collected from the University of Alberta (Edmonton, Canada). Biogas generated

from the UASB reactor was collected with a Tedlar gas bag (VWR International, America). The experiment was divided into seven phases (I-VII) based on organic loading rates (OLR) of 0.4, 1.0, 2.3, 5.1, 9.3, 13.6, and 16.0 g COD/(L·d), respectively; corresponding hydraulic retention times (HRT) were 8 d, 4 d, 2 d, 1 d, 0.5 d, 0.3 d, and 0.25 d from Phases I to VII. The characteristics of the toilet wastewater in each phase are shown in **Table 4.1** and **Table 4.2**. The hydraulic up-flow velocity in the UASB reactor increased from 1.8 to 58.3 mm/h from Phase I to VII. The reactor was operated in each phase for at least 4 weeks, and conditions were changed only after COD removal; the methane production potential ($\text{CH}_4\text{-COD g/ influent COD g}$) was stable for at least two weeks. A relatively consistent COD removal rate and a methane production rate within 5% indicated a stable state for each phase.

Table 4.1. Profiles of COD, VFA, TS and NH₄⁺-N concentrations in influent (untreated toilet wastewater) and effluent and COD_{total} removal efficiency in phases I-VII (unit: g/L, standard deviation is in brackets).

Phases		Phase I (OLR 0.4)	Phase II (OLR 1.0)	Phase III (OLR 2.3)	Phase IV (OLR 5.1)	Phase V (OLR 9.3)	Phase VI (OLR 13.6)	Phase VII (OLR 16.0)
Influent	TCOD	2.8 (0.9)	3.8 (0.6)	4.6 (0.8)	5.1 (1.1)	4.6 (1.0)	4.6 (0.6)	3.8 (0.7)
	suspended COD	1.2 (0.8)	1.5 (0.6)	2.1 (0.6)	3.5 (1.0)	3.0 (1.1)	2.5 (0.8)	1.6 (0.9)
	SCOD	1.9 (0.5)	2.4 (0.8)	2.5 (0.7)	1.6 (0.2)	1.6 (0.6)	2.3 (0.6)	2.2 (0.7)
	VFA- COD	0.3 (0.2)	0.6 (0.2)	0.4 (0.2)	0.4 (0.3)	0.4 (0.2)	0.4 (0.2)	0.4 (0.2)
	TS	2.2 (0.4)	2.6 (0.8)	3.5 (0.8)	4.2 (0.5)	3.3 (0.4)	3.7 (0.3)	2.9 (0.4)
	NH ₄ ⁺ -N	1.0 (0.1)	1.0 (0.1)	0.9 (0.1)	1.0 (0.1)	1.0 (0.1)	0.9 (0.1)	0.9 (0.1)
	Effluent	TCOD	0.7 (0.4)	0.7 (0.1)	0.8 (0.2)	0.9 (0.1)	0.9 (0.1)	0.9 (0.2)
suspended COD		0.1 (0.3)	0.1 (0.1)	0.2 (0.2)	0.4 (0.2)	0.5 (0.2)	0.5 (0.2)	0.4 (0.1)
SCOD		0.5 (0.1)	0.6 (0)	0.6 (0.1)	0.5 (0.1)	0.4 (0)	0.3 (0.1)	0.8 (0.4)
VFA- COD		0.05 (0.02)	0.05 (0.01)	0.06 (0.02)	0.08 (0.03)	0.10 (0.04)	0.13 (0.04)	0.16 (0.02)
NH ₄ ⁺ -N		0.9 (0.1)	0.9 (0.1)	0.9 (0.1)	1.0 (0.1)	0.9 (0.1)	1.0 (0.1)	0.9 (0.1)
TCOD removal efficiency (%)		78.0 (9.6)	85.4 (7.0)	84.7 (4.4)	83.0 (3.5)	76.0 (9.0)	80.9 (2.7)	75.6 (6.0)

Table 4.2. Profiles of Ca²⁺, PO₄³⁻-P, and pH in phases I-VII (unit: mg/L, standard deviation is in brackets).

Phases	Influent			Effluent			Reduced Ca ²⁺ / PO ₄ ³⁻ -P Molar ratio
	Ca ²⁺	PO ₄ ³⁻ -P	pH	Ca ²⁺	PO ₄ ³⁻ -P	pH	
Phase I (OLR 0.4)	92.3 (18.5)	55.1 (16.4)	7.5 (0.2)	58.4 (21.3)	31.9 (8.8)	8.5 (0.1)	1.1
Phase II (OLR 1.0)	89.6 (20.2)	50.8 (9.2)	7.4 (0.1)	54.2 (15.5)	28.4 (6.4)	8.0 (0.2)	1.2
Phase III (OLR 2.3)	86.2 (21.5)	39.1 (8.1)	7.8 (0.4)	52.2 (20.5)	20.5 (6.3)	8.1 (0.2)	1.4
Phase IV (OLR 5.1)	95.9 (20.2)	34.9 (10.7)	7.4 (0.3)	73 (19.2)	25.1 (3.7)	7.8 (0.2)	1.8
Phase V (OLR 9.3)	107.6 (19.2)	81.1 (18.6)	7.5 (0.3)	52.9 (28.4)	32.7 (7.4)	7.9 (0.1)	0.9
Phase VI (OLR 13.6)	120.0 (22.6)	102.8 (19.7)	7.6 (0.2)	50.5 (26.1)	42.0 (9.3)	8.0 (0.1)	0.9
Phase VII (OLR 16.0)	99.4 (16.1)	82.4 (19.8)	7.5 (0.2)	50.2 (16.7)	45.5 (9.4)	8.0 (0.1)	1.0

4.2.2 Water quality characterization and biogas analysis

Influent and effluent samples (20 mL) were collected twice a week and analyzed immediately. The biogas volume was measured every day, and the composition of biogas was measured twice a week. Influent and effluent total COD concentration, soluble COD concentration, suspended COD concentration, phosphate phosphorus and pH were determined according to the standard methods of the American Public Health Association (APHA) (Baird et al., 2017). The preparation of suspended COD and soluble COD samples followed the procedure reported by a previous study (Zhang et al., 2013). Influent and effluent ammonia nitrogen were measured using a Nessler Ammonia Quantification Reagent Kit. Biogas composition was measured with a syringe and

quantified using gas chromatography (GC) (7890B Agilent Technologies, Santa Clara USA; Column: Molsieve 5A 2.44 m 2 mm and Hayesep N 1.83 m 2 mm; carrier gas: argon; column temperature: 100 °C, injector temperature 150 °C, detector temperature 200 °C). Volatile fatty acids (VFAs) concentrations were analyzed by a Dionex ICS-2100 ion chromatograph equipped with an IonPac AS18 column and 4.5 mM carbonate/1.4 mM bicarbonate eluent (Dionex, Sunnyvale, CA). COD balance was calculated as previously reported (Zhang et al., 2021a).

4.2.3 Characterization of granular sludge

Extracellular polymeric substances (EPS) in the sludge granules were extracted using the formaldehyde-sodium hydroxide method with modifications (Liu and Fang, 2002): 5 mL sludge and 0.06 mL of 36.5% formaldehyde were mixed in a 15 mL polyethylene centrifuge tube and stored at 4°C for 1 h; 2 mL of 2N NaOH was added and the mixture was stored at 4 °C for 3 h, then centrifuged at 6000 rpm for 20 min; the supernatant was collected, filtered with a 0.22 µm membrane, and dialyzed for 24 h. Poly-saccharides in the EPS were measured by methods reported (DuBois et al., 1956), and the protein content in the EPS was measured using the modified Lowry method with bovine serum albumin as the standard (Fr/olund et al., 1995). The EPS samples were further used to obtain fluorescence emission-excitation matrix (EEM) spectra.

When each reactor operation phase was completed, the sludge samples were examined for structural morphology with a scanning electron microscope (SEM) (Zeiss Sigma 300 VPPESEM, USA). The element distribution on the sludge surface was determined by energy dispersive X-ray spectroscopy (EDX) (Bruker EDX system, USA). Sludge granules were placed in Petri dishes and photographed with a high-resolution camera (1024 × 768). Four sludge samples were collected at each sampling point. The sludge particle size distribution was determined by measuring the size

of 50 particles randomly selected in each photo. The precipitated species on the sludge surface were examined using X-ray diffraction (XRD) (Rigaku Ultimate IV, Japan). Concentrations of total suspended solids (TSS) and volatile suspended solids (VSS) were determined following standard methods (Baird et al., 2017).

4.2.4 Microbial community analysis

Sludge samples collected at the end of each phase were used for DNA extraction. 1.0 mL of each sludge sample was used for DNA extraction with a DNeasy PowerSoil Kit (QIAGEN, Hilden, Germany), following the manufacturer's protocol. NanoDrop One (ThermoFisher, Waltham, MA) was used to check the purity and concentration of DNA samples. All extracted DNA samples were stored at -20 °C. The microbial communities were analyzed for the 16S rRNA gene sequence. The sequence was amplified by the polymerase chain reaction (PCR) using primer sets with the sequencing adaptors 515F (5'- ACACTGACGACATGGTTCTAC AGTGYCAGCMGCCGCGGTAA-3') and 806R (5'- TACGGTAGCAGAGACT TGGTCTGGACTACNVGGGTWTCTAAT -3') (Apprill et al., 2015; Parada et al., 2016). DNA samples were sent to the Génome Québec Innovation Centre (Montréal, QC, Canada) for barcoding and sequencing on the Illumina Miseq PE250 platform previously described, using primer pair 515F/806R. The forward and reverse reads of the raw sequence were paired, quality-filtered, and chimera were removed using the “DADA2” algorithm in the QIIME2 pipelines (Callahan et al., 2016). Taxonomy was assigned using 99% similarity in the GreenGenes (version 13_8) reference database (McDonald et al., 2012; Werner et al., 2012). The Pearson's product momentum correlation coefficient was employed to assess the degree of correlation; “+” and “-” were used to present strong positive and strong negative correlations when the Pearson's coefficient (r) was > 0.5 and < -0.5.

4.2.5 Statistical analysis

All results are expressed as mean value and standard deviation (SD). Statistical significance was assessed using the student t-test in Microsoft Excel; $p < 0.05$ was statistically significant.

4.3 Results

4.3.1 Reactor performance

Fig. 4.1A shows influent and effluent concentrations of COD and the COD removal rate in the seven phases, each with a different organic loading rate (OLR). The influent total COD (COD_t) concentration was in the range of 2 g/L to 7 g/L. The effluent COD concentration was stable throughout the 250 days of operation (not including the start-up time), and ranged from 0.7 g/L to 1.0 g/L. The COD_t removal rate reached $78.0 \pm 9.6\%$ in Phase I, with an HRT of 8 d, and an OLR of 0.4 g COD/(L·d). The removal rates of COD_t in Phase II (HRT of 4 d, OLR of 1.0 g COD/(L·d)), Phase III (HRT of 2 d, OLR of 2.3 g COD/(L·d)), and Phase IV (HRT of 1 d, OLR of 5.1 g COD/(L·d)) were stable at $85.4 \pm 7.0\%$, $84.7 \pm 4.4\%$, and $83.0 \pm 3.5\%$, respectively. With further OLR increases to 9.3 g COD/(L·d) (Phase V, HRT of 0.5 d), 13.6 g COD/(L·d), (Phase VI, HRT of 0.3 d), and 16.0 g COD/(L·d) (Phase VII, HRT of 0.25 d), the removal rates of COD_t were slightly reduced to $76.0 \pm 9.0\%$ in Phase V, $80.9 \pm 2.7\%$ in Phase VI, and $75.6 \pm 6.0\%$ in Phase VII.

Fig. 4.1B shows the methane production potential (CH_4 -COD g/influent COD g) during the seven phases tested. During the first two phases (Phase I and Phase II), the methane production potential was $38.3 \pm 4.7\%$ and $42.7 \pm 4.0\%$, respectively. The methane production potential further increased in Phase III, and remained stable during Phase III, Phase IV, and Phase V, which

produced methane production potential of $52.7 \pm 9.5\%$, $48.7 \pm 7.6\%$, and $56.6 \pm 5.4\%$, respectively. The methane production potential increased to $58.0 \pm 4.5\%$ and $61.9 \pm 15.3\%$ in Phase VI and Phase VII, respectively.

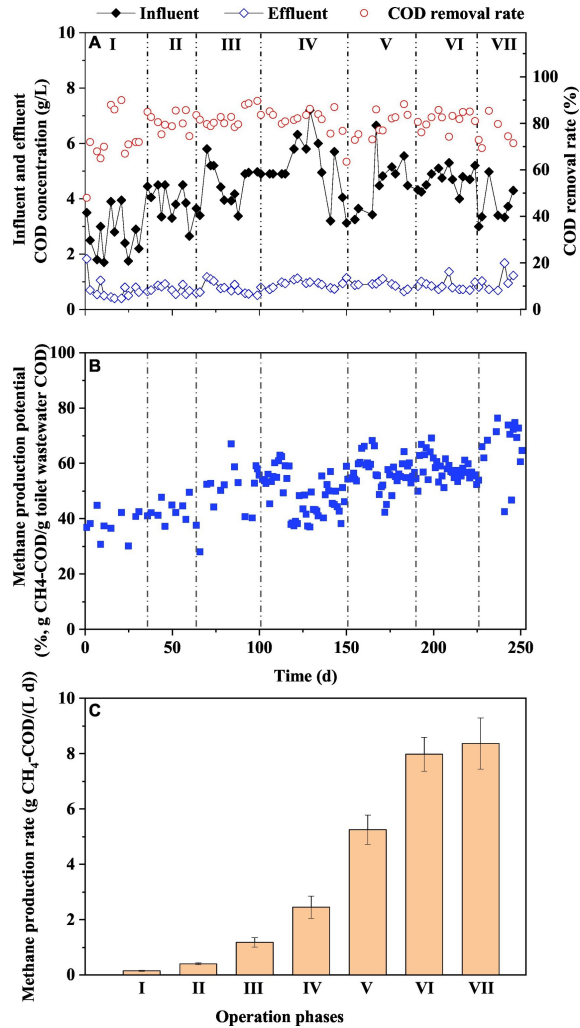


Fig. 4.1. Performance of UASB reactor during seven operation phases (A: Inluent and effluent total COD concentrations and COD removal rate; B: Methane yield; C: Methane production rate).

Our results showed stable reactor operation overall, and a high methane production potential was achieved under high OLR conditions. Our OLR of 16.0 g COD/(L·d) was significantly higher than the highest OLR previously reported, 4.1 g COD/(L·d) (Gao et al., 2019), for toilet wastewater treatment under mesophilic conditions. The detailed profiles of total COD, suspended COD, soluble COD, VFA and ammonia nitrogen concentrations in the influent and the effluent in Phase I-VII are given in **Table 4.1**.

Fig. 4.1C shows methane production rates in the UASB reactor treating toilet wastewater during seven operation phases. Methane production rates increased from 0.2 ± 0.02 g CH₄-COD/(L·d) in Phase I (OLR of 0.4 g COD/(L·d)), to 8.4 ± 0.9 g CH₄-COD/(L·d) in Phase VII (OLR of 16.0 g COD/(L·d)). The highest methane production rate in the present study (8.4 ± 0.9 g CH₄-COD/(L·d)) was higher than the methane production rate in (Gao et al., 2019b) (2.0 ± 0.2 g CH₄-COD/(L·d)), which indicates that a high performance in the UASB reactor was achieved in the present study.

4.3.2 COD mass balance

Fig. 4.2 presents the steady-state COD mass balance in the first six operation phases in the UASB reactor. The partition of influent total COD (COD_t) includes COD converted to methane, COD in the effluent, COD accumulated in the reactor, COD in the waste sludge, and unknown COD. Effluent COD accounted for only 14.6% - 24.4% of the input COD, indicating an effective COD removal throughout the seven phases of operation. The proportion of the input COD that was converted to methane increased significantly from 38.3% in Phase I to 61.9% in Phase VI. The COD accumulated in the UASB reactor varied from 1.0% to 9.8% throughout the operation period. The COD in wasted sludge accounted for 12.2% to 16.9% of the input COD. The sum of the output

COD accounted for 81.3% - 99.5% of the input COD, indicating a satisfactory development of COD balance (Gao et al., 2019b).

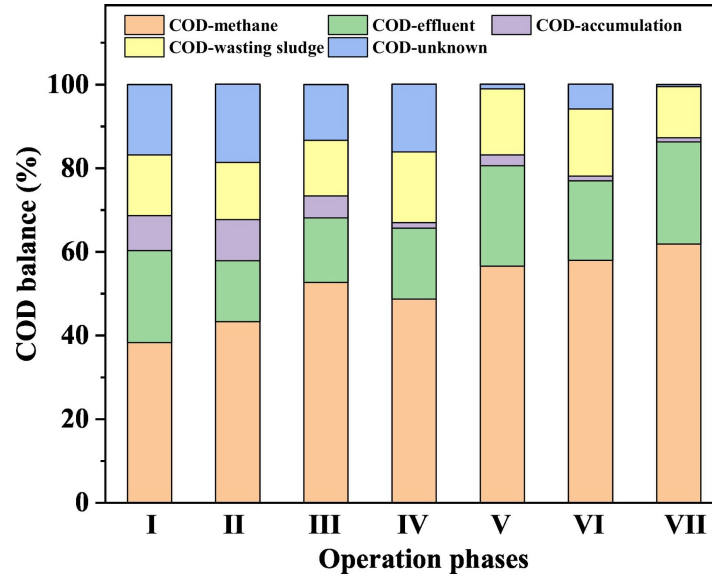


Fig. 4.2. COD mass balance of UASB reactor treating toilet wastewater at different hydraulic retention time (HRT), the partition of influent COD considered includes COD for methane production, effluent COD, COD accumulation in sludge, COD in discharged sludge and unknown COD.

4.3.3 Sludge bed development

Fig. 4.3A shows the seven phases of the UASB reactor operation. Concentrations of total suspended solids (TSS) and volatile suspended solids (VSS) in the seed sludge were 11.7 ± 0.3 g/L and 10.2 ± 0.2 g/L, respectively. The sludge bed height was 22.5 cm (the height of the reactor was 30 cm). In the first three phases, the VSS concentration ranged between 9.1 ± 0.6 g/L and 11.3 ± 0.8 g/L, which is in the range of commonly reported VSS in UASBs treating toilet wastewater (Luostarinen et al., 2007). In Phase IV to Phase VII, the VSS concentration increased

significantly, from 14.2 ± 2.2 g/L to 25.9 ± 0.3 g/L. The TSS followed a trend like that of the VSS throughout the experiment. The slow decrease of the VSS/TSS ratio, from 0.87 ± 0.02 in seed sludge to 0.76 ± 0.01 in Phase VII is in the range of commonly reported studies of granular sludge (Lens et al., 1998; Subramanyam, 2013), and can be attributed to the accumulation of inorganic compounds in the sludge (to be further discussion in Section 4.3.5).

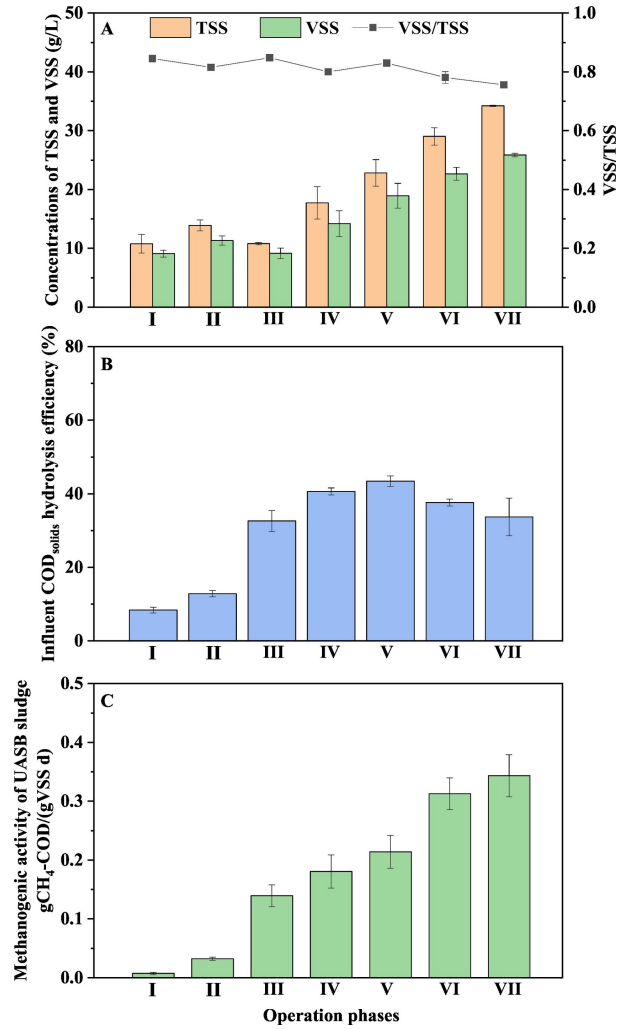


Fig. 4.3. The concentrations of TSS and VSS and the ratio of VSS/TSS (A), the influent COD_{solids} hydrolysis efficiency (B), and methanogenic activity (C) of UASB reactor treating toilet wastewater at different organic loading rates (OLR). Error bars represent one standard deviation.

In the anaerobic treatment of toilet wastewater, the rate-limiting step is the hydrolysis of particulate organic substrates (de Graaff et al., 2010; Gao et al., 2019b). The hydrolysis of solid COD was stable from Phase III to Phase VII (Fig. 4.3B), with a hydrolysis efficiency of $32.6 \pm 2.8\%$ to $43.4 \pm 1.4\%$, indicating a stable condition in the UASB reactor (de Graaff et al., 2010).

The methanogenic capacity of the UASB sludge is shown in **Fig. 4.3C**. The methanogenic activity of the UASB sludge remained stable from Phase III to Phase V, in a range of 0.14 ± 0.002 g CH₄-COD/(gVSS·d) to 0.21 ± 0.03 g CH₄-COD/(gVSS·d). The methanogenic activity increased in Phase VI to 0.31 ± 0.03 g CH₄-COD/(gVSS·d) and Phase VII to 0.34 ± 0.04 g CH₄-COD/(gVSS·d).

4.3.4 Granules size and granule EPS content

Proteins and polysaccharides are the main components in the extracellular polymeric substances (EPS) secreted by anaerobic granular sludge. An EPS content of 96.5-115.8 mg/g VSS was achieved in the granular sludge during mesophilic anaerobic toilet wastewater treatment (**Fig. 4.4**). The sludge had a protein concentration of 91.5-105.6 mg/gVSS (**Fig. 4.4 A**) and a polysaccharide concentration of 3.7-10.2 mg/gVSS. EEM fluorescence spectra of sludge granules in the EPS in Phase I and Phase IV (**Fig. 4.5**) show that the major EPS components contained aromatic protein-like substances (EX/EM 280/360 and 230/360). The average diameter of the sludge granules increased from 0.55 mm in Phase I to 1.1 mm in Phase IV, maintaining an average diameter of 1.1 mm in later phases (**Fig. 4.4B**). Correspondingly, the protein/polysaccharide ratio in the EPS increased from 11.5-15.9 in Phase I to Phase III and increased to 18.3-25.5 in the last phases of the experiment.

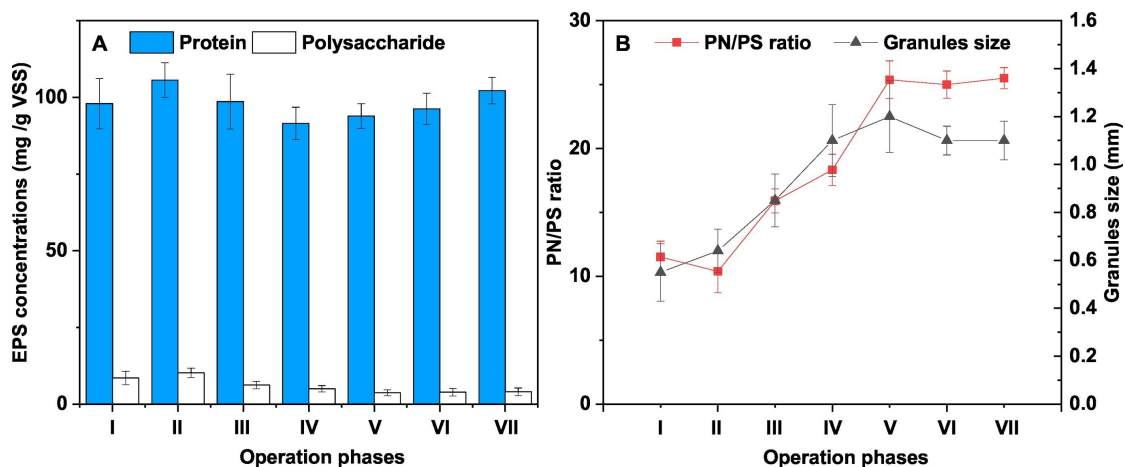


Fig. 4.4. Protein and polysaccharide contents in EPS of the granules (A), granules diameter and PN/PS ratio (B) during the operation phases.

The protein/polysaccharide contents (~ 110 mg/g VSS) in the EPS agree with those reported in previous studies (Ismail et al., 2010; Zhu et al., 2015). The protein in the EPS bonds with cations (Ca^{2+} and Mg^{2+}) and reduces the surface charge of the UASB sludge. Zhu et al. reported that the protein in EPS had a negative linear correlation with the surface charge (Zhu et al., 2015). Gagliano et al. found that the hydrophobicity of the protein enhanced aggregation of the anaerobic biomass (Gagliano et al., 2020). Lu et al. found that a low protein/polysaccharide ratio was associated with poor settleability of the granular sludge, due to the hydrophilic nature of polysaccharides, and that a high polysaccharide concentration decreased the hydrophobicity and led to poor biomass aggregation (Lu et al., 2015). The protein/polysaccharide ratio depends on environmental conditions (temperature, substrate type, salinity), and is often found to be stable in steady-state conditions (Dubé and Guiot, 2019; Hudayah et al., 2019).

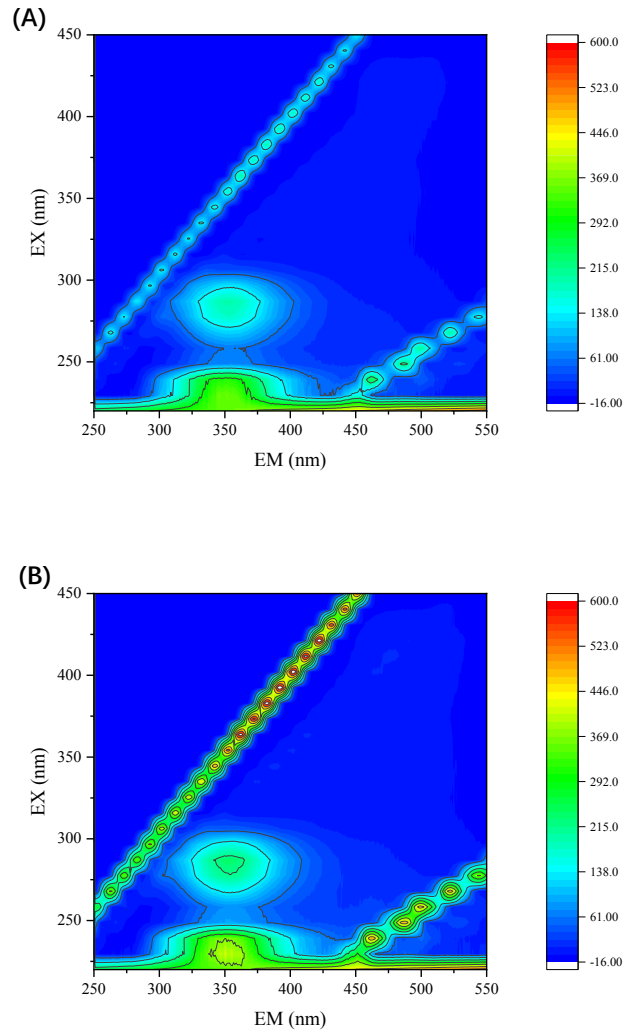


Fig. 4.5. EEM fluorescence spectra of sludge EPS during anaerobic sludge granulation (A) Phase I and (B) Phase IV.

4.3.5 Characteristics of granular sludge in the reactor

Granular sludge was first observed at the end of Phase I of reactor operation. The distribution of granular sludge was relatively consistent from Phase IV to VII. **Fig. 4.6A** shows a digital camera image of the anaerobic granules. At low magnification ($\times 100$), SEM images show the rough surfaces and the porous structures of the granules, revealing channels for the transportation of

substrates and gases, as reported in previous study (Jiraprasertwong et al., 2020). The sludge distribution shown in **Fig. 4.6B** is based on granule diameters of 0.2–0.5 mm (10.8%), 0.5–0.7 mm (20.7%), 0.7–1 mm (11.3%), and ≥ 1 mm (57.2%). Considering sludge particles larger than 0.5 mm to be granular sludge, granular sludge accounted for 89.2% of the UASB sludge bed in this study (Jiraprasertwong et al., 2020).

Fig. 4.6C is a scanning electron microscopy (SEM) image of granules in the UASB reactor; **Fig. 4.6D** shows the SEM energy dispersive X-ray spectroscopy (SEM-EDX) results of the granules shown in **Fig. 4.6C**. Three granules were randomly selected to measure the elemental mole ratio of the granule surface by SEM-EDS. The dominant elements in the granules are carbon ($71.0 \pm 1.6\%$), nitrogen ($2.5 \pm 0.5\%$), oxygen ($22.7 \pm 0.6\%$), sodium ($0.2 \pm 0.05\%$), magnesium ($0.08 \pm 0.03\%$), calcium ($1.3 \pm 0.6\%$), aluminum ($0.1 \pm 0.08\%$), silicon ($0.6 \pm 0.2\%$), sulfur ($0.5 \pm 0.04\%$), chlorine ($0.09 \pm 0.1\%$), and phosphorous ($0.9 \pm 0.3\%$). Based on this information, we assume the granules are composed predominantly of calcium phosphate precipitates, with a Ca/P ratio of 1.49 ± 0.13 (Fig. 4D). The carbon detected in the granules was likely associated with the biomass. The profiles of Ca^{2+} and PO_4^{3-} concentrations in influent and effluent are given in **Table 4.2**. The UASB removed $\text{Ca}^{2+}/\text{PO}_4^{3-}$ -P ratios (0.9-1.8) were close to the SEM-EDS results, indicating that the CaP precipitated in the UASB reactor from the toilet wastewater and contributed to the formation of CaP rich granules.

Fig. 4.6E shows an X-ray diffraction (XRD) pattern of a dried and ground granule from the UASB reactor. XRD analysis identified amorphous calcium phosphate (ACP), $\text{Ca}_3(\text{PO}_4)_2 \cdot x\text{H}_2\text{O}$, a Ca/P ratio of 1.5, tricalcium phosphate (TCP), and $\text{Ca}_3(\text{PO}_4)_2$. This result agreed with the Ca/P ratio of 1.49 ± 0.13 acquired by SEM-EDS analysis.

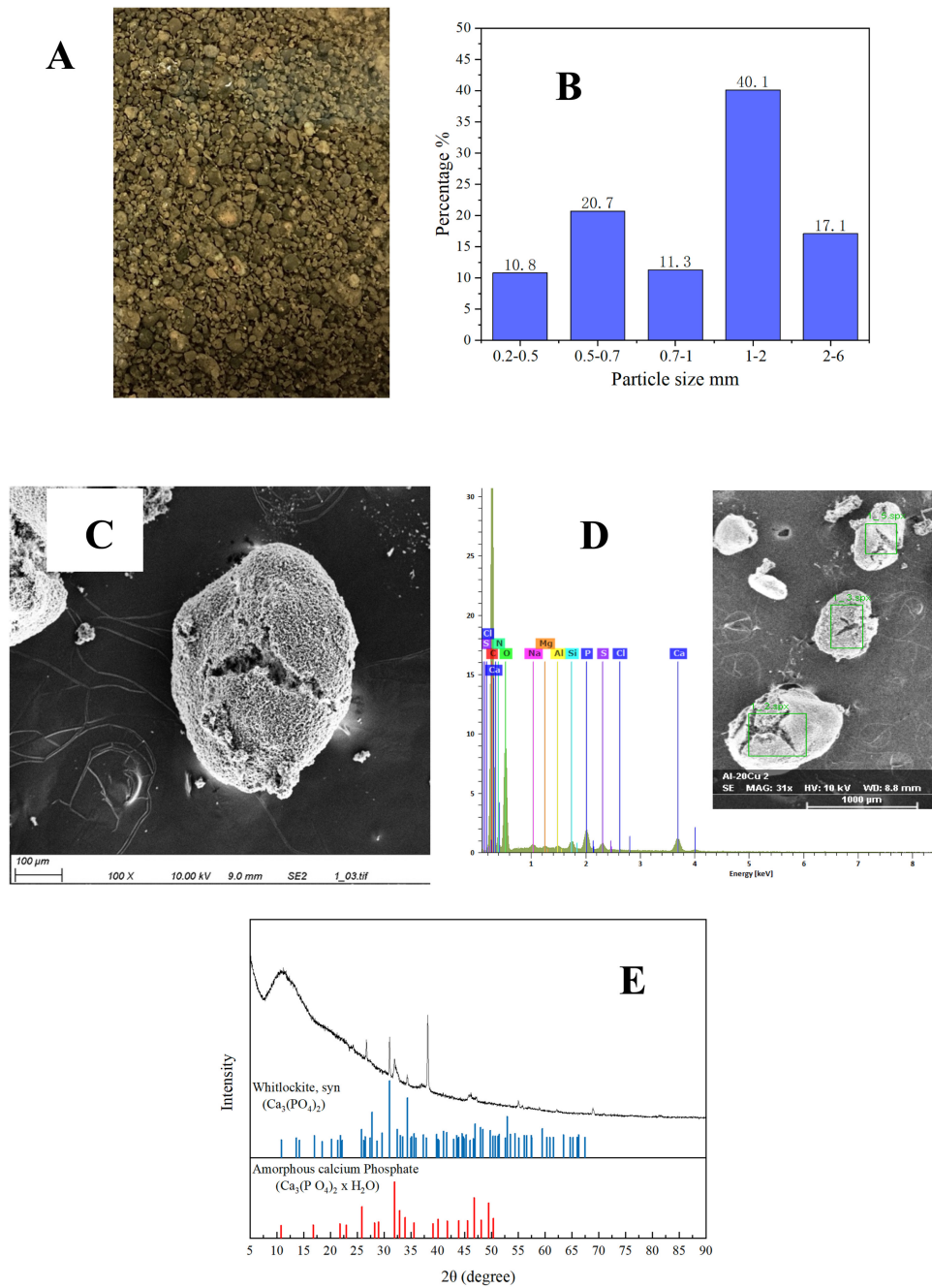


Fig. 4.6. Granular sludge and particle size distribution in UASB reactor (A: Granule formation in the UASB reactor; B: Particle size distribution of granular sludge; C: SEM pictures of granular sludge; D: SEM-EDS images of granules; E: XRD pattern of a granule).

4.3.6 Microbial community

Microbial community analyses were carried out in Phase I, Phase III, and Phase IV. The anaerobic granules started to form in Phases I and II, they grew larger in Phase III, and matured in Phases IV-VII, increasing in diameter from 0.54 mm (Phase I) to 1.1-1.2 mm (Phases IV-VII) (**Fig. 4.7**).

In Phase I, the top 10 Bacterial genera in the anaerobic granules were mainly affiliated with the orders *Bacteroidales* (uncultured 11.8%, *Blvii* 3.9% and *Paludibacter* 1.4%), *Cloacamonales* (uncultured 1.1%, *W22* 5.4%, and *Candidatus Cloacamonas* 3.9%), and *Syntrophobacterales* (*Syntrophus* 5.2%). When the granules had matured, *Syntrophus* was the most abundant (16.2%) in Phase IV, followed by an uncultured genus from the order *Bacteroidales* (9.0%), *W22* (6.2%), and an uncultured genus from the order *SHA-98* (4.2%). The other top Bacterial genera decreased or disappeared in Phase VI. The order *Bacteroidales* was a significant portion of fecal Bacterial population. *Bacteroidales* can hydrolyze and ferment carbohydrates and proteins and contributed to the dominance of the uncultured genera from the order *Bacteroidales* throughout the study period. *Paludibacter* was classified as a VFA producer because of its ability to ferment sugars, and it was enriched from 1.3% in Phase I to 3.1% in Phase IV. *Syntrophus* was highly enriched and increased with an increase in organic loading rate and with the development of granular sludge. *Syntrophus* was reported to be present in anaerobic granules, where it contributed to hydrogen production through hydrolysis and fermentation (Wang et al., 2017).

In the Archaea population, dominant methanogens in the anaerobic granules were diverse. The acetoclastic *Methanosaeta* (17.7%), the hydrogenotrophic *VadinCA11* (28.2%), and *WSA2* (20.4%) were dominant in Phase I. The relative abundance of *Methanosaeta* (8.7% in Phase III and 6.4% in Phase IV), which was the Archaea member believed to be important in granular sludge

formation, decreased with an increase in organic loading rate and with the development of granules in Phases III and IV. In Phase IV, the dominance of *WSA2* (23.1%) was evident, followed by *VadinCA11* (18.0%), *Methanoculleus* (17.4%) and *WCHD3-30* (16.4%), which are all hydrogenotrophic methanogens. Overall, it was observed that the growth of the granules was first promoted with the development of the acidogenic and syntrophic bacteria (*Bacteroidales* and *Syntrophobacterales*) and *Methanosaeta*, as shown in **Fig. 4.7**. Acidogenic bacteria have been reported to be important in sludge granule formation due to their EPS production (Liu and Fang, 2002). However, with further maturation of the granular sludge, syntrophic bacteria *Syntrophus*, together with diverse H₂-utilizing methanogens, proliferated, and eventually resulted in a hydrogenotrophic dominant pathway in Phase IV.

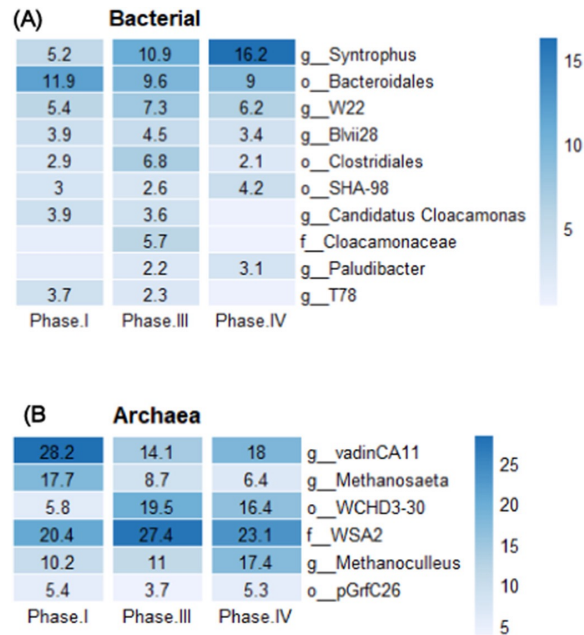


Fig. 4.7. Relative abundances of top 10 bacterial genera (A) and top 6 archaeal genera (B) in the anaerobic granules. Unidentified genera were named using higher taxonomic levels, family and order (f__ and o__).

Interestingly, *Syntrophus* and *Blvii28* are important in direct interspecies electron transfer (DIET) (Guo et al., 2020). There is a potential for DIET in anaerobic granular sludge, depending on environmental conditions (substrate type, organic loading rate, the presence of conductive materials), but no direct proof of DIET has been shown in anaerobic granules. The correlation results show that *Syntrophus*, *SHA.98*, *Paludibacter*, *WCHD3-30*, and *Methanoculleus* had strong positive correlations with the granular size and the protein/polysaccharide ratio (as shown in **Fig. 4.8**).

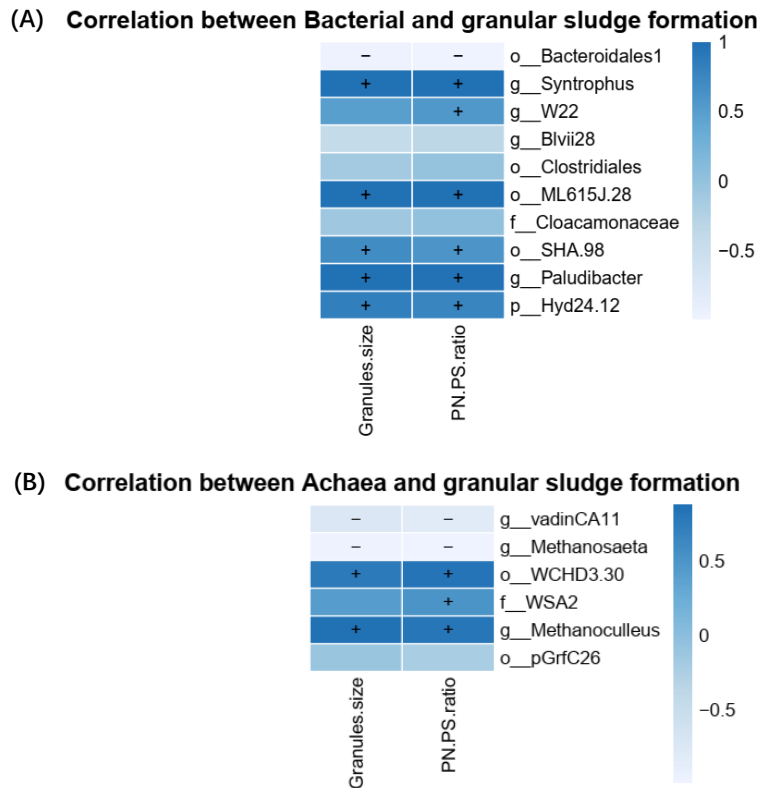


Fig. 4.8. Pearson's correlation between sludge granules microbial community and granules size and PN/PS ratio in the EPS of the granules. The color key indicates the strength of correlation coefficient. (A) Correlation between Bacterial and granular sludge formation; (B) Correlation between Achaea and granular sludge formation.

4.4 Discussion

4.4.1 Anaerobic granules significantly increased the performance of the UASB

The mesophilic anaerobic treatment of toilet wastewater in this study achieved a high OLR of 16.0 kg COD/(m³·d) under a short hydraulic retention time (HRT) of 0.25 d. The removal efficiency and methanogenesis efficiency reached 75.6 ± 6.0% and 61.9 ± 15.3%, respectively. The reactor performance was steady over the entire operation. The high performance was first observed in the anaerobic treatment of toilet wastewater, and this is attributed to the anaerobic granules formed in the sludge bed. (Gao et al., 2019b) did not observe anaerobic granule formation and achieved an OLR of 4.1 kg COD/(m³·d). (Tervahauta et al., 2014b) reported anaerobic granules formed in anaerobic toilet wastewater treatment at 25 °C and a low OLR of 1.1 kg COD/(m³·d).

In the present study, the methanogenic activity of the anaerobic granules was 0.34 ± 0.04 g CH₄-COD/(gVSS·d). Hydrogen and acetate are the main substrates of anaerobic digestion. The observed high methanogenic activity indicated effective hydrogen and acetate utilization in the anaerobic granules. The biodegradation of propionate was thermodynamically favorable only under a low hydrogen partial pressure (10⁻⁴ atm). It requires juxtaposition between acetogens and hydrogen-utilizing methanogens as a prerequisite for syntrophic propionate degradation (Gonzalez-Gil et al., 2001). Otherwise, the accumulation of hydrogen and acetate leads to an increase in the concentration of VFAs and a drop in pH that can result in UASB operation failure (Zhang et al., 2020c).

Anaerobic granules have well-structured multilayers (Macleod et al., 1990), with close proximity between heterogeneous bacteria, syntrophic bacteria, and methanogens (Baloch et al., 2008). This tight spatial arrangement among microorganisms enables microbes involved in the interdependent

anaerobic digestion processes (hydrolysis of organic solids, acidogenesis, acetogenesis, methanogenesis) to achieve an effective syntrophic interaction (Fang et al., 1995; Harmsen et al., 1996; Sekiguchi et al., 1999).

The anaerobic granules achieved a high volatile suspended solids (VSS) concentration (25.9 ± 0.3 g/L). This was attributed to a longer sludge retention time due to the higher density of anaerobic granules compared with the anaerobic floc sludge. The high biomass obtained would be expected to enhance hydrolase excretion and promote hydrolysis efficiency. The hydrolysis efficiency in the present study ($32.6 \pm 2.8\%$ to $43.4 \pm 1.4\%$) was higher than the hydrolysis efficiency reported by (Gao et al., 2019b) ($29.5 \pm 5.2\%$ - $33.2 \pm 5.0\%$), where no anaerobic granules were observed. The high hydrolysis efficiency in the present study enabled a short hydraulic retention time (HRT) of 6 h to be achieved. A short HRT can reduce the reactor volume significantly, extending its application. The methane produced in anaerobic toilet wastewater treatment can be used to heat the UASB reactor.

As demonstrated in this study, $75.6 \pm 6.0\%$ of influent COD and $46.5 \pm 10.8\%$ of phosphate phosphorus (data shown in **Table 4.1** and **Table 4.2**) can be removed from the reactor. However, the treated effluent still contains 0.8 ± 0.1 g/L COD, 0.9 ± 0.04 g/L $\text{NH}_4\text{-N}$ and 32.3 ± 8.9 mg/L $\text{PO}_4^{3-}\text{-P}$. Post-treatment of the UASB effluent is needed to meet the wastewater discharge or reuse standards.

4.4.2 Formation of anaerobic granules in anaerobic toilet wastewater treatment

Only one other research group has reported the formation of anaerobic granules during anaerobic toilet wastewater treatment (Tervahauta et al., 2014b). Interestingly, (de Graaff et al., 2010) did not observe anaerobic granule formation in anaerobic toilet wastewater treatment when operating

a UASB reactor for 951 days. Therefore, it is important for future reactor design and operation to explain the formation of anaerobic granules in anaerobic toilet wastewater treatment.

This study is the first to describe the microbial community in the anaerobic granules in anaerobic toilet wastewater treatment. *Methanosaeta* was an important member of the archaea community (6.4% - 8.7%); other archaea were hydrogenotrophic methanogens. This observation differs from other reported studies of anaerobic granules, in which *Methanosaeta* was the predominant methanogen (Faria et al., 2019). This difference can probably be attributed to the difference in up-flow velocity applied in anaerobic toilet wastewater treatment and traditional anaerobic granular reactors (Van Lier et al., 2016). In particular, a high up-flow velocity was often used in previous studies to select anaerobic granular sludge by washing out biomass unnecessary for granule formation (Van Lier et al., 2016). *Methanosaeta* is known to be more hydrophobic than other methanogens, which allows them to quickly develop as core “biocarriers;” thus, *Methanosaeta* are retained in anaerobic reactors operated with high up-flow velocity (Zheng et al., 2006). Under the stressful condition of high up-flow velocity, extracellular polysaccharide substances (EPS) excreted by Bacteria worked as a glue to build up the microbial multilayers discussed in Section 4.1 (Faria et al., 2019). However, in the present study, the up-flow velocity in the UASB reactor treating toilet wastewater was below 0.1 m/h, which is much lower than the up-flow velocity (> 0.5 m/h) applied in traditional anaerobic granule reactors (Subramanyam, 2013). This means that *Methanosaeta*, working as the nuclei of the granules, might not be very important. The hydrogenotrophic methanogens were able to retain and proliferate in the UASB treating toilet wastewater.

It was noted that calcium phosphate precipitated in the anaerobic granules during anaerobic toilet wastewater treatment. A similar observation has been reported (Tervahauta et al., 2014b; Zhang

et al., 2021a). Positively charged calcium ions may facilitate granular sludge formation by adhering to negatively charged bacterial cells and bridging the sludge aggregates. This process can also be accompanied by the formation of calcium phosphate (under high localized pH [> 7.9] and concentrated Ca^{2+} conditions) (Cunha et al., 2019; Cunha et al., 2018a). Calcium phosphate granules (instead of, or in addition to *Methanosaeta*) might serve as granular sludge nuclei. (Zhang et al., 2021a) reported that the rapid hydrolysis of protein or urea in thermophilic toilet wastewater treatment led to an increase in pH, which could facilitate calcium phosphate precipitation. In the present study, CaP precipitated under undersaturated conditions (supersaturation index < 0), which may be explained by the microbial-induced localized chemical environment (e.g. high located pH and Ca^{2+} concentration) that is thermodynamically favorable for P precipitation. Future studies are needed to better elucidate the mechanism associated with such processes.

The formation of anaerobic granules in the UASB treatment of toilet wastewater has two practical advantages. (1) A critical up-flow velocity is not necessary. A lower up-flow velocity not only benefits the hydrolysis of organic matter present in toilet wastewater, it also avoids the design requirements (strict high height-to-diameter ratios and/or recirculation) to maintain a high up-flow velocity. (2) Anaerobic granules, rich in phosphate, can be easily collected at the bottom of the reactor (due to their higher density) and used as fertilizer, or donated to the phosphate refinery industry. Moving forward, a pilot community-scale demonstration of the high-rate UASB reactor with CaP granular sludge for toilet wastewater treatment will provide field knowledge and further support technology development and implementation.

4.5 Conclusions

This study showed that vacuum toilet wastewater can be effectively treated under mesophilic anaerobic conditions using a UASB reactor at a high organic loading rate (OLR). A chemical oxygen demand (COD) removal efficiency of $75.6 \pm 6.0\%$ and a methane production potential of $61.9 \pm 15.3\%$ were achieved with a hydraulic retention time (HRT) of 0.25 day and an organic loading rate (OLR) of 16.0 g COD/(L·d). The formation of calcium phosphate granular sludge observed in this reactor increased the methanogenic activity of the UASB sludge and enhanced the hydrolysis of particulate COD. Amorphous calcium phosphate (ACP), $\text{Ca}_3(\text{PO}_4)_2 \cdot x\text{H}_2\text{O}$, a Ca/P ratio of 1.5, tricalcium phosphate (TCP), and $\text{Ca}_3(\text{PO}_4)_2$ were the most prominent CaP species in the granules. Protein was dominant in the extracellular polymeric substances (EPS) of the granular sludge, and the high protein/polysaccharide ratio was likely beneficial to granule settleability. A hydrogenotrophic methanogenic pathway was dominant in mature granules, and microbes related to the formation of granules were enriched in this study.

**CHAPTER 5 ANAEROBIC CO-DIGESTION OF POT ALE AND SPENT
CAUSTIC WASTEWATER: IMPACTS ON PERFORMANCE STABILITY
AND MICROBIAL COMMUNITY DYNAMICS**

A version of this chapter has been submitted.³

³ Mou, A., Yang, X., Yu, N., Mohamed A., and Liu, Y. Anaerobic co-digestion of pot ale and spent caustic wastewater: Impacts on performance stability and microbial community dynamics.

5.1 Introduction

The distillery industry, a major contributor to the global economy due to its expansive market and substantial revenue generation, faces pressing environmental challenges that necessitate effective and sustainable waste management solutions (Gunes et al., 2019). In the process of distillery production, for every liter of malt alcohol, approximately 8-15 liters of high-strength organic wastewater are generated (Gunes et al., 2021a). The distillery process comprises four main stages- mashing, fermentation, and two subsequent distillations (Gunes et al., 2019). The first distillation (spirit still) produces pot ale wastewater with a light-yellow color, high COD, low pH, and challenging biodegradability due to spent grains and yeast (Mallick et al., 2010a). The second distillation (wash still) generates spent caustic wastewater, notable for its dark brown color, high pH, high salinity, and biodegradable organics (Moraes et al., 2015). Given the rigorous regulations governing the disposal of distillery wastewater, there is a growing imperative to convert these by-products into economically and environmentally beneficial resources, aligning with global efforts to decarbonize key industries.

Treating wastewater from the distillery industry is crucial due to the need to remove toxic substances before their release into aquatic environments. Some treatment methods, such as coagulation and flocculation, adsorption, and oxidation, aim to eliminate high levels of COD, BOD, total nitrogen, and phosphates to prevent the eutrophication of water bodies (Bes-Piá et al., 2003; Jain et al., 2005; Mohana et al., 2009; Satyawali and Balakrishnan, 2008). However, these methods frequently fall short in terms of cost-effectiveness. In contrast, anaerobic digestion (AD) offers significant environmental benefits by converting various distillery wastewaters into biogas, thus generating bioenergy (Gunes et al., 2019). This process not only improves the energy balance but also enhances the economic viability of the industry. Despite its advantages, AD faces

challenges, particularly with pot ale wastewater, which is difficult to degrade due to its complex carbohydrates like dextrin, spent yeast, and coagulated protein (White et al., 2020). The robust cell walls of spent yeast, composed of phosphomannans, chitins, glucans, and proteins, pose additional barriers to degradation (Mallick et al., 2010a). Mono-digestion of pot ale typically requires a long hydraulic retention time and is further complicated by low biodegradability and inhibition due to its acidic pH and inefficient hydrolysis (Ripoll et al., 2022). To address these challenges, pre-treatment methods such as chemical, mechanical, thermal, and biological processes are employed to enhance hydrolysis of refractory organic matter (Ariunbaatar et al., 2014; Cesaro and Belgiorno, 2014; Toreci et al., 2009). For example, alkaline pre-treatment has proven particularly effective for pot ale, helping to balance its acidity and facilitate the release of cellular substances by swelling particles and solubilizing hemicellulose (Okolie et al., 2022). Conversely, spent caustic wastewater is generally unsuitable for AD due to its extremely high pH (greater than 13). Although pH neutralization can make AD feasible, this process requires substantial acid use, which increases the salinity and toxicity of the wastewater and reduces the efficiency of AD.

Anaerobic digestion of a single waste stream can face challenges at high organic loading rates (OLR), often due to nutrient imbalances, inadequate carbon/nitrogen (C/N) ratios, accumulation of volatile fatty acids (VFA), high total ammoniacal nitrogen, and pH destabilization from low buffering capacity (Kainthola et al., 2019; Xing et al., 2020; Zhu et al., 2008). To address these challenges, anaerobic co-digestion, which represents the simultaneous digestion of two or more types of organic matter, emerges as an effective improvement strategy. This approach not only mitigates the inhibitory effects through dilution but also enhances the C/N ratio, balances nutrients, and improves methane production kinetics, allowing for operation at higher OLRs (Sillero et al.,

2024). Furthermore, co-digestion offers significant economic and technological savings by utilizing shared facilities for managing multiple waste streams simultaneously (Tena et al., 2021). Previous studies have explored various combinations of waste types for co-digestion, including olive mill wastewater with poultry manure, food waste with cattle manure, and food waste with blackwater (Gao et al., 2020; Khoufi et al., 2015; Wang et al., 2020c). Recent studies have identified distillery wastewaters, with their complex organic content, as particularly attractive feedstocks for anaerobic co-digestion (Gunes et al., 2019). Especially, studies focusing on the co-digestion of distillery wastewater have reported enhanced methane production using co-substrates such as distillery sludge with spent yeast, sewage sludge with distillery wastewater, sugarcane press mud with distillery effluent, and distillery wastewater with dairy cattle manure and cheese whey (Akassou et al., 2010; Duguma et al., 2024; Evidente et al., 2021; Ripoll et al., 2022). However, these studies predominantly involved batch experiments to test optimal conditions and often potentially entailed significant transportation costs due to the disparate origins of the co-substrates. There has been no research on the long-term reactor operation of anaerobic co-digestion involving different streams from the same distillery facility.

Therefore, this study aims to assess the feasibility of long-term operation of anaerobic co-digestion of two primary wastewaters generated at a distillery facility: spent caustic wastewater and pot ale wastewater, using up-flow anaerobic sludge blanket (UASB) reactors under mesophilic conditions. The research evaluates the impact of adding spent caustic wastewater as a co-substrate to pot ale wastewater and compares this to the mono-digestion of pot ale wastewater alone. The performance and sludge characteristics of two UASB reactors were analyzed at different organic loading rates. Additionally, this study explores the microbial communities in the anaerobic granular sludge of

both reactors to understand the mechanisms underlying different performance, providing critical insight into the anaerobic co-digestion process of distillery wastewaters.

5.2 Materials and Methods

5.2.1 Distillery wastewater and inoculum

Two types of distillery wastewaters-spent caustic wastewater and pot ale wastewater-were obtained from a Canadian distillery facility and were stored at 4°C prior to use. Spent caustic wastewater was collected from a spent caustic tank during the cleaning process, and pot ale wastewater was obtained from a condensate holding tank following the cleaning of a rectifying column. The characteristics of wastewater were conducted in 48 hours. Anaerobic granular sludge, used as the seed sludge, was collected from an anaerobic reactor treating molasses wastewater from Alberta, Canada.

5.2.2 Batch co-digestion experiments

Different volume ratios of spent caustic wastewater and pot ale wastewater were mixed for one hour. After mixing, pH, TCOD, soluble chemical oxygen demand (SCOD), and total dissolved solids (TDS) of co-substrates were measured. Biochemical methane potential (BMP) tests were performed to assess the methane production potential of co-substrates with different volume ratios. The inoculum, granular sludge, for the BMP test was obtained from a mesophilic anaerobic digester treating molasses wastewater with a VSS of around 25 g/L. For each BMP test, 45 mL of anaerobic granular sludge was mixed with 45 mL substrates and placed into a 167 mL serum bottle. Nine groups of batch experiments were conducted based on different substrates. In the control group, deionized water was mixed with the seed sludge to determine its endogenous methane

production capabilities. Spent caustic wastewater, pot ale wastewater, and their co-substrates (S:P volume ratios of 1:1, 1:2, 1:3, 1:4, 1:5, and 1:6) were used as feedstocks for the experimental groups. The headspace of the bottles was filled with nitrogen gas, sealed with rubber stoppers and aluminum caps, and incubated at 120 rpm and 35°C in darkness. Each experimental setup was replicated three times. The headspace pressures and gas compositions were measured every 1-2 days over a period of 15 days.

5.2.3 Reactor operation

Two lab-scale up-flow anaerobic sludge blanket (UASB) reactors were employed for the distillery wastewater treatment under mesophilic conditions. The feedstocks for the pot ale wastewater UASB reactor (R1) and the co-digestion UASB reactor (R2) consisted of pot ale wastewater and a co-substrate of pot ale wastewater and spent caustic wastewater at a 5:1 volume ratio, respectively. R1 was operated over three stages: stage 1 with an organic loading rate (OLR) of 3.7 ± 0.9 g/L/d, stage 2 at 7.6 ± 3.9 g/L/d, and stage 3 at OLR of 11.2 ± 0.9 g/L/d. The hydraulic retention times (HRTs) of R1 were 19.6 ± 5.3 days, 12.4 ± 4.4 days, and 10.7 ± 0.7 days for stage 1, stage 2, and stage 3, respectively, over a duration of 130 days. R2 was operated through four stages: stage 1 at an OLR of 3.9 ± 0.8 g/L/d, stage 2 at 8.8 ± 2.0 g/L/d, stage 3 at 11.8 ± 2.1 g/L/d, and stage 4 at 13.6 ± 3.8 g/L/d. The HRTs of R2 were 19.8 ± 3.9 days, 11.0 ± 2.0 days, 7.7 ± 1.1 days, and 7.3 ± 2.9 days at stage 1, stage 2, stage 3, and stage 4, respectively, over 200 days. The COD removal and methane production rate were monitored every 2-3 days.

5.2.4 Analytical methods

TCOD, SCOD, ammonia, phosphate, total phosphorus (TP), alkalinity, hardness, total suspended solids (TSS), volatile suspended solids (VSS), and TDS were measured in accordance with the

Standard Methods (APHA, 2012). For biogas collection, foil gas bags (CHROMSPEC™, Brockville, Canada) were utilized. The composition of the biogas was analyzed using a gas chromatograph (GC, 7890B Agilent Technologies, USA) equipped with a Hayesep Q column and a thermal conductivity detector. Helium, with a purity of 99.999 %, was used as the carrier gas. The oven and detector were maintained at temperatures of 100°C and 200°C, respectively.

Methane production rate and hydrolysis efficiency were calculated following a previous study (Mou et al., 2024). Methane production rate is defined as the fraction of influent TCOD that is converted to methane (%), $\text{g CH}_4\text{-COD/g TCOD}$. Hydrolysis efficiency refers to the proportion of the feed particulate COD that is hydrolyzed (%). The influent COD can be apportioned into four distinct pathways: conversion to methane, discharge in effluent, discharge in waste sludge, and accumulation in reactor sludge bed. The mass balance for the influent COD was performed according to the procedures described by the previous study (Mou et al., 2024).

5.2.5 Sludge characteristics

The methane production capacity of the sludge in the reactor was assessed by sampling from the sludge bed at the end of each stable operational stage. To account for the uneven distribution of sludge bed, three samples of 20 mL each were taken from the top, middle, and bottom layers, which were then combined to get a representative sample. The specific methanogenic activity (SMA) of the sludge was measured to determine the capacity to convert acetate or H_2/CO_2 into CH_4 . Additionally, sludge stability was assessed to identify the percentage of biodegradable substrate present in the sludge. The SMA and sludge stability of each sludge sample were evaluated following the methodologies described in previous studies (Mou et al., 2022a; Mou et al., 2024). All tests were conducted in triplicate.

5.2.6 Microbial community analysis

Mixed sludge samples of 2 mL were collected from the top, middle, and bottom of the sludge bed at the end of each stage. These samples were centrifuged at 3000g for 10 mins, and the supernatant was discarded. DNA was extracted from the remaining sludge pellet using a DNeasy PowerSoil Kit (QIAGEN, Hilden, Germany), according to the manufacturer's instructions. Amplification of 16S rRNA genes was performed using the universal primer pairs 515F and 806R on the Illumina MiSeq platform. Sequence analysis was conducted using the DADA2 pipeline in QIIME 2, which provided a 99% match to the Greengenes database. All raw sequence files have been deposited in the National Center for Biotechnology Information (NCBI) under Bioproject PRJNA 985784.

5.3 Results and discussion

5.3.1 Wastewater characteristics

Pot ale wastewater and spent caustic wastewater, originating from different processes in the distillery industry, exhibit markedly distinct characteristics as shown in **Table 5.1**. The pH of spent caustic wastewater was significantly high at 13.2 ± 0.2 , contrasting with pot ale wastewater, with a low pH of 4.0 ± 0.3 . Extreme pH can inhibit microbial activities, which is crucial for anaerobic digestion, thereby necessitating pH adjustments prior to treatment (Nkuna et al., 2022).

TCOD for pot ale wastewater was notably high at 105.5 ± 27.4 g/L compared to 15.3 ± 1.7 g/L for spent caustic wastewater. The SCOD/TCOD ratio, which was an essential factor in AD, indicated the availability of readily biodegradable organic matter. Pot ale wastewater has a lower SCOD/TCOD ratio at 44% compared to spent caustic at 86%, suggesting a large fraction of the organic load was in forms less readily digestible, potentially limiting the digestion process

efficiency. TDS of spent caustic wastewater was high at 50.3 g/L, which can lead to osmotic pressure that can further inhibit microbial activity in AD systems.

In summary, the distinct characteristics of the two wastewater streams highlight the need for pre-treatment, pH neutralization, potential dilution, and co-digestion strategies to address the low pH, high TCOD, and challenging SCOD/TCOD ratios for pot ale wastewater and high pH and high TDS for pot ale wastewater, facilitating a more efficient anaerobic digestion process.

Table 5.1. Characteristics of spent caustic wastewater, pot ale wastewater, and co-digestion wastewater (S:P=1:5). The values are average \pm standard deviation.

Parameters	Unit	Spent caustic wastewater	Pot ale wastewater	Co-digestion wastewater (S:P=1:5)
pH	-	13.2 \pm 0.2	4.0 \pm 0.3	6.9 \pm 0.6
TCOD	g/L	15.3 \pm 1.7	105.5 \pm 27.4	88.3 \pm 19.8
SCOD	g/L	13.2 \pm 3.0	46.7 \pm 14.3	40.7 \pm 9.4
NH ₄ ⁺ -N	mg N/L	118 \pm 33	49 \pm 16	55 \pm 21
PO ₄ ³⁻ -P	mg P/L	46 \pm 21	336 \pm 30	317 \pm 24
TP	mg P/L	257 \pm 41	1476 \pm 105	1390 \pm 79
Alkalinity	mg/L CaCO ₃	19260 \pm 339	Not detected	1150 \pm 50
Ca ²⁺	mg/L Ca	91 \pm 26	88 \pm 6	105 \pm 29
Mg ²⁺	mg/L Mg	14 \pm 4	274 \pm 13	125 \pm 26
TSS	g/L	1.7 \pm 0.6	22.9 \pm 8.2	15.5 \pm 7.1
VSS	g/L	0.3 \pm 0.1	12.1 \pm 4.3	8.6 \pm 1.6
TDS	g/L	50.3 \pm 4.5	24.1 \pm 4.6	28.9 \pm 2.5

5.3.2 Batch experiments of co-digestion

Different volume ratios of spent caustic wastewater (S) and pot ale wastewater (P) were mixed for one hour, after which pH and TCOD/SCOD ratios were measured, as shown in **Fig.5.1A**. The co-substrates pH decreased from 12.56 (S:P volume ratio 1:1) to 6.62 (S:P volume ratio 1:6) due to the increasing proportion of pot ale wastewater in the co-substrates. Notably, at S:P ratios of 1:5

and 1:6, the pH values were 7.60 and 6.62, respectively, aligning with the optimal pH range for anaerobic digestion process (Nkuna et al., 2022). The SCOD/TCOD ratios of co-substrates exceeded that of pot ale wastewater, attributed to the dilutive effect of spent caustic wastewater.

BMP tests were conducted on the co-substrates to assess the methane production potential. As shown in **Fig.5.1B**, the methane production potential after 15 days for spent caustic wastewater and co-substrates with S:P volume ratios from 1:1 to 1:3 remained below 60% due to the inhibitory effects of high pH values. The initial stage showed a longer lag phase for pot ale wastewater compared to the 1:5 and 1:6 volume ratio co-substrates, which can be attributed to low pH values. Furthermore, the final methane production of the 1:5 co-substrate, which was 92%, was higher than that of pot ale wastewater, which was 86%. Therefore, the 1:5 co-substrate was chosen for further long-term co-digestion experiments in UASB reactors due to its neutralized pH and high methane production potential.

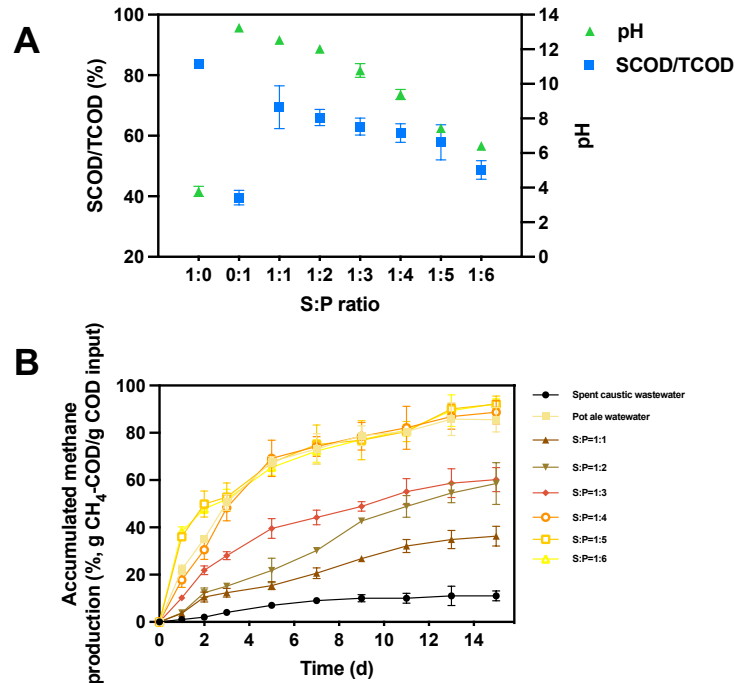


Fig. 5.1. SCOD/TCOD ratios and pH of different spent caustic wastewater: pot ale wastewater (S:P) volume ratio co-digestion wastewater (A) and biochemical methane potential (BMP) of different S:P volume ratio co-digestion wastewater (B). The mixing time for co-digestion wastewater was one hour.

5.3.3 Reactor performance

5.3.3.1 Methane production rate

The feedstocks of control reactor (R1) and co-digestion reactor (R2) were pot ale wastewater and co-substrates (S:P volume ratio of 1:5), respectively. As shown in **Fig. 5.2**, R1 reached a stable and effective methane production rate after 30 days, while R2 was 20 days start-up, which indicated the acclimatization of biomass to the co-substrate. In Stage 1, the OLR of R1 and R2 were 3.7 g/L/d and 3.9 g/L/d, with HRT of 19.6 days and 19.8 days, respectively. In Stage 1, R2 demonstrated a stable methane production of 2.6 g CH₄-COD/L/d, which was 15% higher than that of R1 (3.0 g CH₄-COD/L/d).

At Stage 2, the OLR increased to 7.6 g/L/d for R1 and 8.8 g/L/d for R2, with methane production rates of $62.0 \pm 3.7\%$ and $63.8 \pm 3.9\%$, respectively. Therefore, the methane productions at Stage 2 were 4.7 g CH₄-COD/L/d for R1 and 5.6 g CH₄-COD/L/d for R2, with R2 showing a 19% higher methane production than R1. This was due to the addition of spent caustic wastewater, which enhanced the readily biodegradable organics and balanced the pH values, creating better environmental conditions for effective hydrolysis process and methanogenesis process.

In Stage 3, with the increased OLR, R2 maintained a stable methane production rate (46.9%) with an OLR of 11.8 g/L/d, whereas R1 experienced a sharp decline in methane production rate (31% to 16%), which indicated an overload of the stage with an OLR of 11.2 g/L/d. This may be attributed to the hindered mass transfer with the accumulation of particulate solids in the sludge bed (Gao et al., 2020). At Stage 4, the OLR of R2 increased to 13.6 g/L/d, achieving a methane production rate of 44.0%, indicating a robust system due to the beneficial properties of the co-substrates.

Overall, R2 consistently demonstrated higher methane production across all stages compared to R1 and achieved a higher maximum organic loading rate. These results suggest that co-digestion of spent caustic wastewater and pot ale wastewater effectively enhances both energy recovery efficiency and organic loading capacities.

5.3.3.2 COD removal rate

The influent TCOD, effluent TCOD, and TCOD removal rate of two reactors are presented in **Fig. 5.2**. The influent TCOD of co-substrate ranged from 81 to 110 g/L, which was lower than that of pot ale wastewater (102-116 g/L). This was due to the dilution effect of spent caustic wastewater in co-substrate. The effluent TCOD of R1 increased from 5.6 g/L at Stage 1 to 14.6 g/L at Stage

2, and further to 27.0 g/L at Stage 3. Similarly, the effluent TCOD of R2 rose from 7.6 g/L at Stage 1 to 23.29 g/L at Stage 4. To ensure high-quality effluent and prevent sludge washout, excess sludge was periodically removed from UASB reactors. Correspondingly, the TCOD removal rate of R1 decreased from 94.6% at Stage 1 to 76.5% at Stage 3. However, the TCOD removal rates of R2 were higher than those of R1. This may be due to more particulate COD accumulated in R1's sludge bed due to lower HRT. The TCOD removal rates of two reactors remained higher than 75%, which demonstrated that efficient organic reductions can be achieved under high OLRs.

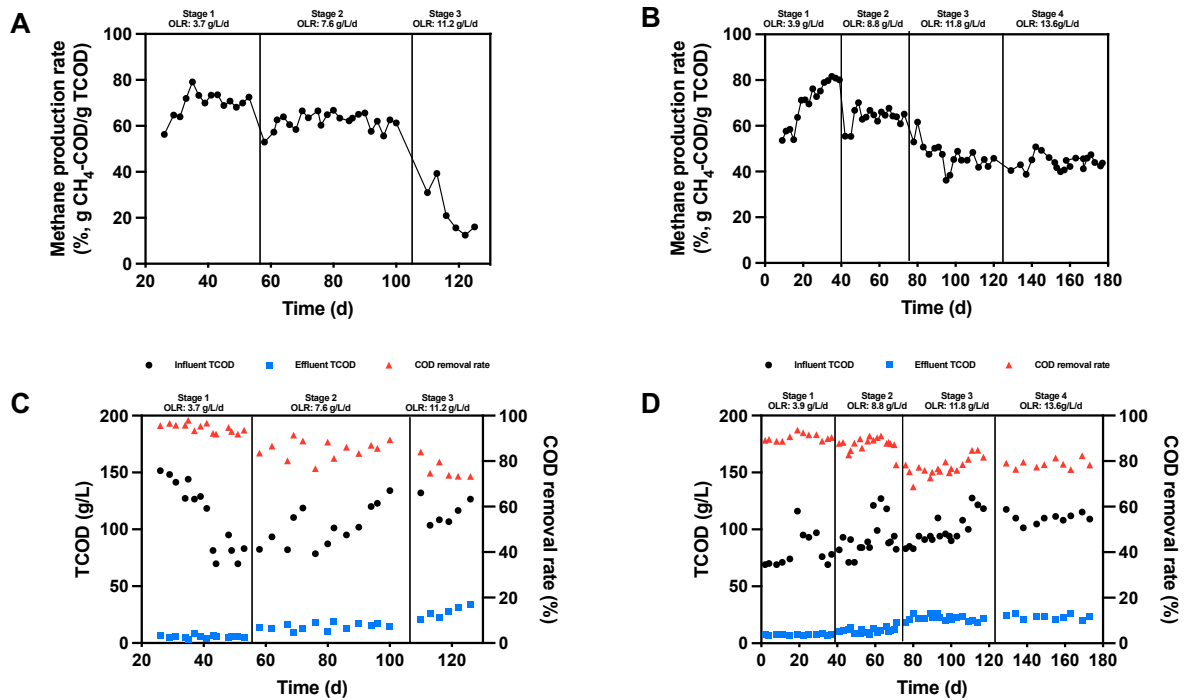


Fig. 5.2. Methane production rate of control reactor (pot ale wastewater) (A) and co-digestion reactor (B) and influent TCOD, effluent TCOD, and COD removal rates of control reactor (C) and co-digestion reactor (D) after long-term operation at different stages.

5.3.4 COD mass balance and hydrolysis efficiency

5.3.4.1 COD mass balance

The distributions of influent COD are divided into five categories: methane production, effluent COD, accumulated COD in the sludge bed, discharged sludge, and unidentified losses (**Fig. 5.3**). In both reactors, R1 and R2, effluent COD represented only 5-20% of the total COD input, indicating efficient organic removal.

At Stage 1 and Stage 2, a significant portion of COD, between 62% and 76%, was transformed into methane. The high conversion rate indicated effective methanogenic activity. However, at Stage 3, the dynamics of R1 shifted significantly. 40% of the COD was found accumulating in the sludge bed rather than being converted into methane (only 23%). This accumulation significantly hindered the methanogenic process in R1, likely due to the low pH of the pot ale wastewater, which potentially lowered the pH of the sludge bed, thus inhibiting methanogenesis.

R2 showed an increase in COD accumulation in the sludge bed as the OLR was increased. This was because as OLR increased, incomplete degradation of organics occurred, leading to particulate COD settling at the bottom of the sludge bed, a phenomenon driven by the reactor's low up-flow velocity. Moreover, as microbial growth was stimulated by higher OLRs, discharged COD from the sludge bed also increased, indicative of an expanding biomass in the sludge bed. This trend was primarily due to the higher daily input of organics, challenging the reactor's microbial community to efficiently process the increased load.

R2 exhibited lower COD accumulation in sludge bed compared to R1. This was attributed to the addition of spent caustic wastewater in R2, which not only neutralized the pH but also provided a

more readily biodegradable substrate. This improvement in substrate facilitated hydrolysis process, thereby enhancing methane production rate. In contrast, while R1 showed lower effluent COD, it also exhibited a reduced methane conversion rate than R2 at Stage 1 and Stage 2. This suggests that a portion of the organics removed in R1 was accumulated in the sludge bed rather than being effectively converted into methane.

Overall, R2 outperformed R1 in terms of methane production rate and organic degradation, with a notably lower proportion of COD remaining in the sludge bed. This result underscores the effectiveness of co-digestion in optimizing the anaerobic treatment process.

5.3.4.2 Hydrolysis efficiency

Pot ale wastewater is characterized by organics with solids, making hydrolysis a critical and limiting step in anaerobic treatment (Gao et al., 2020). To better understand the impact of co-digestions on anaerobic digestion, hydrolysis efficiency of substrates was calculated, as shown in **Fig. 5.3C**.

At Stage 1, the hydrolysis efficiency of R1 was $52.2 \pm 3.9\%$, which was lower than that of R2 ($58.3 \pm 4.4\%$). A similar trend was also observed in Stage 2, with R2 maintaining a higher hydrolysis efficiency of $54.1 \pm 6.0\%$ compared to $48.5 \pm 5.5\%$ in R1. The highest hydrolysis efficiencies of R1 and R2 were observed at Stage 1, corresponding to the highest methane production rate achieved. The enhancement of hydrolysis efficiency of co-substrate could be attributed to microorganism activities, which were likely elevated in the presence of more readily biodegradable substrates through the alkaline nature of spent caustic wastewater acting as a pre-treatment chemical. This could help break down yeast and particulate organics into forms more accessible for microbial digestion (Kim et al., 2011).

However, the hydrolysis efficiency of R2 decreased significantly to $37.3 \pm 1.0\%$ at Stage 3 and $29.0 \pm 3.8\%$ at Stage 4, in accordance with the decreased methane production rate. This reduction can be partly explained by operational challenges, notably sludge retention time (SRT). Proper SRT is essential as it ensures a sufficient population of microbes to effectively hydrolyze organics. Overloaded conditions in Stage 3 and Stage 4 required frequent sludge disposal to manage sludge washout, resulting in a shortened SRT, which was inadequate for maintaining efficient hydrolysis under high organic loading conditions. Additionally, with increased substrate accumulation in sludge bed and higher discharged sludge volumes at high OLRs, the proportion of microorganisms retained in the sludge bed decreased, which further limited the hydrolysis process and subsequently reduced the methane production rate.

Overall, the co-digestion of spent caustic wastewater and pot ale wastewater significantly enhanced hydrolysis efficiency of co-substrate by increasing the proportion of readily biodegradable organics in the solid-rich pot ale wastewater, and then led to higher methane production and higher organic loading capacity compared to reactor using pot ale wastewater alone.

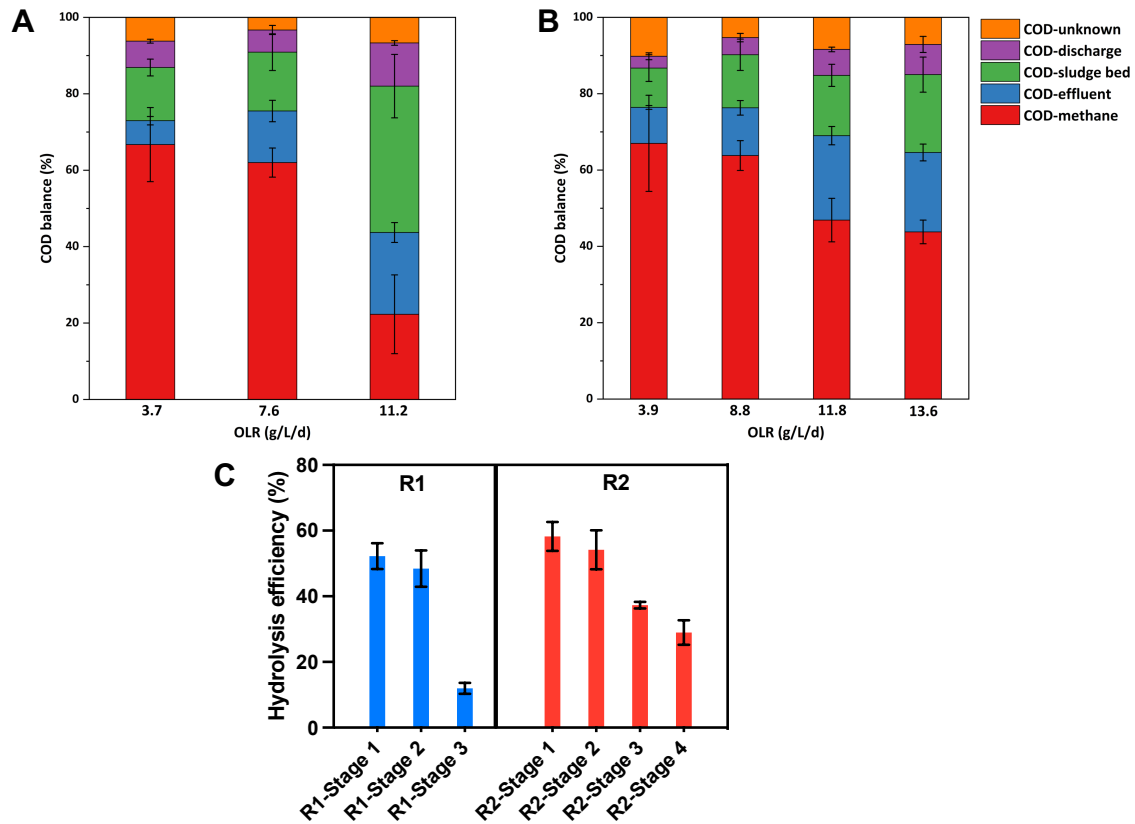


Fig. 5.3. COD balance of control reactor (pot ale wastewater) (A) and co-digestion reactor (B) and hydrolysis efficiency (C) of two reactors after long-term operation at different stages.

5.3.5 Sludge characteristics

5.3.5.1 Sludge-specific methanogenic activity

SMA of sludge is reported to be a crucial indicator for assessing microbial activities and determining the dominant methanogenesis pathway. In this study, two substrates, acetate and H_2 & CO_2 , were employed to identify the dominant methanogenesis pathway (acetoclastic or hydrogenotrophic methanogenesis) for each stage, as shown in **Fig. 5.4**. The SMAs for H_2 & CO_2 exceeded those for acetate in both reactors, suggesting hydrogenotrophic methanogenesis as the dominant pathway.

At Stage 1, the SMA for H₂&CO₂ in R1 was significantly lower at 217 ± 31 mg CH₄-COD/gVSS/d compared to 353 ± 42 mg CH₄-COD/gVSS/d in R2. This result aligns with the observed methane production rates, indicating an enrichment of hydrogenotrophic methanogens in the co-digestion reactor. This trend persisted into Stage 2, where R2 exhibited an SMA H₂&CO₂ that was 43% higher than that of R1. Furthermore, the increased OLR at Stage 2 led to higher SMAs for both reactors, boosting methanogen population and activity.

At Stage 3, SMAs of R1 sharply declined due to overloading stress and low pH, which adversely affected microbial activity. Conversely, R2 maintained higher SMA, consistent with stable methane production rates during this stage. Notably, the differential between SMA for H₂&CO₂ and SMA for acetate was significantly greater in R2 than in R1, while SMA for acetate in both reactors remained relatively consistent, ranging from 165 to 193 mg CH₄-COD/gVSS/d. These observations suggest the potential involvement of syntrophic acetate oxidation (SAO), where acetate is first converted to H₂&CO₂ before methanogenesis, a pathway typically stimulated under high organic loading conditions.

In summary, co-digestion process significantly enhances sludge SMA, particularly favoring hydrogenotrophic methanogenesis. This enhancement indicates that co-digestion could promote a robust population of hydrogenotrophic methanogens, which in turn enhance methane production rates.

5.3.5.2 Sludge stability

Sludge stability assesses the proportion of undigested biodegradable substrates in sludge bed, as illustrated in **Fig. 5.4C**. At Stage 1, the sludge stability was relatively low for both reactors, with R1 at 243 ± 25 mg CH₄-COD/g TCOD and R2 at 157 ± 12 mg CH₄-COD/g TCOD. R2 exhibited

a 55% lower stability than R1, reflecting its higher hydrolysis efficiency which helps reduce substrate accumulation in the sludge bed.

As the OLR increased, sludge stability rose for both reactors, corresponding with a decrease in methane production rates. The highest sludge stability for R1 was 415 ± 12 mg CH₄-COD/g TCOD. High sludge stability often indicates that hydrolysis is the rate-limiting step. Insufficient hydrolysis leads to the accumulation of particulate organics in the sludge bed, replacing active biomass and potentially resulting in sludge wash-out. This accumulation reduces specific methanogenic activities of sludge, potentially leading to reactor failure.

Overall, the addition of spent caustic wastewater to pot ale wastewater in the co-digestion reactor significantly enhanced hydrolysis efficiency, thereby reducing the accumulation of particulate organics in the sludge bed. This improvement allowed the reactor to achieve higher OLRs compared to the control reactor.

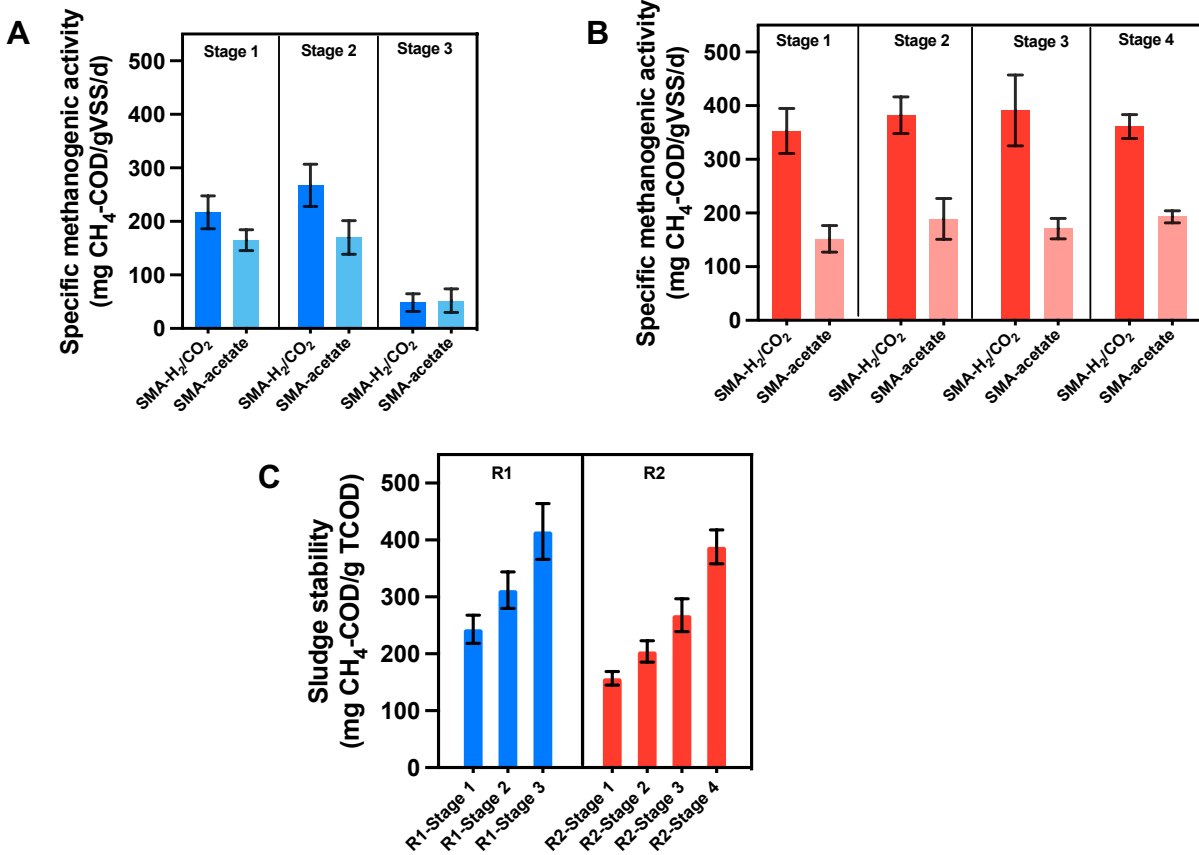


Fig. 5.4. Sludge-specific methanogenic activity (SMA) of control reactor (pot ale wastewater) (A) and co-digestion reactor (B) and sludge stability (C) of two reactors after long-term operation at different stages. The organic loading rates (OLR) of R1 at Stage 1, 2, and 3 were 3.7 g/L/d, 7.6 g/L/d, and 11.2 g/L/d, respectively. The OLR of R2 at Stage 1, 2, 3, and 4 were 3.9 g/L/d, 8.8 g/L/d, 11.8 g/L/d, and 13.6 g/L/d, respectively.

5.3.6 Microbial community

5.3.6.1 Bacterial community

Fig. 5.5A displays the relative abundance of main bacterial communities in the inoculum anaerobic granular sludge and sludge from the control and co-digestion reactors at different stages.

In Stage 1, R2's dominant bacterial genus included *HA73* (28.6%), the unclassified genus in the order *Bacteroidales* (14.9%), unclassified genus in the family *Tissierellaceae* (7.0%), and *Pelotomaculum* (6.2%). For R1, the dominant genera were distinctly different, featuring *HA73* (15.9%) and *Lutispora* (9.6%). *Bacteroidales* is known for its capability to hydrolyze and ferment carbohydrates (Ju et al., 2017), while *Pelotomaculum* can collaborate with methanogens to break terephthalate into simple molecules like benzoate and acetate for methane recovery (Hu et al., 2024). The enrichment of fermentative bacteria and syntrophic bacteria in R2 underscores its higher hydrolysis efficiency and higher methane production at Stage 1.

As the operational OLR increased at Stage 2, *HA73* became more prevalent in both reactors, with its abundance rising to 18.7% in R1 and a significant 52.7% in R2. *HA73* is known to degrade amino acids into acetate, which is a key intermediate in methane production (Giordani et al., 2021). For R1, the fermentative bacteria, such as *Prevotella* and *Lactobacillus*, were also enriched in Stage 2. This adaptation likely reflects the microbial response to increased OLRs.

In subsequent stages, as OLR continued to rise in R2, the bacterial profile shifted. The relative abundance of fermentative bacteria like *HA73* decreased, while *Tissierellaceae* increased, which indicates that *Tissierellaceae* could thrive in high OLR conditions. Simultaneously, the syntrophic bacteria *Pelotomaculum* increased to 4.1% in Stage 3 and 9.2% in Stage 4, aligning with the high methane production rates observed. These shifts highlight the adaptive changes in the microbial community in response to the reactor conditions, promoting efficient hydrolysis and methanogenesis.

Overall, in the co-digestion reactor, the enhancements of hydrolysis efficiency and the ability to adapt to higher OLR were significantly facilitated by the enrichment of both fermentative and

syntrophic bacteria. The microbial dynamism, stimulated by the co-substrates, facilitated the robust operation of reactor under high OLR conditions.

5.3.6.2 Archaeal community

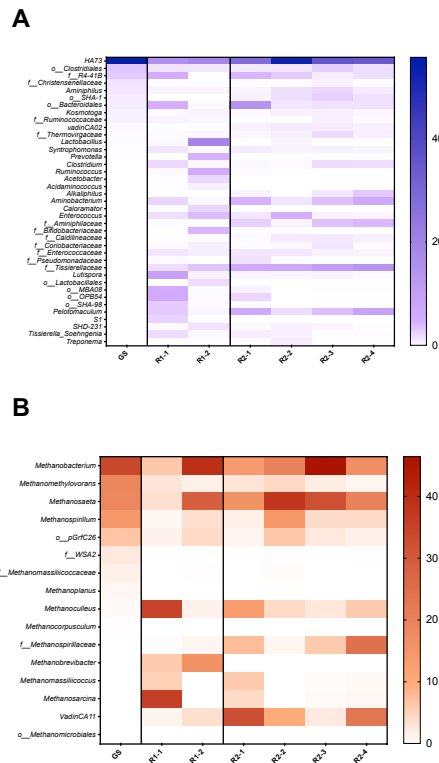
Fig. 5.5B illustrates the relative abundance of archaeal community. At Stage 1, R1 was dominant by *Methanosarcina* (35.9%) and *Methanoculleus* (34.9%), contrasting with R2, where the predominant archaea were *VadinCA11* (32.2%), *Methanosaeta* (15.8%), *Methanobacterium* (14.3%), and *Methanoculleus* (13.4%). The enrichment of hydrogenotrophic methanogens, *Methanobacterium*, *Methanosarcina*, and *Methanoculleus* underscores the dominant hydrogenotrophic pathway in both reactors, which aligns with the SMA findings (Mou et al., 2024). *Methanosaeta* and *Methanosarcina*, known for their roles in acetate degradation and syntrophic interactions that facilitate methanogenesis, were enriched to enhance methane production (Mou et al., 2022a).

At Stage 2, the archaeal community structure changed with the increased OLRs. R1 showed an enrichment of *Methanobacterium* and *Methanobrevibacter*, rising to 38.9% and 15.9%, respectively. For R2, *Methanosaeta*, *Methanobacterium*, and *Methanospirillum* experienced significant increases, which were 37.7%, 20.2%, and 14.8%, respectively. This result aligns with the higher SMA for H₂&CO₂, indicating effective adaptation to elevated organic loading.

At Stage 3 and Stage 4, as the OLR continued to rise in R2, there was a shift toward *Methanobacterium* and unclassified genus in the family *Methanospirillaceae*, suggesting an adaptation to the high organic loading stress. Meanwhile, the abundance of *Methanosaeta* and *Methanospirillum* declined. The robustness of *Methanobacterium* in extreme conditions such as

high OLR supports its role in maintaining system stability and enhancing syntrophic interactions under stress (Chen et al., 2020; Yu et al., 2021).

In summary, the distinct enrichment of methanogens in co-digestion reactor compared to the control reactor underscores the effectiveness of the co-digestion process in adapting to and thriving under high OLR conditions. The diverse and robust archaeal community in the co-digestion reactor not only supports higher hydrolysis efficiency but also enhances methane production.



5.3.7 Implications

The findings of this study provided insights into the operational benefits and underlying mechanisms of anaerobic co-digestion of spent caustic wastewater and pot ale wastewater. By integrating spent caustic wastewater with pot ale wastewater, the co-digestion process effectively mitigated the pH imbalance and enhanced the buffer capacity, significantly improving biodegradability of the co-substrate. The superior performance of the co-digestion reactor was reflected by higher methane production rates, increased hydrolysis efficiency and improved sludge stability. These improvements stemmed from the neutralized pH, balanced nutrients, enhanced microbial viability and activities in the co-digestion reactor. The enrichment of robust microorganisms and syntrophic interactions of bacteria and archaea can effectively convert organics into methane, even as the OLR increases. Furthermore, the higher hydrolysis efficiency and lower sludge stability values observed in the co-digestion reactor indicate more breakdown of organics, minimizing the accumulation of particulate substrates that often leads to system instability. This integration of enhanced microbial robustness, efficient hydrolysis, and stable reactor operation highlights the co-digestion reactor's enhanced capacity to handle higher OLRs, outperforming the mono-digestion system.

5.4 Conclusion

This study demonstrates the significant advantages of anaerobic co-digestion of spent caustic wastewater and pot ale wastewater in enhancing biogas production and organic loading capacities in long-term UASB operations. By mixing these wastewater streams, the co-digestion process effectively neutralized pH imbalances, diluted toxic substrates and increased readily biodegradable organics, fostering a robust microbial structure. This condition supported efficient

syntrophic interactions, hydrolysis and methanogenesis process, outperforming mono-digestion system. This study underscores the potential of co-digestion to optimize wastewater treatment in the distillery industry, and also offers a pathway towards sustainable energy recovery and reduced environmental impact.

**CHAPTER 6 SPATIAL DISTRIBUTIONS OF GAC IN UASB REACTORS
INFLUENCE METHANE PRODUCTION TREATING LOW AND HIGH
SOLID-CONTENT WASTEWATER**

*Part of this chapter has been published in Bioresource Technology.*⁴

*Part of this chapter has been submitted.*⁵

⁴ Mou, A., Yu, N., Sun, H., Liu, Y. 2022. Spatial distributions of granular activated carbon in up-flow anaerobic sludge blanket reactors influence methane production treating low and high solid-content wastewater. *Bioresource Technology*, 363, 127995.

⁵ Mou, A., Yu, N., Yang, X., Khalil, M., and Liu, Y. Enhancing methane production in up-flow anaerobic sludge blanket (UASB) reactor: the role of granular activated carbon (GAC) placement and substrate solid content on biofilm community dynamics.

6.1 Introduction

The anaerobic digestion (AD) of organic material involves redox reactions and electron transfer (Jadhav et al., 2021; Nguyen et al., 2021). Complex organic matter is hydrolyzed by bacteria to soluble volatile fatty acids (VFAs), VFAs are transformed to acetic acids, H₂, and CO₂, then methane is produced by microorganisms, mainly by archaea (Feng et al., 2021; Sharma et al., 2019). Anaerobic digestion is sensitive to temperature, pH, and free ammonia (Sharma et al., 2019). When treating high solid-content wastewater (such as blackwater, food waste and waste activated sludge), the hydrolysis process was usually the rate-limiting step. It is observed that the potential of biogas production from high solid-content wastewater greatly depends on the operating parameters, such as carbon-to-nitrogen ratios, temperature, and pH in anaerobic digestion (Jain et al., 2015; Zhou and Hu, 2017; Zhou et al., 2021). Also, different digestion approaches were also applied to treat high solid-content wastewater, such as continuous stirred tank reactor (CSTR), sequential batch anaerobic composting (SEBAC), anaerobic phased solids digester (APSD), up-flow anaerobic sludge blanket (UASB) (Jain et al., 2015; Tyagi et al., 2018). It has been found that two-step/multi-step anaerobic digestion is the best approach for anaerobic digestion (Jain et al., 2015). However, the application of anaerobic digestion to high solid-content wastewater is still relatively limited. This has been due to slowly biodegradable components and the waste's heterogeneous nature, which makes process control challenging. Therefore, pre-treatment methods, such as mechanical, thermal, chemical, and biological, of high solid-content wastewater, were applied before anaerobic digestion to improve biogas production (Yu et al., 2020; Zhou et al., 2018; Zhou et al., 2019). Microbial interspecies electron transfer (in which hydrogen acts as an electron donor and the electron shuttle) can accelerate syntrophic methanogenesis. Methanogenesis is the final step in the anaerobic degradation of organic carbon. The low partial

pressure of hydrogen in syntrophic methanogenesis can make methanogenesis the rate-limiting step in anaerobic digestion (Nguyen et al., 2021; Yu et al., 2021c).

Direct interspecies electron transfer (DIET) between microorganisms does not rely on the diffusion of electron carriers such as hydrogen (Park et al., 2018). Recently, conductive materials such as biochar, carbon nanotubes, iron-based oxide, granular activated carbon (GAC), powdered activated carbon, and magnetite have been demonstrated as electron conduits that stimulate DIET and, ultimately, methane production (Barua and Dhar, 2017; Dang et al., 2016; Nguyen et al., 2021). GAC is commonly utilized as a medium for efficient biomass growth and redox reactions. The high surface area of GAC stimulates microbial growth and shortens the cell-to-cell distance, facilitating DIET between bacteria and methanogens (Barua and Dhar, 2017; Liu et al., 2012; Yu et al., 2021c).

With its inherently hydrophobic surface and porous structure, GAC serves as an exceptional support material for microbial attachment, fostering biofilm formation, and potentially facilitating DIET during syntrophic metabolism (Cayetano et al., 2022; Park et al., 2018; Zhao et al., 2015). The development of biofilms on GAC in UASB reactors is a multistage process that initiates with the adhesion of free-floating microorganisms to the GAC surface (Flemming and Wingender, 2010; Xia et al., 2022; Zhuravleva et al., 2022). This attachment subsequently transitions into micro-colonial formation as the microbes proliferate on the GAC surface (Flemming and Wingender, 2010). Eventually, the biofilm continues to develop structurally, forming a three-dimensional structure (Flemming and Wingender, 2010; Xia et al., 2022). The proximity of cells within a biofilm dramatically reduces the metabolite diffusion distance and enhances collaboration between related species, thereby optimizing the bioconversion processes (Cayetano et al., 2022). Previous studies have proved the crucial role of biofilms formed on GAC in improving the

efficiency of anaerobic digestion processes (Yu et al., 2021). Bacteria and methanogens associated with biofilms formed on GAC surface are in proximity, which reduces diffusion constraints and allows for electrons to be more readily exchanged among species (Cayetano et al., 2022; Li et al., 2021b). Moreover, some studies suggest that GAC has the potential to adsorb hydrogen gas produced by fermentative bacteria in anaerobic digesters, therefore providing a readily available substrate for hydrogenotrophic methanogens present on the GAC surface (Jin et al., 2007). This interplay between GAC and biofilm explains the significance of biofilms on GAC in enhancing the efficiency of UASB reactors.

In an up-flow anaerobic sludge blanket (UASB) reactor treating organic material, the added GAC settles at the bottom of the reactor. Because the settling of GAC can restrict its contact with microbes, a more effective approach is required to optimize the contact area between GAC and sludge. A larger GAC surface area could promote DIET kinetics in anaerobic digestion (Barua and Dhar, 2017). Recently, Yu et al. (Yu et al., 2021c) demonstrated significantly improved UASB performance with self-floating GAC (by encasing GAC in plastic carriers) amendment, as compared to settled GAC, treating glucose as the carbon source. However, no other study examined the effectiveness of settled and floating GAC when treating wastewater with more complex water characteristics.

Our current study explored the effect of settled and self-floating GAC on the performance of UASB reactors treating wastewater with three different solid contents under mesophilic conditions. The impacts of the spatial distributions of GAC on the UASB reactor performance were evaluated, and the mechanisms that promoted anaerobic digestion with self-floating GAC were investigated.

6.2 Materials and methods

6.2.1 Reactor design and operation

Three laboratory-scale UASB reactors (R1, R2, R3), supplemented with 25 g/L of settled (R1), self-floating (SF, R2), or settled + self-floating (R3) GAC (pellet diameter 3 mm, Acurel® Extreme Activated Filter Carbon Pellets, USA) (**Fig. 6.1**), were operated continuously under mesophilic temperature (35 °C) for 170 days. The GAC added to R1 settled to the bottom of the reactor (GAC is denser than water). The GAC added to R2 was packed with polyethylene (PE) plastic media (1 inch in diameter, Powkoo, Canada); each PE plastic media ball contained one gram of GAC. The low-density plastic carriers enabled the GAC to float to the upper layer of the sludge blanket. The R3 reactor contained both unpacked GAC (10 g/L) and floating GAC (15 g/L).

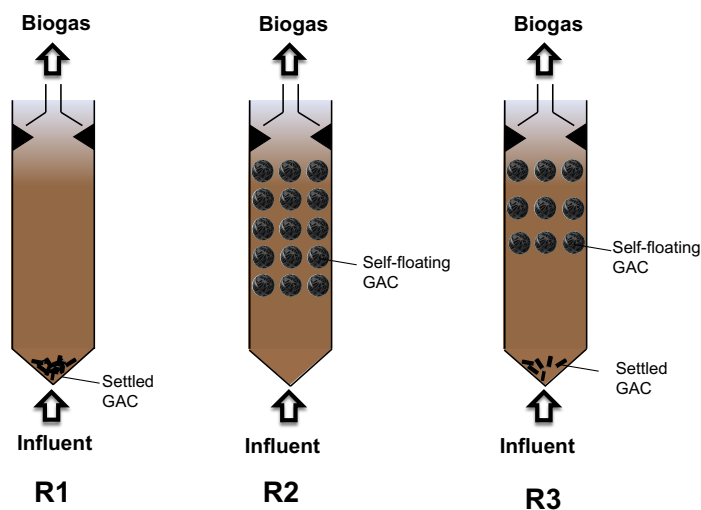


Fig. 6.1. The schematic layout of three UASB reactors.

The UASBs were operated in three stages after start-up (day 0-60): stage 1 (day 61-94), stage 2 (day 95-137), and stage 3 (day 138-170). Feedstock solid-content ratios (a ratio between soluble chemical oxygen demand (SCOD)/total chemical oxygen demand (TCOD): < 10% as high solid-

content, 40%-60% as medium solid-content, and > 90% as low solid-content) were applied in stages 1, 2, and 3, respectively. The hydraulic retention time (HRT) was 7 days in the three stages of reactor operations.

6.2.2 Seed sludge and substrates

Inoculum sludge with a volatile solids (VS) concentration of 7.5 g/L was obtained from a full-scale anaerobic digester at a wastewater treatment plant (WWTP) located in Edmonton, Alberta, Canada. The synthetic wastewater being digested was prepared using commercial dog food (Salmon and Sweet Potato Dog Food, Kirkland Signature, USA). Dog food was ground for 1 minute using an electric grinder (2500 W, 50 Hz) before being added to the reactors in stage 1 (Sun et al., 2022). To reduce the solid contents of feedstock in stages 2 and 3, the dog food was treated with thermal hydrolysis process (THP; high-pressure boiling followed by rapid decompression) in a 2 L batch hydrothermal reactor (Parr 4848, maximum temperature: 350 °C, maximum pressure: 1900 psi; Parr Instrument Company, Moline, IL, USA); the sample was mixed at 150 rpm during the hydrolysis. Sodium carbonate (Na_2CO_3) was utilized to adjust the pH of the hydrolyzed dog food to 7.5. An operating temperature of 150 °C and an exposure time of 60 mins were applied (Mohammad Mirsoleimani Azizi et al., 2021).

6.2.3 Analytical methods

Total suspended solids (TSS), volatile suspended solids (VSS), total solids (TS), VS, and chemical oxygen demand (COD) were measured using standard methods (Baird et al., 2017). Biogas was collected using 10 L foil gas bags (Chromatographic Specialties Inc., Brockville, Canada). The volumes of biogas were quantified using a measuring syringe. Biogas compositions were characterized using gas chromatography (7890B, Agilent Technologies, Santa Clara, US). The pH

was measured using a benchtop pH meter (B40PCID, VWR, SympHony). The methane yields were calculated based on the method described in (Sun et al., 2021). The hydrolysis efficiency of the feedstock was calculated using Equation (5-1) (Gao et al., 2019b):

$$\text{Hydrolysis efficiency (\%)} = \frac{SCOD_{t_2} - SCOD_{t_0} + COD_{CH_4}}{TCOD_{t_0} - SCOD_{t_0}}, \quad (6-1)$$

where $SCOD_{t_2}$ is the effluent SCOD of the UASB reactor, $SCOD_{t_0}$ is the influent SCOD, COD_{CH_4} is the COD converted to methane, and $TCOD_{t_0}$ is the influent TCOD.

6.2.4 Sludge characterization

To measure the maximum methane production in the reactor, at the completion of each stage, samples were collected at the upper and lower layers of the sludge blanket in each reactor. Each sludge sample was tested for its specific methanogenic activity (SMA) (the capability of the sludge to convert H_2/CO_2 or acetate into methane). The sludge samples were incubated for two weeks to remove the residue organics in sludge before the SMA tests. The sludge sample was diluted with deionized water to 10 mL and added to a serum bottle (working volume = 37 mL). An SMA batch test was performed on each sludge sample using H_2/CO_2 (volume ratio = 4:1) or acetate (1 g/L) as a substrate to measure the activities of hydrogenotrophic or acetoclastic methanogens. In the test for H_2/CO_2 , H_2/CO_2 was used to flush the headspace of bottles to provide a substrate. When acetate was applied as the substrate, the bottles were purged with nitrogen gas to establish an anaerobic environment. All bottles were sealed with rubber stoppers and aluminum caps and the bottles were cultivated using a shaker (35 °C, 120 rpm).

6.2.5 Microbial community analysis

Upon the completion of each operational stage, 2 grams of bottom GAC, top GAC, and the sludge flocs around GAC were collected from each of the three reactors. The bottom GAC and top GAC samples were washed with deionized water to detach loosely bound biomass or suspended sludge from the biofilm that had developed on the GAC. The sludge flocs surrounding GAC samples were centrifuged at 4000 g for 10 mins to remove the supernatant. The DNA extractions from the GAC biofilm and sludge pellet were performed using a DNeasy PowerSoil Kit (QIAGEN, Hilden, Germany), in accordance with the manufacturer's instructions. The concentrations of extracted DNA samples from biofilm and floc sludge were determined by NanoDrop One (ThermoFisher, Waltham, MA, USA). The polymerase chain reaction (PCR) was conducted on the Illumina MiSeq platform. 16S rRNA genes in the biofilm and sludge samples were amplified using the universal primer pairs 515F and 806R.

6.2.6 Microbial community analysis and gene predictions

The analysis of DNA sequence was conducted utilizing the QIIME 2 DADA2 pipeline, matching with 99% similarity with respect to the Greengenes database (version 13_8). Microbial communities were analyzed in R software (version 4.2.0). The "corrplot" package was employed to analyze the correlation between the operational parameters, reactor performance, sludge activities, and microbial communities. The "vegan" package was used for the principal component analysis (PCA). Based on 16S rRNA gene amplicon sequences data, predictions of metagenome and annotations of functional genes were performed. Gene prediction was facilitated using Phylogenetic Investigation of Communities by Reconstruction of Unobserved States (PICRUSt) on the Kyoto Encyclopedia of Genes and Genomes (KEGG) database (Langille et al., 2013). Raw

sequence files have been stored at the National Center for Biotechnology Information (NCBI) under Bioproject PRJNA 985778 and PRJNA 879213. Statistical significance was determined by a p -value of less than 0.05.

6.3 Results and Discussion

6.3.1 Wastewater characteristics

Dog food, a high solid-content wastewater surrogate, contains crude protein, crude fat, and crude fiber, which is a suitable representation of complex feedstock with high solid content compared with the feedstock of acetate, glucose, yeast extract and milk powder. Also, pre-hydrolyzed dog food could provide a way to control the solid contents of feedstocks due to its stable performance.

The synthetic wastewater characteristics in the three stages are summarized in **Table 6.1**. The influent TCOD for three stages remained stable at ~ 14 g/L. The average influent soluble COD was 1.0 ± 0.3 g/L in stage 1, which corresponds to SCOD/TCOD ratio $< 10\%$. With thermal hydrolysis pre-treatment, influent SCOD increased to 7.5 ± 1.3 g/L in stage 2 and 13.0 ± 1.6 g/L in stage 3. The SCOD/TCOD ratios for stage 2 and stage 3 were 40-60% and $> 90\%$, respectively. Therefore, wastewater influent from stages 1, 2, and 3 can be categorized as high solid-content wastewater, medium solid-content wastewater, and low solid-content wastewater, respectively. To evaluate the impact of THP on methane yield, the biomethane potentials (BMPs) of influent wastewater at three stages were measured and compared, which showed that the BMPs were similar ($P > 0.05$) for wastewater influent from stage 1 to stage 3, which were $88.6 \pm 4.0\%$ in stage 1, $88.8 \pm 2.9\%$ in stage 2, and $90.0 \pm 4.1\%$ in stage 3, indicating that THP pre-treatment did not impact wastewater digestibility.

Table 6.1. Synthetic wastewater characteristics in the three stages of reactor operations. The values are average \pm standard deviation.

Parameters	Unit	Stage 1	Stage 2	Stage 3
pH	—	7.5 ± 0.2	7.5 ± 0.2	7.5 ± 0.2
TCOD ^a , (n=20)	g/L	14.0 ± 1.4	14.0 ± 2.0	14.0 ± 1.4
SCOD ^b , (n=20)	g/L	1.0 ± 0.3	7.5 ± 1.3	13.0 ± 1.6
SCOD/TCOD, (n=20)	%	<10	40-60	>90
BMPs ^c , (n=3)	%, g CH ₄ -COD/g TCOD	88.6 ± 4.0	88.8 ± 2.9	90.0 ± 4.1

a: total chemical oxygen demand.

b: soluble chemical oxygen demand.

c: biomethane potentials.

6.3.2 Reactor performance

6.3.2.1 Methane yield

The three GAC-amended UASB reactors — R1 (with settled GAC), R2 (with self-floating GAC), and R3 (with self-floating + settled GAC) — were fed with 14 g/L wastewater with a low SCOD/TCOD ratio (high solid-content) in the mesophilic condition in stage 1. Compared to the addition of settled GAC, the addition of self-floating GAC significantly enhanced the methane yield (**Fig. 6.2**). During the stable state operation in stage 1, the methane yields of R2 and R3 were $74.2 \pm 3.7\%$ and $65.1 \pm 3.8\%$, respectively, which were higher than the methane yield observed in R1 ($58.3 \pm 1.4\%$). R2 exhibited a 14.0% higher methane yield than R3.

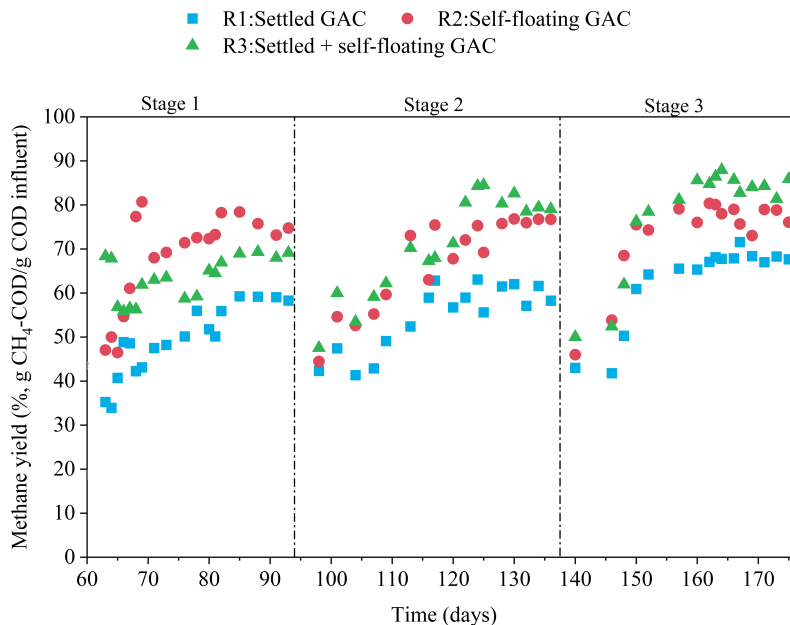


Fig. 6.2. Methane yield in R1, R2, and R3 during the three stages of reactor operations.

During stage 2, with reduced feedstock solid content (SCOD/TCOD ratio of feedstock: 40%-60%, medium solid-content wastewater), the methane yield of R3 increased to $77.1 \pm 6.3\%$. However, no significant change ($P > 0.05$) in methane yield was observed in R1 and R2 between stage 1 and stage 2.

During stage 3, with further reduced solid content (when the reactors were operating with low solid-content wastewater), R3 achieved the highest methane yield ($83.4 \pm 3.3\%$). The methane yields of R1 and R2 also increased to $67.4 \pm 1.9\%$ and $77.3 \pm 2.3\%$, respectively.

Overall, the addition of self-floating GAC (in R2 and R3) improved the methane yield in both low and high solid-content wastewater. In the AD of organic material in wastewater with high solid content, the reactor containing self-floating GAC (R2) achieved a higher methane yield than the reactor containing settled GAC (R1) and the reactor containing settled + self-floating GAC (R3).

However, the reactor containing the settled + self-floating GAC (R3) exhibited the highest methane yield among the three GAC-amended reactors when the feedstock was wastewater with low and medium solid contents.

6.3.2.2 Chemical oxygen demand balance

After UASB treatment, the fate of influent COD includes: (I) discharged sludge; (II) accumulated sludge in the sludge bed; (III) effluent solids; (IV) methane; and (V) unknown (**Fig. 6.3**). In stage 1, the influent COD accumulation in the settled sludge was significantly higher ($14.7 \pm 1.3\%$) in R1 (settled GAC only) than the COD accumulation in R2 ($9.3 \pm 1.0\%$) and R3 ($11.9 \pm 2.2\%$) sludge. Hydrolysis is often the rate-limiting step in the anaerobic digestion of high solid-content wastewater (Duan et al., 2012; Gao et al., 2019a; Gao et al., 2019b). **Fig. 6.4** shows that in stage 1, the hydrolysis efficiencies in R2 ($75.2 \pm 5.7\%$) and R3 ($67.7 \pm 4.0\%$) were higher than that in R1 ($55.7 \pm 2.7\%$). These data suggested that the addition of self-floating GAC will achieve a higher hydrolysis efficiency than the addition of settled GAC when treating high solid-content wastewater. This could be explained by the higher biomass concentration (VSS 30.5 ± 2.3 g/L) at the self-floating GAC amended reactors (R2) bottom than the reactor amended with settled GAC only (R1, VSS 21.8 ± 3.1 g/L) that facilitated hydrolysis process (Yu et al., 2021c). Further, the self-floating GAC contributed to the stimulation of methanogenesis at the upper reactor region, facilitating the downstream conversion of the fermentation products, which reduced the intermediates inhibition and allowed the AD of high-solid wastewater to proceed in a way that complies with the sequential reaction steps.

In stage 2 and stage 3, the COD accumulation in the sludge decreased, indicating hydrolysis was no longer the rate-limiting step in the three UASB reactors. R3 produced the highest level of methane among the three reactors.

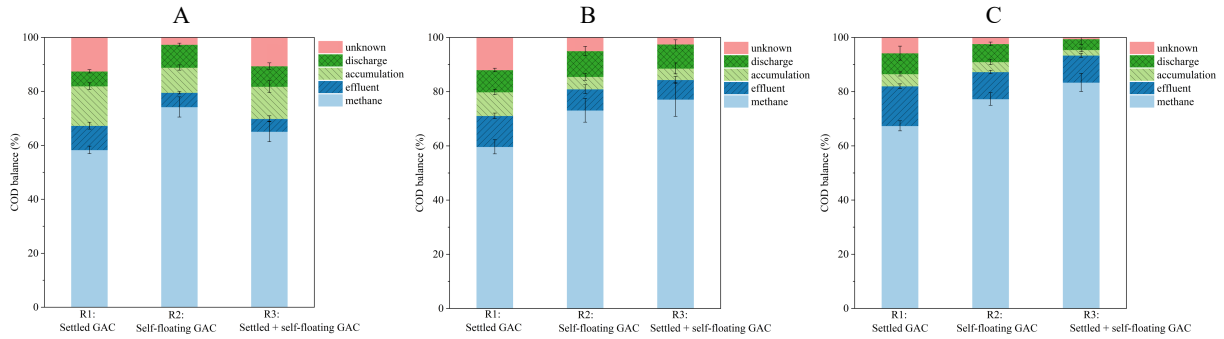


Fig. 6.3. COD balance in R1, R2, and R3 reactors (A: stage 1; B: stage 2; C: stage 3).

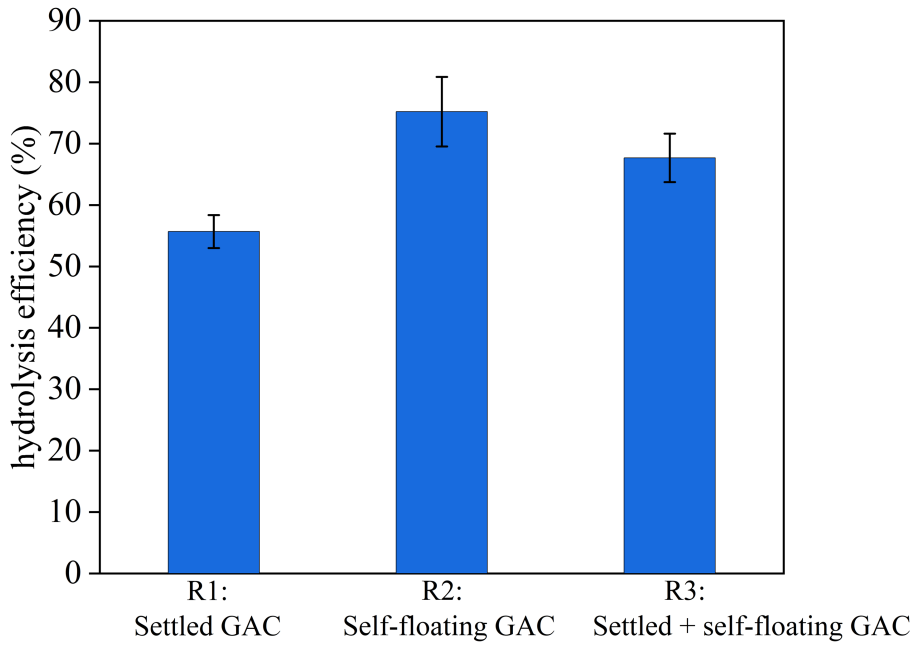


Fig. 6.4. Hydrolysis efficiency of high solid-content wastewater in stage 1 of reactor operations.

6.3.3 Sludge characteristics

As shown in **Fig. 6.5**, the methanogenic activities of microbes using H_2/CO_2 were significantly greater than the methanogenic activities of microbes using acetate in the three stages of the three reactors. This demonstrated that hydrogenotrophic methanogenesis was the main pathway in these reactors.

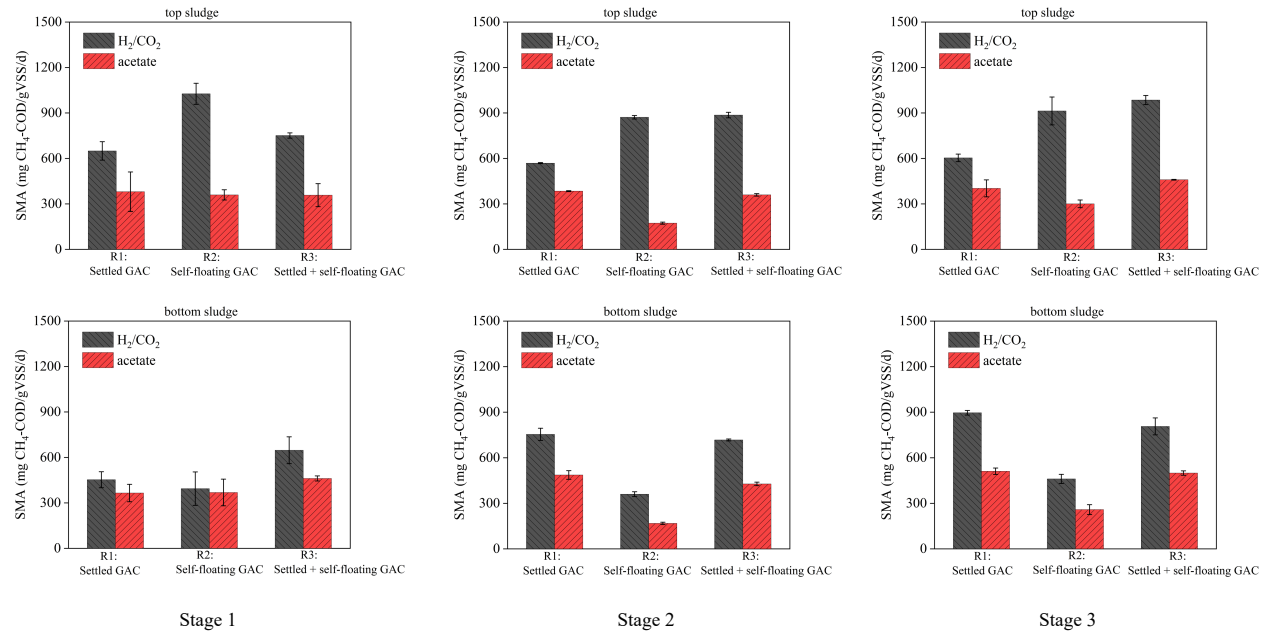


Fig. 6.5. Spatial sludge specific methanogenic activity (SMA) for acetate and H_2/CO_2 in three stages of reactor operations.

In stage 1, the SMAs of the top sludge and the bottom sludge in R2 (the best performing reactor in stage 1, with self-floating GAC) were distinctive. In the top layer of sludge in R2, the hydrogenotrophic SMA was the highest (1026 ± 70 mg CH_4 -COD/gVSS/d) among the sludge in all three reactors in stage 1. However, the hydrogenotrophic SMA in the bottom layer of sludge in R2 was the lowest (394 ± 110 mg CH_4 -COD/gVSS/d) among the sludge in all three reactors in stage 1. These results indicated that methanogenesis mainly occurred toward the top layer of the

sludge, likely due to the presence of the self-floating GAC. Combined with the hydrolysis results shown in **Fig. 6.4**, the results in R2 suggested that hydrolysis took place mostly toward the bottom layer of sludge, in accordance with the results published in (Yu et al., 2021c). With both settled and self-floating GAC, the hydrogenotrophic SMA in the top layer of sludge in R3 was also higher than the hydrogenotrophic SMA in R1, indicating the presence of self-floating GAC in R3 improved top layer sludge SMA. Interestingly, there were no clear spatial differences in the hydrogenotrophic SMA of the sludge in R1 in stage 1.

In comparison to stage 1, SMA (for both H₂/CO₂ and acetate) of R1 in the bottom sludge increased significantly in stage 2. This may be attributed to the reduced solids accumulation on the bottom of R1 reactor at stage 2 (**Fig. 6.3**). It was observed that the hydrogenotrophic SMA in the bottom sludge (754 ± 40 mg CH₄-COD/gVSS/d) was higher than the hydrogenotrophic SMA in the top sludge (569 ± 3 mg CH₄-COD/gVSS/d) of R1 reactor in stages 2. In stage 2, using H₂/CO₂ as a substrate, the SMAs in the top sludge layer (886 ± 18 mg CH₄-COD/gVSS/d) and the bottom sludge layer (717 ± 6 mg CH₄-COD/gVSS/d) of R3 were both higher than the SMAs in stage 1. This corresponded to an improved methane yield in R3 in stage 2.

In stage 3, when treating low solid-content wastewater, the SMAs for H₂/CO₂ and for acetate of R3 (with self-floating + settled GAC) were the highest compared with SMAs of R3 in stage 1 and stage 2. When the hydrolysis process was not the rate-limiting step (stage 3), the settled GAC in R3 promoted methanogenic activity at the bottom of the reactor, while the self-floating GAC promoted further methanogenesis at the top of the reactor, combination of which may have attributed to the high methane yield observed in R3 reactor in stage 3.

6.3.4 Microbial community

6.3.4.1 Bacterial community

Fig. 6.6 shows the relative abundance of representative bacterial communities in the three UASB reactors in the three stages of reactor operations. The dominant bacteria in R1 in stage 1 were an unclassified genus in class *Mollicutes* (8.21% at the top sludge and 10.94% at the bottom sludge, respectively) and an unclassified genus in order *Bacteroidales* (8.13% at the top sludge and 7.71% at the bottom sludge, respectively). *AUTHM297* and an unclassified genus in order *Fusobacteriales* were dominant in the bottom of R2 during stage 1; *Fusobacteriales* has been reported to catabolize macro-molecules into smaller substrates to conserve energy (Abid et al., 2021; Muturi et al., 2021); *AUTHM297* has been observed in anaerobic digestions and can survive in environments with highly degraded organic matter (Liu et al., 2020b). *Fusobacteriales*, 5.53% at the top of R2 and 12.88% at the bottom of R2 in stage 1, indicated that the hydrolysis of macro-molecules mainly occurred on the bottom of the reactors containing self-floating GAC (R2 and R3). A relatively higher abundance of *AUTHM297* was observed in R2 and R3. This implied that R2 and R3 contained more degraded organic matter than R1 and was consistent with the hydrolysis efficiency results (**Fig. 6.4**).

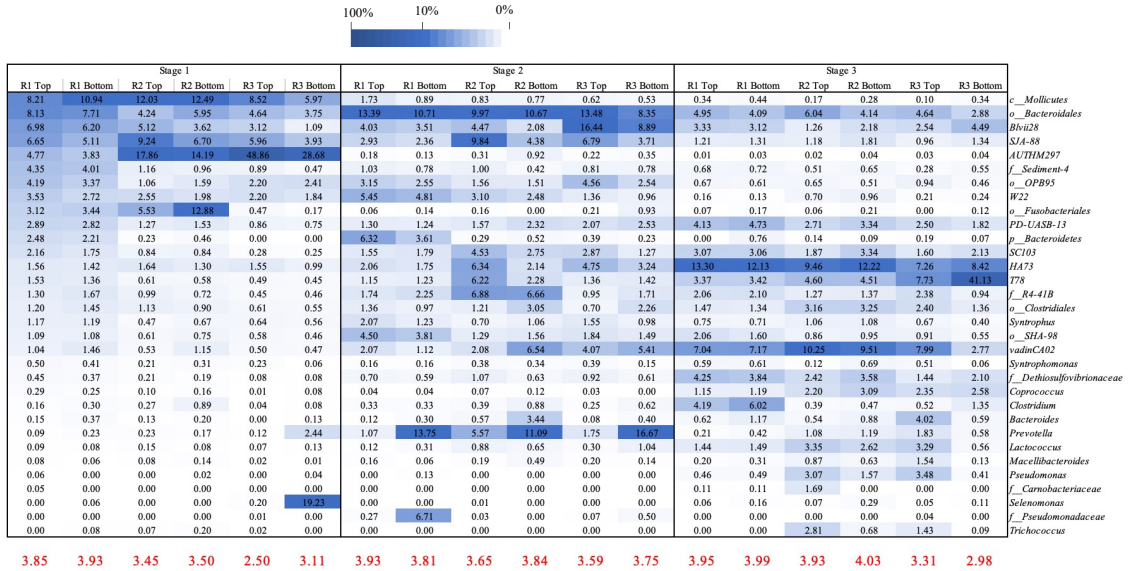


Fig. 6.6. Relative abundance of bacterial communities at the genus level. Taxonomic names are shown for genus level or higher level (family: f; order: o; class: c; p: phylum) if not identified at the genus level. The Shannon diversity is reported at the bottom of the heatmap.

An unclassified genus in order *Bacteroidales* was enriched in all three reactors during stage 2. The main fermentation products of *Bacteroidales* are acetate and succinate (Mercado et al., 2022) In stage 2, among the three reactors, *Blvii28* had the highest relative abundance (16.44% on the top and 8.88% on the bottom) in R3. *Blvii28* is a hydrogen-producing fermenter that can form a syntrophic relationship with hydrogenotrophic methanogens (Su et al., 2014). Thus, *Blvii28* could be responsible for the high methane yield of R3 in stage 2 (Fig. 6.2). With the presence of self-floating GAC during stage 2, R2 and R3 reactors had a higher relative abundance of *SJA-88* in the top sludge layer than in the bottom sludge layer. *SJA-88* is a saccharolytic bacteria, which can ferment glucose and produce VFAs (Yao et al., 2022). The presence of self-floating GAC enabled the enrichment of different microbes in different layers of sludge, assisting anaerobic digestion. *Prevotella*, which uses glucose and fiber disaccharides to produce acetate (Leng et al., 2021), was

more abundant on the bottom layer of sludge than on the top layer of sludge in all three reactors in stage 2. The spatial differences in the abundance of *Prevotella* among the three reactors could be due to the accumulation of feeding on the bottom of three reactors.

HA73 was enriched in the three reactors during stage 3, and likely contributed to the degradation of amino acids into acetate (Giordani et al., 2021; Yu et al., 2022). This could be due to the presence of more soluble amino acids in the feed after thermal hydrolysis. The dominant bacteria at the bottom of R3 was *T78* (41.13%), which can degrade peptone into acetate. Hence, the fermentation of organics mainly occurred in the bottom sludge layer of R3, and this enabled more effective anaerobic digestion. *Syntrophus* and *Syntrophomonas*, which can act as syntrophic fatty acid metabolizers, were also enriched in the three reactors in stage 3. *Syntrophus* can produce e-pili and multiply through DIET. *Syntrophomonas* was reported to be a DIET participant and can be greatly enriched on the GAC surface (Yu et al., 2021c).

6.3.4.2 Archaeal community

The relative abundances of archaeal communities in the three UASB reactors in the three stages of anaerobic digestion are shown in **Fig. 6.7**. Archaeal diversity was indicated by Shannon diversity index value. Top layer of sludge bed of R2 (2.11) and R3 (1.93) had higher archaeal diversity than top layer of sludge bed of R1 (1.79) at stage 1, indicating that GAC ascent increased the archaeal diversity of top sludge at stage 1. There was no significant difference in dominant genera between the top sludge and the bottom sludge in R1 during stage 1: *Methanoseata* (37.78% top, 39.84% bottom), an unclassified genus in family *WSA2* (17.39% top, 16.26% bottom), an unclassified genus in family *Methanomassiliicoccaceae* (12.36% top, 10.10% bottom), *Methanobacterium* (11.40% top, 12.60% bottom). However, the addition of self-floating GAC in

R2 enriched different genera in top and bottom sludge layers: *Methanoseata* (36.08% bottom, 21.49% top), an unclassified genus in family *WSA2* (20.41% top, 15.83% bottom). Similar to findings in (Yu et al., 2021c), these results demonstrated that self-floating GAC played a significant role in controlling the spatial distributions of the microbial communities in the UASB reactors. The relative abundance of *Methanospirillum* in the top sludge layer of R2 was the highest (7.12%) of the three reactors in stage 1. *Methanospirillum* was also enriched in R3. *Methanospirillum* has been reported to produce electrically conductive archaeum, which enables long-range electron transfer (Li et al., 2018; Lin et al., 2017). Thus, the addition of self-floating GAC might have stimulated the growth of DIET-active microorganisms, which could explain the high methane yield achieved in R2 during stage 1.

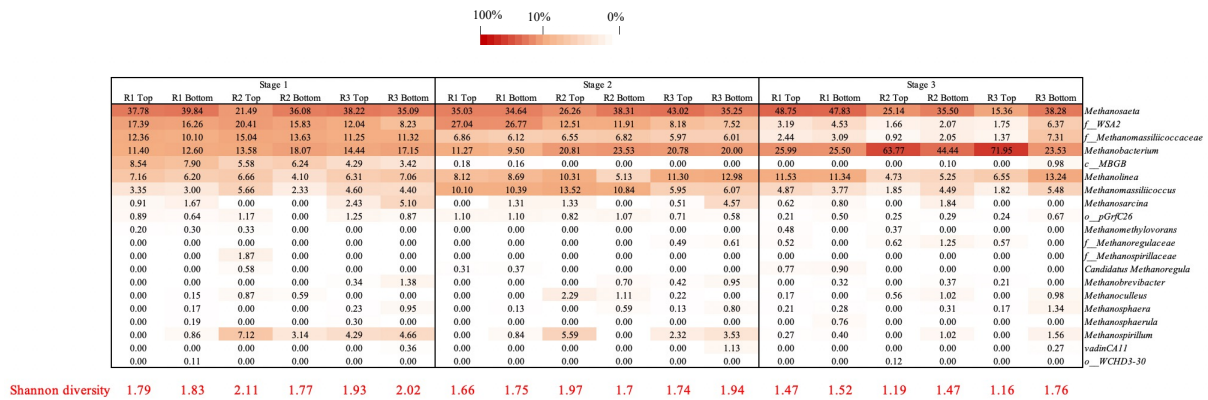


Fig. 6.7. Relative abundance of archaeal communities at the genus level. Taxonomic names are shown for genus level or higher level (family: f_; order: o_; class: c_) if not identified at the genus level. The Shannon diversity is reported at the bottom of the heatmap.

In stage 2, *Methanosarcina* and *Methanospirillum* were enriched in the sludge at the bottom of R1 (1.31% and 0.84%), the top of R2 (1.33% and 5.59%), the top of R3 (0.51% and 2.32%), and the bottom of R3 (4.57% and 3.53%) — that is, all the sludge layers that had received GAC

supplements. The results indicated that the addition of GAC might have stimulated the growth of *Methanosarcina*, the potentially DIET-active methanogenic archaea that can accept extracellular electrons (Song et al., 2010b; Yu et al., 2021). *Methanosarcina* could have contributed to the high methane yield in the three reactors. DIET-active methanogenic archaea were enriched in the top and bottom layers of sludge in R3 and could be associated with the higher methane yield in stage 2.

In stage 3, *Methanobacterium* was the dominant archaea in the top layer of sludge in R2 (63.77%) and in the top layer of sludge in R3 (71.95%). *Methanobacterium*, a strict hydrogenotrophic methanogen, is commonly found in the biofilm growing on the cathode of a bio-electrochemical system, indicating a potential participation in electron capture (Abid et al., 2021; Yu et al., 2021). These results may be related to the addition of self-floating GAC in R2 and R3 reactors.

6.3.5 Microbial community of GAC-biofilms

VSS concentrations of both flocs and biofilms, which was a critical factor influencing anaerobic digestion performance. At the end of each operational stage, VSS concentrations in flocs significantly exceeded those in biofilms. Biofilm-associated VSS concentrations spanned from 0.6 to 1.2 g/L, constituting 4.8% to 7.0% of the UASB reactors' total biomass.

Despite the relatively low biomass of biofilms, their hypothesized role in enhancing methane production has been supported by evidence of close proximity of syntrophic bacteria and methanogenic archaea on GAC surfaces, allowing direct hydrogen utilization by hydrogenotrophic methanogens. Thus, the contribution of GAC biofilm biomass to methane yield should not be underestimated. To further explore these interactions, especially when treating different solid-content wastewater, this study collected and analyzed both suspended flocs and GAC surface

biofilms to identify and understand the bacterial and archaeal community compositions involved (Fig. 6.8).

6.3.5.1 Bacterial community of biofilms

Fig. 6.8A illustrates the relative abundance of primary bacteria genera in both the suspended sludge near GAC and the biofilms on the GAC in three reactors. During the treatment of high solid-content wastewater, there was a notable distinction between the dominant bacteria in the suspended sludge and those in the GAC biofilms across all three reactors. Additionally, the bacterial communities of biofilms exhibited significant variation depending on GAC locations.

In Stage 1, top-GAC biofilms in R2 and R3 displayed enrichment of syntrophic bacteria, notably including *Geobacter* and *Syntrophus*. *Geobacter*, an anaerobic iron-reducing bacteria, can degrade acetate in an iron-reducing environment, serving as an electron donor for DIET with methanogens in AD (Jung et al., 2022). *Syntrophus* can facilitate anaerobic degradation via the DIET pathway by producing electrically-conductivity pili (Walker et al., 2020). These bacteria are integral to the DIET process, enhancing methanogenic performance. *Geobacter*, *Syntrophus*, *Syntrophomonas*, *Syntrophobacter*, and *Syntrophorhabdus* have been proven to be the syntrophic bacteria involved in the DIET process (Dang et al., 2022; Zhang et al., 2022b). The ratios of these syntrophic bacteria in the suspended sludge surrounding GAC and the biofilms attached to GAC are depicted in **Fig. 6.8B**. The ratios of syntrophic bacteria in the GAC biofilm were greatly higher than those in the suspended sludge across three stages, underscoring the importance of GAC biofilm as the site of the DIET process. In Stage 2, the presence of *Syntrophus* in the top-GAC biofilm of R3 highlighted the supportive role of top GAC in DIET, correlating with increased methane production of R3. During Stage 3, top-GAC biofilms exhibited a higher abundance of syntrophic bacteria compared

to bottom-GAC biofilms, emphasizing top-GAC's crucial role in facilitating the syntrophic reactions and subsequently enhancing reactor performance.

During three stages, notable variations in bacterial compositions were observed between suspended sludge and GAC biofilms, particularly the top-GAC biofilms. This underscores the significant influence of GAC-associated biofilms, particularly those located at the top, in optimizing wastewater treatment processes through the promotion of syntrophic interactions.

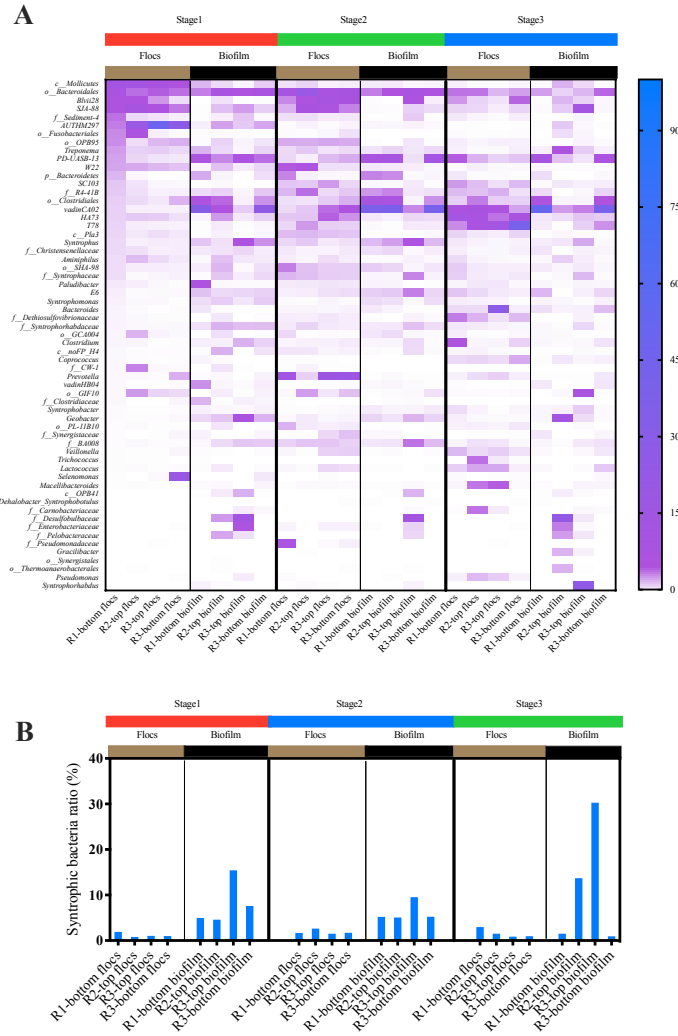


Fig. 6.8. Relative abundance of the main bacteria genera (A) and syntrophic bacteria ratio (B) of suspended sludge surrounding GAC and biofilm attached on GAC of three reactors (R1: bottom GAC-amended UASB; R2: top GAC-amended UASB; R3: bottom+top GAC-amended UASB) under three stages (Stage 1: high solid-content wastewater; Stage 2: medium solid-content wastewater; Stage 3: low solid-content wastewater). Taxonomic names are shown for genus level or higher level (family: f_; order: o_; class: c_; p: phylum) if not identified at the genus level.

6.3.5.2 Archaeal community of biofilms

Fig. 6.9 illustrates the genus-level relative abundance of the archaeal community and the Shannon diversity index for both flocs adjacent to GAC and biofilms formed on GAC. The biofilms on top GAC consistently exhibited higher archaeal diversity compared to those on the bottom GAC across all three stages. This difference was particularly pronounced in Stage 3, where the Shannon index of top-GAC biofilms ranged from 1.5 to 1.8, as compared to 0.5 to 0.6 for bottom-GAC biofilms. The vertical distribution of archaeal diversity suggests that the addition of top GAC may facilitate a more diverse archaeal community in the biofilm, potentially due to varied substrate gradients and increased contact area between top GAC and substrates. Additionally, the disparity in archaeal diversity between top-GAC and bottom-GAC biofilms was more pronounced when treating low solid-content wastewater, in contrast to high solid-content wastewater. This observation could be attributed to higher concentrations of soluble substrates, such as VFA, at the top of the reactors during low solid-content wastewater treatment (Mou et al., 2024).

In Stage 1, *Methanobacterium* (53.2%-78.8%) and *Methanosaeta* (10.9%-23.8%) were the dominant genera in GAC biofilms, exhibiting a distinct microbial composition compared to flocs. Notably, *Methanospirillum* was significantly enriched in top-GAC biofilm, constituting 3.6% in top GAC of R2 and 7.0% in top GAC of R3. Additionally, *Methanolinea*, an unidentified genus from the *WSA2* family, and *Methanomassiliicoccaceae* family were notably enriched in top-GAC biofilm of R2. The enrichment of these hydrogenotrophic methanogens, including *Methanobacterium*, *Methanospirillum*, *Methanolinea* and *WSA2*, are known for metabolizing formate, hydrogen, and carbon dioxide into methane (Lee et al., 2017; Sun et al., 2020), indicating a thriving pathway of hydrogenotrophic methanogenesis. *Methanosaeta* primarily converts acetate into methane and carbon dioxide (Zhang et al., 2021b). Recent studies describe *Methanosaeta*'s

ability to accept electrons via DIET for reducing carbon dioxide to methane (Cerrillo et al., 2018). The enrichment of *Methanospirillum* in the top-GAC biofilm aligned with previous findings of its involvement in DIET (Walker et al., 2019; Yu et al., 2021). Furthermore, the domination of *Methanobacterium* and *Methanosaeta* in GAC biofilms, indicative of their role in the DIET process, has been reported previously (Yu et al., 2021; Zheng et al., 2020). This result indicates that the observed higher methane yield could be attributed to the GAC amendment, particularly the role of top-GAC biofilm in enriching DIET-related archaea.

In Stage 2, the dominant archaea in GAC biofilms were *Methanobacterium*, *Methanosaeta*, and *Methanosarcina*. Notably, *Methanosarcina* showed a significant increase in top-GAC biofilm, reaching 3.8% in top-GAC biofilm of R2 and 5.2% in top-GAC biofilm of R3. *Methanosarcina* is distinguished by the metabolic versatility, exhibiting a high maximum specific growth rate and a notable half-saturation coefficient, particularly under conditions of increased organic loading rates (De Vrieze et al., 2012). It has been reported in coastal sediment environments, *Geobacter* and *Methanosarcina* have been reported to establish syntrophic DIET partners facilitated by conductive materials (Rotaru et al., 2018). The enhanced relative abundance of *Methanosarcina* and *Geobacter* in top-GAC biofilm suggests a potential establishment of DIET in this stage. This enhancement appears to be directly correlated with the enhanced methane yield observed in UASB with top GAC, especially in R3. These results underscore the critical role of the top-GAC biofilm in promoting DIET, thereby enhancing the reactors' performance.

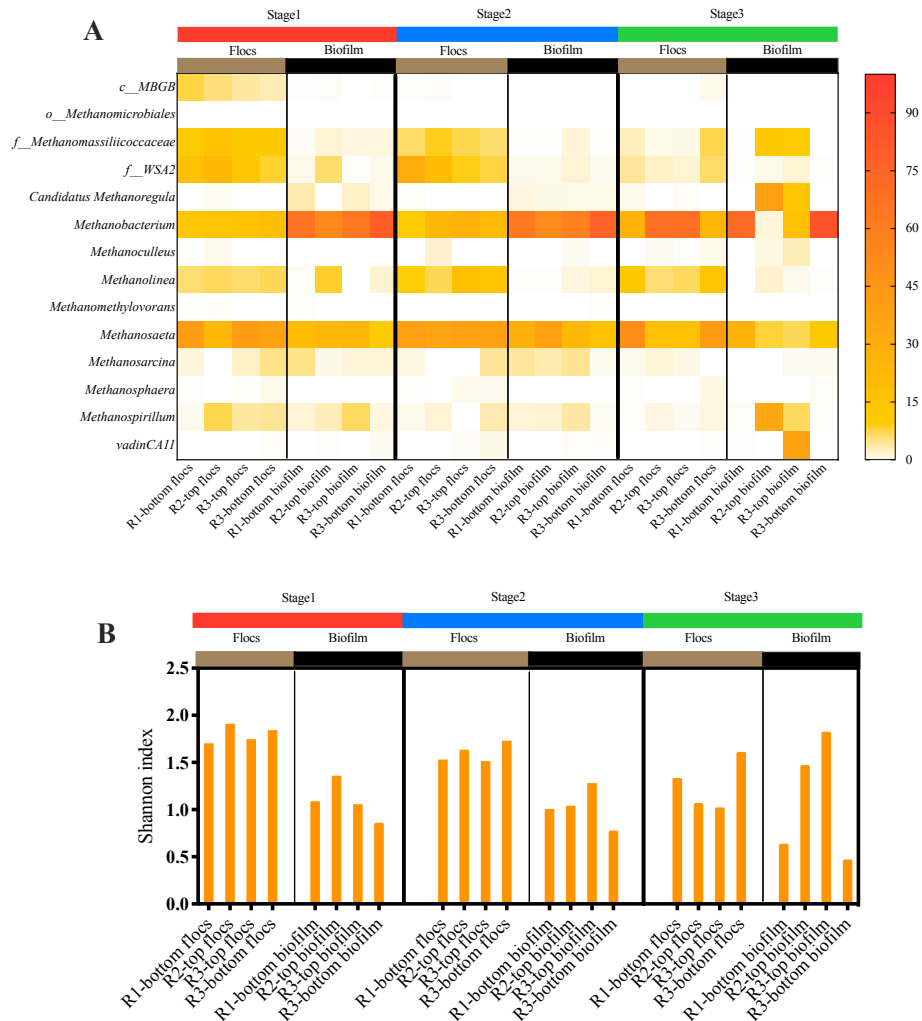


Fig. 6.9. Relative abundance of archaea genera (A) and Shannon index (B) of flocs surrounding GAC and biofilm attached on GAC of three reactors (R1: bottom GAC-amended UASB; R2: top GAC-amended UASB; R3: bottom+top GAC-amended UASB) under three stages (Stage 1: high solid-content wastewater; Stage 2: medium solid-content wastewater; Stage 3: low solid-content wastewater). Taxonomic names are shown for genus level or higher level (family: f_; order: o_; class: c_; p: phylum) if not identified at the genus level.

In Stage 3, *Methanobacterium* and *Methanosaeta* were the predominant archaea in bottom-GAC biofilms. The prevalent archaea in top-GAC biofilm of R2 were *Candidatus Methanoregula*, *Methanospirillum*, and an unidentified genus from *Methanomassiliicoccaceae* family, while top-GAC biofilm of R3 predominantly comprised *VadinCA11*, *Methanobacterium*, and *Candidatus Methanoregula*. This marked a distinction from the archaeal communities observed in Stage 1 and Stage 2. *Methanoregula*, identified as a hydrogenotrophic methanogen, has been suggested as a potential electro-active archaea related to DIET (Walker et al., 2020). The enrichment of *Candidatus Methanoregula* in top-GAC biofilm when treating low solid-content wastewater aligned with previous findings (Yu et al., 2021). These results indicate a differential enrichment of DIET-related archaea in response to varying solid content in wastewater. This divergence was attributed to the addition of bottom GAC in R3, which likely impacted the spatial distribution of intermediates and consequently enriched distinct dominant archaea in the top-GAC biofilm.

Overall, top-GAC biofilm exhibited higher archaeal diversity, with distinct microbial compositions dominated by DIET-related hydrogenotrophic methanogens. This variation was likely attributed to differential substrate availability and physical characteristics of the top GAC environment. Furthermore, top-GAC biofilms facilitated the syntrophic interaction between syntrophic bacteria and hydrogenotrophic methanogens, then enhancing methane production. Meanwhile, the compositions of dominant archaeal communities varied in response to the solid content of the wastewater, indicating a dynamic interaction between biofilm locations and wastewater characteristics.

6.3.6 Predictions of functional genes

Fig. 6.10 represents the predicted metagenomic functions within the flocs and GAC-associated biofilms across the three stages of wastewater treatment, revealing the functional potential of the microbial communities within the UASB reactors.

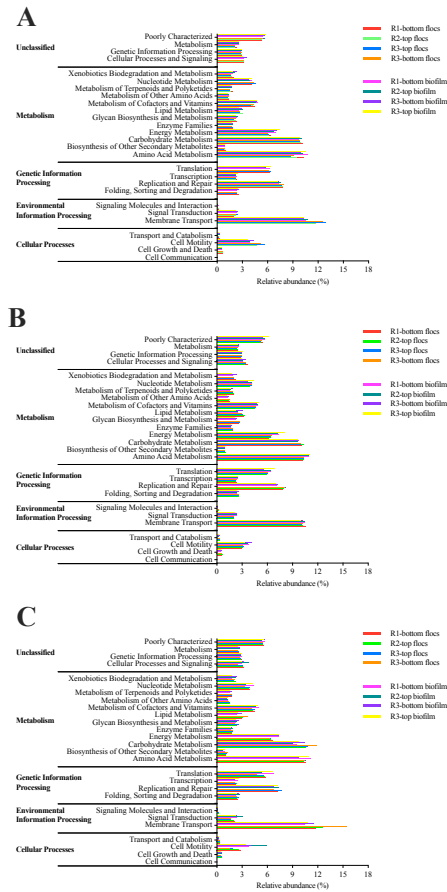


Fig. 6.10. Predicated metagenome functions of flocs surrounding GAC and biofilm attached on GAC of three reactors (R1: bottom GAC-amended UASB; R2: top GAC-amended UASB; R3: bottom+top GAC-amended UASB) under three stages. Stage 1: high solid-content wastewater (A); Stage 2: medium solid-content wastewater (B); Stage 3: low solid-content wastewater (C).

When treating high solid-content substrates, a higher prevalence of genes involved in xenobiotics biodegradation and metabolism in the biofilms, especially in the top-GAC biofilms of R2 and R3, was predicted, compared to the flocs. This indicates an active role of these biofilms in the degradation of complex organic compounds. Additionally, the top GAC biofilms exhibited an increased relative abundance of genes associated with carbohydrate metabolism, which aligned with the enhanced hydrolysis efficiency observed in reactors with top GAC. In contrast, flocs exhibited a high prevalence of cell motility function, indicative of conductive pili growth crucial for cell-to-cell attachment and electron transfer (Yu et al., 2021c). However, this function was less pronounced in GAC biofilms than in flocs, possibly due to limited interactions between the substrates and biofilms under high solid-content conditions.

At Stage 2, there was a notable increase in functions related to metabolism of cofactors and vitamins in the GAC biofilms. This suggests that the microbial communities in GAC biofilms may have a greater capacity for synthesizing essential growth factors, potentially enhancing overall metabolic activity and stability under medium solid-content conditions. Meanwhile, there was an increase in environmental information processing functions, such as signal transduction, and cellular processes including cell motility on GAC biofilms. This shift likely resulted from the increased concentration of soluble substrate concentration in wastewater. These findings provide insights into the efficiency of electron transfer process in GAC biofilms, correlating with the enhanced methane yield during medium solid-content wastewater treatment. Notably, biofilms at the R3 bottom location displayed heightened functions in xenobiotics biodegradation and metabolism and lipid metabolism, suggesting an intensified hydrolysis process. Additionally, these biofilms exhibited an increased prevalence of cellular processes, signaling functions, and cell motility, highlighting their enhanced role in cell-to-cell attachment and electron transfer.

These observations underline the significant impact of the bottom-GAC biofilm of R3 on the hydrolysis and methanogenesis efficiency, contributing to improved energy recovery at this stage.

At Stage 3, there was a shift towards cellular processes and signaling, particularly in the top-GAC biofilms of R2 and R3. This shift could be indicative of an active microbial community responding to lower solid content substrates by increasing cellular maintenance and stress response mechanisms. Moreover, the R2-top biofilm showed greater activity in cellular processes and signaling, signal transduction, and cell motility compared to the R3-top biofilm. This difference was attributed to the absence of bottom GAC in R2, leading to an increased organic load on top-GAC biofilm of R2 and thus enhancing electron transfer. On the other hand, the presence of R3 bottom GAC alleviated the substrate loads for top GAC, resulting in a higher energy recovery efficiency at Stage 3.

These functional gene prediction findings further demonstrated the varying functionalities of GAC biofilms in response to different solid content in wastewater. In high solid-content environments, GAC biofilms predominantly enhanced metabolism-related functions, suggesting their superior capacity to decompose complex organics. Conversely, in a low solid-content environment, the biofilms showed their crucial role in metabolic processes and electron transfer efficiency. The presence of top GAC appeared to enhance functional potential of the biofilm-associated microbial communities. These observations indicate that the functionality of GAC biofilms was highly adaptable, responding distinctly to varying solid-content levels in wastewater, thereby impacting the efficiency of wastewater treatment processes, as the biofilms provided a robust platform for complex biochemical interactions essential for efficient wastewater treatment.

6.3.7 Principal component analysis (PCA)

The composition of microbial community was influenced by operational parameters, including wastewater solid contents, GAC locations, GAC volumes, VSS, methane yield, and hydrolysis efficiency. A principal component analysis was conducted, applying biplot scaling to emphasize the distances between samples, as depicted in Fig.5. The PCA models for bacterial (Fig. 6.11A) and archaeal (Fig. 6.11B) communities accounted for 44.55% and 75.63% of the total variance observed within the respective microbial communities.

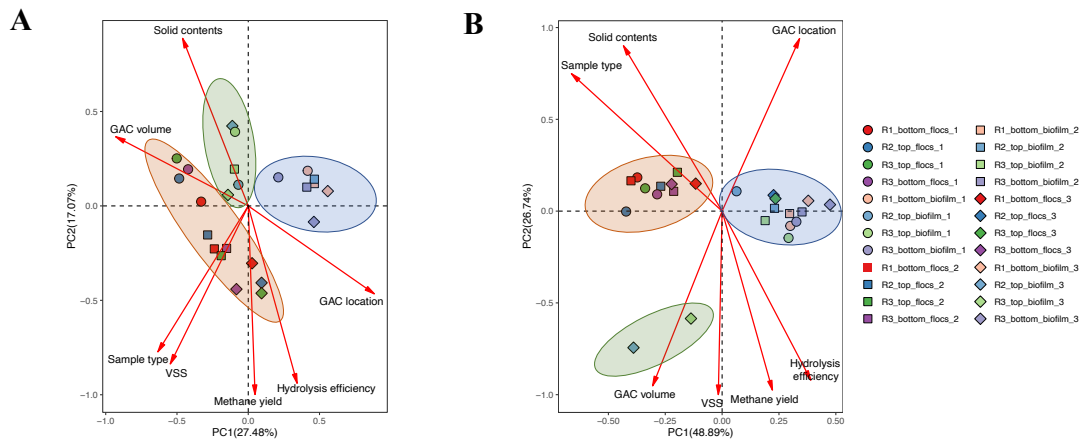


Fig. 6.11. Principal component analysis (PCA) of bacteria (A) and archaea (B) community of flocs and biofilm of three reactors (R1: bottom GAC-amended UASB; R2: top GAC-amended UASB; R3: bottom+top GAC-amended UASB) under three stages (Stage 1: high solid-content wastewater; Stage 2: medium solid-content wastewater; Stage 3: low solid-content wastewater).

In the context of bacterial communities, a distinct clustering of flocs was observed, which was closely associated with VSS concentrations. Conversely, biofilm communities, particularly those associated with the top layer of GAC across all stages, were grouped together and oriented toward

the left side of the biplot. This orientation indicates a correlation with factors such as solid contents, hydrolysis efficiency, and methane yield, suggesting that the top GAC fostered a unique bacterial community. In contrast, samples from bottom-GAC biofilms were positioned toward the right side of the biplot, signifying a strong connection with the GAC location and volume.

For the archaeal communities, a pronounced separation was evident. The flocs displayed clustering which was tightly correlated with the solid contents. For biofilm communities, the top GAC samples from Stage 3 (R2 and R3), were closely grouped, implying a selective pressure exerted by the top GAC in forming a specific archaeal community during the treatment of low solid content wastewater. This selection was potentially more conducive to methanogenesis, as suggested by the directional vectors pointing toward methane yield. This aligned with the high methane yields observed in R2 and R3.

Overall, the PCA findings highlighted the distinct influences of GAC amendment in UASB on the microbial community, with solid content emerging as a significant factor in shaping the distinct bacterial and archaeal communities of top-GAC and bottom-GAC biofilms, thus directly impacting the efficiency of wastewater treatment processes.

6.3.8 Correlation matrix analysis

Fig. 6.12 illustrates the correlation matrix derived from Pearson's product-moment calculations between operational parameters (GAC position, sample type, and substrate solid content) and reactor performance (hydrolysis and methanogenesis), sludge activities (SMA for H₂/CO₂ and SMA for acetate), and microbial community (archaea ratio and bacteria ratio).

The matrix revealed a markedly positive correlation between hydrolysis efficiency and both SMA-H₂ and methanogenesis efficiency, suggesting that efficient hydrolysis could provide a conducive environment for methanogenesis by producing intermediates. Also, there was a notable strong positive correlation between methanogenesis efficiency and SMA-H₂, highlighting the substantial contribution of the hydrogenotrophic methanogenesis pathway to methane yield. The spatial positioning of GAC emerged as influential, with bottom GAC displaying a positive association with SMA-acetate and top GAC with SMA-H₂, underlining the effect of GAC placement on the methanogenesis pathway. Moreover, GAC biofilm correlated positively with the ratios of syntrophic bacteria, archaea ratio, and hydrogenotrophic methanogens ratio, implying that biofilms may provide a supportive place for these communities, thereby facilitating DIET processes.

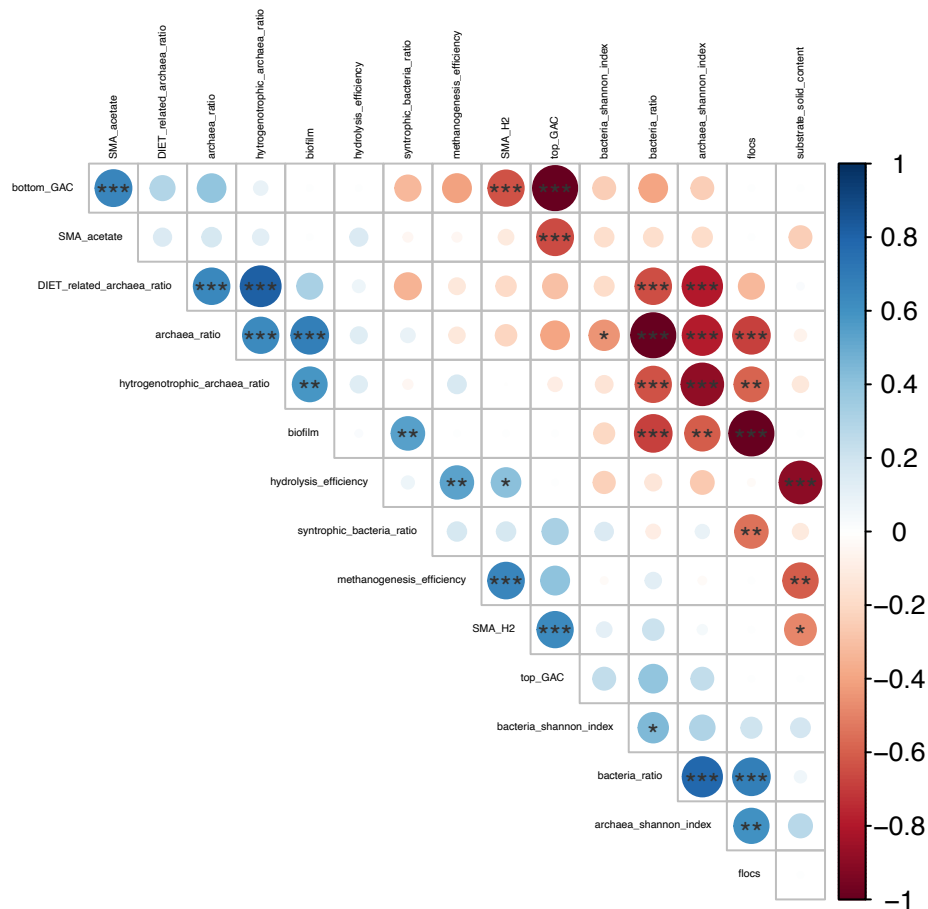


Fig. 6.12. Correlation of operational parameters with reactor performance, sludge activities, and microbial community. The color bar indicates Pearson correlation coefficient. Significance labeled (*) for $p < 0.05$, () for $p < 0.01$, (***) for $p < 0.001$.**

Hydrolysis efficiency showed a significant negative correlation with solid content of substrates, indicating that hydrolysis process was a rate-limited step when treating high solid-content wastewater. Additionally, sample type, representing the distinction between flocs and biofilm, showed significant correlations with microbial community diversity ratios, suggesting that the physical form of the biomass influences microbial diversity and structure.

In summary, the correlation patterns provided insights into the interactions among operational parameters and biological processes within the reactors. GAC positioning correlated with microbial communities and overall reactor performance, indicating that the strategic placement of GAC can be a critical factor in optimizing reactor performance. Moreover, the significant role of GAC biofilm in DIET processes was underscored, further emphasizing their contribution to the overall performance of the reactor system.

6.3.9 Implications

This study provided critical insights into the role of biofilm development on GAC in enhancing the performance of UASB reactors treating wastewater with varying solid contents. It underscored the strategic importance of GAC placement, revealing how top-GAC and bottom-GAC biofilms, in contrast to floc-based communities, distinctly enhanced treatment efficiency and methane production. Specifically, in high solid-content conditions, top GAC markedly boosted hydrolysis and methanogenesis by optimizing microbial interactions. In this process, hydrolysis bacteria were enriched on bottom flocs, while methanogenesis archaea predominate at the top flocs. GAC biofilms further specialized, with bottom-GAC biofilms hosting hydrolytic bacteria like *Bacteroidales*, and top-GAC biofilms favoring the syntrophic interaction of syntrophic bacteria and methanogenic microbes, such as *Geobacter*, *Syntrophus*, *Methanobacterium*, and *Methanosaeta*, which could reduce diffusion constraints and assist direct or indirect interspecies electron exchange. In low solid-content conditions, GAC at both top and bottom synergistically enhanced methanogenesis. Bottom-GAC biofilms played a significant role by enriching hydrogenotrophic archaea such as *Methanobacteria*, mitigating intermediate inhibition, while top biofilms targeted residual substrates through enrichment of syntrophic bacteria, such as *Geobacter* and *Syntrophorhabdus*, and hydrogenotrophic archaea such as *Methanoregula*. The enrichment of

hydrogenotrophic archaea on GAC biofilm was in accordance with previous studies demonstrating hydrogen adsorption onto carbon materials, suggesting GAC's potential to capture hydrogen produced by fermentative bacteria and syntrophic acetate oxidizers in AD process (Florentino et al., 2019; Jin et al., 2007). This capability could enable hydrogenotrophic methanogens on conductive surfaces to directly utilize the adsorbed hydrogen. The microbial community's analysis revealed the positive impacts of GAC biofilms on methane production, facilitating close proximity between syntrophic bacteria and hydrogenotrophic methanogens.

The gene prediction, PCA, and correlation findings highlighted GAC biofilm's dynamic adaptability across varying solid contents, predominantly boosting metabolic functions for complex organic decomposition in high solid-content wastewater. This adaptability underscored GAC biofilms' essential role in metabolic efficiency and electron transfer. The microbial communities of GAC biofilms demonstrated variability in response to the solid content of the substrates. Furthermore, the functional roles of biofilms on the top and bottom GAC exhibited distinct differences. Additionally, the composition of microbial communities enriched on the top GAC was influenced by the presence of bottom GAC in the system. These comprehensive analyses demonstrated that adaptability was critical for improving wastewater treatment processes through enhanced biochemical interactions and operational efficiencies.

6.4 Conclusions

Improved methane production was achieved when self-floating GAC was supplied in UASB reactor treating high solid-content wastewater, where fermentation process was enhanced on the bottom layer of the reactor while the methanogenesis process was improved on the top layer of the reactor. However, when treating low and medium solid-content wastewater, settled + self-

floating GAC can reduce VFA, making anaerobic process more effective. The DIET participants were enriched in GAC-amended reactors, especially the self-floating GAC reactor. These results demonstrated the significance of optimizing the reactor design when treating different kinds of wastewater. Also, this study conclusively demonstrated the positive role of GAC biofilms in enhancing methane production and overall efficiency of UASB reactors across varying solid-content wastewaters. The strategic placement of GAC, both at the top and bottom of reactors, fostered distinct microbial communities that specialize in optimizing hydrolysis and methanogenesis processes. This differentiation in microbial function and community composition, especially in response to high and low solid-content conditions, illustrated the critical adaptability and impact of GAC biofilms on the anaerobic digestion process. Through targeted microbial enrichment and functional specialization, GAC biofilms significantly contributed to more effective and environmentally sustainable wastewater treatment strategies.

**CHAPTER 7 ENHANCING METHANE PRODUCTION AND ORGANIC
LOADING CAPACITY FROM HIGH SOLID-CONTENT WASTEWATER
IN MODIFIED GRANULAR ACTIVATED CARBON (GAC)-AMENDED
UP-FLOW ANAEROBIC SLUDGE BLANKET (UASB)⁶**

A version of this chapter has been published in Science of the Total Environment

⁶ Mou, A., Yu, N., Yang, X., Liu, Y. 2024. Enhancing methane production and organic loading capacity from high solid-content wastewater in modified granular activated carbon (GAC)-amended up-flow anaerobic sludge blanket (UASB). *Science of The Total Environment*, 906, 167609.

7.1 Introduction

Anaerobic digestion (AD), utilizing functional microorganisms in the stages of hydrolysis, acidogenesis, acetogenesis, and methanogenesis, is an efficient and cost-effective way to recover energy from organic waste and wastewater (Mou et al., 2022b). AD is susceptible to changes in operational and environmental aspects, including organic loading rate (OLR), hydraulic retention time (HRT), pH, and temperature (Gao et al., 2019a). The OLR is a critical operation parameter, as it can either positively or negatively impact microbial activities, reaction kinetics, and biogas production. A low OLR can result in microorganism starvation or the development of microorganisms with low activity, whereas an OLR increase can promote rapid microbial growth, enhancing substrate degradation and overall biogas yields (Xu et al., 2018; Zhang et al., 2021a). However, surpassing the optimal OLR can hinder methanogen multiplication, causing acidogenesis to dominate methanogenesis. Such variations can result in the acidification of the digester due to the build-up of volatile fatty acids (VFAs) (Xu et al., 2018). The influence of OLR on the AD microbiome and methane production is substantial, as various studies have examined predominant bacteria and archaea variations and their dynamics concerning different OLR and HRT parameters (Gao et al., 2019b; Zhang et al., 2021b; Zhang et al., 2020d).

Methane production is restricted due to the gradual metabolism of fatty acids by obligate syntrophic microorganisms that transform fatty acids to CO₂ and acetate (Zhang et al., 2022d). Methanogens employ the electrons derived from metabolic process to convert CO₂ to CH₄. Increasing short-chain fatty acid production rates during a high OLR can result in an accumulation of intermediate products, destabilizing the methanogenic community (Yu et al., 2021c; Zhang et al., 2020d). Hence, accelerating the pace of syntrophic metabolism could potentially optimize methanogenesis. During syntrophic metabolism, electrons can be transferred to methanogens

directly or indirectly. In the case of indirect electron transfer, hydrogen or formate usually function as interspecies electron mediators. Direct interspecies electron transfer (DIET) can occur through nonbiological conductive materials like biochar, carbon cloth, and granular activated carbon (GAC) (Lin et al., 2018; Mo et al., 2023; Zhao et al., 2015; Zhou et al., 2023). These materials facilitate electron transfer between syntrophic partners, and recent research has demonstrated that DIET can significantly improve the conversion of VFAs to methane (Dang et al., 2022; Guo et al., 2022). Mathematical simulations have demonstrated that the rates of DIET can exceed interspecies hydrogen transfer rates by a factor of 8.6 (Storck et al., 2016). This electron transfer rate enhancement enables the employment of a higher OLR and reduces acid stress in the digester. Consequently, digesters active with DIET can manage relatively higher OLRs compared to traditional digesters.

Recently, spatial distributions of GAC in up-flow anaerobic sludge blanket (UASB) were evaluated (Mou et al., 2022a; Yu et al., 2021c). When GAC was supplied to the upper portion of the UASB, fermentation was improved at reactor's bottom and methanogenesis was increased at reactor's top. The spatial distribution of GAC in a bioreactor was found to impact the formation and distribution of microenvironments within the bioreactor; this influenced the kinds, growth, and activities of the microorganisms (Lee et al., 2021; Liu et al., 2020a; Maloney et al., 2002). A uniform distribution of GAC throughout the bioreactor provided microorganisms with equal access to the GAC surface area. However, when GAC was preferentially placed in certain areas of the reactor, microorganisms aggregated and attached to the GAC surface in these areas (Zhang et al., 2021b). This could lead to the formation of distinct microbial communities with different metabolic pathways and functions. Placements of GAC in different areas of the reactor have been shown to improve the contact between microorganisms and substrate (Yu et al., 2021c), and to

enhance the removal rates of organic matter from wastewater. Thus, the spatial distribution of GAC in bioreactor systems could impact microbiome development and reactor performance by influencing the formation of microenvironments, hydrodynamics, and mass transfer. Proper placement of GAC could lead to improved reactor performance and the formation of diverse microbial communities with distinct metabolic functions (Yu et al., 2021c; Zhang et al., 2022d). Therefore, careful consideration of GAC spatial distribution is crucial in the design and operation of bioreactor systems. Previous studies of GAC distributions in reactors treating wastewaters predominantly targeted low solid content wastewaters, such as glucose (Yu et al., 2021c; Zhang et al., 2022c). No comprehensive study has been conducted to understand the effects of GAC distributions in the treatment of high solid-content wastewaters, particularly in relation to high organic loading treatments.

To assess the potential of bottom and top GAC application in AD processes and gain a clear understanding of its applicability, three UASB reactors were tested: one with bottom GAC, one with top GAC, and one with bottom+top GAC. The organic loading capacity of high solid-content wastewater was measured. The performance and stability at high OLRs of the three UASB reactors were measured. Furthermore, the potential mechanism was uncovered via spatial microbial community analysis, which was expected to provide insight into anaerobic treatment of high solid-content wastes.

7.2 Materials and methods

7.2.1 Design and operation of the reactors

Three lab-scale UASB reactors (R1, R2, and R3) were continuously operated at a mesophilic temperature (35 °C) for 150 days, with 25 g/L of bottom GAC (pellet diameter 0.1 inches, Acurel®

Extreme Activated Filter Carbon Pellets, USA) (R1), top GAC (R2), and bottom+top GAC (R3). The GAC introduced to R1 settled at the reactor's bottom. The GAC added to R2 was packed together with polyethylene (PE) plastic media balls (1 inch in diameter, Powkoo, Canada) (**Fig. 7.1**). Each PE plastic media ball contained one gram GAC. And R3 had both bottom and top GAC (10 g/L and 15 g/L, respectively) (Mou et al., 2022a). The three UASB reactors were amended with identical GAC concentrations, but their distributions differed. In the bottom GAC reactor (R1), the settled GAC occupied the reactor's bottom, constituting only 3% of its volume. In contrast, the top GAC reactor (R2) had its GAC, encased in plastic media, spread across the middle and upper sections, making up about 50% of the reactor's total volume. Meanwhile, the bottom+top GAC reactor had both bottom and top GAC (within plastic media), which together accounted for 30% of its volume. The GAC utilized originated from coconut shells, boasting a surface area ranging from 800 to 1500 m²/g and a typical pore size between 2 to 50 nm. Prior to the experiment, the GAC underwent a thorough rinse with deionized water. Three UASBs were operated in three stages: Stage 1 (Day 0-60), Stage 2 (Day 61-110), and Stage 3 (Day 111-150). The OLRs increased stepwise, from 2.0 ± 0.2 g/L/d in Stage 1 to 4.0 ± 0.3 g/L/d in Stage 2, and to 6.0 ± 0.2 g/L/d in Stage 3, through decreases in HRT from 7.0 days in Stage 1, to 3.5 days in Stage 2, and to 2.3 days in Stage 3.



Fig. 7.1. The top-GAC bio-balls.

7.2.2 Seed sludge and wastewater

The initial sludge, sourced from a municipal wastewater treatment plant's anaerobic digester in Edmonton, Alberta, Canada, had a volatile suspended sludge (VSS) concentration of 7 g/L. High solid-content synthetic wastewater was prepared using commercial dog food. The total chemical oxygen demand (TCOD) and the soluble chemical oxygen demand (SCOD) of the high solid-content synthetic wastewater were 14.0 ± 1.4 g/L and 1.0 ± 0.3 g/L, respectively. Feedstock solid-content ratios (SCOD/TCOD ratio) $< 10\%$ were defined as high solid-content wastes (Mou et al., 2022a). The feedstock was adjusted with sodium carbonate to a pH of 7.5 before being pumped into the reactors.

7.2.3 Analytical techniques and calculations

7.2.3.1 Analytical techniques

Total suspended solids (TSS), VSS, total solids (TS), volatile solids (VS), and chemical oxygen demand (COD) were analyzed in accordance with the Standard Methods (Baird et al., 2017). Foil gas bags with a 10 L capacity (CHROMSPEC™, Brockville, Canada) were used for biogas collection. The compositions of the biogas were determined using a gas chromatograph (GC, 7890B Agilent Technologies, USA) equipped with a Hayesep Q column and a thermal conductivity detector. Helium gas, with a purity level of 99.999%, functioned as the carrier gas. The designated temperatures for the oven and detector were set at 100 °C and 200 °C, respectively. To analyze volatile fatty acids (VFA) such as acetate, propionate, and butyrate, an ionic chromatography (IC, DIONEX ICS-2100, ThermoFisher, USA) was utilized. This instrument was equipped with a conductivity detector and an IonPac AS18 Analytical Column (2 × 250 mm).

Before the analysis, samples were filtered through 0.22 µm membrane filters (Fisher Scientific, CA).

7.2.3.2 Methane yield calculations

The methane yield was calculated using Equation (7-1) (Zhang et al., 2019):

$$\text{Methane yield} = \frac{64 \cdot P \cdot V_d \cdot C_d}{R \cdot T \cdot \text{TCOD}_d} \times 100\% \quad (7-1)$$

Where *Methane yield*: the fraction of influent TCOD that is converted to methane (%; g CH₄-COD/g TCOD); *P*: atmosphere pressure (kPa); *V_d*: biogas volume on day d (L); *C_d*: methane percentage in biogas on day d (%); *R*: gas law constant (L·kPa/(K·mol)); *T*: gas temperature (K); *COD_d*: total COD input on day d (g TCOD); *64*: conversion factor of 1 mol methane to 64 g COD.

7.2.3.3 Chemical oxygen demand (COD) balance calculations

The influent COD can be apportioned into four distinct pathways: converted to methane, discharged in effluent, discharged waste sludge, and accumulated in reactor sludge bed. The mass balance for the influent COD is shown in Equation (7-2) (Sun et al., 2022):

$$\text{COD}_{\text{influent}} Q \Delta t = \sum_{i=1}^{i=\Delta t} \text{COD}_{\text{methane}} V_i + \text{COD}_{\text{effluent}} Q \Delta t + \text{COD}_{\text{discharge}} V_{\text{discharge}} + (\text{COD}_{\text{sludge}, \Delta t} V_{\Delta t} - \text{COD}_{\text{sludge}, 0} V_0) \quad (7-2)$$

Where *Δt*: the duration of COD mass balance test (d); *COD_{influent}*, *COD_{effluent}*, and *COD_{discharge}*: the COD concentrations of influent, effluent, and discharged sludge (g/L); *COD_{sludge,0}*: the COD of sludge in the reactor sludge bed at *t=0* (g/L); *COD_{sludge, Δt}*: the COD of sludge in the reactor sludge bed at *t=Δt* (g/L); *COD_{methane}*: the COD of methane (g/L); *Q*: the volumetric flow rate (L/d); *V_i*:

the methane volume at $t=i$ (L); $V_{discharge}$: the volume of discharged waste sludge (L); $V_{\Delta t}$ and V_0 : the volumes of sludge in the reactor at $t=\Delta t$ and $t=0$, respectively (L).

7.2.3.4 Hydrolysis efficiency calculations

The hydrolysis efficiency was calculated using Equation (7-3) (Sun et al., 2021):

$$\text{Hydrolysis efficiency} = \frac{COD_{CH_4} + SCOD_{effluent} - SCOD_{influent}}{TCOD_{influent} - SCOD_{influent}} \times 100\% \quad (7-3)$$

Where *Hydrolysis efficiency*: the percentage of the feed particulate COD that is hydrolyzed (%); COD_{CH_4} : the COD converted to the produced methane (g/L); $SCOD_{effluent}$: the soluble COD in the effluent (g/L); $SCOD_{influent}$: the soluble COD in the feed (g/L); $TCOD_{influent}$: the total COD in the feed (g/L); $SCOD_{influent}$: the soluble COD in the feed (g/L).

7.2.4 Sludge characterization

The maximal methane production capacity of the sludge in the reactor was determined by sampling from the top and bottom sludge. The specific methanogenic activity (SMA) and sludge stability of each sludge sample were evaluated. SMA was measured to evaluate the ability of sludge to transfer acetate or H_2/CO_2 into CH_4 . The measurement of sludge stability identified the percentage of biodegradable substrate within the sludge. All tests were performed in triplicate.

7.2.5 Analysis of microbial community

Sludge samples, each of 2 mL, from top and bottom sludge blanket, were centrifuged at 3000g for 10 mins with the supernatant subsequently discarded. As per the guidelines provided by the manufacturer, DNA was extracted from the remaining sludge pellet using a DNeasy PowerSoil Kit (QIAGEN, Hilden, Germany). The polymerase chain reaction (PCR) process was conducted

on the Illumina MiSeq platform. 16S rRNA genes were amplified using the universal primer pairs 515F and 806R. The DADA2 pipeline in QIIME 2 was utilized for DNA sequence analysis, offering a 99% match to the Greengenes database. All raw sequence files were stored at the National Center for Biotechnology Information (NCBI) under Bioproject PRJNA 985778.

7.2.6. Analysis of statistical significance

The data's statistical significance was assessed using a Student's T-test. *P* values below 0.05 were deemed statistically significant.

7.3 Results and Discussion

7.3.1 Reactor performance

7.3.1.1 Methane yield, chemical oxygen demand removal, and effluent pH

Three UASB reactors were fed with wastewater having a high solid content of 14 g COD/L and operated at a mesophilic temperature of 35 °C for 150 days. The OLRs were gradually increased from 2.0 ± 0.2 g/L/d in Stage 1 to 4.0 ± 0.3 g/L/d in Stage 2, then to 6.0 ± 0.2 g/L/d in Stage 3. The three reactors were differentiated based on the placement of GAC, with R1 having GAC placed at the bottom, R2 having GAC placed at the top, and R3 having GAC placed at the bottom and the top. Variations in methane yields, effluent COD concentrations, and effluent pH in the three UASBs at each stage are shown in **Fig. 7.2**.

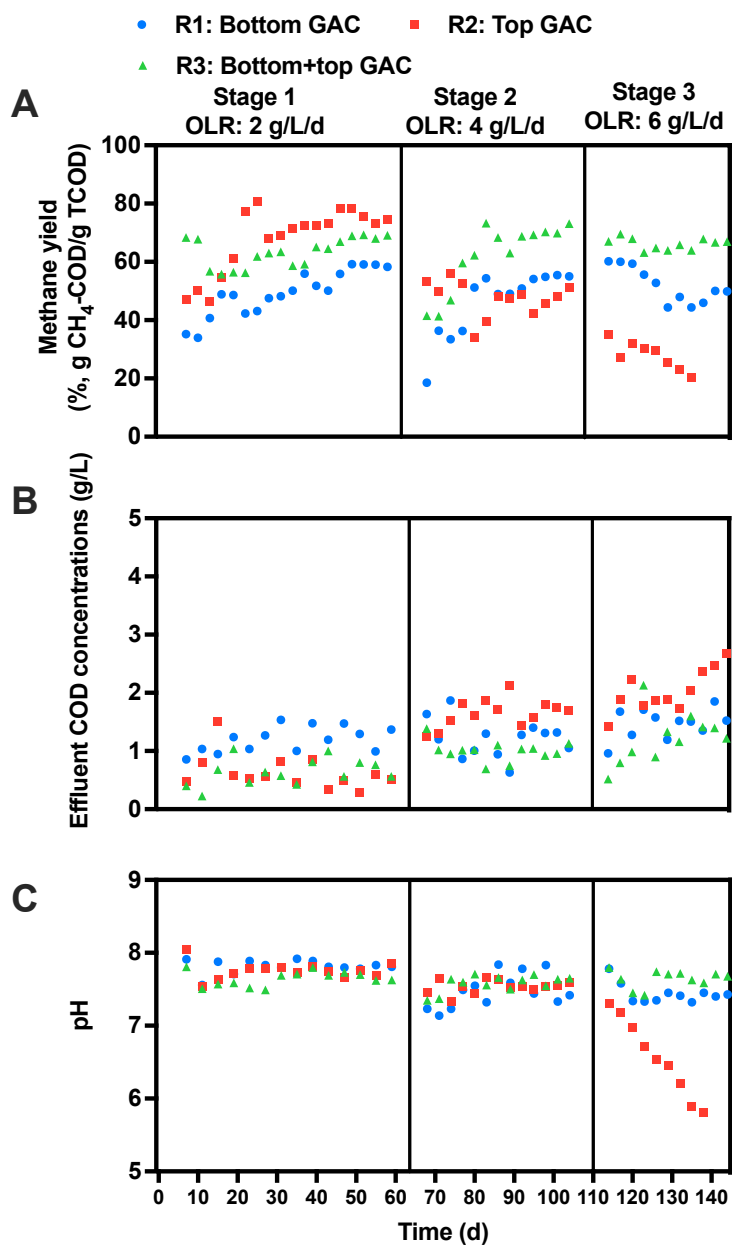


Fig. 7.2. Reactor performances: (A) Methane yield, (B) effluent chemical oxygen demand (COD) concentrations and (C) effluent pH.

During Stage 1, R2 and R3 reactors exhibited higher methane yields than R1 (**Fig. 7.2A**). At an OLR of 2.0 ± 0.2 g/L/d, R2 had a methane yield of $74 \pm 4\%$ (g CH₄-COD/g TCOD), R3 had a methane yield of $65 \pm 4\%$ (g CH₄-COD/g TCOD), and R1 had a methane yield of $58 \pm 1\%$ (g CH₄-

COD/g TCOD). In a previous study, the methane yield in a UASB reactor without GAC was reported to be 47.9% (g CH₄-COD/g TCOD) (Sun et al., 2022). This result was notably lower than those observed in the three GAC-amended UASB reactors in this study. This finding suggests that the addition of either bottom or top GAC, or both, had the potential to enhance methane yield. The methane yield of R2 exceeded that of R3 by 14%. In Stage 2, as the OLR increased, R3 demonstrated the highest methane yield: $67 \pm 5\%$ (g CH₄-COD/g TCOD). In Stage 2 the methane yields of R1 and R2 decreased to $52 \pm 3\%$ (g CH₄-COD/g TCOD) and $47 \pm 6\%$ (g CH₄-COD/g TCOD), respectively. In Stage 3, at an OLR of 6.0 ± 0.2 g/L/d, R3 maintained a stable methane yield, whereas R2 experienced a sharp decline in methane yield ($28 \pm 5\%$, g CH₄-COD/g TCOD). The methane yield of R1 declined to $47 \pm 3\%$ (g CH₄-COD/g TCOD) in Stage 3.

In the first stage, the effluent COD concentration of R1 was 1.2 ± 0.2 g/L, R2 was 0.6 ± 0.3 g/L, and R3 was 0.6 ± 0.2 g/L (**Fig. 7.2B**). These results suggest that top GAC improved reactor performance regarding effluent COD levels at low OLRs. Following an increase in OLR to 4.0 ± 0.3 g/L/d in Stage 2, the effluent COD concentration of R1 remained at 1.2 ± 0.3 g/L, while the effluent COD concentrations of R2 and R3 rose to 1.7 ± 0.2 g/L and 1.0 ± 0.2 g/L, respectively. As the OLR increased to 6.0 ± 0.2 g/L/d during Stage 3, the effluent COD concentrations of all three reactors increased.

The addition of GAC at the top of the reactor had a positive impact on reactor performance with respect to methane yield and effluent COD during the treatment of high solid-content wastewater at a low OLR. As the OLR increased, the methane yield and the effluent COD quality of R2 declined rapidly and failed completely in Stage 3 due to acid accumulation, as shown by the sharp decrease in pH in Stage 3 (**Fig. 7.2C**). However, the performance of R1 and R3, which had GAC at the bottom, remained stable under high OLR conditions. This implies that having GAC at the

bottom of the reactor had a favorable impact on reactor performance at high OLRs. In the case of R1, the methane yield decreased in Stage 3 whereas the effluent COD concentration remained at the same level from Stage 1 to Stage 3, indicating an increase in COD accumulation in the UASB, attributed to the COD designated for microorganism growth and the particulate COD in the sludge bed that remains unhydrolyzed. Conversely, the methane yield of R3 increased, but effluent COD quality decreased, suggesting a decrease in COD accumulation in the reactor. This implies that, under high OLR conditions, high solid-content wastewater can be effectively converted to energy when reactor's bottom and top both contained GAC (R3).

7.3.1.2 Chemical oxygen demand mass balance

The fate of influent COD can be categorized into five outcomes: produced methane, effluent COD, accumulated COD in the sludge bed, discharged sludge, and unidentified COD (**Fig. 7.3**). In Stage 1, R1 exhibited a considerable COD accumulation in the sludge ($14.7 \pm 1.3\%$). Additionally, $58.3 \pm 1.4\%$ of the influent COD was transformed into methane, while only $9.0 \pm 1.3\%$ of influent COD was detected in the effluent. In contrast, the reactors with top GAC (R2 and R3) demonstrated a significantly higher percentage of methane conversion, with $74.2 \pm 3.7\%$ and $65.1 \pm 3.8\%$ influent COD being converted to methane, respectively. Consequently, enhanced effluent quality and decreased COD accumulation were observed in the reactors amended with GAC at the top. A higher amount of energy was harvested in the form of biomethane from top GAC-amended reactors (R2 and R3).

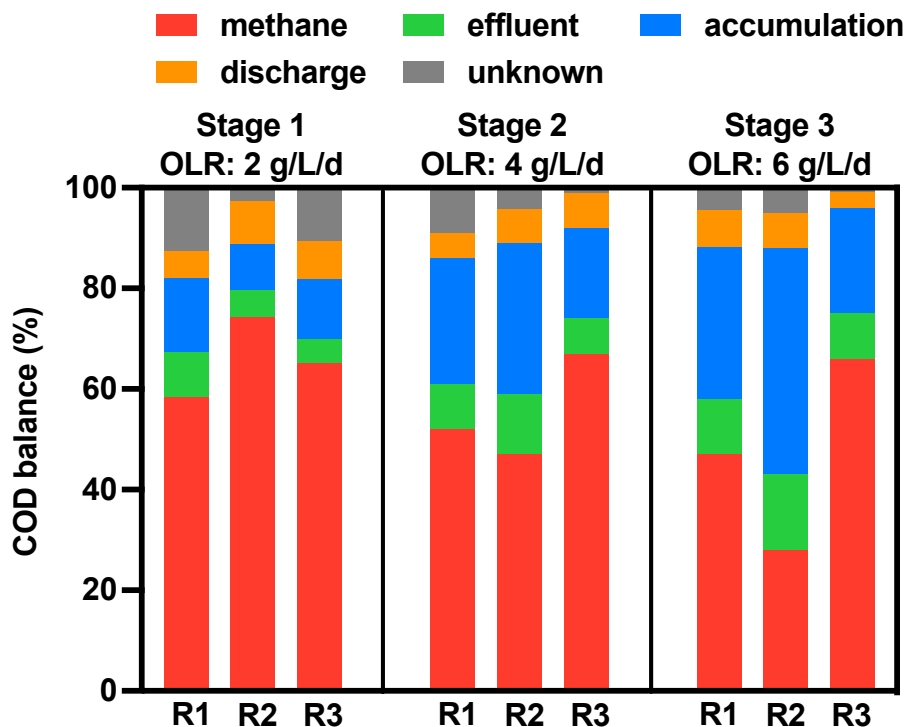


Fig. 7.3. Chemical oxygen demand (COD) mass balance of three reactors (R1: bottom GAC; R2: top GAC; R3: bottom+top GAC) at different organic loading rates (OLRs).

During Stage 2, COD accumulation rose in all three reactors. The reactor with only top GAC (R2) displayed a significant COD accumulation ($30.2 \pm 5.9\%$) in the sludge bed. Furthermore, $47.4 \pm 6.0\%$ of influent COD was transformed into methane, while $11.8 \pm 1.7\%$ of influent COD was present in the effluent in R2. In contrast, the reactors with GAC amended at the bottom (R1 and R3) demonstrated higher methane productions ($52.4 \pm 2.6\%$ for R1 and $67.4 \pm 4.6\%$ for R3) and lower COD accumulations ($25.1 \pm 2.6\%$ for R1 and $17.9 \pm 2.6\%$ for R3) than the reactor without bottom GAC (R2). This suggests that the inclusion of bottom GAC in the reactor had a favorable influence on methane production.

In Stage 3 (OLR was 6 ± 0.2 g/L/d), the produced methane in R2 experienced a sharp drop, reaching $27.9 \pm 4.8\%$. However, accumulated COD and effluent COD rose to $45.0 \pm 4.5\%$ and $14.5 \pm 2.6\%$, respectively, both of which were considerably higher than those observed in Stage 1 and Stage 2. Compared to R2, R1 and R3 (with bottom GAC) demonstrated stable operation, exhibiting lower COD accumulation in the sludge bed, and reduced effluent COD.

In summary, the placement of GAC at the top of the reactor contributed to a reduction in COD accumulation in the sludge bed at low OLR conditions. Additionally, the addition of GAC to reactor's bottom enhanced the effluent COD quality and minimized the COD accumulation in the sludge bed at elevated OLR conditions. The amendment of both bottom and top GAC in the reactor could potentially boost energy recovery and improve effluent COD quality when processing high solid-content wastewater at a high OLR.

7.3.2 Hydrolysis efficiency

Hydrolysis frequently represents the step that restricts the overall rate of AD process when dealing with substrates containing high solids (Ellacuriaga et al., 2021; Sun et al., 2022). To better understand the influence of the spatial distribution of GAC on anaerobic digestion, hydrolysis efficiencies of high solid-content substrates were calculated, as displayed in **Fig. 7.4**. In Stage 1, R2 demonstrated the highest hydrolysis efficiency ($74.2 \pm 3.7\%$), while R1 exhibited the lowest hydrolysis efficiency ($63.7 \pm 7.2\%$). This result aligns with the increased methane production and increased COD reduction in R2 (**Fig. 7.2**). Additionally, the high hydrolysis efficiency in R2 clarified the low accumulation of COD in the sludge bed (**Fig. 7.3**). These observations confirm that the addition of GAC to the top of a reactor can stimulate the hydrolysis efficiency of high solid-content substrates, as previously reported (Mou et al., 2022a; Yu et al., 2021c).

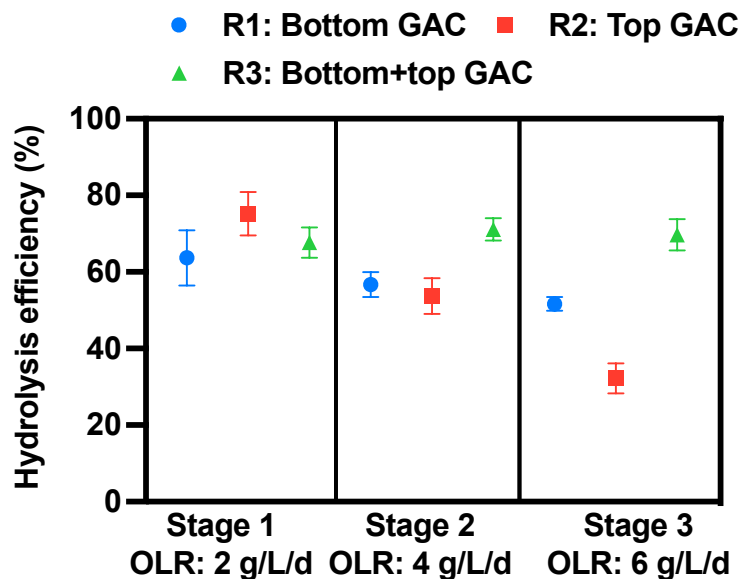


Fig. 7.4. Hydrolysis efficiency of three reactors at different organic loading rates (OLRs).

Upon raising the OLR in Stage 2, the reactors with bottom GAC displayed increased hydrolysis efficiencies ($56.7 \pm 3.3\%$ for R1 and $71.1 \pm 2.9\%$ for R3) compared to the reactor without bottom GAC (R2) ($53.7 \pm 4.7\%$). The fact that the hydrolysis efficiency of R1 in Stage 2 decreased relative to Stage 1 might account for the increased COD accumulation in the sludge bed. The results suggest that the placement of GAC at the bottom of a USAB can enhance the hydrolysis of high solid-content substrates under high OLR conditions.

Following a further OLR increase to 6 ± 0.2 g/L/d, the hydrolysis efficiency of R2 plummeted to $32.2 \pm 3.9\%$, corresponding with a substantial COD accumulation. At the elevated OLR, the hydrolysis efficiency of R1 dropped to $51.7 \pm 1.8\%$, which might explain the reduced methane yield and increased COD accumulation. Although the OLR increased to 6 ± 0.2 g/L/d in Stage 3, no significant difference ($p > 0.05$) was observed in hydrolysis efficiencies in R3. This suggests that the addition of GAC to both the top and the bottom of a reactor might improve syntrophic

degradation activities by enhancing methanogenesis and stimulating fermentation under a high OLR.

During the low OLR stage, the top GAC promoted methanogenesis process, enabling the conversion of fermentation products and reducing intermediated inhibition, thus allowing high solid wastewater anaerobic digestion to proceed in accordance with sequential reaction steps. However, following an OLR increase, the reduced HRT resulted in insufficient contact time between substrates and microorganisms. Thus, introducing both top and bottom GAC in the reactor could improve methanogenesis and further stimulate the hydrolysis, allowing for efficient energy recovery under high OLR conditions.

7.3.3 Volatile fatty acids (VFAs) concentrations

In three UASB reactors, mixed liquor samples were collected from both the top and bottom layers of the sludge blanket to evaluate the spatial distributions of VFA during stable operational conditions. **Fig. 7.5** illustrates that during Stage 1, R1 displayed the highest VFA concentration at the top layer, which was 442 mg/L. This suggests limited degradation of intermediates in R1's top layer, which lacked bottom GAC. Conversely, R2's bottom had the highest VFA concentration of 875 mg/L among the three reactors, suggesting a dominant fermentation process in its bottom layer. The VFA concentrations in the top layers of R2 and R3 were 247 mg/L and 313 mg/L, respectively, both of which were lower than that of R1. This reduction can be ascribed to the addition of top GAC in both R2 and R3. Notably, even though both R2 and R3 were amended with top GAC, their VFA distributions differed, attributed to the presence of bottom GAC in R3. The findings imply that VFA-to-methane conversion was primarily enhanced in R2's top layer, while a distinct fermentation zone was present in R2's bottom layer, enhancing energy recovery.

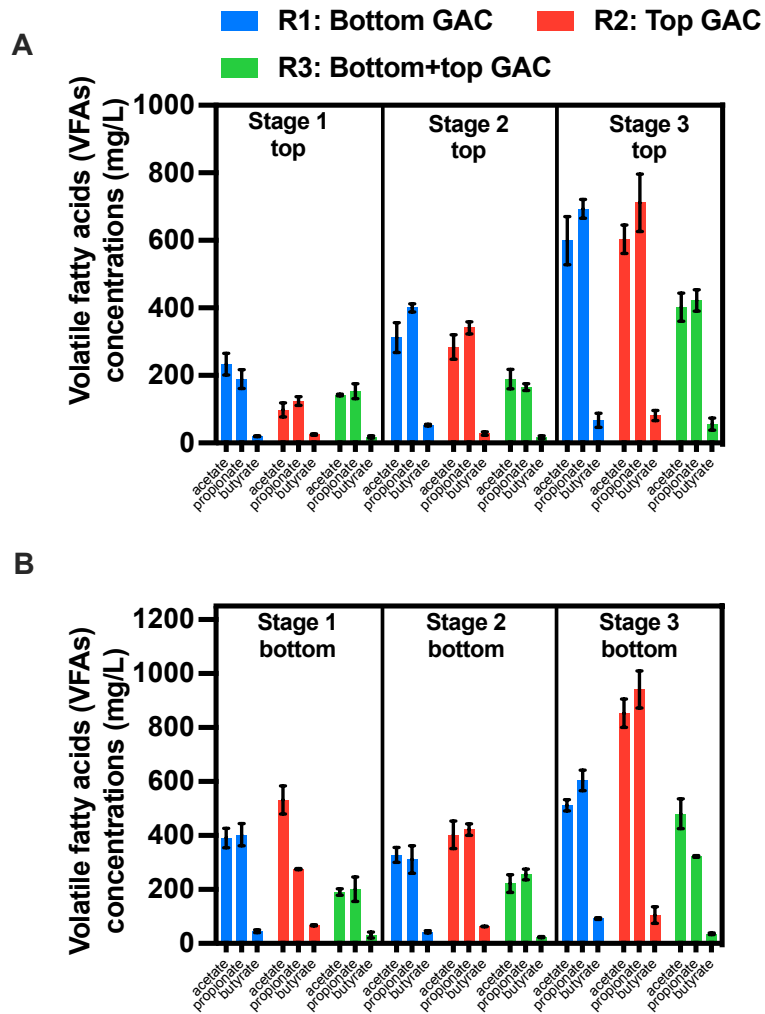


Fig. 7.5. Volatile fatty acids (VFAs) concentrations in terms of acetate, propionate, and butyrate of top layer (A) and bottom layer (B) of three reactors at different organic loading rates (OLRs).

In Stage 2, the VFA concentrations in the top layers of R2 and R3 were 653 mg/L and 371 mg/L, respectively. Both values were lower than R1's VFA, which could be attributed to the presence of top GAC in R2 and R3. It is noteworthy that R2's top VFA concentration exceeded that of R3, a deviation from the observations in Stage 1. The elevated OLR in Stage 2 amplified the VFA inhibition loading. Furthermore, the presence of bottom GAC in R3 facilitated VFA consumption

in the bottom layer, subsequently reducing the VFA concentration in the top layer. This observation aligns with the enhanced performance of R3 during Stage 2.

In Stage 3, R3's top and bottom layers consistently showed the lowest VFA concentrations among all reactors. This result can be attributed to the combined effects of top and bottom GAC, which enhanced the methanogenesis process throughout the reactor. As a result, VFA inhibition was reduced, likely accounting for R3's higher methane yield under high OLR conditions. Conversely, the VFA accumulation in R2's layers provides insight into its operational failure during Stage 3.

In summary, under low OLR conditions, fermentation and methanogenesis processes are segregated within different layers of the top GAC reactor (R2). However, under high OLR conditions, the presence of both bottom and top GAC in R3 facilitated faster VFA consumption, thereby alleviating VFA inhibition.

7.3.4 Sludge stability

To understand the roles of GAC at different spatial locations and clarify the accumulation of particulate COD in the reactors at different OLRs, sludge stability was examined in three reactors' top and bottom sludge beds (**Fig. 7.6**). High sludge stability indicates the existence of a substantial fraction of the biodegradable substrate in the sludge. For three reactors, the bottom sludge bed exhibited markedly higher stability in comparison to the top sludge bed at three stages, suggesting that particulate COD mainly accumulated in the bottom layer of sludge due to the high solid content of the wastewater.

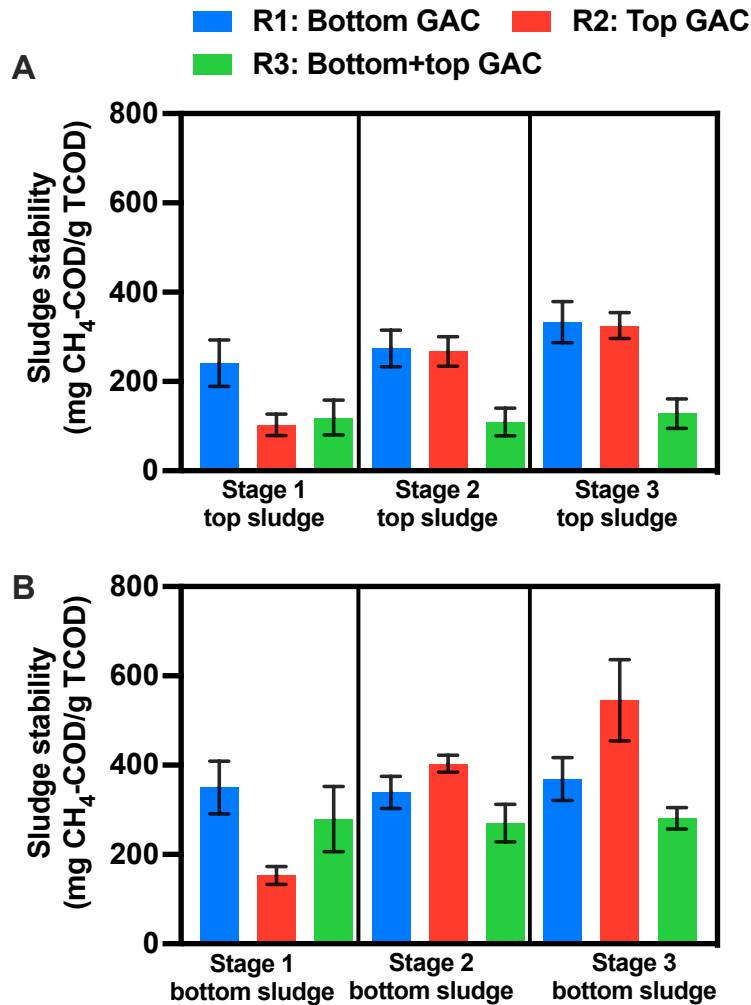


Fig. 7.6. Sludge stability of top layer (A) and bottom layer (B) of three reactors at different organic loading rates (OLRs). Stage 1: OLR was 2.0 ± 0.2 g/L/d; Stage 2: OLR was 4.0 ± 0.3 g/L/d; Stage 3: OLR was 6.0 ± 0.2 g/L/d.

In Stage 1, R1 had the highest sludge stability at top layer (241 ± 52 mg CH₄-COD/g TCOD) and bottom layer (350 ± 59 mg CH₄-COD/g TCOD). Among three reactors, in Stage 1, R2 displayed the lowest sludge stability at both the bottom layer (153 ± 20 mg CH₄-COD/g TCOD) and the top layer (103 ± 24 mg CH₄-COD/g TCOD), indicating a low accumulation of biodegradable COD. The R3's top sludge exhibited a lower biodegradability than R1's top sludge. However, the sludge

stability at R3's bottom was higher than that at R2's bottom. This might be attributed to the dominance of fermentative bacteria in R2's bottom sludge, leading to the formation of a fermentation zone located in reactor's bottom layer, which makes anaerobic process more efficient. These observations suggest that the hydrolysis might occur in the bottom sludge bed as a result of top GAC addition, wherein top GAC could stimulate methanogenesis in top sludge bed, promoting the conversion of fermentation products, reducing the inhibition of intermediates, and ultimately accelerating the hydrolysis in the bottom sludge bed under low OLR conditions.

At Stage 2, the sludge stability at R1's bottom remained at 339 ± 36 mg CH₄-COD/g TCOD, and the sludge stability at R1's top increased to 274 ± 41 mg CH₄-COD/g TCOD. This suggests that the elevated COD accumulation in R1 during Stage 2 (**Fig.7.3**) occurred in the upper layer of the sludge bed. This was potentially due to the absence of GAC at the top of R1. The R2's bottom sludge exhibited increased stability at a high OLR (403 ± 19 mg CH₄-COD/g TCOD) compared to the bottom sludge of R1 and R3, which both contained GAC at the bottom. This suggests that GAC placed at reactor's bottom can improve methanogenesis efficiency when the reactor is operated at a high OLR. The elevated sludge stability observed in R2's top sludge (267 ± 33 mg CH₄-COD/g TCOD) could be attributed to a large accumulation of solids substrates at reactor's bottom, raising sludge bed height and resulting in an accumulation of particulate COD in the upper layer as the sludge bed ascends.

At Stage 3, the sludge stability at R2's bottom exhibited a significant rise to 545 ± 91 mg CH₄-COD/g TCOD. This could be due to the lack of GAC at R2's bottom. In comparison, the sludge stability in R3's top sludge (128 ± 33 mg CH₄-COD/g) was lower than in R1's top sludge (333 ± 46 mg CH₄-COD/g TCOD) at a high OLR. This could be explained by the introduction of top

GAC in R3, where fast consumption of intermediates could reduce the intermediates inhibition and allow the hydrolysis process to proceed efficiently.

To summarize, the addition of top GAC reduced the buildup of particulate COD in the reactor at low OLRs. When GAC was placed at reactor's bottom, the sludge stability decreased at high OLRs. Thus, the spatial analysis of sludge stability outcomes proved the distinct influence of GAC spatial locations on anaerobic processes under different OLR conditions.

7.3.5 Specific methanogenic activities of sludge

To gain insight into the effects of bottom GAC and/or top GAC on sludge activities, the SMA was analyzed at top and bottom sludge (**Fig. 7.7**). At Stage 1, R2's top sludge had the highest hydrogenotrophic SMA (1026 ± 70 mg CH₄-COD/gVSS/d) compared to R1's and R3's top sludge, whereas R2's bottom sludge presented a lowest hydrogenotrophic SMA of 394 ± 110 mg CH₄-COD/gVSS/d among three reactors. This suggests that the placement of GAC at the top of R2 stimulated the activity of hydrogenotrophic methanogens in the sludge at the top of the reactor. R3's bottom sludge had a higher hydrogenotrophic SMA (751 ± 17 mg CH₄-COD/gVSS/d) compared to R3's top sludge (650 ± 61 mg CH₄-COD/gVSS/d). However, R3's top sludge showed a lower hydrogenotrophic SMA than R2's top sludge; this result might be due to VFA consumption by methanogens in R3's bottom and then the VFA starvation of methanogens in the sludge at R3's top in the low OLR condition.

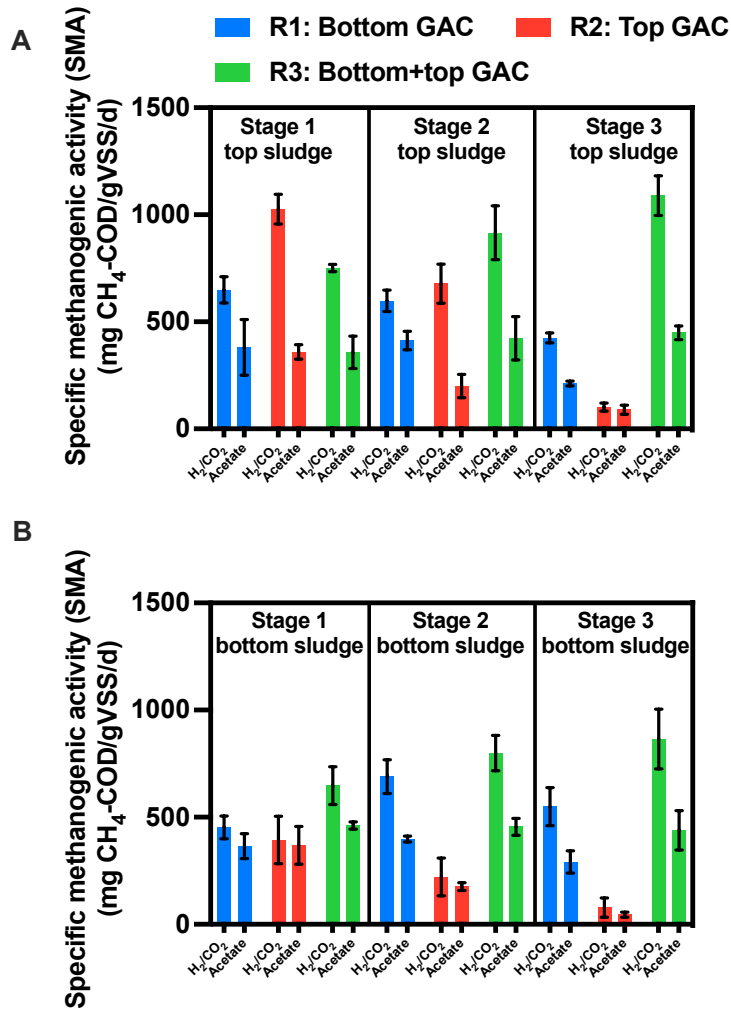


Fig. 7.7. Sludge specific methanogenic activities (SMAs) of top layer (A) and bottom layer (B) of three reactors at different organic loading rates (OLRs).

In Stage 2, there was a higher hydrogenotrophic SMA in R1's bottom sludge (689 ± 79 mg CH₄-COD/gVSS/d) compared to that in R2's bottom sludge (221 ± 88 mg CH₄-COD/gVSS/d), suggesting that the placement of GAC at bottom improved the hydrogenotrophic methanogenic activity at a high OLR. In Stage 2, R2's top sludge had a hydrogenotrophic SMA of 678 ± 91 mg CH₄-COD/gVSS/d, whereas R1's top sludge had a hydrogenotrophic SMA of 598 ± 50 mg CH₄-COD/gVSS/d. This finding suggests that the placement of top GAC had a positive impact on the

hydrogenotrophic methanogenic activity. In Stage 2, R3's top and bottom sludge showed the highest hydrogenotrophic SMAs (916 ± 126 mg CH₄-COD/gVSS/d in the top sludge and 799 ± 82 mg CH₄-COD/gVSS/d in the bottom sludge) among the three reactors. This explained the high methane yield achieved in R3 in Stage 2.

In Stage 3, as the OLR rose to 6.0 ± 0.2 g/L/d, R2 exhibited low hydrogenotrophic SMAs in both top (102 ± 19 mg CH₄-COD/gVSS/d) and bottom (78 ± 45 mg CH₄-COD/gVSS/d) sludge, indicating decreased microbial methanogenic activities and therefore reactor failure. In correlation with the sludge stability findings presented in **Fig. 7.6**, this was attributed to the excessive production of intermediates like VFAs during hydrolysis in the bottom sludge bed. The efficient utilization of intermediates was also hindered due to an insufficient contact time of substrates and microorganisms after the HRT was decreased. Subsequently, the pH in R2 decreased sharply due to the accumulation of intermediates, leading to a reduction in microbial activities. Compared to Stage 2, lower hydrogenotrophic SMAs were measured in R1's top (435 ± 23 mg CH₄-COD/gVSS/d) and bottom (549 ± 89 mg CH₄-COD/gVSS/d), likely because of the intermediate inhibition at Stage 3. In R1, the hydrogenotrophic SMA in bottom sludge was higher than that in top sludge. This was a consequence of the addition of bottom GAC to R1, which accelerated hydrogenotrophic methanogenesis by enabling effective electron transfer and mitigated the intermediate inhibition on microbial methanogenic activity in R1's bottom sludge. Of the three reactors, R3 showed the highest hydrogenotrophic SMAs in both top (1089 ± 93 mg CH₄-COD/gVSS/d) and bottom (865 ± 139 mg CH₄-COD/gVSS/d) sludge layers, corresponding to a stable operation and an efficient energy recovery in R3 at Stage 3. These findings suggest that the additions of GAC to reactor's top and bottom layers can stimulate hydrogenotrophic methanogenic activities in sludge at high OLRs. The addition of bottom GAC to R3 facilitated effective electron

transfer by methanogens. Unconsumed intermediates flowed to the top of R3 where they were effectively consumed due to the addition of top GAC. Moreover, the effective consumption of inhibiting intermediates further accelerated the hydrolysis. It is concluded that the additions of GAC to reactor's top and bottom layers can enhance both system stability and reactor performance by promoting fermentation and improving VFA conversion efficiency across the entire reactor.

In all three stages, the top sludge of R3 exhibited higher hydrogenotrophic SMAs compared to the top sludge of R1. This observation can be attributed to the addition of top GAC in R3 reactor, which is known to boost electron transfer efficiency. Notably, despite both R1 and R3 possessing bottom GAC throughout the three stages, the bottom sludge of R3 still demonstrated higher hydrogenotrophic SMAs relative to R1's bottom sludge. This phenomenon might be explained by the role of top GAC in stimulating methanogenesis in the upper reactor region. Such stimulation aids in the downstream conversion of fermentation products, thereby mitigating intermediate inhibitions, particularly hydrogen inhibition. Consequently, it promoted hydrogenotrophic methanogenic activities in the bottom sludge.

In summary, under low OLR conditions, methanogenesis was primarily promoted in R2's upper layer, whereas a fermentation zone was situated at R2's lower layer. However, at high OLRs, the presence of bottom GAC became more pronounced, as methanogenesis alleviated the inhibition of intermediates. R3 (bottom+top GAC) exhibited high reactor stability and good performance at high OLRs, effectively promoting fermentation and the conversion of intermediates throughout the reactor.

7.3.6 Microbial community

To enhance comprehension of the microbial spatial distributions in reactors with the additions of different spatial locations of GAC, the relative abundance of representative bacterial communities and archaeal communities at top sludge and bottom sludge were analyzed, as shown in **Fig. 7.8**.

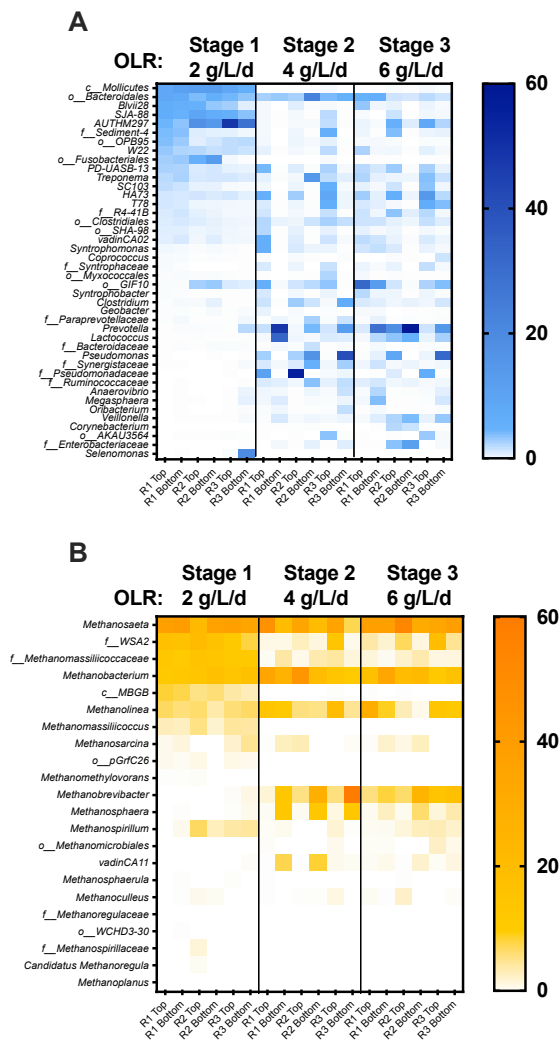


Fig. 7.8. Relative abundance of main bacterial (A) and archaeal (B) communities at the genus level of three reactors (R1: bottom GAC; R2: top GAC; R3: bottom+top GAC) at top and bottom sludge.

7.3.6.1 Bacterial community

In Stage 1, *Blvii28*, *SJA-88*, an unclassified genus in the class *Mollicutes*, and an unclassified genus in the orders *Bacteroidales* were the dominant bacteria in R1's bottom and top sludge (**Fig. 7.8A**). These dominant bacteria displayed a similar relative abundance in R1's top and bottom sludge, indicating no bacterial spatial difference in R1. In R2's bottom sludge, the dominant bacteria were *AUTHM297* (14.2%), an unclassified genus in the order *Fusobacteriales*, and an unclassified genus in the class *Mollicutes*. *Fusobacteriales* primarily hydrolyzes macromolecules into smaller substrates for energy conservation (Mou et al., 2022a). The relative abundance of an unclassified genus in the order *Fusobacteriales* was greater in R2's bottom sludge (12.9%) than in R2's top sludge (5.5%). This finding implies that the majority of macromolecular hydrolysis occurred at the bottom of the reactor that was supplemented with GAC at the top (R2), corroborating the hydrolysis efficiency findings. The presence of *AUTHM297* has been detected in other anaerobic reactors and has been shown to persist in environments rich in significantly degraded organic matter (Ahmad et al., 2020). The relative abundance of *AUTHM297* in R2's top sludge (17.9%) was higher than that in R2's bottom sludge (14.2%), suggesting that a large amount of highly degraded organic matter was present in R2's top layer. This observation might indicate that methanogenesis primarily took place in R2's top layer.

In Stage 2, *Prevotella* and *Lactococcus* were the predominant bacteria (82.2% of the bacterial population) in R1's bottom sludge. In three reactors, the relative abundance of *Prevotella* was higher in bottom sludge than in top sludge. *Prevotella* ferments carbohydrates into short-chain fatty acids (Kutlar et al., 2022). The relative abundances of *Prevotella* and *Lactococcus* were higher in R1's and R3's bottom sludge, both of which had GAC appended to the bottom, than in R2's bottom sludge, which had no GAC at the bottom. This observation suggests that, when the

OLR was increased, the hydrolysis primarily occurred at the bottom of reactors due to the addition of bottom GAC. Notably, the relative abundance of *Pseudomonas* in bottom sludge (16.6% of R2 and 40.4% of R3) was higher than that in the top sludge (3.0% of R2 and 0.1% of R3) when GAC was added to the top of the reactor (R2 and R3). *Pseudomonas* has been reported to degrade organic matter (Ng et al., 2005). This finding indicates that the addition of top GAC enhanced hydrolysis process at reactor's bottom, which was consistent with the findings on hydrolysis efficiency and sludge stability. The relative abundance of the syntrophic bacteria *Syntrophomonas*, *Syntrophobacter*, and *Geobacter*, which participate in DIET (Zhang et al., 2022d), was higher in R2's top sludge (2.1%) and R3's top sludge (1.6%) than in bottom sludge (0.7% for R2 and 0.1% for R3). These results suggest that DIET was stimulated by the addition of top GAC in Stage 2.

In Stage 3, the dominant bacteria in R1's bottom sludge were *Prevotella*, an unclassified genus of the order *Bacteroidales*, and *Methanosphaera*, all of which are fermentative bacteria participating in the breakdown of carbohydrates (Zhang et al., 2022d). The enrichment of these fermentative bacteria in R1's bottom sludge was attributed to the effective consumption of fermentative intermediates with the addition of bottom GAC at high OLR, which could facilitate fermentation process without intermediate inhibition. The relative abundance of *Syntrophomonas* of R1's bottom sludge increased to 2.1% in Stage 3. *Syntrophomonas* functions as a syntrophic fatty acid metabolizer and has been reported to participate in DIET (Yu et al., 2021c). This observation highlights the positive impact of bottom GAC on anaerobic process at a high OLR. The fermentative bacteria *Prevotella*, *Pseudomonas*, *T78*, *HA73*, and *Treponema*, which can hydrolyze macromolecules, amino acids, glucose, and peptone (Qiu et al., 2019), were enriched in R3's bottom sludge at a high OLR. The high relative abundance of fermentative bacteria in R3 can account for the high hydrolysis efficiency at a high OLR. The high relative abundance of

fermentative bacteria in R3's bottom suggested an increased production of intermediates, such as VFA. These intermediates subsequently served as substrates for methanogenic archaea. The efficient metabolic conversion of these intermediates by methanogenic archaea is crucial for maintaining low sludge stability, especially at high OLRs. The fact that syntrophic bacteria, including *Syntrophomonas*, *Syntrophobacter*, and *Geobacter*, increased from 0.1% to 0.7% in R3's bottom sludge when the OLR was increased, suggests that the placement of GAC at the bottom of the reactor stimulated DIET and accelerated methanogenesis.

7.3.6.2 Archaeal community

As shown in **Fig. 7.8B**, hydrogenotrophic methanogens and acetoclastic methanogens were identified in all three reactors, corroborating the SMA results. In Stage 1, *Methanosaeta*, an unclassified genus in the family *WSA2*, an unclassified genus in the family *Methanomassiliicoccaceae*, and *Methanobacterium* were the prevailing archaea in three reactors' top and bottom sludge. There was no notable difference between R1's top and bottom sludge in the relative abundances of dominant genera. However, substantial differences were observed in the relative abundances of dominant archaea in R2's and R3's top and bottom sludge. These results imply that the additions of top GAC influence the spatial distributions of archaeal communities in R2 and R3. *Methanosarcina* was enriched in R1 (1.7%) and R3 (5.1%), particularly in the bottom sludge layers. These findings align with prior research (Dang et al., 2016; Xu et al., 2015). Notably, the highest relative abundances of *Methanospirillum* and *Methanomassiliicoccus* were observed in R2's top sludge at 7.1% and 5.7%, respectively. *Methanomassiliicoccus* has been reported to thrive in electrochemically assisted anaerobic reactors (Im et al., 2019), while *Methanospirillum* has been identified as a significant member of the microbial community that adheres to carbon cloth surfaces and potentially engages in DIET with *Geobacter* in the presence of GAC (Lee et al.,

2016; Lei et al., 2016). Consequently, the placement of GAC at the top of a reactor might encourage *Methanospirillum*, a well-known hydrogen-utilization methanogen, which might be linked to the predominant hydrogenotrophic methanogenesis pathway, as illustrated in **Fig. 7.7**. *Methanomassiliicoccus* and *Methanospirillum* have been associated with reactors that are processing complex organic matter, and these microorganisms have demonstrated an ability to survive in environments rich in volatile fatty acids (Lei et al., 2016; Wang et al., 2020b). These findings suggest that R2's top sludge had a higher VFA concentration. A high VFA concentration would help to explain the high hydrolysis efficiency observed in R2 during Stage 1.

When the OLR was increased to 4.0 ± 0.3 g/L/d in Stage 2, there was a shift in archaea dominance in all three reactors. In R1's top sludge, the prevalent archaea became *Methanosaeta* (46.1%), *Methanobacterium* (34.4%), and *Methanolinea* (13.7%), while the primary archaea in R1's bottom sludge consisted of *Methanobacterium* (26.7%), *Methanosaeta* (20.0%), and *Methanosphaera* (12.6%). The distinctions between R1's top and bottom sludge were significant, suggesting that the impact of bottom GAC placement became more pronounced when the OLR was increased. Additionally, the relative abundance of *Methanobacterium* and *Methanosphaera*, both hydrogenotrophic methanogens, increased with the OLR increment, possibly due to the breakdown of complex organics and the subsequent release of a substantial amount of hydrogen (Wang et al., 2022; Zhao et al., 2017). In line with this observation, the relative abundance of *Methanobacterium* in R2's top sludge increased to its highest level (44.1%) among the three reactors as the acidification rate accelerated at R2's bottom after the OLR was raised. Thus, this observation can potentially explain the high hydrogenotrophic SMA results of R2's top sludge at Stage 2. The relative abundance of *Methanobrevibacter*, which uses hydrogen as an electron donor was 60.1% in R3's bottom sludge at Stage 2. The sharp increase in the relative abundance of

Methanobacterium could account for the high hydrogenotrophic SMA observed in R3's bottom sludge. Thus, the GAC at the bottom of R3 has a substantial influence on methanogenesis in the UASB after the OLR was increased.

7.3.7 Implications

The findings of this study indicate that under varying organic loading rates, diverse GAC amendment approaches exert distinctly different effects on methanogenic activities. In this work, at a low OLR, the introduction of GAC at the top of a UASB reactor facilitated methane recovery by enabling GAC contact with the sludge, eliminating the need for mechanical stirring. The different placements of GAC produced microenvironments in the UASBs enabling a distinct separation between the fermentation zone and methanogenesis zone. This special arrangement improved the hydrolysis efficiency of high solid-content substrates and reduced the accumulation of biodegradable COD within the sludge bed. Throughout the entire depth of R2, the increase in hydrogenotrophic methanogenic activities was detected. The syntrophic bacteria *Geobacter* was enriched in R2's bottom sludge bed and the methanogenesis archaea *Methanospirillum* was enriched in R2's top sludge bed under low OLR conditions.

At high OLR conditions, the bottom GAC emerged as a significant factor in alleviating the inhibition of intermediates resulting from accelerated fermentation process. The simultaneous additions of both bottom and top GAC established dual microenvironments surrounding the GAC within UASB reactor. The bottom microenvironment accelerated methanogenesis process, subsequently promoting hydrolysis by consuming intermediates, while the top microenvironment could consume residual intermediates. The development of two microenvironments rendered the UASB more efficient and resilient under high OLR conditions. Additionally, the microbial

hydrogenotrophic methanogenesis activities were improved as the OLR increased throughout the top and bottom GAC-amended UASB (R3). Following the OLR increase, the syntrophic bacteria *Syntrophomonas*, *Syntrophobacter*, and *Geobacter*, and the hydrogenotrophic archaea *Methanobacterium*, *Methanobrevibacter*, *Methanosphaera*, and *Methanospirillum*, were enriched, demonstrating an enhanced syntrophic metabolism throughout the top and bottom of the R3.

7.4 Conclusions

The application of top GAC to UASB at a low OLR resulted in enhanced methane production. This led to improved fermentation in the reactor's bottom layer and boosted methanogenesis in the top layer. However, at a challenging organic loading capacity, the addition of GAC to the reactor's bottom and top layer improved syntrophic metabolism and improved anaerobic activity. Microbes involved in DIET were enriched in reactors amended with GAC. These findings show that reactor design should be based on a variable organic loading capacity.

CHAPTER 8 CONCLUSIONS AND RECOMMENDATIONS

8.1 Thesis overview

Anaerobic digestion (AD) presents a promising approach for the pollutant removal and production of valuable products such as volatile fatty acids (VFAs) and biogas from organic waste and wastewater. Despite extensive exploration across diverse waste streams, AD is susceptible to disruptions from inhibition factors such as low temperatures, pH fluctuations, substrate characteristics, and toxicants, often leading to unsatisfactory performance. These inhibitory factors can impact different steps of AD process. Therefore, it is crucial to maintain a balance throughout each step.

To enhance bioenergy recovery from high-strength waste and wastewater, this thesis developed four low-cost or low-energy-input strategies, each targeting specific steps of AD process. Four representative waste types were selected: thickened waste activated sludge (TWAS), blackwater, distillery wastewater, and synthetic high-strength wastewater. The selection of treatment strategies was informed by the distinctive properties and inhibitions affecting the AD steps for each type of waste and wastewater.

The hydrolysis process is the first step of AD process, where substrates with high particulate waste experience rate-limiting conditions. TWAS was selected as the representative waste with limitation of hydrolysis due to the inherent recalcitrance of sludge cell walls and extracellular polymeric substances (EPS), which are crucial but difficult-to-degrade components of the organic fraction. To address this challenge, $\text{Ca}(\text{ClO})_2$ pre-treatment was employed for TWAS treatment. Batch experiments were conducted with varying dosages of $\text{Ca}(\text{ClO})_2$, resulting in improved solubility and biodegradability of TWAS, accompanied by a reduction in sludge volume.

And then, the syntrophic interactions between each step are also important. Substrates with high VFA, particulate solids and soluble contents can inhibit syntrophic interactions in AD process. Blackwater was selected as representative household wastewater, which contains high solid materials such as toilet paper and undigested plant matter and high soluble contents. Moreover, the presence of high ammonia contents in blackwater can also inhibit the syntrophic interactions. Furthermore, blackwater contributes about 75% of phosphorous content in domestic sewage. Based on these characteristics of blackwater, calcium phosphate granular sludge was successfully cultivated in the up-flow anaerobic sludge blanket (UASB) reactor, enabling phosphorous recovery. The calcium phosphate granular sludge also provided proximity of syntrophic interactions between bacteria and methanogens, while resisting ammonia inhibitions, thereby aiding the system in achieving high organic loading rate (OLR). Another representative industry wastewater used in this thesis is distillery wastewater, particularly pot ale wastewater and spent caustic wastewater, which presents challenges in anaerobic digestion due to extreme pH, high nutrient loads, and the presence of lignin and yeast. These factors can inhibit syntrophic activities of AD process. To address these challenges, anaerobic co-digestion of pot ale wastewater and spent caustic wastewater was investigated. This approach demonstrated enhanced methane production rates and organic loading capacities compared to mono-digestion. It effectively mitigated pH imbalance, increased hydrolysis efficiency, and improved the activities of hydrogenotrophic methanogens. Additionally, the syntrophic relationships between bacteria and methanogens in these systems were significantly improved.

The methanogenesis process usually faces inhibitions due to the inefficient electron transfer from bacteria to archaea. Previous research contributed to the development of a modified UASB reactor that achieved phase separation within a single unit, optimizing fermentation processes near the

wastewater inlet and enhancing methanogenesis along the reactor column. Subsequently, the modified UASB reactor was optimized with various placements of granular activated carbon (GAC). Synthetic high-strength wastewater was used as the complex substrate to mimic different solid-content wastewater. Following continuous long-term operations, the novel modified UASB reactors achieved high methane yield and organic loading capacities. The addition of top GAC accelerated methanogenesis process, followed by the VFA consumption, and then enhanced the hydrolysis efficiency, in the end achieving the whole AD process balance.

8.2 Conclusions

This doctoral thesis focuses on investigating innovative, cost-effective, and efficient AD technologies targeting specific steps to enhance energy recovery from representative high-strength waste and wastewater. The key findings underscore the importance of cultivating functional microbiomes and balancing AD process to improve performance. The conclusions drawn include:

Calcium hypochlorite pre-treatments to enhance thickened waste activated sludge (TWAS) hydrolysis

- The use of calcium hypochlorite to enhance hydrolysis of TWA was thoroughly investigated. Findings presented in Chapter 3 demonstrate the effectiveness of 5-20% $\text{Ca}(\text{ClO})_2$ (based on total suspended solids) in improving the solubility and biodegradability of TWAS. This treatment led to a significant reduction in sludge volume (65%) post-aerobic digestion compared to untreated TWAS (35%). While lower doses of $\text{Ca}(\text{ClO})_2$ (5-10%) markedly improved digestion efficiency through mechanisms such as cell lysis and decomposition of extracellular polymeric substances (EPS). Higher concentrations (>20%) were found to inhibit microbial activity, thereby slowing the release of dissolved organic compounds. These laboratory tests provided essential

information on optimal dosages, retention times, and operational mechanisms for the calcium hypochlorite pre-treatment strategy.

Calcium phosphate granular sludge for blackwater to enhance syntrophic interactions

- The effects of calcium phosphate granular sludge on the performance of mesophilic UASB for blackwater treatment were demonstrated in Chapter 4. Results revealed the successful development of calcium phosphate granules in the mesophilic UASB reactor treating blackwater, enabling phosphorus recovery alongside achieving a high OLR of 16 g/L/d and a short hydraulic retention time (HRT) of 0.25 days, leading to high methane production. Microbial analysis demonstrated the proliferation of syntrophic bacteria *Syntrophus*, in conjunction with diverse H₂-utilizing methanogens, ultimately establishing a hydrogenotrophic dominant pathway in the UASB reactor. The integration of reactor performance and microbial community analysis underscored the role of calcium phosphate granular sludge in enhancing methanogenic activities and facilitating the hydrolysis of particulate chemical oxygen demand (COD). The formation of anaerobic granules within the UASB treatment of blackwater provides two practical advantages: eliminating the necessity for a critical up-flow velocity, thus benefiting organic matter hydrolysis, and enabling easy collection of phosphate-rich granules at the reactor bottom for potential utilization as fertilizer or in the phosphate refinery industry. This study provides crucial practical insights into simultaneously recovering energy and nutrients for blackwater treatment.

Co-digestion of spent caustic wastewater and pot ale wastewater to improve syntrophic activities

- The feasibility of continuous operation of co-digestion for spent caustic wastewater and pot ale wastewater was extensively investigated in Chapter 5. The study demonstrated that co-digestion significantly enhanced methane production rates and organic loading capacities

compared to mono-digestion (pot ale wastewater). This study showed that mixing these two distinct wastewater streams can mitigate pH imbalance and increase the availability of readily biodegradable organic matter, thereby creating an optimized environment for robust microbial communities. The co-digestion UASB reactor achieved a high methane yield of 76% at an OLR of 3.9 g/L/d and challenged the highest OLR of 13.6 g/L/d with the methane yield of 44%. The microbial community analysis revealed robust methanogens and syntrophic bacteria, which facilitated efficient substrate conversion into biogas. This study underscores the effectiveness of co-digestion in enhancing the sustainability of wastewater treatment in distillery industry.

Modified UASB reactors with different GAC spatial distributions to realize phase separation and enhance methanogenesis

- Chapters 6 and 7 demonstrated the impacts of GAC spatial distributions (bottom, top, and bottom+top) in UASB reactors on methane production, organic loading capacity, and dynamics of microbial communities in flocs and biofilms treating high, medium, and low solid-content wastewater. Chapter 6 revealed that, for high solid-content wastewater, the configuration with GAC positioned at the top yielded the highest methane yield (74 %), followed by the combination of bottom and top GAC (65%), and bottom GAC (58%). In contrast, for low solid-content wastewater, all configurations improved methane yield, with the bottom+top GAC achieving the highest methane yield (83%). Further analysis of microbial communities indicated a significant influence of GAC locations on the spatial distribution of the microbial consortium, enriched differently according to the substrate's solid content. When treating high solid-content wastewater, fermentation bacteria were enriched on the bottom layer of the reactor, whereas the hydrogenotrophic methanogens dominated the top layer of the reactor. However, when treating low and medium solid-content wastewater, the potential direct interspecies electron transfer (DIET)

participants were enriched in granular activated carbon (GAC)-amended reactors, especially the top GAC reactor. This study demonstrates the significance of optimizing the reactor design when treating different solid-content wastewater.

- The methanogenic activities observed in the suspended sludge of three different UASB reactors, as detailed in Chapter 6, did not show significant variation. This suggests a pronounced influence of the GAC biofilm on methane production. Additionally, Chapter 6 compares microbial communities in biofilms that developed on the GAC at the bottom and top of these reactors. High solid-content wastewater favored syntrophic bacteria dominance in top-GAC biofilms, whereas low solid-content conditions enriched hydrogenotrophic methanogens; *Methanobacteria* was predominantly found in bottom-GAC biofilms, whereas *Methanoregula* was enriched in top-GAC biofilms. This distinction underscores GAC-biofilm microbial communities' potential to enhance methane production.

- The findings from Chapter 7 suggested that top GAC placement enhanced hydrolysis process and methanogenesis process separately, potentially beneficial for treating high solid-content wastewater under high OLRs. Three UASB reactors described in Chapter 6 were operated to treat high solid-content wastewater with different OLRs. The results showed that at a low OLR, top GAC placement resulted in the highest methane yield at 74%. However, at high OLRs, reactors with GAC at both bottom and top achieved the highest methane production at 66%. The application of top GAC to UASB at a low OLR resulted in enhanced methane production. This led to improved fermentation in the reactor's bottom layer and boosted methanogenesis in the top layer. However, at a challenging organic loading capacity, the addition of GAC to the reactor's bottom and top layer improved syntrophic metabolism and improved anaerobic activity.

Microorganisms involved in DIET were enriched in reactors amended with GAC. These findings show that reactor design should be based on a variable organic loading capacity.

8.3 Recommendations

This thesis has introduced four strategic, low-energy-input approaches designed to enhance energy recovery from high-strength waste and wastewater. These strategies target specific AD steps and are customized to handle four representative wastewater types: TWAS for centralized system, blackwater from decentralized system, pot ale wastewater from distillery industry, and synthetic high-strength wastewater, chosen based on the unique inhibitory properties affecting each AD step. Based on the findings from this thesis, there are recommendations for future studies.

This thesis has illuminated the efficiency of calcium hypochlorite pre-treatment in enhancing TWAS hydrolysis at different dosages and offered insights into its optimal application. Therefore, in the future, the use of calcium hypochlorite pre-treatment can be expanded across different waste types to improve hydrolysis rates. Future research should continue to investigate dosage levels and integration methods to maximize solubility and biodegradability. Meanwhile, these findings are grounded in laboratory-scale experiments yet, requiring for expansive research to validate their efficiency in full-scale operations. Therefore, it becomes essential to start large-scale studies that not only replicate these laboratory successes but also address the variability inherent in WAS characteristics and operational conditions.

The study of blackwater treatment through UASB reactors underscores the potential for nutrient and energy recovery. It also highlights the necessity for subsequent treatment phases to align the effluent quality with reuse standards. This challenge appeals to the innovation of novel technologies and two-stage reactors capable of mitigating nutrients, pathogens, micropollutants,

and residual organic matter in an integrated, efficient method. Given the significant health and environmental risks posed by the accumulation of micropollutants in blackwater, there is a critical need for advanced monitoring techniques and risk assessments. These techniques should aim to comprehensively understand and mitigate the impacts of such contaminants, facilitating the development of effective removal strategies within new sanitation systems.

Additionally, the potential of co-digestion of high-strength industrial wastewater, particularly from distillery facilities, presents a promising solution for enhancing biogas production while mitigating environmental impacts and reducing the cost of transportation of wastewater. Future studies can focus on optimizing the co-digestion process in terms of substrate combinations, reactor design, and operational parameters to maximize energy recovery and minimize residual wastes. This includes evaluating the economic and environmental benefits of integrating co-digestion into existing wastewater treatment infrastructures and exploring the feasibility of scale-up to industrial levels.

Further, the addition of GAC in UASB reactors has been shown to enhance methanogenic activity in the lab scale, yet the translation of this innovation to full-scale bioreactors poses significant questions regarding practical implementation and cost-effectiveness. Also, there are demands to investigate a wider array of conductive materials and to identify minimum GAC quantities that achieve desired outcomes, thereby enhancing the economic accessibility of the technology.

This thesis also focuses on the varied nature of waste and wastewater from centralized, decentralized systems, and distillery industry, calling for a broader investigation of other wastes, such as food waste and other industrial wastewater, such as molasses wastewater and refinery wastewater. This thesis has an advanced understanding of microbial community development and

functional pathways for different high-strength wastewater treatments at the DNA level. Delving into RNA-level and proteomic analyses could unveil the critical microorganisms involved, offering deeper insights that might bridge the gap between theoretical knowledge and its application in environmental engineering.

BIBLIOGRAPHY

- Abid M, Wu J, Seyedsalehi M, Hu Y-y, Tian G. Novel insights of impacts of solid content on high solid anaerobic digestion of cow manure: Kinetics and microbial community dynamics. *Bioresource Technology* 2021; 333: 125205.
- Abu-Dahrieh J, Orozco A, Groom E, Rooney D. Batch and continuous biogas production from grass silage liquor. *Bioresource Technology* 2011; 102: 10922-10928.
- Ahmad F, Sakamoto IK, Adorno MAT, Motteran F, Silva EL, Varesche MBA. Methane Production from Hydrogen Peroxide Assisted Hydrothermal Pretreatment of Solid Fraction Sugarcane Bagasse. *Waste and Biomass Valorization* 2020; 11: 31-50.
- Akassou M, Kaanane A, Crolla A, Kinsley C. Statistical modelling of the impact of some polyphenols on the efficiency of anaerobic digestion and the co-digestion of the wine distillery wastewater with dairy cattle manure and cheese whey. *Water Science and Technology* 2010; 62: 475-483.
- Alipour Z, Azari A. COD removal from industrial spent caustic wastewater: A review. *Journal of Environmental Chemical Engineering* 2020; 8: 103678.
- Almeida MC, Butler D, Friedler E. At-source domestic wastewater quality. *Urban Water* 1999; 1: 49-55.
- Alphenaar A. *Anaerobic Granular Sludge : Characterization, and Factors Affecting Its Functioning*. Wageningen University and Research, Netherlands, 1994, pp. 215.
- Ambaye TG, Rene ER, Dupont C, Wongrod S, van Hullebusch ED. Anaerobic Digestion of Fruit Waste Mixed With Sewage Sludge Digestate Biochar: Influence on Biomethane Production. *Frontiers in Energy Research* 2020; 8.
- APHA. *Standard Methods for the Examination of Water and Wastewater*, 2012.

- Appels L, Baeyens J, Degève J, Dewil R. Principles and potential of the anaerobic digestion of waste-activated sludge. *Progress in Energy and Combustion Science* 2008; 34: 755-781.
- Apprill A, McNally S, Parsons R, Weber L. Minor revision to V4 region SSU rRNA 806R gene primer greatly increases detection of SAR11 bacterioplankton. *Aquatic Microbial Ecology* 2015; 75: 129-137.
- Aquino SF, Stuckey DC. Integrated model of the production of soluble microbial products (SMP) and extracellular polymeric substances (EPS) in anaerobic chemostats during transient conditions. *Biochemical Engineering Journal* 2008; 38: 138-146.
- Ariunbaatar J, Panico A, Esposito G, Pirozzi F, Lens PNL. Pretreatment methods to enhance anaerobic digestion of organic solid waste. *Applied Energy* 2014; 123: 143-156.
- Awasthi SK, Joshi R, Dhar H, Verma S, Awasthi MK, Varjani S, et al. Improving methane yield and quality via co-digestion of cow dung mixed with food waste. *Bioresource Technology* 2018; 251: 259-263.
- Baek G, Kim J, Kim J, Lee C. Role and Potential of Direct Interspecies Electron Transfer in Anaerobic Digestion. *ENERGIES* 2018; 11.
- Baird RB, Eaton AD, Rice EW, Bridgewater L. Standard methods for the examination of water and wastewater. Vol 23: American Public Health Association Washington, DC, 2017.
- Baloch MI, Akunna JC, Kierans M, Collier PJ. Structural analysis of anaerobic granules in a phase separated reactor by electron microscopy. *Bioresource Technology* 2008; 99: 922-929.
- Bamba JNY, Almendrala MC, Caparanga AR, Doma BT. Effect of Biochemical Pretreatment and Nutrient Supplementation on Anaerobic Co-Digestion of Sugarcane Press Mud and Distillery Effluent. *IOP Conference Series: Earth and Environmental Science* 2021; 801: 012001.

Barrena R, Traub JE, Gil CR, Goodwin JAS, Harper AJ, Willoughby NA, et al. Batch anaerobic digestion of deproteinated malt whisky pot ale using different source inocula. *WASTE MANAGEMENT* 2018; 71: 675-682.

Barua S, Dhar BR. Advances towards understanding and engineering direct interspecies electron transfer in anaerobic digestion. *Bioresource Technology* 2017; 244: 698-707.

Batstone DJ, Picioreanu C, van Loosdrecht MCM. Multidimensional modelling to investigate interspecies hydrogen transfer in anaerobic biofilms. *Water Research* 2006; 40: 3099-3108.

Bes-Piá A, Mendoza-Roca JA, Alcaina-Miranda MI, Iborra-Clar A, Iborra-Clar MI. Combination of physico-chemical treatment and nanofiltration to reuse wastewater of a printing, dyeing and finishing textile industry. *Desalination* 2003; 157: 73-80.

Bradford MM. A rapid and sensitive method for the quantitation of microgram quantities of protein utilizing the principle of protein-dye binding. *Analytical Biochemistry* 1976; 72: 248-254.

Burger G, Parker W. Investigation of the impacts of thermal pretreatment on waste activated sludge and development of a pretreatment model. *Water research* 2013; 47: 5245-5256.

Burgess JE, Pletschke BI. Hydrolytic enzymes in sewage sludge treatment: a mini-review. *Water Sa* 2008; 34: 343-350.

Cabrita TM, Santos MT. Biochemical Methane Potential Assays for Organic Wastes as an Anaerobic Digestion Feedstock. *Sustainability*. 15, 2023.

Callahan BJ, McMurdie PJ, Rosen MJ, Han AW, Johnson AJA, Holmes SP. DADA2: High-resolution sample inference from Illumina amplicon data. *Nature Methods* 2016; 13: 581-583.

- Capodaglio AG. Taking the water out of “wastewater”: An ineluctable oxymoron for urban water cycle sustainability. *Water Environment Research* 2020; 92: 2030-2040.
- Capodaglio AG, Callegari A, Ceconet D, Molognoni D. Sustainability of decentralized wastewater treatment technologies. *Water Practice and Technology* 2017; 12: 463-477.
- Capson-Tojo G, Moscoviz R, Ruiz D, Santa-Catalina G, Trably E, Rouez M, et al. Addition of granular activated carbon and trace elements to favor volatile fatty acid consumption during anaerobic digestion of food waste. *Bioresource Technology* 2018; 260: 157-168.
- Cayetano RDA, Kim G-B, Park J, Yang Y-H, Jeon B-H, Jang M, et al. Biofilm formation as a method of improved treatment during anaerobic digestion of organic matter for biogas recovery. *Bioresource Technology* 2022; 344: 126309.
- Cerrillo M, Viñas M, Bonmatí A. Anaerobic digestion and electromethanogenic microbial electrolysis cell integrated system: Increased stability and recovery of ammonia and methane. *Renewable Energy* 2018; 120: 178-189.
- Cesaro A, Belgiorno V. Pretreatment methods to improve anaerobic biodegradability of organic municipal solid waste fractions. *Chemical Engineering Journal* 2014; 240: 24-37.
- Chae K-J, Choi M-J, Lee J, Ajayi FF, Kim IS. Biohydrogen production via biocatalyzed electrolysis in acetate-fed bioelectrochemical cells and microbial community analysis. *International Journal of Hydrogen Energy* 2008; 33: 5184-5192.
- Chaggu EJ, Sanders W, Lettinga G. Demonstration of anaerobic stabilization of black water in accumulation systems under tropical conditions. *Bioresource technology* 2007; 98: 3090-3097.
- Chen H, Wei Y, Liang P, Wang C, Hu Y, Xie M, et al. Performance and microbial community variations of a upflow anaerobic sludge blanket (UASB) reactor for treating monosodium

- glutamate wastewater: Effects of organic loading rate. *Journal of Environmental Management* 2020; 253: 109691.
- Chen L, Fang W, Chang J, Liang J, Zhang P, Zhang G. Improvement of Direct Interspecies Electron Transfer via Adding Conductive Materials in Anaerobic Digestion: Mechanisms, Performances, and Challenges. *FRONTIERS IN MICROBIOLOGY* 2022; 13.
- Chen W, Westerhoff P, Leenheer JA, Booksh K. Fluorescence excitation– emission matrix regional integration to quantify spectra for dissolved organic matter. *Environmental science & technology* 2003; 37: 5701-5710.
- Chen Y, Cheng JJ, Creamer KS. Inhibition of anaerobic digestion process: A review. *Bioresource Technology* 2008; 99: 4044-4064.
- Chen Z, Zhang W, Wang D, Ma T, Bai R, Yu D. Enhancement of waste activated sludge dewaterability using calcium peroxide pre-oxidation and chemical re-flocculation. *Water Research* 2016; 103: 170-181.
- Chiang PF, Claire MJ, Han S, Maurice NJ, Giwa AS. Effectiveness of Torrefaction By-Products as Additive in Vacuum Blackwater under Anaerobic Digestion and Economic Significance. *Processes* 2023; 11: 3330.
- Chon D-H, Rome M, Kim YM, Park KY, Park C. Investigation of the sludge reduction mechanism in the anaerobic side-stream reactor process using several control biological wastewater treatment processes. *Water Research* 2011; 45: 6021-6029.
- Cunha JR, Morais S, Silva JC, Van Der Weijden RD, Hernández Leal La, Zeeman G, et al. Bulk pH and carbon source are key factors for calcium phosphate granulation. *Environmental science & technology* 2019; 53: 1334-1343.

- Cunha JR, Schott C, van der Weijden RD, Leal LH, Zeeman G, Buisman C. Calcium addition to increase the production of phosphate granules in anaerobic treatment of black water. *Water Research* 2018a; 130: 333-342.
- Cunha JR, Schott C, van der Weijden RD, Leal LH, Zeeman G, Buisman C. Calcium phosphate granules recovered from black water treatment: A sustainable substitute for mined phosphorus in soil fertilization. *Resources, Conservation and Recycling* 2020; 158: 104791.
- Cunha JR, Tervahauta T, van der Weijden RD, Temmink H, Hernández Leal La, Zeeman G, et al. The effect of bioinduced increased pH on the enrichment of calcium phosphate in granules during anaerobic treatment of black water. *Environmental science & technology* 2018b; 52: 13144-13154.
- Dang H, Yu N, Mou A, Zhang L, Guo B, Liu Y. Metagenomic insights into direct interspecies electron transfer and quorum sensing in blackwater anaerobic digestion reactors supplemented with granular activated carbon. *Bioresource technology* 2022; 352: 127113.
- Dang Y, Holmes DE, Zhao Z, Woodard TL, Zhang Y, Sun D, et al. Enhancing anaerobic digestion of complex organic waste with carbon-based conductive materials. *Bioresource Technology* 2016; 220: 516-522.
- Dang Y, Sun D, Woodard TL, Wang L-Y, Nevin KP, Holmes DE. Stimulation of the anaerobic digestion of the dry organic fraction of municipal solid waste (OFMSW) with carbon-based conductive materials. *Bioresource Technology* 2017; 238: 30-38.
- De Anda J, López-López A, Villegas-García E, Valdivia-Aviña K. High-Strength Domestic Wastewater Treatment and Reuse with Onsite Passive Methods. *Water* 2018; 10: 99.

- de Graaff M, Bijmans MFM, Abbas B, Euverink G-JW, Muyzer G, Janssen AJH. Biological treatment of refinery spent caustics under halo-alkaline conditions. *Bioresource Technology* 2011; 102: 7257-7264.
- de Graaff MS, Temmink H, Zeeman G, Buisman CJN. Anaerobic Treatment of Concentrated Black Water in a UASB Reactor at a Short HRT. *Water* 2010; 2: 101-119.
- De Vrieze J, Hennebel T, Boon N, Verstraete W. Methanosarcina: The rediscovered methanogen for heavy duty biomethanation. *Bioresource Technology* 2012; 112: 1-9.
- Deng YY, Blok K, van der Leun K. Transition to a fully sustainable global energy system. *Energy Strategy Reviews* 2012; 1: 109-121.
- Dewil R, Baeyens J, Appels L. Enhancing the use of waste activated sludge as bio-fuel through selectively reducing its heavy metal content. *Journal of Hazardous Materials* 2007; 144: 703-707.
- Dhar H, Kumar S, Kumar R. A review on organic waste to energy systems in India. *Bioresource Technology* 2017; 245: 1229-1237.
- Dionisi D, Bruce SS, Barraclough MJ. Effect of pH adjustment, solid-liquid separation and chitosan adsorption on pollutants' removal from pot ale wastewaters. *Journal of Environmental Chemical Engineering* 2014; 2: 1929-1936.
- Duan N, Dong B, Wu B, Dai X. High-solid anaerobic digestion of sewage sludge under mesophilic conditions: Feasibility study. *Bioresource Technology* 2012; 104: 150-156.
- Dubé C-D, Guiot SR. Characterization of the protein fraction of the extracellular polymeric substances of three anaerobic granular sludges. *AMB Express* 2019; 9: 23.
- DuBois M, Gilles KA, Hamilton JK, Rebers PA, Smith F. Colorimetric Method for Determination of Sugars and Related Substances. *Analytical Chemistry* 1956; 28: 350-356.

- Duguma A, Bekele T, Geda A. Biogas Production through Anaerobic Codigestion of Distillery Wastewater Sludge and Disposable Spent Yeast. *International Journal of Chemical Engineering* 2024; 2024: 5510471.
- Ellacuriaga M, Cascallana JG, González R, Gómez X. High-Solid Anaerobic Digestion: Reviewing Strategies for Increasing Reactor Performance. *Environments* 2021; 8: 80.
- Erkan HS. Waste activated sludge disintegration by hydroxyl and sulfate radical-based oxidation: a comparative study. *Environmental Science-Water Research & Technology* 2019; 5: 2027-2040.
- Evidente RC, Almendrala MC, Caparanga AR, Pamintuan KR, Mendoza JA. Anaerobic Codigestion of Press mud and Molasses-based Distillery Wastewater for Enhanced Biogas Production. *IOP Conference Series: Earth and Environmental Science* 2021; 943: 012017.
- Fang HHP, Chui HK, Li YY. Microstructural analysis of UASB granules treating brewery wastewater. *Water Science and Technology* 1995; 31: 129-135.
- Faria CV, Souza DF, Pontes TM, Amaral MCS, Fonseca FV. Strategies of anaerobic sludge granulation in an EGSB reactor. *Journal of Environmental Management* 2019; 244: 69-76.
- Feng D, Guo X, Lin R, Xia A, Huang Y, Liao Q, et al. How can ethanol enhance direct interspecies electron transfer in anaerobic digestion? *Biotechnology Advances* 2021; 52: 107812.
- Feng X, Deng J, Lei H, Bai T, Fan Q, Li Z. Dewaterability of waste activated sludge with ultrasound conditioning. *Bioresource Technology* 2009; 100: 1074-1081.
- Fernández del Castillo A, Garibay MV, Senés-Guerrero C, Orozco-Nunnelly DA, de Anda J, Gradilla-Hernández MS. A review of the sustainability of anaerobic reactors combined with constructed wetlands for decentralized wastewater treatment. *Journal of Cleaner Production* 2022; 371: 133428.

- Flemming H-C, Wingender J. The biofilm matrix. *Nature Reviews Microbiology* 2010; 8: 623-633.
- Florentino AP, Sharaf A, Zhang L, Liu Y. Overcoming ammonia inhibition in anaerobic blackwater treatment with granular activated carbon: the role of electroactive microorganisms. *Environmental Science-Water Research & Technology* 2019; 5: 383-396.
- Fr/olund B, Griebe T, Nielsen PH. Enzymatic activity in the activated-sludge floc matrix. *Applied Microbiology and Biotechnology* 1995; 43: 755-761.
- Friedler E, Brown DM, Butler D. A study of WC derived sewer solids. *Water Science and Technology* 1996; 33: 17-24.
- Gadirli G, Pilarska AA, Dach J, Pilarski K, Kolasa-Więcek A, Borowiak K. Fundamentals, Operation and Global Prospects for the Development of Biogas Plants—A Review. *Energies*. 17, 2024.
- Gagliano MC, Sudmalis D, Pei R, Temmink H, Plugge CM. Microbial Community Drivers in Anaerobic Granulation at High Salinity. *Frontiers in Microbiology* 2020; 11.
- Gao M, Zhang L, Florentino AP, Liu Y. Performance of anaerobic treatment of blackwater collected from different toilet flushing systems: Can we achieve both energy recovery and water conservation? *Journal of Hazardous Materials* 2019a; 365: 44-52.
- Gao M, Zhang L, Guo B, Zhang Y, Liu Y. Enhancing biomethane recovery from source-diverted blackwater through hydrogenotrophic methanogenesis dominant pathway. *Chemical Engineering Journal* 2019b; 378: 122258.
- Gao M, Zhang L, Liu Y. High-loading food waste and blackwater anaerobic co-digestion: Maximizing bioenergy recovery. *Chemical Engineering Journal* 2020; 394: 124911.

- Gautam P, Kumar S, Lokhandwala S. Advanced oxidation processes for treatment of leachate from hazardous waste landfill: A critical review. *Journal of Cleaner Production* 2019; 237: 117639.
- Gholipour S, Mehrkesh P, Azin E, Nouri H, Rouhollahi AA, Moghimi H. Biological treatment of toxic refinery spent sulfidic caustic at low dilution by sulfur-oxidizing fungi. *Journal of Environmental Chemical Engineering* 2018; 6: 2762-2767.
- Ghyoot W, Verstraete W. Anaerobic digestion of primary sludge from chemical pre-precipitation. *Water Science and Technology* 1997; 36: 357-365.
- Giordani A, Brucha G, Santos KA, Rojas K, Hayashi E, Alves MMS, et al. Performance and Microbial Community Analysis in an Anaerobic Hybrid Baffled Reactor Treating Dairy Wastewater. *Water, Air, & Soil Pollution* 2021; 232: 403.
- Godvin Sharmila V, Kumar G, Sivashanmugham P, Piechota G, Park J-H, Adish Kumar S, et al. Phase separated pretreatment strategies for enhanced waste activated sludge disintegration in anaerobic digestion: An outlook and recent trends. *Bioresource Technology* 2022; 363: 127985.
- Gonzalez A, Hendriks A, Van Lier J, de Kreuk M. Pre-treatments to enhance the biodegradability of waste activated sludge: elucidating the rate limiting step. *Biotechnology advances* 2018; 36: 1434-1469.
- Gonzalez-Gil G, Lens PNL, Van Aelst A, Van As H, Versprille AI, Lettinga G. Cluster Structure of Anaerobic Aggregates of an Expanded Granular Sludge Bed Reactor. *Applied and Environmental Microbiology* 2001; 67: 3683-3692.

- Goodwin JAS, Finlayson JM, Low EW. A further study of the anaerobic biotreatment of malt whisky distillery pot ale using an UASB system. *Bioresource Technology* 2001; 78: 155-160.
- Goodwin JAS, Stuart JB. Anaerobic-digestion of malt whiskey distillery pot ale using upflow anaerobic sludge blanket reactors. *Bioresource Technology* 1994; 49: 75-81.
- Graham J, Peter B, Walker G, Wardlaw A, Campbell E. Characterisation of the pot ale profile from a malt whisky distillery. *Worldwide Distilled Spirits Conference: Science and sustainability*. Nottingham University Press/The Institute of Brewing and Distilling, 2012.
- Gros M, Ahrens L, Levén L, Koch A, Dalahmeh S, Ljung E, et al. Pharmaceuticals in source separated sanitation systems: Fecal sludge and blackwater treatment. *Science of The Total Environment* 2020; 703: 135530.
- Gunes B, Stokes J, Davis P, Connolly C, Lawler J. Pre-treatments to enhance biogas yield and quality from anaerobic digestion of whiskey distillery and brewery wastes: A review. *Renewable and Sustainable Energy Reviews* 2019; 113: 109281.
- Gunes B, Stokes J, Davis P, Connolly C, Lawler J. Modelling and optimisation of the biogas yield after hybrid alkaline-ultrasonic pre-treatment in the early stages of anaerobic digestion of pot ale to shorten the processing time. *Process Safety and Environmental Protection* 2021a; 146: 43-53.
- Gunes B, Stokes J, Davis P, Connolly C, Lawler J. Optimisation of anaerobic digestion of pot ale after thermochemical pre-treatment through Response Surface Methodology. *Biomass & Bioenergy* 2021b; 144.

- Guo B, Zhang L, Sun H, Gao M, Yu N, Zhang Q, et al. Microbial co-occurrence network topological properties link with reactor parameters and reveal importance of low-abundance genera. *npj Biofilms and Microbiomes* 2022; 8: 1-13.
- Guo B, Zhang Y, Zhang L, Zhou Y, Liu Y. RNA-based spatial community analysis revealed intra-reactor variation and expanded collection of direct interspecies electron transfer microorganisms in anaerobic digestion. *Bioresource Technology* 2020; 298.
- Hai FI, Yang S, Asif MB, Sencadas V, Shawkat S, Sanderson-Smith M, et al. Carbamazepine as a Possible Anthropogenic Marker in Water: Occurrences, Toxicological Effects, Regulations and Removal by Wastewater Treatment Technologies. *Water* 2018; 10: 107.
- Hamza RA, Iorhemen OT, Tay JH. Advances in biological systems for the treatment of high-strength wastewater. *Journal of Water Process Engineering* 2016; 10: 128-142.
- Harmsen HJ, Kengen HM, Akkermans AD, Stams AJ, de Vos WM. Detection and localization of syntrophic propionate-oxidizing bacteria in granular sludge by in situ hybridization using 16S rRNA-based oligonucleotide probes. *Applied and Environmental Microbiology* 1996; 62: 1656-1663.
- He D, Xiao J, Wang D, Liu X, Fu Q, Li Y, et al. Digestion liquid based alkaline pretreatment of waste activated sludge promotes methane production from anaerobic digestion. *Water Research* 2021; 199: 117198.
- Hong K-J, Tarutani N, Shinya Y, Kajiuchi T. Study on the Recovery of Phosphorus from Waste-Activated Sludge Incinerator Ash. *Journal of Environmental Science and Health, Part A* 2005; 40: 617-631.
- Hu L, Heng S, Kudisi D, Liu Y, Liu Z, Lu X, et al. Dual-chamber up-flow fluidized hollow-fiber anaerobic membrane bioreactor (UF-HF-AnMBR) treating synthetic purified terephthalic

- acid wastewater: Granular sludge regranulation and methane production. *Chemical Engineering Journal* 2024; 486: 150292.
- Hudayah N, Suraraksa B, Chaiprasert P. Impact of EPS and chitosan combination on enhancement of anaerobic granule quality during simultaneous microbial adaptation and granulation. *Journal of Chemical Technology & Biotechnology* 2019; 94: 3725-3735.
- Im S, Yun Y-M, Song Y-C, Kim D-H. Enhanced anaerobic digestion of glycerol by promoting DIET reaction. *Biochemical Engineering Journal* 2019; 142: 18-26.
- Ismail SB, de La Parra CJ, Temmink H, van Lier JB. Extracellular polymeric substances (EPS) in upflow anaerobic sludge blanket (UASB) reactors operated under high salinity conditions. *Water Research* 2010; 44: 1909-1917.
- Jadhav DA, Yu Z, Hussien M, Kim J-H, Liu W, Eisa T, et al. Paradigm shift in Nutrient-Energy-Water centered sustainable wastewater treatment system through synergy of bioelectrochemical system and anaerobic digestion. *Bioresource Technology* 2024; 396: 130404.
- Jadhav P, Nasrullah M, Zularisam AW, Bhuyar P, Krishnan S, Mishra P. Direct interspecies electron transfer performance through nanoparticles (NPs) for biogas production in the anaerobic digestion process. *International Journal of Environmental Science and Technology* 2021.
- Jain N, Bhatia A, Kaushik R, Kumar S, Joshi HC, Pathak H. Impact of Post-Methanation Distillery Effluent Irrigation on Groundwater Quality. *Environmental Monitoring and Assessment* 2005; 110: 243-255.

- Jain S, Jain S, Wolf IT, Lee J, Tong YW. A comprehensive review on operating parameters and different pretreatment methodologies for anaerobic digestion of municipal solid waste. *Renewable and Sustainable Energy Reviews* 2015; 52: 142-154.
- Jin H, Lee YS, Hong I. Hydrogen adsorption characteristics of activated carbon. *Catalysis Today* 2007; 120: 399-406.
- Jin N. The effect of phosphate buffer on improving the performance of autothermal thermophilic aerobic digestion for sewage sludge. *RSC advances* 2018; 8: 9175-9180.
- Jiraprasertwong A, Seneesrisakul K, Pornmai K, Chavadej S. High methanogenic activity of a three-stage UASB in relation to the granular sludge formation. *Science of The Total Environment* 2020; 724: 138145.
- Ju F, Lau F, Zhang T. Linking Microbial Community, Environmental Variables, and Methanogenesis in Anaerobic Biogas Digesters of Chemically Enhanced Primary Treatment Sludge. *Environmental Science & Technology* 2017; 51: 3982-3992.
- Jung S, Kim M, Lee J, Shin J, Shin SG, Lee J. Effect of magnetite supplementation on mesophilic anaerobic digestion of phenol and benzoate: Methane production rate and microbial communities. *Bioresource Technology* 2022; 350: 126943.
- Kainthola J, Kalamdhad AS, Goud VV. Optimization of methane production during anaerobic co-digestion of rice straw and hydrilla verticillata using response surface methodology. *Fuel* 2019; 235: 92-99.
- Kang H-J, Lee S-H, Lim T-G, Park H-D. Effect of inoculum concentration on methanogenesis by direct interspecies electron transfer: Performance and microbial community composition. *Bioresource Technology* 2019; 291: 121881.

- Kang H-J, Lee S-H, Lim T-G, Park H-D. Effect of microbial community structure in inoculum on the stimulation of direct interspecies electron transfer for methanogenesis. *Bioresource Technology* 2021; 332: 125100.
- Kavitha S, Brindha GJ, Gloriana AS, Rajashankar K, Yeom IT, Banu JR. Enhancement of aerobic biodegradability potential of municipal waste activated sludge by ultrasonic aided bacterial disintegration. *Bioresource technology* 2016; 200: 161-169.
- Kavitha S, Kumar SA, Yogalakshmi K, Kaliappan S, Banu JR. Effect of enzyme secreting bacterial pretreatment on enhancement of aerobic digestion potential of waste activated sludge interceded through EDTA. *Bioresource technology* 2013; 150: 210-219.
- Kennedy KJ, Thibault G, Droste RL. Microwave enhanced digestion of aerobic SBR sludge. *Water Sa* 2007; 33: 261-270.
- Khoufi S, Louhichi A, Sayadi S. Optimization of anaerobic co-digestion of olive mill wastewater and liquid poultry manure in batch condition and semi-continuous jet-loop reactor. *Bioresource Technology* 2015; 182: 67-74.
- Kim H-W, Nam J-Y, Shin H-S. A comparison study on the high-rate co-digestion of sewage sludge and food waste using a temperature-phased anaerobic sequencing batch reactor system. *Bioresource Technology* 2011; 102: 7272-7279.
- Kothari R, Pandey AK, Kumar S, Tyagi VV, Tyagi SK. Different aspects of dry anaerobic digestion for bio-energy: An overview. *Renewable and Sustainable Energy Reviews* 2014; 39: 174-195.
- Kujawa-Roeleveld K, Elmitwalli T, Zeeman G. Enhanced primary treatment of concentrated black water and kitchen residues within DESAR concept using two types of anaerobic digesters. *Water Science and Technology* 2006; 53: 159-168.

- Kujawa-Roeleveld K, Fernandes T, Wiryawan Y, Tawfik A, Visser W, Zeeman G. Performance of UASB septic tank for treatment of concentrated black water within DESAR concept. *Water Science and Technology* 2005; 52: 307-313.
- Kumar A, Samadder SR. Performance evaluation of anaerobic digestion technology for energy recovery from organic fraction of municipal solid waste: A review. *Energy* 2020; 197: 117253.
- Kutlar FE, Tunca B, Yilmazel YD. Carbon-based conductive materials enhance biomethane recovery from organic wastes: A review of the impacts on anaerobic treatment. *Chemosphere* 2022; 290: 133247.
- Langille MGI, Zaneveld J, Caporaso JG, McDonald D, Knights D, Reyes JA, et al. Predictive functional profiling of microbial communities using 16S rRNA marker gene sequences. *Nature Biotechnology* 2013; 31: 814-821.
- Lau PL, Trzcinski AP. A review of modified and hybrid anaerobic baffled reactors for industrial wastewater treatment. *Water Science and Engineering* 2022; 15: 247-256.
- Layden NM, Kelly HG, Mavinic DS, Moles R, Bartlett J. Autothermal thermophilic aerobic digestion (ATAD)—Part II: Review of research and full-scale operating experiences. *Journal of Environmental Engineering and Science* 2007; 6: 679-690.
- Lee B, Park J-G, Shin W-B, Tian D-J, Jun H-B. Microbial communities change in an anaerobic digestion after application of microbial electrolysis cells. *Bioresource Technology* 2017; 234: 273-280.
- Lee J, Kwon D, Kim J. Long-term performance evaluation of granular activated carbon fluidization and biogas sparging in anaerobic fluidized bed membrane bioreactor:

- Membrane fouling and micropollutant removal. *Process Safety and Environmental Protection* 2021; 154: 425-432.
- Lee J-Y, Lee S-H, Park H-D. Enrichment of specific electro-active microorganisms and enhancement of methane production by adding granular activated carbon in anaerobic reactors. *Bioresource Technology* 2016; 205: 205-212.
- Lee NM, Welander T. Reducing sludge production in aerobic wastewater treatment through manipulation of the ecosystem. *Water Research* 1996; 30: 1781-1790.
- Lei Y, Sun D, Dang Y, Chen H, Zhao Z, Zhang Y, et al. Stimulation of methanogenesis in anaerobic digesters treating leachate from a municipal solid waste incineration plant with carbon cloth. *Bioresource Technology* 2016; 222: 270-276.
- Leng X, Usman M, Salama E-S, Ni H, Zhou T, Jeon B-H, et al. Development of an innovative MFC-biosensor for real-time monitoring of anaerobic digestion for biogas production: Controlled substrate feeding strategy. *Journal of Environmental Chemical Engineering* 2021; 9: 106703.
- Lens Pv, Van Den Bosch M, Pol LH, Lettinga G. Effect of staging on volatile fatty acid degradation in a sulfidogenic granular sludge reactor. *Water Research* 1998; 32: 1178-1192.
- Li J, Wang Q, Liang J, Li H, Guo S, Gamal El-Din M, et al. An enhanced disintegration using refinery spent caustic for anaerobic digestion of refinery waste activated sludge. *Journal of Environmental Management* 2021a; 284: 112022.
- Li L, Xu Y, Dai X, Dai L. Principles and advancements in improving anaerobic digestion of organic waste via direct interspecies electron transfer. *Renewable and Sustainable Energy Reviews* 2021b; 148: 111367.

- Li W, Khalid H, Zhu Z, Zhang R, Liu G, Chen C, et al. Methane production through anaerobic digestion: Participation and digestion characteristics of cellulose, hemicellulose and lignin. *Applied Energy* 2018; 226: 1219-1228.
- Li Y, Chen Y, Wu J. Enhancement of methane production in anaerobic digestion process: A review. *Applied Energy* 2019; 240: 120-137.
- Li YC, Wang YL, Li ZW. Optimization of Extraction Process of Water-Soluble Polysaccharides from *Porphyra* by Response Surface Methodology. *Advanced Materials Research* 2014; 864-867: 526-530.
- Liang J, Huang J, Zhang S, Yang X, Huang S, Zheng L, et al. A highly efficient conditioning process to improve sludge dewaterability by combining calcium hypochlorite oxidation, ferric coagulant re-flocculation, and walnut shell skeleton construction. *Chemical Engineering Journal* 2019; 361: 1462-1478.
- Liang J, Huang S, Dai Y, Li L, Sun S. Dewaterability of five sewage sludges in Guangzhou conditioned with Fenton's reagent/lime and pilot-scale experiments using ultrahigh pressure filtration system. *Water research* 2015; 84: 243-254.
- Liang T, Elmaadawy K, Liu B, Hu J, Hou H, Yang J. Anaerobic fermentation of waste activated sludge for volatile fatty acid production: Recent updates of pretreatment methods and the potential effect of humic and nutrients substances. *Process Safety and Environmental Protection* 2021; 145: 321-339.
- Lim SJ, Kim T-H. Applicability and trends of anaerobic granular sludge treatment processes. *Biomass & Bioenergy* 2014; 60: 189-202.

- Lin R, Cheng J, Ding L, Murphy JD. Improved efficiency of anaerobic digestion through direct interspecies electron transfer at mesophilic and thermophilic temperature ranges. *Chemical Engineering Journal* 2018; 350: 681-691.
- Lin R, Cheng J, Zhang J, Zhou J, Cen K, Murphy JD. Boosting biomethane yield and production rate with graphene: The potential of direct interspecies electron transfer in anaerobic digestion. *Bioresource Technology* 2017; 239: 345-352.
- Liu F, Rotaru A-E, Shrestha PM, Malvankar NS, Nevin KP, Lovley DR. Promoting direct interspecies electron transfer with activated carbon. *Energy & Environmental Science* 2012; 5: 8982-8989.
- Liu H, Fang HHP. Extraction of extracellular polymeric substances (EPS) of sludges. *Journal of Biotechnology* 2002; 95: 249-256.
- Liu J, Liu T, Chen S, Yu H, Zhang Y, Quan X. Enhancing anaerobic digestion in anaerobic integrated floating fixed-film activated sludge (An-IFFAS) system using novel electron mediator suspended biofilm carriers. *Water Research* 2020a; 175: 115697.
- Liu T, Schnürer A, Björkmalm J, Willquist K, Kreuger E. Diversity and Abundance of Microbial Communities in UASB Reactors during Methane Production from Hydrolyzed Wheat Straw and Lucerne. *Microorganisms* 2020b; 8.
- Liu Y, Tay J-H. State of the art of biogranulation technology for wastewater treatment. *Biotechnology Advances* 2004; 22: 533-563.
- Lu X, Zhen G, Estrada AL, Chen M, Ni J, Hojo T, et al. Operation performance and granule characterization of upflow anaerobic sludge blanket (UASB) reactor treating wastewater with starch as the sole carbon source. *Bioresource Technology* 2015; 180: 264-273.

- Luo C, Lü F, Shao L, He P. Application of eco-compatible biochar in anaerobic digestion to relieve acid stress and promote the selective colonization of functional microbes. *Water Research* 2015; 68: 710-718.
- Luo J, Huang W, Zhang Q, Guo W, Wu Y, Feng Q, et al. Effects of different hypochlorite types on the waste activated sludge fermentation from the perspectives of volatile fatty acids production, microbial community and activity, and characteristics of fermented sludge. *Bioresource Technology* 2020: 123227.
- Luostarinen S, Sanders W, Kujawa-Roeleveld K, Zeeman G. Effect of temperature on anaerobic treatment of black water in UASB-septic tank systems. *Bioresource technology* 2007; 98: 980-986.
- Macleod FA, Guiot SR, Costerton JW. Layered structure of bacterial aggregates produced in an upflow anaerobic sludge bed and filter reactor. *Applied and Environmental Microbiology* 1990; 56: 1598-1607.
- Mainardis M, Buttazzoni M, Goi D. Up-Flow Anaerobic Sludge Blanket (UASB) Technology for Energy Recovery: A Review on State-of-the-Art and Recent Technological Advances. *Bioengineering* 2020; 7: 43.
- Malila R, Lehtoranta S, Viskari EL. The role of source separation in nutrient recovery – Comparison of alternative wastewater treatment systems. *Journal of Cleaner Production* 2019; 219: 350-358.
- Mallick P, Akunna JC, Walker GM. Anaerobic digestion of distillery spent wash: Influence of enzymatic pre-treatment of intact yeast cells. *Bioresource Technology* 2010a; 101: 1681-1685.

- Mallick P, Akunna JC, Walker GM. Benefits of enzymatic pre-treatment of intact yeast cells for anaerobic digestion of distillery pot ale. *Distilled spirits: new horizons: energy, environmental and enlightenment*, 2010b, pp. 197-201.
- Maloney SW, Adrian NR, Hickey RF, Heine RL. Anaerobic treatment of pinkwater in a fluidized bed reactor containing GAC. *Journal of Hazardous Materials* 2002; 92: 77-88.
- Martins G, Salvador AF, Pereira L, Alves MM. Methane Production and Conductive Materials: A Critical Review. *Environmental Science & Technology* 2018; 52: 10241-10253.
- Massoud MA, Tarhini A, Nasr JA. Decentralized approaches to wastewater treatment and management: Applicability in developing countries. *Journal of Environmental Management* 2009; 90: 652-659.
- Matheri AN, Ndiweni SN, Belaid M, Muzenda E, Hubert R. Optimising biogas production from anaerobic co-digestion of chicken manure and organic fraction of municipal solid waste. *Renewable and Sustainable Energy Reviews* 2017; 80: 756-764.
- McDonald D, Price MN, Goodrich J, Nawrocki EP, DeSantis TZ, Probst A, et al. An improved Greengenes taxonomy with explicit ranks for ecological and evolutionary analyses of bacteria and archaea. *The ISME Journal* 2012; 6: 610-618.
- McHugh S, O'Reilly C, Mahony T, Colleran E, O'Flaherty V. Anaerobic Granular Sludge Bioreactor Technology. *Reviews in Environmental Science and Biotechnology* 2003; 2: 225-245.
- Mercado JV, Koyama M, Nakasaki K. Short-term changes in the anaerobic digestion microbiome and biochemical pathways with changes in organic load. *Science of The Total Environment* 2022; 813: 152585.

- Merrylin J, Kaliappan S, Kumar SA, Yeom I-T, Banu JR. Enhancing aerobic digestion potential of municipal waste-activated sludge through removal of extracellular polymeric substance. *Environmental Science and Pollution Research* 2014; 21: 1112-1123.
- Mo F, Song C, Zhou Q, Xue W, Ouyang S, Wang Q, et al. The optimized Fenton-like activity of Fe single-atom sites by Fe atomic clusters-mediated electronic configuration modulation. *Proceedings of the National Academy of Sciences* 2023; 120: e2300281120.
- Mohammad Mirsoleimani Azizi S, Dastyar W, Meshref MNA, Maal-Bared R, Ranjan Dhar B. Low-temperature thermal hydrolysis for anaerobic digestion facility in wastewater treatment plant with primary sludge fermentation. *Chemical Engineering Journal* 2021; 426: 130485.
- Mohana S, Acharya BK, Madamwar D. Distillery spent wash: Treatment technologies and potential applications. *Journal of Hazardous Materials* 2009; 163: 12-25.
- Moraes BS, Zaiat M, Bonomi A. Anaerobic digestion of vinasse from sugarcane ethanol production in Brazil: Challenges and perspectives. *Renewable and Sustainable Energy Reviews* 2015; 44: 888-903.
- Mou A, Yu N, Sun H, Liu Y. Spatial distributions of granular activated carbon in up-flow anaerobic sludge blanket reactors influence methane production treating low and high solid-content wastewater. *Bioresource Technology* 2022a; 363: 127995.
- Mou A, Yu N, Yang X, Liu Y. Enhancing methane production and organic loading capacity from high solid-content wastewater in modified granular activated carbon (GAC)-amended up-flow anaerobic sludge blanket (UASB). *Science of The Total Environment* 2024; 906: 167609.

- Mou A, Yu N, Zhang L, Sun H, Liu Y. Calcium Hypochlorite Pretreatment Enhances Waste-Activated Sludge Degradation during Aerobic Digestion. *Journal of Environmental Engineering* 2022b; 148: 04022002.
- Muga HE, Mihelcic JR. Sustainability of wastewater treatment technologies. *Journal of Environmental Management* 2008; 88: 437-447.
- Muturi SM, Muthui LW, Njogu PM, Onguso JMa, Wachira FN, Opiyo SO, et al. Metagenomics survey unravels diversity of biogas microbiomes with potential to enhance productivity in Kenya. *PLOS ONE* 2021; 16.
- Ng PJ, Fleet GH, Heard GM. Pesticides as a source of microbial contamination of salad vegetables. *International Journal of Food Microbiology* 2005; 101: 237-250.
- Nguyen LN, Vu MT, Abu Hasan Johir M, Pernice M, Ngo HH, Zdarta J, et al. Promotion of direct interspecies electron transfer and potential impact of conductive materials in anaerobic digestion and its downstream processing - a critical review. *Bioresource Technology* 2021; 341: 125847.
- Nkuna R, Roopnarain A, Rashama C, Adeleke R. Insights into organic loading rates of anaerobic digestion for biogas production: a review. *Critical Reviews in Biotechnology* 2022; 42: 487-507.
- Noutsopoulos C, Andreadakis A, Kouris N, Charchousi D, Mendrinou P, Galani A, et al. Greywater characterization and loadings – Physicochemical treatment to promote onsite reuse. *Journal of Environmental Management* 2018; 216: 337-346.
- Nsair A, Onen Cinar S, Alassali A, Abu Qdais H, Kuchta K. Operational Parameters of Biogas Plants: A Review and Evaluation Study. *Energies*. 13, 2020.

- Okolie JA, Tabat ME, Ogbaga CC, Okoye PU, Davis P, Gunes B. Economic and environmental assessments of a novel integrated process for biomethane production and ammonia recovery from pot ale. *Chemical Engineering Journal* 2022; 446: 137234.
- Parada AE, Needham DM, Fuhrman JA. Every base matters: assessing small subunit rRNA primers for marine microbiomes with mock communities, time series and global field samples. *Environmental Microbiology* 2016; 18: 1403-1414.
- Paritosh K, Kesharwani N. Biochar mediated high-rate anaerobic bioreactors: A critical review on high-strength wastewater treatment and management. *Journal of Environmental Management* 2024; 355: 120348.
- Park J-H, Kang H-J, Park K-H, Park H-D. Direct interspecies electron transfer via conductive materials: A perspective for anaerobic digestion applications. *Bioresource Technology* 2018; 254: 300-311.
- Park ND, Helle SS, Thring RW. Combined alkaline and ultrasound pre-treatment of thickened pulp mill waste activated sludge for improved anaerobic digestion. *Biomass and Bioenergy* 2012; 46: 750-756.
- Pasalari H, Gholami M, Rezaee A, Esrafil A, Farzadkia M. Perspectives on microbial community in anaerobic digestion with emphasis on environmental parameters: A systematic review. *Chemosphere* 2021; 270: 128618.
- Peng H, Zhang Y, Tan D, Zhao Z, Zhao H, Quan X. Roles of magnetite and granular activated carbon in improvement of anaerobic sludge digestion. *Bioresource Technology* 2018; 249: 666-672.

- Phayungphan K, Rakmak N, Promraksa A. Application of monod two-substrate kinetics with an intermediate for anaerobic co-digestion of distillery wastewater and molasses/glycerol waste in batch experiments. *Water Practice and Technology* 2020; 15: 1068-1082.
- Qiu L, Deng YF, Wang F, Davaritouchaee M, Yao YQ. A review on biochar-mediated anaerobic digestion with enhanced methane recovery. *Renewable and Sustainable Energy Reviews* 2019; 115: 109373.
- Rajendran K, Mahapatra D, Venkatraman AV, Muthuswamy S, Pugazhendhi A. Advancing anaerobic digestion through two-stage processes: Current developments and future trends. *Renewable and Sustainable Energy Reviews* 2020; 123: 109746.
- Ripoll V, Agabo-García C, Perez M, Solera R. Improvement of biomethane potential of sewage sludge anaerobic co-digestion by addition of “sherry-wine” distillery wastewater. *Journal of Cleaner Production* 2020; 251: 119667.
- Ripoll V, Solera R, Perez M. Kinetic modelling of anaerobic co-digestion of sewage sludge and Sherry-wine distillery wastewater: Effect of substrate composition in batch bioreactor. *Fuel* 2022; 329: 125524.
- Rose C, Parker A, Jefferson B, Cartmell E. The Characterization of Feces and Urine: A Review of the Literature to Inform Advanced Treatment Technology. *Critical Reviews in Environmental Science and Technology* 2015; 45: 1827-1879.
- Rosso D, Larson LE, Stenstrom MK. Aeration of large-scale municipal wastewater treatment plants: state of the art. *Water Science and Technology* 2008; 57: 973-978.
- Rotaru A-E, Calabrese F, Stryhanyuk H, Musat F, Shrestha PM, Weber HS, et al. Conductive Particles Enable Syntrophic Acetate Oxidation between *Geobacter* and *Methanosarcina* from Coastal Sediments. *mBio* 2018; 9: 10.1128/mbio.00226-18.

- Satyawali Y, Balakrishnan M. Wastewater treatment in molasses-based alcohol distilleries for COD and color removal: A review. *Journal of Environmental Management* 2008; 86: 481-497.
- Sekiguchi Y, Kamagata Y, Nakamura K, Ohashi A, Harada H. Fluorescence In Situ Hybridization Using 16S rRNA-Targeted Oligonucleotides Reveals Localization of Methanogens and Selected Uncultured Bacteria in Mesophilic and Thermophilic Sludge Granules. *Applied and Environmental Microbiology* 1999; 65: 1280-1288.
- Sharma D, Mahajan R, Goel G. Insights into direct interspecies electron transfer mechanisms for acceleration of anaerobic digestion of wastes. *International Journal of Environmental Science and Technology* 2019; 16: 2133-2142.
- Sillero L, Solera R, Perez M. Effect of temperature and bagasse addition on anaerobic co-digestion of brewery waste by biochemical methane potential test. *Fuel* 2024; 357: 129737.
- Singh NK, Kazmi AA, Starkl M. A review on full-scale decentralized wastewater treatment systems: techno-economical approach. *Water Science and Technology* 2014; 71: 468-478.
- Slompo NDM, Quartaroli L, Zeeman G, da Silva GHR, Daniel LA. Black water treatment by an upflow anaerobic sludge blanket (UASB) reactor: a pilot study. *Water Science and Technology* 2019.
- Song L-J, Zhu N-W, Yuan H-P, Hong Y, Ding J. Enhancement of waste activated sludge aerobic digestion by electrochemical pre-treatment. *Water research* 2010a; 44: 4371-4378.
- Song M, Shin SG, Hwang S. Methanogenic population dynamics assessed by real-time quantitative PCR in sludge granule in upflow anaerobic sludge blanket treating swine wastewater. *Bioresource Technology* 2010b; 101: S23-S28.

- Song T, Li S, Yin Z, Bao M, Lu J, Li Y. Hydrolyzed polyacrylamide-containing wastewater treatment using ozone reactor-upflow anaerobic sludge blanket reactor-aerobic biofilm reactor multistage treatment system. *Environmental pollution (Barking, Essex : 1987)* 2021; 269: 116111-116111.
- Storck T, Viridis B, Batstone DJ. Modelling extracellular limitations for mediated versus direct interspecies electron transfer. *The ISME Journal* 2016; 10: 621-631.
- Strong PJ, Burgess JE. Treatment methods for wine-related and distillery wastewaters: a review. *Bioremediation journal* 2008; 12: 70-87.
- Su X-L, Tian Q, Zhang J, Yuan X-Z, Shi X-S, Guo R-B, et al. *Acetobacteroides hydrogenigenes* gen. nov., sp. nov., an anaerobic hydrogen-producing bacterium in the family Rikenellaceae isolated from a reed swamp. *International journal of systematic and evolutionary microbiology* 2014; 64: 2986-2991.
- Subramanyam R. Physicochemical and Morphological Characteristics of Granular Sludge in Upflow Anaerobic Sludge Blanket Reactors. *Environmental Engineering Science* 2013; 30: 201-212.
- Sun H, Yang X, Yu N, Gong X, Zhang L, Liu Y. Impact of feedwater protein contents on calcium phosphate mineralization in anaerobic digesters. *Journal of Environmental Chemical Engineering* 2021; 9: 106445.
- Sun H, Yu N, Mou A, Yang X, Liu Y. Effluent recirculation weakens the hydrolysis of high-solid content feeds in upflow anaerobic sludge blanket reactors. *Journal of Environmental Chemical Engineering* 2022; 10: 107913.
- Sun M, Zhang Z, Lv M, Liu G, Feng Y. Enhancing anaerobic digestion performance of synthetic brewery wastewater with direct voltage. *Bioresource Technology* 2020; 315: 123764.

- Tassew FA, Bergland WH, Dinamarca C, Kommedal R, Bakke R. Granular sludge bed processes in anaerobic digestion of particle-rich substrates. *Energies* 2019; 12: 2940.
- Tay J-H, Tay ST-L, Liu Y, Show KY, Ivanov V. *Biogranulation technologies for wastewater treatment: Microbial granules*: Elsevier, 2006.
- Tena M, Perez M, Solera R. Benefits in the valorization of sewage sludge and wine vinasse via a two-stage acidogenic-thermophilic and methanogenic-mesophilic system based on the circular economy concept. *Fuel* 2021; 296: 120654.
- Tervahauta T, Rani S, Hernández Leal L, Buisman CJN, Zeeman G. Black water sludge reuse in agriculture: Are heavy metals a problem? *Journal of Hazardous Materials* 2014a; 274: 229-236.
- Tervahauta T, van der Weijden RD, Flemming RL, Leal LH, Zeeman G, Buisman CJ. Calcium phosphate granulation in anaerobic treatment of black water: a new approach to phosphorus recovery. *Water research* 2014b; 48: 632-642.
- Tiehm A, Nickel K, Zellhorn M, Neis U. Ultrasonic waste activated sludge disintegration for improving anaerobic stabilization. *Water Research* 2001; 35: 2003-2009.
- Toreci I, Kennedy KJ, Droste RL. Evaluation of continuous mesophilic anaerobic sludge digestion after high temperature microwave pretreatment. *Water Research* 2009; 43: 1273-1284.
- Turkdogan-Aydinli FI, Yetilmezsoy K, Comez S, Bayhan H. Performance evaluation and kinetic modeling of the start-up of a UASB reactor treating municipal wastewater at low temperature. *Bioprocess and Biosystems Engineering* 2011; 34: 153-162.
- Tyagi VK, Fdez-Güelfo LA, Zhou Y, Álvarez-Gallego CJ, Garcia LIR, Ng WJ. Anaerobic co-digestion of organic fraction of municipal solid waste (OFMSW): Progress and challenges. *Renewable and Sustainable Energy Reviews* 2018; 93: 380-399.

- Tyagi VK, Lo S-L. Enhancement in mesophilic aerobic digestion of waste activated sludge by chemically assisted thermal pretreatment method. *Bioresource technology* 2012; 119: 105-113.
- Ushani U, Kavitha S, Johnson M, Yeom IT, Banu JR. Upgrading the hydrolytic potential of immobilized bacterial pretreatment to boost biogas production. *Environmental Science and Pollution Research* 2017; 24: 813-826.
- Van de Velden M, Dewil R, Baeyens J, Josson L, Lanssens P. The distribution of heavy metals during fluidized bed combustion of sludge (FBSC). *Journal of Hazardous Materials* 2008; 151: 96-102.
- Van Lier J, Van Der Zee F, Frijters C, Ersahin M. Development of anaerobic high-rate reactors, focusing on sludge bed technology. *Anaerobes in Biotechnology* 2016: 363-395.
- Vavilin VA, Rytov SV, Lokshina LY, Pavlostathis SG, Barlaz MA. Distributed model of solid waste anaerobic digestion: Effects of leachate recirculation and pH adjustment. *Biotechnology and Bioengineering* 2003; 81: 66-73.
- Velmurugan B, Arathy EC, Hemalatha R, Philip JE, Alwar Ramanujam R. Anaerobic co-digestion of fruit and vegetable wastes and primary sewage sludge. *Journal of environmental science & engineering* 2010; 52: 19-22.
- Walker DJF, Martz E, Holmes DE, Zhou Z, Nonnenmann SS, Lovley DR. The Archaeum of *Methanospirillum hungatei* Is Electrically Conductive. *mBio* 2019; 10: 10.1128/mbio.00579-19.
- Walker DJF, Nevin KP, Holmes DE, Rotaru A-E, Ward JE, Woodard TL, et al. Syntrophus conductive pili demonstrate that common hydrogen-donating syntrophs can have a direct electron transfer option. *The ISME Journal* 2020; 14: 837-846.

- Wang F, Ji M, Lu S. Influence of ultrasonic disintegration on the dewaterability of waste activated sludge. *Environmental progress* 2006; 25: 257-260.
- Wang G, Gao X, Li Q, Zhao H, Liu Y, Wang XC, et al. Redox-based electron exchange capacity of biowaste-derived biochar accelerates syntrophic phenol oxidation for methanogenesis via direct interspecies electron transfer. *Journal of Hazardous Materials* 2020a; 390: 121726.
- Wang G, Li Q, Li Y, Xing Y, Yao G, Liu Y, et al. Redox-active biochar facilitates potential electron transfer between syntrophic partners to enhance anaerobic digestion under high organic loading rate. *Bioresource Technology* 2020b; 298: 122524.
- Wang H, Zhang Y, Angelidaki I. Ammonia inhibition on hydrogen enriched anaerobic digestion of manure under mesophilic and thermophilic conditions. *Water Research* 2016; 105: 314-319.
- Wang Q, Kuninobu M, Kakimoto K, I-Ogawa H, Kato Y. Upgrading of anaerobic digestion of waste activated sludge by ultrasonic pretreatment. *Bioresource Technology* 1999; 68: 309-313.
- Wang Q, Wei W, Liu S, Yan M, Song K, Mai J, et al. Free ammonia pretreatment improves degradation of secondary sludge during aerobic digestion. *ACS sustainable chemistry & engineering* 2018a; 6: 1105-1111.
- Wang Q, Yuan Z. Enhancing aerobic digestion of full-scale waste activated sludge using free nitrous acid pre-treatment. *Rsc Advances* 2015; 5: 19128-19134.
- Wang Y, Feng M, Liu Y, Li Y, Zhang B. Comparison of three types of anaerobic granular sludge for treating pharmaceutical wastewater. *Journal of Water Reuse and Desalination* 2017; 8: 532-543.

- Wang Y, Li W, Wang Y, Turap Y, Wang Z, Zhang Z, et al. Anaerobic co-digestion of food waste and sewage sludge in anaerobic sequencing batch reactors with application of co-hydrothermal pretreatment of sewage sludge and biogas residue. *Bioresource Technology* 2022; 364: 128006.
- Wang Y, Wang Z, Zhang Q, Li G, Xia C. Comparison of bio-hydrogen and bio-methane production performance in continuous two-phase anaerobic fermentation system between co-digestion and digestate recirculation. *Bioresource Technology* 2020c; 318: 124269.
- Wang Y, Zhao J, Wang D, Liu Y, Wang Q, Ni B-J, et al. Free nitrous acid promotes hydrogen production from dark fermentation of waste activated sludge. *Water research* 2018b; 145: 113-124.
- Wang Z, Y C, Zhang B, Ahmed Z, Ahmad M. Environmental degradation, renewable energy, and economic growth nexus: Assessing the role of financial and political risks? *Journal of Environmental Management* 2023; 325: 116678.
- Weemaes MPJ, Verstraete WH. Evaluation of current wet sludge disintegration techniques. *Journal of Chemical Technology & Biotechnology* 1998; 73: 83-92.
- Wei W, Chen X, Peng L, Liu Y, Bao T, Ni B-J. The entering of polyethylene terephthalate microplastics into biological wastewater treatment system affects aerobic sludge digestion differently from their direct entering into sludge treatment system. *Water research* 2020; 190: 116731-116731.
- Welling CM, Varigala S, Krishnaswamy S, Raj A, Lynch B, Piascik JR, et al. Resolving the relative contributions of cistern and pour flushing to toilet water usage: Measurements from urban test sites in India. *Science of The Total Environment* 2020; 730: 138957.

- Wen C, Dai Z, Cheng F, Cheng H, Yang Z, Cai Q, et al. Review on research achievements of blackwater anaerobic digestion for enhanced resource recovery. *Environment, Development and Sustainability* 2024; 26: 1-31.
- Wendland C, Deegener S, Behrendt J, Toshev P, Otterpohl R. Anaerobic digestion of blackwater from vacuum toilets and kitchen refuse in a continuous stirred tank reactor (CSTR). *Water Science and Technology* 2007; 55: 187-194.
- Werner JJ, Koren O, Hugenholtz P, DeSantis TZ, Walters WA, Caporaso JG, et al. Impact of training sets on classification of high-throughput bacterial 16s rRNA gene surveys. *The ISME Journal* 2012; 6: 94-103.
- White JS, Stewart KL, Maskell DL, Diallo A, Traub-Modinger JE, Willoughby NA. Characterization of Pot Ale from a Scottish Malt Whisky Distillery and Potential Applications. *ACS Omega* 2020; 5: 6429-6440.
- Wilderer PA, Schreff D. Decentralized and centralized wastewater management: a challenge for technology developers. *Water Science and Technology* 2000; 41: 1-8.
- Wu J, Yang Q, Luo W, Sun J, Xu Q, Chen F, et al. Role of free nitrous acid in the pretreatment of waste activated sludge: Extracellular polymeric substances disruption or cells lysis? *Chemical Engineering Journal* 2018; 336: 28-37.
- Xia A, Feng D, Huang Y, Zhu X, Wang Z, Zhu X, et al. Activated Carbon Facilitates Anaerobic Digestion of Furfural Wastewater: Effect of Direct Interspecies Electron Transfer. *ACS Sustainable Chemistry & Engineering* 2022; 10: 8206-8215.
- Xia S, Zhou Y, Eustance E, Zhang Z. Enhancement mechanisms of short-time aerobic digestion for waste activated sludge in the presence of cocoamidopropyl betaine. *Scientific Reports* 2017; 7: 13491.

- Xing B-S, Han Y, Cao S, Wang XC. Effects of long-term acclimatization on the optimum substrate mixture ratio and substrate to inoculum ratio in anaerobic codigestion of food waste and cow manure. *Bioresource Technology* 2020; 317: 123994.
- Xu R, Yang Z-H, Zheng Y, Liu J-B, Xiong W-P, Zhang Y-R, et al. Organic loading rate and hydraulic retention time shape distinct ecological networks of anaerobic digestion related microbiome. *Bioresource Technology* 2018; 262: 184-193.
- Xu S, He C, Luo L, Lü F, He P, Cui L. Comparing activated carbon of different particle sizes on enhancing methane generation in upflow anaerobic digester. *Bioresource Technology* 2015; 196: 606-612.
- Xu Y, Lu Y, Zheng L, Wang Z, Dai X. Perspective on enhancing the anaerobic digestion of waste activated sludge. *Journal of Hazardous Materials* 2020; 389: 121847.
- Yang L, Si B, Zhang Y, Watson J, Stablein M, Chen J, et al. Continuous treatment of hydrothermal liquefaction wastewater in an anaerobic biofilm reactor: Potential role of granular activated carbon. *Journal of Cleaner Production* 2020; 276.
- Yang Y, Zhang Y, Li Z, Zhao Z, Quan X, Zhao Z. Adding granular activated carbon into anaerobic sludge digestion to promote methane production and sludge decomposition. *Journal of Cleaner Production* 2017; 149: 1101-1108.
- Yao Y, Gan Z, Zhou Z, Huang Y-X, Meng F. Carbon sources driven supernatant micro-particles differentiate in submerged anaerobic membrane bioreactors (AnMBRs). *Chemical Engineering Journal* 2022; 430: 133020.
- Yenigün O, Demirel B. Ammonia inhibition in anaerobic digestion: A review. *Process Biochemistry* 2013; 48: 901-911.

- Yin Q, Wu G. Advances in direct interspecies electron transfer and conductive materials: Electron flux, organic degradation and microbial interaction. *Biotechnology Advances* 2019; 37: 107443.
- Yu N, Guo B, Liu Y. Shaping biofilm microbiomes by changing GAC location during wastewater anaerobic digestion. *Science of The Total Environment* 2021; 780: 146488.
- Yu N, Guo B, Zhang Y, Zhang L, Zhou Y, Liu Y. Different micro-aeration rates facilitate production of different end-products from source-diverted blackwater. *Water Research* 2020; 177: 115783.
- Yu N, Guo B, Zhang Y, Zhang L, Zhou Y, Liu Y. Self-fluidized GAC-amended UASB reactor for enhanced methane production. *Chemical Engineering Journal* 2021c; 420: 127652.
- Yu N, Mou A, Sun H, Liu Y. Anaerobic digestion of thickened waste activated sludge under calcium hypochlorite stress: Performance stability and microbial communities. *Environmental Research* 2022; 212: 113441.
- Yu N, Sun H, Mou A, Liu Y. Calcium hypochlorite enhances the digestibility of and the phosphorus recovery from waste activated sludge. *Bioresource Technology* 2021d; 340: 125658.
- Yuan H, Yu B, Cheng P, Zhu N, Yin C, Ying L. Pilot-scale study of enhanced anaerobic digestion of waste activated sludge by electrochemical and sodium hypochlorite combination pretreatment. *International Biodeterioration & Biodegradation* 2016; 110: 227-234.
- Yuan H, Zhu N. Progress in inhibition mechanisms and process control of intermediates and by-products in sewage sludge anaerobic digestion. *Renewable and Sustainable Energy Reviews* 2016; 58: 429-438.

- Zeeman G, Sanders W. Potential of anaerobic digestion of complex waste(water). *Water Science and Technology* 2001; 44: 115-122.
- Zhang L, Guo B, Mou A, Li R, Liu Y. Blackwater biomethane recovery using a thermophilic upflow anaerobic sludge blanket reactor: Impacts of effluent recirculation on reactor performance. *Journal of Environmental Management* 2020a; 274: 111157.
- Zhang L, Guo B, Zhang Q, Florentino A, Xu R, Zhang Y, et al. Co-digestion of blackwater with kitchen organic waste: Effects of mixing ratios and insights into microbial community. *Journal of Cleaner Production* 2019; 236: 117703.
- Zhang L, Hendrickx TLG, Kampman C, Temmink H, Zeeman G. Co-digestion to support low temperature anaerobic pretreatment of municipal sewage in a UASB-digester. *Bioresource Technology* 2013; 148: 560-566.
- Zhang L, Mou A, Guo B, Sun H, Anwar MN, Liu Y. Simultaneous phosphorus recovery in energy generation reactor (SPRING): High rate thermophilic blackwater treatment. *Resources, Conservation and Recycling* 2021a; 164: 105163.
- Zhang L, Mou A, Sun H, Zhang Y, Zhou Y, Liu Y. Calcium phosphate granules formation: Key to high rate of mesophilic UASB treatment of toilet wastewater. *Science of The Total Environment* 2021b; 773: 144972.
- Zhang L, Yuan Y, Zhang Y, Liu Y. Exploring key factors in anaerobic syntrophic interactions: Biomass activity, microbial community, and morphology. *Bioresource Technology* 2022a; 363: 127852.
- Zhang L, Zhang Y, Yuan Y, Mou A, Park S, Liu Y. Impacts of granular activated carbon addition on anaerobic granulation in blackwater treatment. *Environmental Research* 2022b; 206: 112406.

- Zhang Q, Wu Y, Luo J, Cao J, Kang C, Wang S, et al. Enhanced volatile fatty acids production from waste activated sludge with synchronous phosphorus fixation and pathogens inactivation by calcium hypochlorite stimulation. *Science of The Total Environment* 2020b; 712: 136500.
- Zhang Q, Yang Y, Hou L-a, Zhu H, Zhang Y, Pu J, et al. Recent advances of carbon-based additives in anaerobic digestion: A review. *Renewable and Sustainable Energy Reviews* 2023; 183: 113536.
- Zhang Q, Zhang L, Guo B, Liu Y. Mesophiles outperform thermophiles in the anaerobic digestion of blackwater with kitchen residuals: Insights into process limitations. *Waste Management* 2020c; 105: 279-288.
- Zhang X, Jiao P, Wang Y, Wu P, Li Y, Ma L. Enhancing methane production in anaerobic co-digestion of sewage sludge and food waste by regulating organic loading rate. *Bioresource Technology* 2022c; 363: 127988.
- Zhang Y, Guo B, Dang H, Zhang L, Sun H, Yu N, et al. Roles of granular activated carbon (GAC) and operational factors on active microbiome development in anaerobic reactors. *Bioresource Technology* 2022d; 343: 126104.
- Zhang Y, Guo B, Zhang L, Liu Y. Key syntrophic partnerships identified in a granular activated carbon amended UASB treating municipal sewage under low temperature conditions. *Bioresource Technology* 2020d; 312: 123556.
- Zhao Z, Li Y, Quan X, Zhang Y. Towards engineering application: Potential mechanism for enhancing anaerobic digestion of complex organic waste with different types of conductive materials. *Water Research* 2017; 115: 266-277.

- Zhao Z, Zhang Y, Woodard TL, Nevin KP, Lovley DR. Enhancing syntrophic metabolism in up-flow anaerobic sludge blanket reactors with conductive carbon materials. *Bioresource Technology* 2015; 191: 140-145.
- Zheng D, Angenent LT, Raskin L. Monitoring granule formation in anaerobic upflow bioreactors using oligonucleotide hybridization probes. *Biotechnology and Bioengineering* 2006; 94: 458-472.
- Zheng S, Liu F, Wang B, Zhang Y, Lovley DR. Methanobacterium Capable of Direct Interspecies Electron Transfer. *Environmental Science & Technology* 2020; 54: 15347-15354.
- Zhou J, Wang JJ, Baudon A, Chow AT. Improved Fluorescence Excitation-Emission Matrix Regional Integration to Quantify Spectra for Fluorescent Dissolved Organic Matter. *Journal of environmental quality* 2013; 42: 925-930.
- Zhou Q, Song C, Wang P, Zhao Z, Li Y, Zhan S. Generating dual-active species by triple-atom sites through peroxymonosulfate activation for treating micropollutants in complex water. *Proceedings of the National Academy of Sciences* 2023; 120: e2300085120.
- Zhou QX, Hu XG. Systemic Stress and Recovery Patterns of Rice Roots in Response to Graphene Oxide Nanosheets. *Environmental Science & Technology* 2017; 51: 2022-2030.
- Zhou QX, Li DD, Wang T, Hu XG. Leaching of graphene oxide nanosheets in simulated soil and their influences on microbial communities. *Journal of Hazardous Materials* 2021; 404.
- Zhou QX, Ma SL, Zhan SH. Superior photocatalytic disinfection effect of Ag-3D ordered mesoporous CeO₂ under visible light. *Applied Catalysis B-Environmental* 2018; 224: 27-37.

- Zhou QX, Yue ZK, Li QZ, Zhou RR, Liu L. Exposure to PbSe Nanoparticles and Male Reproductive Damage in a Rat Model. *Environmental Science & Technology* 2019; 53: 13408-13416.
- Zhou Y, Li R, Guo B, Zhang L, Zhang H, Xia S, et al. Three-dimension oxygen gradient induced low energy input for grey water treatment in an oxygen-based membrane biofilm reactor. *Environmental Research* 2020; 191: 110124.
- Zhu H, Parker W, Basnar R, Proracki A, Falletta P, Béland M, et al. Biohydrogen production by anaerobic co-digestion of municipal food waste and sewage sludges. *International Journal of Hydrogen Energy* 2008; 33: 3651-3659.
- Zhu L, Zhou J, Lv M, Yu H, Zhao H, Xu X. Specific component comparison of extracellular polymeric substances (EPS) in flocs and granular sludge using EEM and SDS-PAGE. *Chemosphere* 2015; 121: 26-32.
- Zhu X, Yang Q, Li X, Zhong Y, Wu Y, Hou L, et al. Enhanced dewaterability of waste activated sludge with Fe (II)-activated hypochlorite treatment. *Environmental Science and Pollution Research* 2018; 25: 27628-27638.
- Zhuravleva EA, Shekhurdina SV, Kotova IB, Loiko NG, Popova NM, Kryukov E, et al. Effects of various materials used to promote the direct interspecies electron transfer on anaerobic digestion of low-concentration swine manure. *Science of The Total Environment* 2022; 839: 156073.
- Zou R, Tang K, Hambly AC, Wunsch UJ, Andersen HR, Angelidaki I, et al. When microbial electrochemistry meets UV: The applicability to high-strength real pharmaceutical industry wastewater. *Journal of Hazardous Materials* 2022; 423: 127151.